

University of Nottingham
UK | CHINA | MALAYSIA

Faculty of Medicine and Health Sciences
School of Medicine

Investigation of the role of CD24 gene in the progression of colorectal cancer

By

Zaki Hakami

Thesis submitted to the University of Nottingham
For the Degree of Doctor of Philosophy

May 2021

Declaration

I declare that this thesis entitles 'Investigation of the role of CD24 gene in the progression of colorectal cancer' has been authored by Zaki Hakami, and I confirm that all data presented in this thesis are my own works that were generated during the study period at the University of Nottingham unless otherwise stated. No part of this thesis has been submitted for any other degree or type of qualification at any other institution.

Zaki Hakami, May 2021

Acknowledgements

First and foremost, I would like to express my thanks and gratitude to **ALLAH Almighty**, who has given me the knowledge and success to complete this thesis. I would also like to express my sincerest gratitude to my principal supervisor, Professor Mohammad Ilyas, for his continued support, help, guidance, and encouragement during my PhD period. In addition, I would like to thank Jazan University for funding my PhD project.

Further, I would like to express the deepest appreciation to Dr Teresa Raposo for training, assistance and advice. Also, I would like to thank all my colleagues, the current and past members, in the Pathology Research Group and the Division of Cancer and Stem cells for their support, cooperation and assistance.

Finally, I am deeply thankful to my family, especially my mother, wife, siblings, and sons, for their constant prayers, unconditional love, support, and patience during the period of study.

Dedication

This thesis is dedicated to my beloved wife Suha and my dearest sons Abdulaziz and Nawaf for their tremendous love, support, motivation, patience, and sacrifices throughout my PhD studies.

List of Abbreviations

ALDH	Aldehyde dehydrogenase
Angptl4	Angiopoietin-like-4
APC	Adenomatous polyposis coli
BCA	Bicinchoninic acid
BCR	B cell receptor
Bp	Base pairs
BSA	Bovine serum albumin
CA	Cancer antigen
Ca19-9	Cancer antigen 19-9/Carbohydrate antigen 19-9
CBF1	C protein factor 1
CD24	Cluster of differentiation 24
cDNA	Complementary DNA
CEA	Carcinoembryonic antigen
CIMP	CpG island methylator phenotype
CIN	Chromosomal instability
CM	Conditioned Medium
Co-IP	Co-immunoprecipitation
CpG	Cytosine phosphate Guanine
CRC	Colorectal cancer
CSC	Cancer stem cells
CT	Computed tomography
CTC	Circulating tumour cells
Cten	C terminal tensin like
DAPI	4’,6-diamidino-2-phenylindole
DLL	Delta-like protein family
DMEM	Dulbecco’s Modified Eagle’s Medium
DMSO	Dimethyl sulfoxide
DNA	Deoxyribonucleic acid
DRG	Dorsal root ganglion

E. coli	Escherichia coli
ECGM	Endothelial cell growth medium
ECL	Enhanced chemiluminescence
ECM	Extracellular matrix
EDTA	Ethylenediaminetetraacetic acid
EGF	Epidermal growth factor
EGFR	Epidermal growth factor receptor
ELISA	Enzyme-linked immunosorbent assay
EMT	Epithelial-mesenchymal transition
EpCAM	Epithelial cellular adhesion molecule
E selectin	Endothelial selectin
ESI	Electrospray ionisation ion trap
EVC	Empty vector control
FACS	Fluorescence-activated cell sorting
F-actin	Filamentous actin
FAK	Focal Adhesion Kinase
FBS	Fetal Bovine Serum
Fc	Fragment crystallisable
FIT	Faecal occult blood
GlcNAc	β-O-N-acetylglucosamine
GPI	Glycosylphosphatidylinositol
HIF1-α	Hypoxia-inducible factor 1 alpha
HNPCC	Hereditary non-polyposis colorectal cancer
HSA	Heat-stable antigen
HUVEC	Human umbilical vein endothelial cells
ILK	Integrin-Linked Kinase
ITGB1	Integrin beta-like 1
JAG	Jagged protein
KRAS	Kirsten rat sarcoma
L1CAM	L1 cell adhesion molecule
LEF	Lymphoid enhancer-binding factor

LGR5	Leucine-rich repeat-containing G protein-coupled receptor 5
L selectin	Leukocyte selectin
LUC	Luciferase
mAB	Monoclonal Antibody
MALDI	Matrix-assisted laser desorption ionisation
MAPK	Mitogen-activated protein kinase
miRNA	MicroRNA
MLH	MutL homolog
M-MLV	Murine leukaemia viruses
MMP	Metalloproteinase
MMR	Mismatch repair
MSI	Microsatellite instability
MUC1	Mucin 1
NF-κB	Nuclear factor-kappa B
NICD	Notch intracellular domain
NTC	No template control
ORF	Open reading frame
PBGD	Porphobilinogen deaminase
PBS	Phosphate-buffered saline
PCR	Polymerase chain reaction
PE-38	Pseudomonas exotoxin-38
PET	Positron emission tomography
PIK3CA	Phosphatidylinositol 3-kinase catalytic alpha polypeptide
P selectin	Platelet selectin
PSGL-1	P-selectin glycoprotein ligand
PTK	Protein tyrosine kinase
PVDF	Polyvinylidene difluoride
RIPA	Radio immunoprecipitation assay
RTK	Receptor tyrosine kinases

SDM	Site-directed mutagenesis
SH2	Src homology 2
Sialyl-T	Sialyl-tumour antigen
Siglec	Sialic acid-binding Ig-like lectin
siRNA	Small interfering RNA
STAT3	Signal transducer and activator of transcription 3
STR	Short tandem repeat
TBS	Tris-buffered saline
TCF	T cell factor
TGFβ	Transforming growth factor-beta
TGFβR2	transforming growth factor-beta receptor 2
TNF-α	Tumour necrosis factor-alpha
TNM	Tumour Node Metastasis
TP53	Tumour protein P53
uPA	Urokinase-type plasminogen activator
VEGF	Vascular endothelial growth factor
WT	Wild-Type

Abstract

Cluster of differentiation (CD) 24 is a glycosyl-phosphatidylinositol (GPI) anchor protein. CD24 is a heavily glycosylated protein, containing 16 putative *O*-glycosylation sites and two putative *N*-glycosylation sites. In colorectal cancer (CRC) and many other cancers, CD24 induces stemness, cell motility (both migration and invasion) and, through interaction with endothelium, possibly metastasis. The mechanisms by which it exerts these activities are not known. Therefore, this thesis aimed to (i) investigate the role of the putative *N*-glycosylation sites in mediating CD24 function, (ii) define the signalling pathways and ligands that mediate CRC cell adhesion to endothelium and metastasis, and (iii) delineate CD24 involvement in CRC angiogenesis.

(i) *N*-glycosylation target sites on CD24 include asparagine residues at N36 and N52. Using site directed mutagenesis, each site was mutated to glutamine both individually ($CD24^{N36Q}$ and $CD24^{N52Q}$) and in combination ($CD24^{N[36,52]Q}$). The mutant clones were expressed ectopically in the CRC cell lines HCT116 and SW480 cells (CRC cell lines with low endogenous CD24 expression). The activity of the mutant CD24 was compared to known activities of wild-type CD24 ($CD24^{WT}$). The expression of $CD24^{N36Q}$ and $CD24^{N52Q}$ resulted in increased cell motility compared to empty vector control (EVC) but was significantly less than that induced by $CD24^{WT}$. However, the expression of $CD24^{N[36,52]Q}$ resulted in a near-complete loss of cell motility induction. Complementing this, analysis of downstream

targets and F-actin staining demonstrated reduced induction of known CD24 targets and reduced cadherin-switch by the mutant vectors.

(ii) CD24 is thought to act as a ligand for the endothelial molecule P-selectin to promote metastasis. To test the effect of the CD24 /P-selectin interaction on cell function, expression of CD24 was modulated by the CRC cell lines HCT116 and SW620 followed by either stimulation with recombinant P-selectin or co-culture with endothelial cells. Firstly, the interaction of P-selectin/CD24 was confirmed by co-immunoprecipitation. Adhesion assays showed that this interaction increased adhesion between epithelial and endothelial cells and that loss of either CD24 or P-selectin resulted in a reduction of adhesion. This interaction also promoted trans-endothelial migration by the epithelial cells. A positive feedback loop of P-selectin/CD24 interaction was observed, whereby P-selectin stimulation increased CD24 expression in CRCs. In addition, this interaction triggered known downstream signalling molecules associated with migration and invasion. Stimulation of the cells expressing $CD24^{N[36,52]Q}$ with P-selectin failed to induce cell motility and adhesion compared to $CD24^{WT}$.

(iii) Angiogenesis is an important part of establishing metastasis and, given CD24's putative role in tumour metastasis, we investigated the role of CD24 in promoting angiogenesis. In order to test this role, CD24 expression was modulated in CRC cell lines (ectopically expressed in the low-expressing HCT116/ SW480 and silenced in the high-expressing SW620) and the expression of vascular endothelial growth factor (VEGF)-A (a potent

angiogenesis inducer) and angiostatin (an inhibitor of angiogenesis) were assessed by Western blot and qPCR. CD24 was shown to be an inducer of VEGF-A expression and an inhibitor of angiostatin. Transfection of cells with $CD24^{N[36,52]Q}$ resulted in failure to induce VEGF-A or inhibit angiostatin. The conditioned medium was collected from the above-transfected cells to study the effect of CD24-induced secreted products on endothelial cells. The conditioned medium from CD24-expressing cells significantly induced the proliferation and migration, and tube formation of endothelial cells, whereas CD24 silencing had an opposite effect. Integrin-linked kinase (ILK) has been shown to be a target of CD24 and, in order to ascertain whether this may be a mediator of CD24 function, CD24 was forcibly expressed with a simultaneous ILK knockdown. The loss of ILK resulted in a failure of CD24 to induce VEGF-A expression.

In summary, this thesis demonstrated that each of the *N*-glycosylation sites contributes partially to the functional activities of CD24 and that these appear to be additive. Further studies are necessary to elucidate the exact mechanisms behind these activities. Moreover, CD24 may promote adhesion to the endothelium and stimulation of trans-endothelial migration through its interaction with P-selectin. Our data also indicated that CD24 up-regulates VEGF-A expression and promotes CRC angiogenesis via its downstream target, ILK. Collectively, this work has highlighted novel observations about the function of CD24 in several cellular processes in CRC *in vitro* and laid a foundation for research on the role of this gene in CRC metastasis.

Thesis-related publications and participated in conferences

Preprints

Hakami, Z., T. P. Raposo, A. Alsulaiman, W. Dalleywater, H. Otifi, C. Horobin, K. Garrie and M. Ilyas (2021). "N-glycosylation of CD24 mediates cell motility but inhibits cell proliferation in colorectal cancer." bioRxiv: 2021.2005.2002.442315.

In progress publications

Hakami Z, Raposo TP, Alsulaiman A, Dalleywater W, Otifi H, Horobin C, Garrie K, Ilyas M, *N*-glycosylation of CD24 mediates cell motility but inhibits cell proliferation in colorectal cancer (Manuscript submitted)

Alsulaiman A, **Hakami Z**, Ilyas M, CD24 up-regulate Notch1/Cten pathways-mediated cell motility in colorectal cancer (Manuscript in preparation).

Hakami Z, Ilyas M, CD24 mediates Colorectal cancer cells adhesion to endothelial cells and transendothelial migration via binding to P-selectin (Manuscript in preparation)

Presentations and conference communications

Hakami Z, Raposo TP, Ilyas M, P-selectin/CD24 interaction induced invasion, migration and activates CD24 downstream molecules in Colorectal

Cancer. The Nottingham Molecular Pathology Node (NMPN) Annual General Meeting, 12th October 2018/ Nottinghamshire County. (Poster)

Hakami Z, Ilyas M, The Role of CD24/P-selectin Complex in the Progression of Colorectal Cancer. 12th Joint Meeting of the British Division of the International Academy of Pathology and the Pathological Society of Great Britain & Ireland, 2-4 July 2019, Leeds, UK. (Poster)

Hakami Z, Ilyas M, CD24 Modulates Angiogenesis in Colorectal Cancer. 12th Joint Meeting of the British Division of the International Academy of Pathology and the Pathological Society of Great Britain & Ireland, 2-4 July 2019, Leeds, UK. (Poster)

Hakami Z, Ilyas M, CD24/P-Selectin Binding Mediates Colorectal Cancer Cell Invasion, Adhesion to the endothelium, and Trans-endothelial Migration. EACR-OECI Joint Virtual Conference on the Molecular Pathology Approach to Cancer, 23-24 March 2021. (Poster)

Table of Contents

Contents

Declaration ..... **i**
Acknowledgements ..... **ii**
Dedication ..... **iii**
List of Abbreviations ..... **iv**
Abstract ..... **viii**
Thesis-related publications and participated in conferences ..... **xi**
Preprints ..... **xi**
In progress publications ..... **xi**
Presentations and conference communications ..... **xi**
Table of Contents ..... **xiii**
List of Figures ..... **xix**
List of Tables ..... **xxii**
Chapter 1: General Introduction **1**
1.1 The Health Burden of Colorectal Cancer (CRC) **1**
1.2 Diagnostic tools and the staging of CRC **2**
1.3 Pathogenesis of CRC **5**
1.3.1 Chromosomal Instability (CIN) Pathway 7
1.3.2 Microsatellite Instability (MSI) Pathway 9
1.3.3 CpG Island Methylator Phenotype (CIMP) Pathway: 10
1.3.4 Other factors involved in CRC pathogenesis 12
1.4 Cancer Metastasis **13**
1.4.1 General Overview 13
1.4.2 Colorectal Cancer Metastasis 15
1.4.3 Sequential Steps of Metastasis 15
1.4.3.1 Cell Motility and Invasion 15
1.4.3.1.1 Epithelial-mesenchymal transition (EMT) 16
1.4.3.2 Intravasation and Survival in Circulation 18
1.4.3.3 Extravasation 19
1.4.3.4 Colonisation and Establishment of a Secondary Tumour 20
1.4.4 The Role of Cancer Stem Cells (CSCs) in colorectal cancer pathogenesis 21

1.4.4.1 Origin and characteristics of CSCs 21
1.4.4.2 Role of Colorectal CSCs in Metastasis 21
1.5 The CD24 gene 24
1.5.1 Genomic Structure 24
1.5.2 Proteomic Structure 25
1.5.3 CD24 Expression and Function 28
1.5.3.1 Expression in normal tissues 28
1.5.3.2 Expression in Cancer 29
1.5.4 CD24 Proposed Signalling Mechanism 30
1.5.5 CD24-Associated Signalling Molecules 32
1.5.5.1 Notch-1 33
1.5.5.2 Cten 34
1.5.5.3 FAK 36
1.5.5.4 ILK 37
1.5.6 CD24 Ligands 38
1.5.6.1 P-selectin 38
1.5.6.2 Other Ligands 40
1.5.7 Protein Glycosylation 41
1.5.7.1 Common Types of Protein Glycosylation 41
1.5.7.1.1 N-linked glycosylation 41
1.5.7.1.2 O-linked glycosylation 42
1.5.7.1.3 Glypiation 43
1.5.7.2 *N*-glycans Association with Cancers 43
1.5.7.3 CD24 Glycosylation 45
1.5.8 CD24 as a therapeutic target for cancer 46
1.6 Hypothesis and Aims 48
1.6.1 The role of *N*-glycosylation sites in CD24 in CRC progression 48
1.6.2 The Role of CD24/P-selectin in CRC metastasis 49
1.6.3 Investigation of the association of CD24 with CRC Angiogenesis 50
Chapter 2: Material and Methods 51
2.1 Cell culture 51
2.1.1 Cell lines 51
2.1.2 Cell maintenance 52
2.1.3 Freezing cells and Thawing 53
2.1.4 Cell counting 54
2.2 Cloning 54

2.2.1 Bacterial transformation 54
2.2.2 Plasmid purification 55
2.2.3 DNA quantification 56
2.3 Transient transfection 57
2.3.1 Gene overexpression 57
2.3.2 Gene knockdown 57
2.3.3 Co-transfection 58
2.4 P-selectin stimulation 59
2.5 Western blotting 60
2.5.1 Protein extraction 60
2.5.2 Protein quantification 60
2.5.3 SDS-polyacrylamide gel electrophoresis 61
2.5.4 Western blot re-probing 65
2.6 *N*-glycosylation digestion 65
2.7 Co-immunoprecipitation 66
2.8 Real-time quantitative PCR (qPCR) 67
2.8.1 Primers 67
2.8.2 RNA extraction 68
2.8.3 Complementary DNA (cDNA) synthesis 69
2.8.4 RT-qPCR reaction 70
2.9 Immunofluorescence 70
2.9.1 CD24 and PSGL-1 staining 70
2.9.2 F-actin staining 71
2.10 Site-directed mutagenesis (SDM) 72
2.10.1 Primer designing 72
2.10.2 Standard PCR 73
2.10.3 Agarose gel electrophoresis 74
2.10.4 DNA purification from the agarose gel slice 74
2.10.5 Ligation and Bacterial transformation 75
2.10.6 DNA purification (Miniprep) 76
2.10.7 Direct sequencing 77
2.11 In vitro functional studies 77
2.11.1 PrestoBlue cell viability assay 77
2.11.2 Transwell migration assay 78
2.11.3 Wound healing assay 79
2.11.4 Matrigel invasion assay 79

2.11.5 Adhesion assay 80
2.11.6 Trans-endothelial migration assay 81
2.12 Angiogenesis 82
2.12.1 Conditioned media preparation 82
2.12.2 Tube formation assay 82
2.12.3 Enzyme-linked immunosorbent assay (ELISA) 83
2.13 Flow cytometry 85
2.14 SWA11 antibody purification 86
2.15 Statistical analysis 87
Chapter 3: Investigation of the role of *N*-glycosylation sites on CD24 in CRC 88
3.1 Introduction 88
3.2 Results: 91
3.2.1 $CD24^{WT}$ has no role in cell proliferation in CRC cells but induces cell motility 91
3.2.2 Mutating of functional sites of CD24 involved in CRC progression 94
3.2.2.1 Construction $CD24^{N36Q}$ and $CD24^{N52Q}$ plasmids 94
3.2.2.2 Validation of $CD24^{N36Q}$ and $CD24^{N52Q}$ mutation by direct sequencing 96
3.2.2.3 Construction of $CD24^{N[36, 52]Q}$ plasmid 99
3.2.2.4 Validation of $CD24^{N[36,52]Q}$ mutation by direct sequencing 101
3.2.3 Mutant constructs show overexpression of CD24 103
3.2.4 Transfection efficiency of CD24 and CD24 mutant constructs in CRC cells 106
3.2.5 Loss of CD24 *N*-glycosylation sites results in increased cell proliferation 108
3.2.6 Loss of CD24 *N*-glycosylation sites results in loss of motility induction 111
3.2.7 Loss of CD24 *N*-glycosylation sites result in loss of activation of downstream targets and reduction in EMT 114
3.3 Discussion 120
3.4 Summary of findings 125
Chapter 4: Investigation of the role of CD24/P-selectin binding in CRC metastasis 126
4.1 Introduction 126
4.2 Results 129
4.2.1 Stimulation of CD24 positive cell line (SW620) with recombinant P-selectin 129

4.2.2 P-selectin activates CD24 and its downstream signalling molecules 132
4.2.3 CD24 binds to P-selectin 136
4.2.4 P-selectin stimulation does not alter CRC cell proliferation, but it induces cell motility 137
4.2.5 The CD24-P-selectin interaction regulates the adhesion of CRC cells to endothelial cells 140
4.2.6 CD24-P-selectin interaction mediates trans-endothelial migration .. 146
4.2.7 Loss of CD24 *N*-glycosylation disrupts CD24/P-selectin interaction and signalling pathway activation 149
4.2.8 Loss of *N*-glycosylation in CD24 inhibits P-selectin-mediated cell adhesion and transendothelial migration. 151
4.3 Discussion 154
4.4 Summary of findings 158
Chapter 5: Investigating the association between CD24 and angiogenesis 159
5.1 Introduction 159
5.2 Results 163
5.2.1 CD24 stimulates the expression of VEGF in CRC cells 163
5.2.2 CD24 enhances VEGF-A secretion to promote endothelial cell proliferation, migration, and vascular tube formation 166
5.2.3 CD24 promoted VEGFA expression depending on ILK 171
5.2.4 CD24 enhanced endothelial cells proliferation, migration and tube formation via ILK/VEGFA signalling axis 176
5.2.5 Loss of *N*-glycosylation of CD24 reduced the expression level of the ILK/VEGF signalling pathway 181
5.2.6 Loss of *N*-glycosylation inhibits CD24-mediated endothelial cell proliferation, migration, and tubes formation 183
5.3 Discussion 187
5.4 Summary of findings 192
Chapter 6: General Discussion 193
6.1 Introduction 193
6.2 Key findings 196
6.2.1 Mapping of the functional sites in CD24 that contribute to CRC progression 196
6.2.1.1 Validation of CD24 expression and its impact role on the cellular contexts involving proliferation, invasion, and migration in CRC 196
6.2.1.2 *N*-glycosylation sites appear to be important for CD24 to induce its activities 197
6.2.1.3 CD24 involvement in induction of the EMT 199

6.2.2 P-selectin activates CD24 in CRC 200
6.2.3 The potential role of CD24 in the initiation of CRC angiogenesis 204
6.3 Summary 207
6.4 Limitations 208
6.5 Future directions 209
References 213
Appendices I
Appendix I. Homo sapiens CD24 gene, Complete cDNA I
Appendix II. Cell lines authentication certificate II
Appendix III. SWA11 (CD24) antibody purification V
Appendix IV. Transwell assays data analysis VI
Appendix V. Stimulation of SW480-expressing CD24 with P-selectin VII
Appendix VI. Optimisation of CD24 and ILK siRNA VIII

List of Figures

Figure 1.1 Overview of TNM staging for colorectal adenocarcinoma. 4

Figure 1.2 CRC progression from adenoma to carcinoma. 6

Figure 1.3 CMS classification of CRC. 7

Figure 1.4 Simplified representation of the metastatic process. 14

Figure 1.5 Different methods of cell migration 16

Figure 1.6 The role of EMT in cancer metastasis 18

Figure 1.7 Clonal conversion of the crypt. 23

Figure 1.8 Primary amino acid sequences for mouse and human CD24 26

Figure 1.9 A simplified schema of the protein structure of CD24 27

Figure 1.10 Schematic showing the possible associations of CD24 with partner receptors and ligands 31

Figure 1.11 Network showing CD24 signalling pathways in CRC. 32

Figure 1.12 The interaction of P-selectin with its ligands on activated platelets and endothelium 39

Figure 2.1 Flow diagram showing the process of the experimental plan for site-directed mutagenesis (SDM). 72

Figure 2.2 Illustration demonstrates the experimental steps of adhesion assay 81

Figure 2.3 Representation of VEGF-A standard dilution ranging from 1000 to 15.6 pg/ml. 85

Figure 3.1 The sequence of CD24 glycosylation. 90

Figure 3.2 CD24 force expression and knockdown in CRC cells. 91

Figure 3.3 CD24 does not affect cell proliferation but induces migration and invasion in CRC cells. 93

Figure 3.4 Construction of CD24 single mutant plasmids 95

Figure 3.5 Gene sequencing analysis of $CD24^{WT}$ and $CD24^{N36Q}$ and $CD24^{N52Q}$ using Finch software. 97
Figure 3.6 Mutant constructs alignment using (BLAST2) tool..... 99
Figure 3.7 Construction of CD24 double mutant plasmids. 100
Figure 3.8 Gene sequencing analysis of $CD24^{N[36,52]Q}$ using Finch software and alignment tool (BLAST2). 102
Figure 3.9 The expression level of CD24 shows variable glycosylation in the mutant constructs. 105
Figure 3.10 Evaluation of transfection efficiency of $CD24^{WT}$ and CD24 mutant constructs by flow cytometry..... 108
Figure 3.11 Mutations in the *N*-glycosylation sites of CD24 influence cell proliferation. 110
Figure 3.12 *N*-glycosylation mutation causes inhibition in CD24-induced cell invasion and migration..... 114
Figure 3.13 CD24 *N*-glycosylation inhibit the EMT mechanism in CRC cells. ... 116
Figure 3.14 Loss of *N*-glycosylation inhibits CD24-mediated EMT phenotype alteration. 119
Figure 4.1 PSGL-1 does not express in CRC cells. 130
Figure 4.2 Stimulation of SW620 with P-selectin activates CD24 and its downstream target, Cten. 131
Figure 4.3 P-selectin/CD24 signalling pathways..... 135
Figure 4.4 Interaction of P-selectin with CD24 as determined by Co-IP..... 137
Figure 4.5 CD24/P-selectin binding did not alter cell proliferation, instead increasing cell motility. 139
Figure 4.6 CD24 regulates the adhesion of CRC cells to endothelial cells. 141
Figure 4.7 Western blot of CD24 in HCT116 and SW620, P-selectin in HUVEC. 143

Figure 4.8 interaction of CD24/P-selectin regulates the adhesion of CRC cells to endothelial cells.....145
Figure 4.9 CD24/P-selectin interaction regulates trans-endothelial migration. 148
Figure 4.10 *N*-glycosylation mutation impairs CD24/P-selectin signalling in CRC. 150
Figure 4.11 Western blot of $CD24^{N[36,52]Q}$ after stimulation with P-selectin and knockdown of P-selectin in HUVECs. 152
Figure 4.12 Loss of *N*-glycosylation in CD24 ($CD24^{N[36,52]Q}$) inhibits the HCT116 adhesion and transmigration through HUVEC cell monolayers. 153
Figure 5.1 CD24 regulates VEGF-A expression in CRC cells. 165
Figure 5.2 The effect of conditioned medium (CM) from CD24-expressing cells on HUVEC's cell proliferation and migration. 169
Figure 5.3 The effect of conditioned medium (CM) from CD24-expressing cells on angiogenesis. 171
Figure 5.4 CD24 mediates VEGF-A expression via ILK in CRC cell lines. 175
Figure 5.5 CD24 mediates angiogenesis via the VEGF-A/ILK signalling axis. ..180
Figure 5.6 Loss of N-glycosylation disrupts ILK/VEGF-A signalling axis 182
Figure 5.7 Loss of *N*-glycosylation in CD24 inhibits HUVEC cell proliferation and migration. 184
Figure 5.8 Loss of *N*-glycosylation in CD24 inhibits HUVEC tube formation.....186
Figure 6.1 Summary diagram for CD24 signalling pathways following P-selectin stimulation in CRC cells.....203

List of Tables

Table 2.1 The properties of the cell lines used for the study 51

Table 2.2 Mutation profiling for the significant oncogenes in the used cells 52

Table 2.3 siRNA sequences used in knockdown and co-transfection 59

Table 2.4 List of the antibodies used for Western blot 63

Table 2.5 Primers used for RT-qPCR 67

Table 2.6 Site-directed mutagenesis Primers 73

Table 2.7 The component and concentration of the ligation reaction 76

Chapter 1: General Introduction

1.1 The Health Burden of Colorectal Cancer (CRC)

CRC arises most typically in the epithelial lining of the large intestines in the form of adeno (or glandular) carcinoma. The process occurs when epithelial cells capture a range of either epigenetic changes or gene mutations that confer an advantage on them. Nearly all CRC originates from abnormal and uncontrolled growth of cells to form polyps. Such growths frequently acquire further mutations and become cancerous and then go on to spread into the lymph or blood vessels, allowing them to metastasise to lymph nodes and other sites in the body [1].

CRC is the third most common cancer globally, yet it has the second-highest cancer mortality rate [2]. About one million people each year are diagnosed with CRC worldwide, with a slightly higher prevalence in men than women [3]; 56% of CRC cases in the UK are seen in males, with 44% in females [4].

As with most cancers, CRC incidence increases significantly with age in most developed countries. In the UK, about three-quarters of all CRC cancers are confirmed in patients aged 60 and above [4], with the average age of diagnosis being approximately 70 [5].

Age-related increases in incidence rates may be attributed to the fact that cell DNA damage tends to accumulate over time as well as being linked to prior exposure to CRC risk factors and multiple biological processes.

Epidemiologists have also linked lifestyles in industrialised Western nations with increases in the prevalence of CRC. They believe that the observed increase in CRC cases is at least in part due to unhealthy diets that include excessive consumption of red meat and high-fat foods and a lack of food rich in fibres and vitamins. Other risk factors that have been associated with increased CRC incidence include alcohol consumption, reduced physical fitness, smoking, and obesity [6, 7].

Thus, despite the improved patient surveillance, better diagnosis, and advanced treatment seen in most affluent countries, an urgent need to understand the malignant transformation stages of CRC to help identify ways to reduce the high death rates associated with this cancer remains [8].

1.2 Diagnostic tools and the staging of CRC

A majority of CRC patients experience obvious initial symptoms such as abdominal discomfort and pain, haematochezia (blood in the stool), or persistent changes in bowel habits [9]. Several diagnostic tools can be used to determine the occurrence of CRC. These include non-invasive diagnostic examinations, such as the faecal immunohistochemical test (FIT), which is a sensitive indicator of bleeding in the large intestine or rectum. Other tests also include blood levels of non-enzymatic tumour markers such as carcinoembryonic antigen (CEA) and cancer antigen (CA) 19-9 [10]. However, such examinations are insufficient by themselves to diagnose

CRC; further confirmation based on more invasive screening tests is required, and this generally involves either colonoscopy or sigmoidoscopy. These are both effective tools for determining tumour location as well as facilitating tissue biopsy for histopathological examination [10, 11]. Computed tomography (CT) scans, or positron emission tomography (PET) scans, are also used for cancer staging, i.e. to determine how the cancer is metastasising to nearby tissues such as lung, liver, or other major organs, allowing a clearer picture of cancer staging [12].

Tumour Node Metastasis (TNM) system is the most common pathological classification tool used to determine prognostic outcomes in CRC. TNM staging is based on multiple criteria, including the extent of bowel wall invasion, lymph node involvement, and distant tissue metastasis (Figure 1.1).

Tumour cell wall extension and invasion (T) is graded from T1 to T4.

T1: the tumour invades the submucosa.

T2: the tumour penetrates the muscularis propria.

T3: the tumour invades the subserosa or pericolic/perirectal tissue.

T4: the tumour invades the neighbouring organs and perforates the visceral peritoneum.

There are also three categories of lymph node involvement.

N0: no lymph node metastasis.

N1: involvement of 1 to 3 lymph nodes.

N2: tumour metastasis in 4 or more lymph nodes.

Finally, an M1 rating indicates tumour metastasis to distant tissues, while M0 means no distant metastasis has been detected.

Histopathological examination and TNM staging are thus both crucial factors in determining prognosis and treatment strategies for CRC [11, 13].

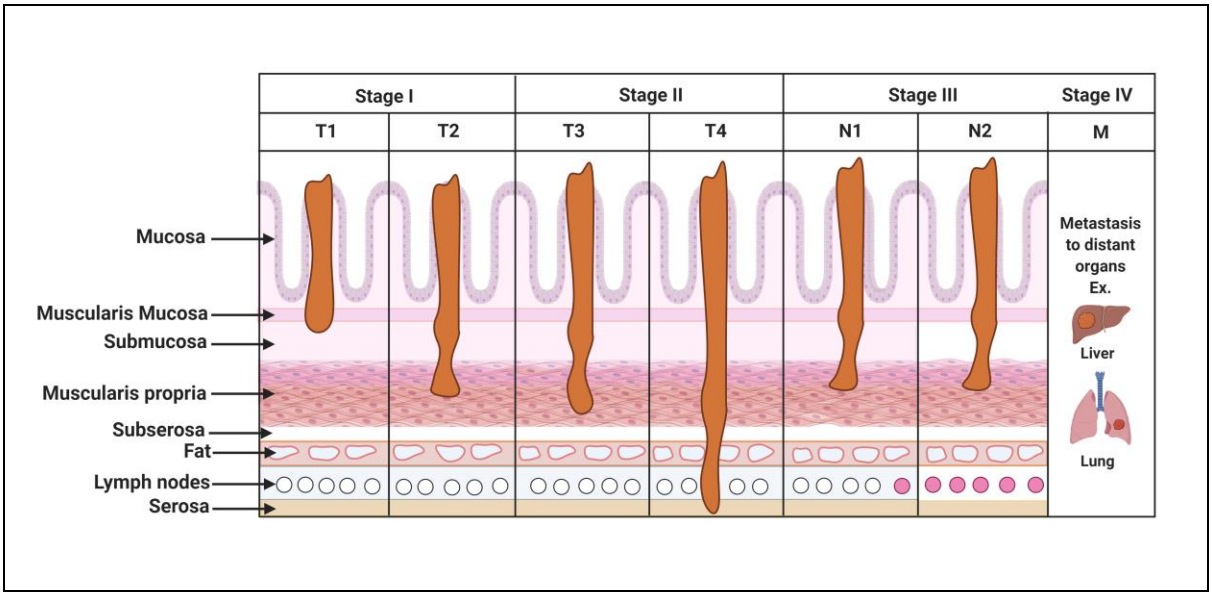


Figure 1.1 Overview of TNM staging for colorectal adenocarcinoma.

TNM staging in colorectal adenocarcinoma. (T) Tumour invasion, categorised from T1 to T4; (N) Regional lymph node involvement, assessed as N0 to N2; and (M) Metastasis to distant organs, given as either M0, no metastasis detected or M1, presence of metastasis. Adopted from *Harrison's*, 19th Ed.

1.3 Pathogenesis of CRC

CRC is generally sporadic, developing from normal colonic epithelium to form benign precursor lesions known as adenomas which then evolve into carcinomas. This is known as the "adenoma-carcinoma sequence" and is driven by the accumulation of mutations or genetic alterations that correspond to histologic changes [14]. The most commonly mutated genes found in CRC include adenomatous polyposis coli (*APC*), tumour protein 53 (*TP53*), and Kirsten rat sarcoma (*KRAS*).

The steps involved in the process by which normal epithelium transforms into carcinoma in CRC; these were first identified by Fearon and Vogelstein [15]. They noted that early adenoma and dysplastic crypt foci are formed in a process associated with mutations in the *APC* gene. After this, an intermediate adenoma is formed, driven by a mutation in *KRAS*, which is followed by late adenoma development as a consequence of the loss of chromosome *18q* and *Smad 4* mutation (Figure 1.2). Throughout this progression from colorectal adenoma to adenocarcinoma, microsatellite instability and chromosomal instability tend to increase, particularly as malignant transformation occurs [16, 17].

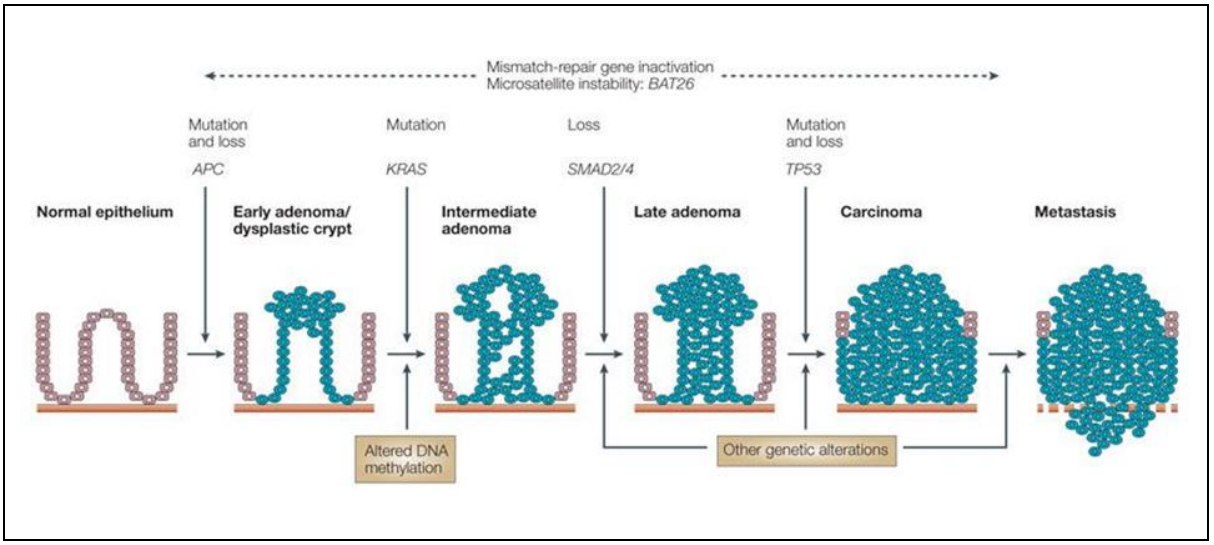


Figure 1.2 CRC progression from adenoma to carcinoma.

A multi-step model of CRC tumorigenesis from normal epithelium through adenoma to carcinoma as a consequence of chromosomal abnormalities and mutations [16].

CRCs are heterogeneous tumours in their specific genetic and molecular configuration [18]. There are several classifications of CRC that depend on both the genetic and molecular basis; the most recently described is the consensus molecular subtype (CMS) classification, which is a new classification framework based on the use of pooled gene expression data from all cohorts [19], (Figure 1.3). An alternative classification involves dividing CRCs into three major pathways: chromosomal instability (CIN), microsatellite instability (MSI), and the CpG island methylator phenotype (CIMP) [20].

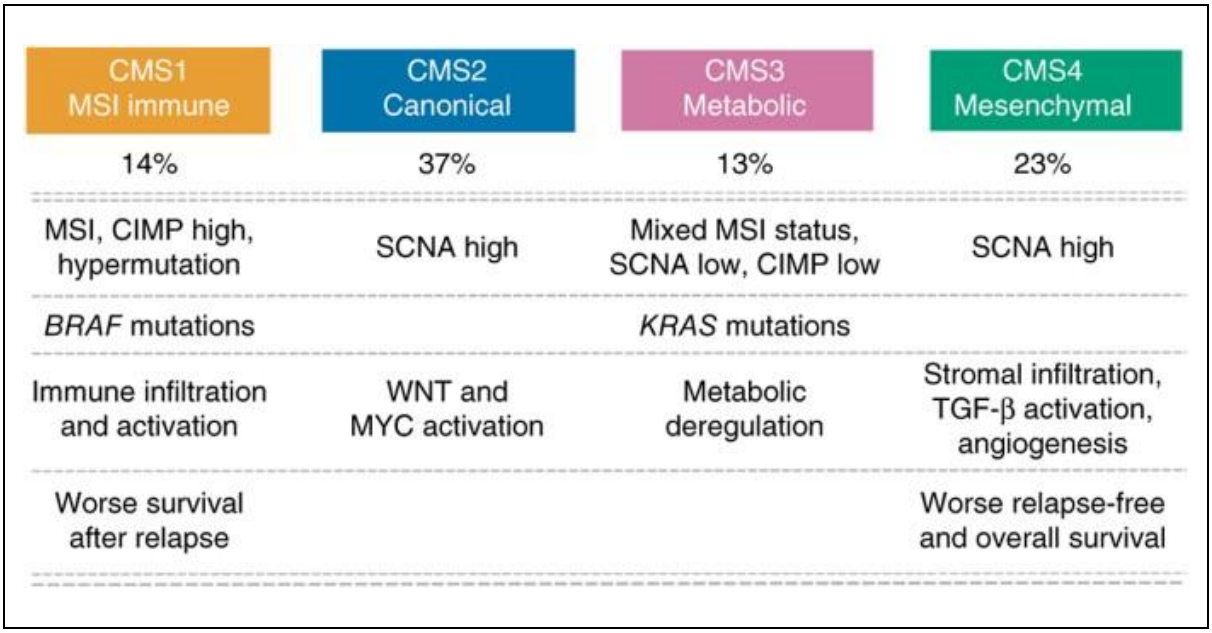


Figure 1.3 CMS classification of CRC.

The biological and clinical features of each CMS subtype. CMS1 (microsatellite instability immune) is hypermutated with MSI, immunity upgraded and rich in CIMP and *BRAF* mutations, and contributes up to 14% of all cases. CMS2 (canonical) constitutes 37% of all cases; they show profound WNT and MYC signalling activation. CMS3 contributes to 13% of cases with metabolic dysregulation with *KRAS*, low somatic copy number alteration (SCNA) level, and low CIMP. Finally, CMS4 has named the mesenchymal subtype with a 23% share of all cases; they have activation of transforming growth factor–β (TGF-β) and tend to be invasive and angiogenetic [21, 22].

1.3.1 Chromosomal Instability (CIN) Pathway

CIN is present in between 70 to 85% of CRC cases [23]. The two crucial components of this pathway are loss of heterozygosity -when one allele is lost-, and a simultaneous imbalance in the number of chromosomes (aneuploidy). CIN creates conditions that are favourable to increases in mutational burden, beginning with *APC* mutation and potentially followed

by mutational inactivation of the tumour suppressor gene, *TP53*, and/or mutational activation of a key oncogene, *KRAS*.

APC mutation is found in between 34 to 70 % of sporadic adenomas and sporadic CRC, and the majority of these *APC* mutations are frameshift or nonsense mutations, leading to a production of truncated proteins with functional abnormalities [24]. Normally, the overexpression of *APC* inhibits cell cycle transition from the G1 phase to the S phase and play a role in regulating the degradation of β-catenin [14]. Mutation in the *APC* gene, therefore, results in Wnt signalling activation due to a failure in the degradation of β-catenin, leading to stabilising β-catenin in the cytoplasm and translocating it to the nucleus where it can bind to transcription factors such as T cell factor/lymphoid enhancer-binding factor (TCF/LEF) and may lead to enhanced transcription of many target genes [25]. This may result in the induction of cancer cell proliferation, migration and epithelial-mesenchymal transition [26].

TP53 is frequently seen to be mutated in CRC; normally, it enhances cell cycle arrest in G1 and promotes DNA repair before cells engage in the DNA replication process. The mutation of *TP53* occurs in the later stages of tumorigenesis, playing a vital role in apoptosis and tumour evasion of cell cycle arrest [14, 27]. The occurrence of a molecular alteration in the *18q* chromosome is often associated with a loss of *TP53* [28], and the *18q* chromosome allelic loss has thus been connected with distant metastasis and reduced overall survival in CRC patients [29, 30].

KRAS mutations are found in 30 to 60% of CRC cases during their transition from adenoma to carcinoma [31]. Activation of *KRAS* results in the induction of several cellular pathways, including cell proliferation, cell motility, apoptosis, survival, cytoskeleton organisation, and inflammatory response [32]. Specific to CIN, subsequent mutations in other genes such as phosphatidylinositol-4,5-bisphosphate 3-kinase catalytic subunit alpha (PIK3CA), and the *SMAD 4* and *SMAD 2* of transforming growth factor pathway have also been observed [15, 32, 33].

1.3.2 Microsatellite Instability (MSI) Pathway

The MSI pathway is an outcome of the mutation or inactivation of the DNA mismatch repair (MMR) system, which has the function during DNA replication of correcting mismatched nucleotides. This pathway is seen in around 15% of sporadic CRC cases, and it appears in more than 94% of tumour in patients with Lynch syndrome (also known as hereditary non-polyposis colorectal cancer (HNPCC) syndrome). This is an autosomal dominant genetic disorder due to a germline mutation of the MMR gene which causes colorectal and other cancers [30].

Microsatellites are simple repetitive DNA sequences which are particularly prone to mismatched base pairs and insertion/deletion loops. They occur in both the coding and non-coding regions of the DNA, and they can result in the production of truncated proteins by means of frameshift mutations in the coding regions or multiple alleles of different sizes in the non-coding region [34, 35].

The family members of DNA-MMR system include MutL homolog 1 (*MLH1*), located on chromosome 3p21; MutS homolog 2 (*MSH2*), located on chromosome 2p16; MutS homolog 6 *(MSH6)*, located on chromosome 2p16; and postmeiotic segregation increased 2 *(PMS2)*, located on chromosome 7p22 [36].

Inactivation of these genes generally results in defective repairs of any inserted or deleted mutations occurring in microsatellite sequences, which consequently leads to the ongoing accumulation of mutations within these regions [37]. In most sporadic CRC (between 83 and 100%), MSI is caused by silencing of *MLH1* by hypermethylation of the promoter; however, Lynch Syndrome (HNPCC) accounts for up to 4% of all CRC cases, being caused by a germline loss-of-function mutation of members of the MMR system[38]. MSI-CRC shows different patterns of high-frequency mutation rates to CIN pathways in *BRAF* V600E, *BAX,* and transforming growth factor-beta receptor II (TGFβR2), and a lower frequency of mutation in *Kras* and the *P53* gene [30, 31].

1.3.3 CpG Island Methylator Phenotype (CIMP) Pathway:

The CIMP pathway occurs due to alterations in DNA methylation patterns that usually occur in CpG dinucleotide sequences (CpG islands) within promotor regions in genes [39]. This pathway accounts for up to 20% of all CRC cases.

The CpG islands are located within gene-promoter regions with extensive runs of CpG dinucleotides, which regulate more than 50% of the human

genome. In normal cells, two epigenetic modification processes occur, DNA methylation and DNA demethylation, and these are maintained in a precise balance. However, this balance may be altered or disrupted in cancer cells, changing the DNA methylation pattern so that the gene promoter regions (CpG sites) that are typically unmethylated in healthy cells commonly become hypermethylated in cancerous cells. Unlike the focal regions of hypermethylation, cancer DNA is thus also subject to diffuse genomic hypomethylation [40, 41]. The process of DNA methylation is catalysed by DNA methyltransferases (DNMT) enzyme by adding a methyl group to the fifth position of the cytosine residues, resulting in a production of 5-methylcytosine.

The hypermethylation of these promoter regions results in transcriptional inactivation of tumour suppressor genes that are important in cell cycle regulation, tumour suppression, DNA repair, angiogenesis, and invasion.

Shen *et al*. identified three distinct groups of CIMP pathways in CRC. These groups include CIMP1 tumours, which are characterised by MSI-H and *BRAF* mutations (80% and 53%, respectively); CIMP2 tumours, which are associated with 92% of *KRAS* mutations and lower frequency of MSI, *BRAF* mutations. The last group is CIMP-negative tumours, which are associated with higher rates of *P53* mutations and lower rates of MSI, *BRAF*, and *KRAS* mutations [42].

Although the mechanisms leading to CIMP have not yet been fully elucidated, initial studies have indicated that *BRAF* mutation is an early

event in the CIMP pathway, highlighting a possible association between CIMP and MSI-H in sporadic CRC. These studies also argue that not only is the *BRAF* oncogene mutation commonly seen in CIMP-H CRC, but it is also related to accelerated cell growth and the progression of carcinogenesis, and thus to increased mortality rates in colon cancer cases [30, 43].

1.3.4 Other factors involved in CRC pathogenesis

In addition to the pathways specifically noted, other factors may contribute to CRC development, including microRNAs (miRNAs) and other genes that may be upregulated but not necessarily mutated. MiRNAs are a class of short non-coding RNA nucleotides (20 to 22 nucleotides) that regulate protein expression by inhibiting the translation of messenger RNA (mRNA) in genes with functions such as cell development, differentiation, proliferation, and apoptosis. In CRC, a huge number of miRNAs play a role in pathogenesis, and such miRNAs may be downregulated or upregulated in CRC cases, thus working either as tumour suppressor genes or oncogenes [30].

Many inflammatory markers are also associated with CRC progression through stimulation of cell proliferation, invasion, apoptosis, and metastasis. These markers include tumour necrosis factor-alpha (TNF-α), interleukin-6, C-reactive protein and signal transducer and activator of transcription 3 (STAT3) [30, 44].

Multiple genes are upregulated or downregulated in CRC, and some of these genes may show altered regulation without having any obvious biological

relevance to CRC. An example of such a gene is *CD24*, which has, however, been shown to affect tumour biology [30] and may, therefore, be of significance to CRC progression.

1.4 Cancer Metastasis

1.4.1 General Overview

Cancer metastasis is the spread of cancer cells from a primary lesion to distal organs, which is ultimately responsible for most cancer fatality [45]. It is vital to note that such dissemination entails a plethora of cellular mechanisms being adopted by the cancerous cells, including migration, evading immune scrutiny by hindering anti-tumorigenic activities, escaping, and having significant control of tissue micro-environments.

Metastasis is a sophisticated process that entails cancer cells breaking away from the primary tumour, thus undertaking migration, followed by the invasion of both lymphatic and blood vessels. To metastasise, such cells must detach from their primary sites, endure the pressures within the blood vessels, circulate in the bloodstream, and colonise new cellular surroundings in a secondary site (Figure 1.4). Once cancer cells spread past their original primary sites in this way, however, they increase the risk of death. As a result, metastasis and activating invasion have become the hallmarks of cancer, based on their contribution to the ever-increasing number of cancer-related fatalities worldwide. Spread to nearby organs and tissues and seeding at distant sites, forming metastases are the

characteristics of cancer malignancy, and some researches have reported that almost 90% of the cancer deaths are attributed to metastases [46, 47]. Generally, therefore, cancer deaths are not connected to the primary lesion but are instead the result of cancer metastasis.

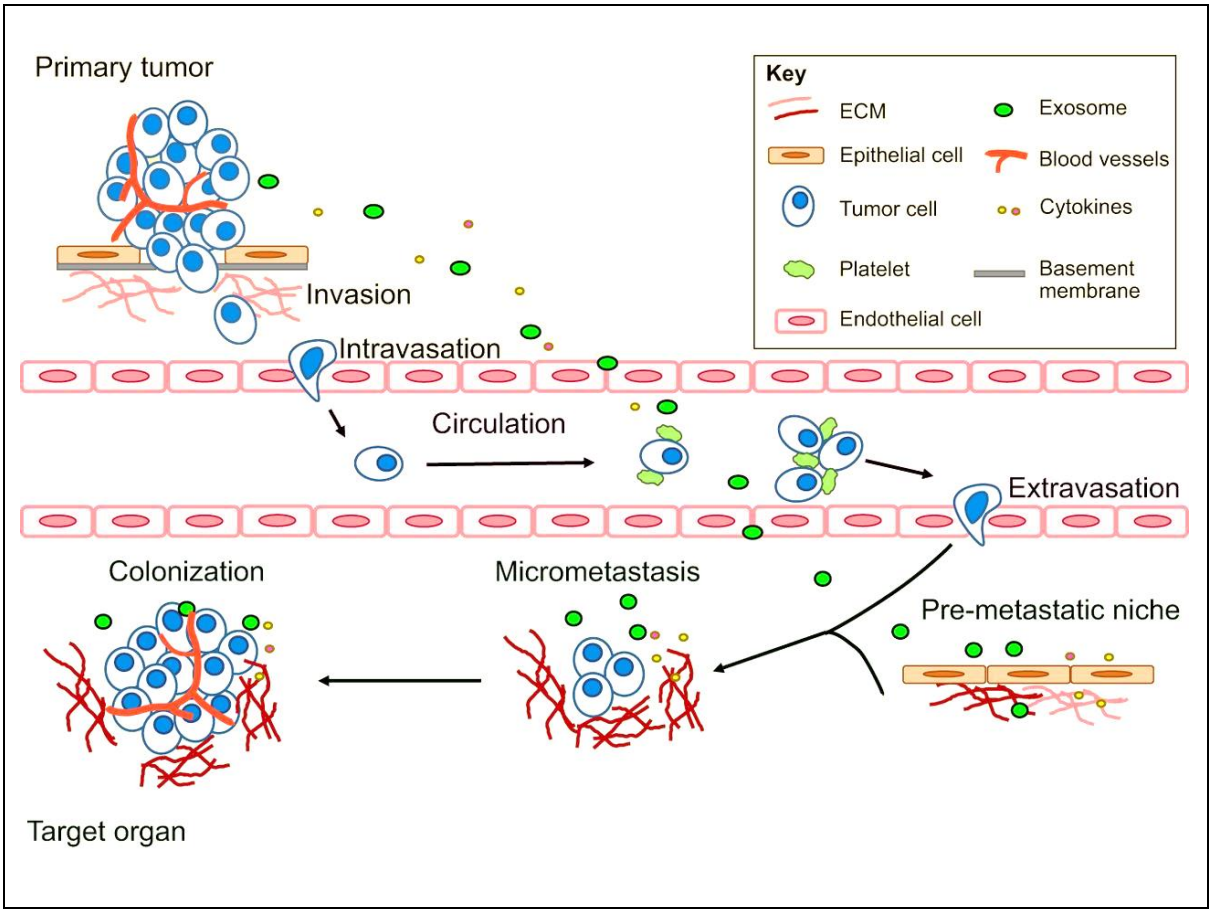


Figure 1.4 Simplified representation of the metastatic process.

The cancer cells break away from the primary tumour to conduct migration and invasion of the extracellular matrix (ECM). Various factors, such as exosomes and cytokines, are secreted from the primary site to facilitate tumour cell motility into the blood vessels. The cells thus intravasate and enter the circulation. The circulating tumour cells are coated with platelets and bind to the endothelium. After this, the tumour cells exit the vasculature in a process known as extravasation. The final step of metastasis is colonisation, which begins with the establishment of one or more secondary tumours. Following the spread of

micrometastases to distant organs, they may become dormant for years before eventually multiplying and becoming macrometastases to complete such colonisation [48].

1.4.2 Colorectal Cancer Metastasis

Approximately 20% of CRC cases present with metastasis and a further 35 to 45% develop metastatic recurrence [49], leading to a 5-year OS of <10% [50].

Recent developments in metastasis research have contributed to an expanded comprehension of CRC at both the molecular and cellular levels and identify stem cell-associated biomarkers such as CD24 [51]. Metastasis, as noted, requires several processes involving the activation of various biomarkers produced by cancer cells or adjacent cells. This thesis thus aims to examine the effect and contribution of the *CD24* gene to various steps leading to metastasis more closely.

1.4.3 Sequential Steps of Metastasis

1.4.3.1 Cell Motility and Invasion

Cell motility in tumour cells can lead to tumour metastasis. The motility of tumour cells into the tissues contiguous to the principal tumour is generally the first step of such spread.

Cancer cells thus use various mechanisms to invade tissues. They may move as single cells, epithelial sheets, or detached clusters via either amoeboid or mesenchymal cell types of motility [52]. There is plasticity in

the methods of cell migration and cancer cells may go through morphological or phenotypical conversions, as joint amoeboid, mesenchymal to amoeboid, and epithelial-mesenchymal transitions (EMT) (Figure 1.5).

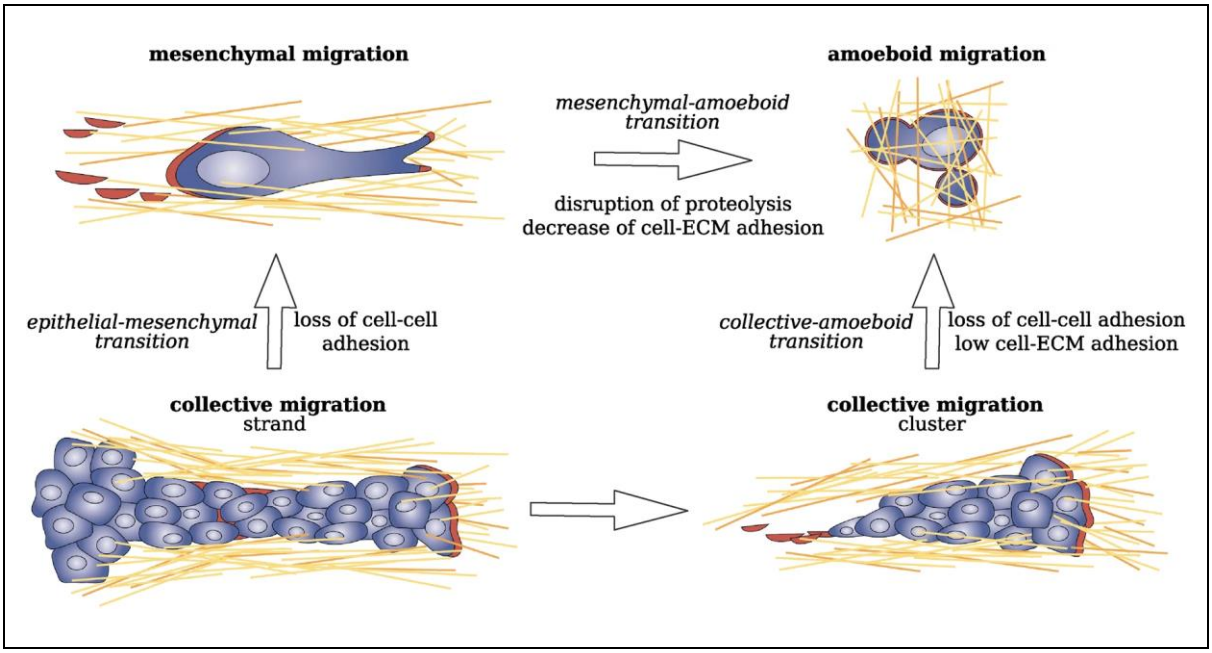


Figure 1.5 Different methods of cell migration.

During migration, cancer cells undergo a variety of morphological and phenotypic transitions, such as epithelial-mesenchymal transition and mesenchymal–amoeboid transition [53, 54].

1.4.3.1.1 *Epithelial-mesenchymal transition (EMT)*

Over the past decade, EMT has been confirmed as an essential process in cancer and metastasis development. EMT leads to a change in the phenotype of the epithelial cells and also is seen in processes such as wound healing and embryogenesis. EMT is molecularly characterised by the cell losing its epithelial characteristics [52]. Epithelial cells are normally defined as stationary, polarised cells that are interconnected by adherens,

tight or gap junctions, desmosomes and integrins. Apical-basal polarity may be derived from interactions with the basement membrane [55].

The loss of epithelial cadherin (E-cadherin) disrupts the cell-cell interactions and apical-basal polarity as E-cadherin uses extracellular domains to bind with E-cadherin of the neighbouring cells. To connect adherens junctions with the actin cytoskeleton and facilitate intracellular signalling, β- catenin, α- catenin, and p120-catenin bind with the E-cadherin in the intracellular region [56]. The transcriptional repressors ZEB2, SNAI1, SNAI2 and Twist down-regulate E-cadherin in a process that subsequently strips adherens junctions and translocates β-catenin to the centre of the cell, leading to a change of expression in cadherin from the E- to N-Cadherin. This change, known as the cadherin-switch, enhances cell motility after EMT transformation. Thus, EMT-transformed cells release themselves from their epithelial cells clusters and can move as single cells [56] (Figure 1.6). Multiple factors have been highlighted as having a biological role in the induction of EMT, but the most dominant factor is TGF-β, which activates Smad and leads to transcriptional repression of E-cadherin [57].

Examining EMT in CRC shows evidence of up-regulation and down-regulation of several EMT biomarkers associated with CRC progression such as E- and N-cadherins, Vimentin, and snail. The overexpression of N-cadherin, Vimentin, and the snail transcription factor all allow for cancer progression, reducing survival times and facilitating lymph node metastasis

[58-60]. Similarly, loss or down-regulation of E-cadherin in CRC tissue has been correlated with poor prognosis and distant metastasis [61].

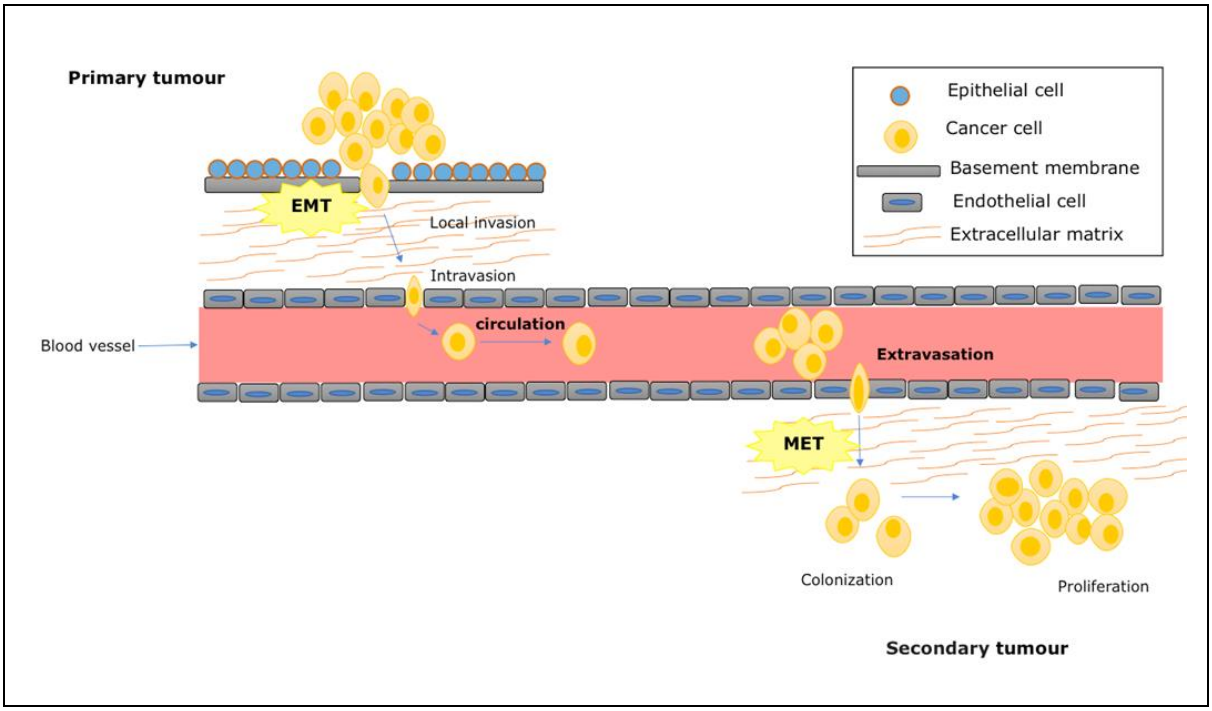


Figure 1.6 The role of EMT in cancer metastasis

To metastasise, tumour cells must detach from the primary site, undergo EMT, invade the extracellular matrix, migrate through blood circulation and finally colonise at a secondary site.

1.4.3.2 Intravasation and Survival in Circulation

After tumour cells undergo changes to their epithelial properties to become mesenchymal, they are able to enter the blood and lymphatic vessels. Various proteases are secreted to facilitate tumour cell invasion into the blood vessels, and these are the same ones used in the invasion process, which are the metalloproteinase (MMP)-1, -2, and -9 matrices. The urokinase-type plasminogen activator (uPA/uPAR) system is also activated

during this process [62]. These proteases breakdown the extracellular matrix (ECM), paving the way for the exodus of tumour cells into the blood and lymph vessels.

Blood is not, however, a conducive milieu for circulating tumour cells (CTC), and thus very few CTCs survive to trigger distant metastasis. The inevitable presence of immune cells and other killer factors leads to the death of over 99% of CTCs in the bloodstream [62], despite tumour cells secreting MMP-2/ -14, cathepsin B, cancer procoagulant, and thrombin to protect themselves from surveillant immunity cells. Tumour cell-induced platelet aggregation, in which platelets gather around the tumour cells, eventually forms a coat that helps cancer cells survive in the hostile environment of the bloodstream and facilitates extravasation. In CRC, these processes are further mediated by molecules expressed on the cancer cell surface, such as CD24, which can bind to the adhesion molecules and growth factors expressed on platelets and endothelial cells such as selectins and VEGF [63].

1.4.3.3 Extravasation

Extravasation is the process whereby CTCs leave the circulatory system. To achieve this, the CTCs secrete factors such as MMP-1/-2 and angiopoietin-like-4 (Angptl4) that are responsible for inducing vascular hyper-permeability. Extravasation is thus a dynamic process mediated by the expression of pro-metastatic genes such as integrin-beta 1 (*ITGB1*), *VEGF-A*, and Twist. These cause the vasculature of various organs to become

primed with molecules and receptors such as selectins or even to release chemokines or exosomes, which induce specific tumour cells to favour certain tissue environments [64, 65].

1.4.3.4 Colonisation and Establishment of a Secondary Tumour

The final step of metastasis is colonisation, marked by the establishment of a secondary tumour in one or more secondary organ sites. In such cases, the primary neoplasm sheds cancer cells that commence an enzymatic invasion of the target host's extracellular matrices. While during this invasion process, multiple cancer cells undergo apoptosis, which can be attributed to the physical forces applied to them as they pass through the host defence mechanisms and microvasculature of the secondary organs; the few that survive are sufficient in many cases to colonise selective organs [66]. These sites are recognised by organ-specific adhesion molecules found on the surface of the microvascular endothelial cells, such as selectins, while the attachment of the tumour cells to these microvascular endothelial cells facilitates the establishment of secondary tumour colonies. In technical terms, the tumour cells have specific receptors that bind to ligands present on endothelial cells, such as selectins. This binding may recognise components of the vascular basement membrane, which further trigger extravasation and the establishment of secondary tumours [65].

1.4.4 The Role of Cancer Stem Cells (CSCs) in colorectal cancer pathogenesis

1.4.4.1 Origin and characteristics of CSCs

CSCs are clusters of self-replicating cancer cells capable of self-renewal based on their multipotent characteristics [67]. These cells may be the basis of metastasis due to their ability to adapt to tumour microenvironments. CSCs are however also characterised by their inability to survive in the absence of a specific set of environmental requirements, which includes cytokines.

CSCs originate from tissue-specific stem cells [68]. They are imbued with the capacity to regenerate and differentiate, thus supporting the progression of cancer via cloning, self-regeneration, growth, homing, and proliferation, being capable of replicating in both homeostatic and abnormal conditions. In addition, CSCs can morph into differentiated cells as required [68]. CSC functions include maintaining specialised microenvironments in the cells that promote cancer progression.

1.4.4.2 Role of Colorectal CSCs in Metastasis

Ongoing research into metastasised cancer occurrence has suggested a relationship between cancer stem cells and metastasised cancer growth [69].

CSCs, require specific microenvironment conditions to survive [70], though these environments also then provide appropriate conditions in which

cancerous cells can spread and metastasise into tissues. CSCs can also encode instructions to unaffected cells, altering several transmitters usually found in healthy stem cells to morph these into cancer inducing transmitters such as Smad, APK/ERK, JAK/STAT, PTEN, Pi3K/AKT, Notch, and Hedgehog [69].

Steinbichler *et al*. found that CSCs possess a self-generating nature due to the presence of characteristics including tumour cell plasticity, differentiation, and dormancy, capabilities that increase the cells adaptability and allow them to form metastasised tissues [69]. The recurrence of metastasised tissues thus almost entirely relies on the functionality of CSCs.

Intestinal crypts are the main storage facility for stem cells; mutated cancer cells thus generally originate in these crypts, then spread to the epithelial lining and replace normal crypts [71] and CD24 is found among several genes that are highly expressed in these stem cell sites [72]. Technically, the mutated stem cells within the colonic crypt and epithelium can expand within niche via a process known as niche succession; then, all the progeny of stem cell lineage occupy the whole crypt and this process is known as a clonal expansion [71] (Figure 1.7). In CRC, CSCs also play a vital role in metastasis and recurrence [73]. Colorectal CSCs share several biological features with stem cells, such as activation of various signalling pathways, such as Wnt/β-catenin, Notch, TGF-β and Hedgehog [74]. CSCs can be identified by the expression of several cell surface markers, including CD24,

CD44, CD133, Lgr-5, EpCAM and ALDH. CD24 is thus considered an auxiliary stem cell marker and, as such, plays a crucial role in the observation of CRC development and differentiation.

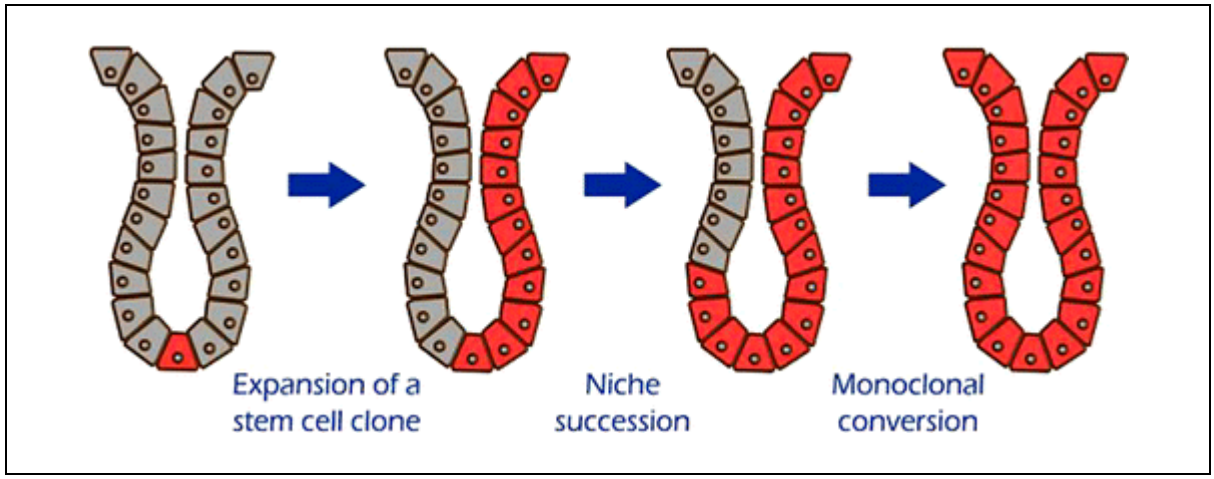


Figure 1.7 Clonal conversion of the crypt.

As mutation occurs, the stem cells located at the base of the crypt are transformed; then, the transformed cells proliferate and spread to the transit-amplifying population. Eventually, these cells occupy the normal crypt [71].

1.5 The CD24 gene

1.5.1 Genomic Structure

The cluster of differentiation 24 (*CD24*), also known as signal transducer *CD24*, has been of significant interest to investigators in cancer studies since 1987 when Springer *et al*. were the first to report the discovery of *CD24* in mice. In their study, *CD24* was labelled as a heat-stable antigen (HSA) due to its resistance to intense heat [75]. The murine *CD24* gene was initially cloned in 1990, at which point it was found to encode a small protein that, in its mature form, was composed of 30 amino acids [76]. Three mouse *CD24* genes were identified: one located on chromosome 10 was termed *CD24a* to distinguish it from the other two, which were found to be intronless and non-expressed genes located on chromosome 8 and chromosome 14 [77]. The human *CD24* gene was discovered in 1991 [78], being found, based on in situ hybridisation analysis, on chromosome 6q21. Identical but non-functional sequences of the human *CD24* gene were also identified on chromosomes 1p, 15q21-q22, 20q11.21, and Yq11, though these otherwise identical *CD24* genes lack expression and are thus known as pseudogenes [79, 80].

The messenger RNA (mRNA) for CD24 contains 2,179 base pairs, while the open reading frame (ORF) consists of only 243 base pairs, where the initiation point begins at 368 and terminates at 610 (see Appendix I). CD24 mRNA is characterized by the presence of two regulatory regions within the CD24 1.2 kb promoter at sites -446 and -840, relative to the initiation

codon ATG, which were identified as putative binding sites for TCF / LEF transcription factors. The deletion of these sites, particularly -446, was found to increase CD24 transcription as the binding of TCF-4 to these sites has a main role in suppressing CD24 transcription; thus, it was suggested that CD24 is a true target for the Wnt signalling pathway [81].

1.5.2 Proteomic Structure

In terms of protein structure, the complementary DNA (cDNA) of CD24 can be translated into 80 amino acids in humans and 78 amino acids in mice. Both human and mouse CD24 protein structures share similarities, particularly in terms of their extensive *N*- and *O*-glycosylation forms. However, two extra amino acids (serine and threonine) are present in the mature form of the human protein that differentiates it from the mouse protein (Figure 1.8).

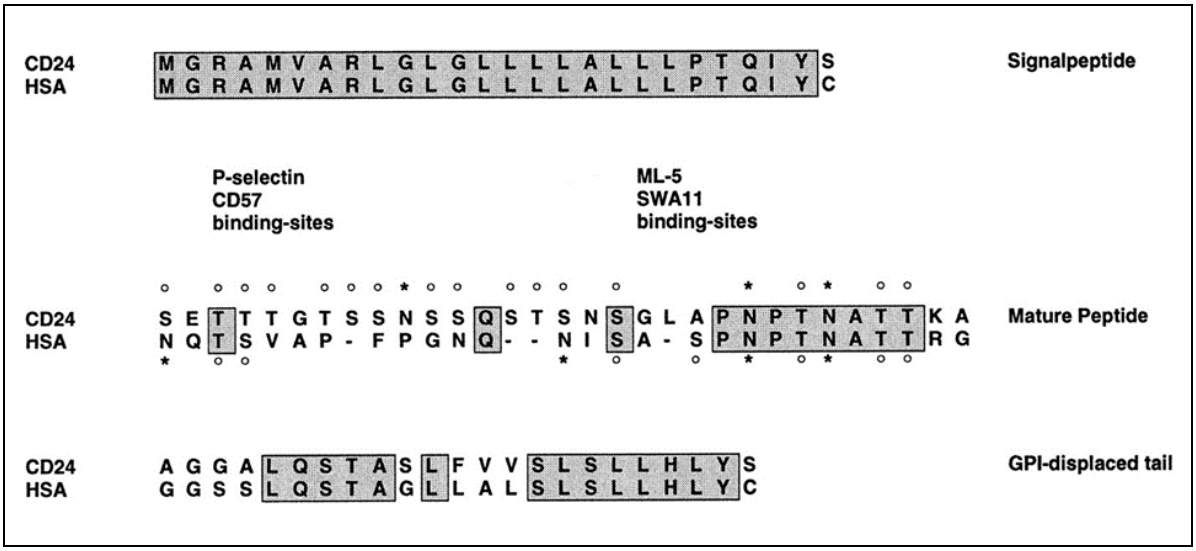


Figure 1.8 Primary amino acid sequences for mouse and human CD24.

Potential *N*-glycosylation sites are indicated with asterisk marks, while *O*-glycosylation sites are indicated with a ring on each amino acid. P-selectin and CD57 antibody binding sites and the specific monoclonal antibodies for CD24 (SWA11 and ML-5) are also indicated [82]. Abbreviations: HAS, heat-stable antigen; GPI, glycosylphosphatidylinositol.

The human CD24 whole protein with its 80 amino acids has an *N*-terminal signal peptide (26 amino acids) and a C-terminal region with a GPI-displaced tail consisting of 27 to 29 amino acids. The role of the *N*-terminal signalling peptide is to localise CD24 on the cell surface, and the C-terminal region, also known as a GPI-displaced tail, is thought to be a pro-peptide, with the GPI anchor connecting to the C-terminal region of mature CD24. Both regions are cleaved after this as a result of the posttranslational modification process in the endoplasmic reticulum, at which point the *N*-terminal signalling peptide is removed, and the C-terminal (GPI attachment signal peptide) is also cleaved at the ω site, which is carried out by GPI

transamidase. Removal of both regions leaves the mature form attached to the surface membrane by means of a GPI anchor [78, 83, 84] (Figure 1.9).

The mature form of CD24 has two potential *N*- and 16 potential *O*-glycosylation sites, which render it a mucin-like protein. This massive glycosylation causes its molecular weight to range from 30 kDa to 70 kDa, and it has been suggested that the biological activity of CD24 depends on these glycosylation patterns.

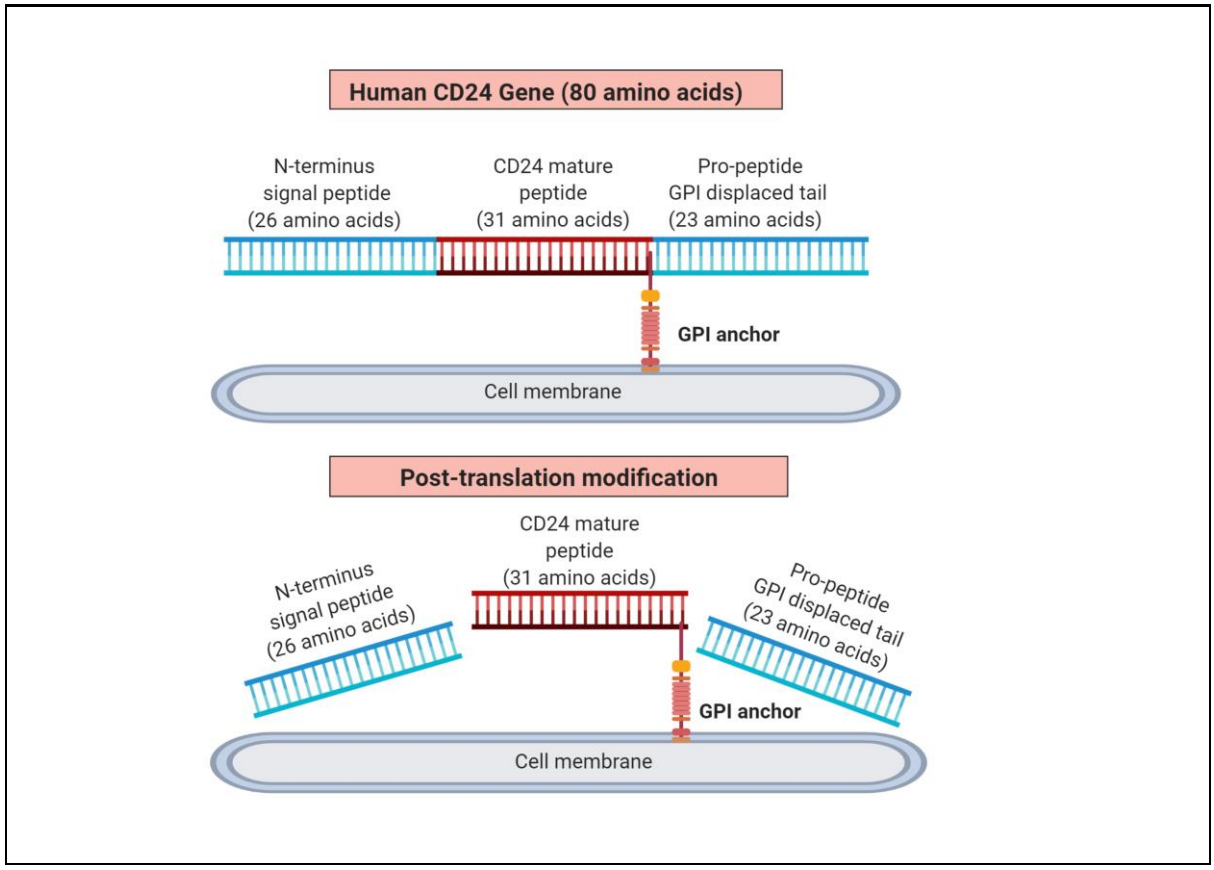


Figure 1.9 A simplified schema of the protein structure of CD24.

The human CD24 protein (80 amino acids) contains an N-terminal signal peptide (26 amino acids) and a C-terminal region with a GPI-displaced tail (27 to 29 amino acids). These two regions are detached during the posttranslational modification process, leaving the mature form of CD24 (31 amino acids) bound to the cell membrane via the GPI anchor. Abbreviations: GPI, glycosylphosphatidylinositol.

1.5.3 CD24 Expression and Function

1.5.3.1 Expression in normal tissues

The *CD24* gene typically has a diverse range of expression in normal tissue, with high expression levels having been identified in multiple lineages of haematopoietic cells, including most B cells, immature T cells, neutrophils, monocytes, macrophages and dendritic cells. However, *CD24* expression in B cells tends to gradually reduce or disappear completely during differentiation to the mature stage (plasma cell). *CD24* is additionally expressed in neuronal cells, muscle cells, pancreatic cells, numerous epithelial cells (intestinal epithelium, renal tubular epithelium, and keratinocytes), and gastric tissue [80, 85, 86].

Functionally, *CD24* has been used as a marker for haematopoietic and neuronal cell differentiation since its discovery. It has also been seen to act as a co-stimulatory molecule for T cell clonal expansion, which in turn is considered a significant genetic checkpoint for the regulation of T-cell homeostatic proliferation and autoimmunity. It also plays a role in regulating B-cell differentiation, activation, proliferation, and apoptosis [85-88], as well as playing a major role in neural development, neurite growth and neural migration [89]. Finally, *CD24* overexpression in the normal colon cells has been used to isolate Lgr5+ colonic epithelial stem cells in mice [90].

1.5.3.2 Expression in Cancer

Along with its diverse expression in normal tissues, overexpression of CD24 has been found in multiple autoimmune and inflammatory diseases and a variety of tumours. CD24 is expressed in many solid tumours, such as breast cancer, pancreatic cancer, oesophageal squamous cell carcinoma, non-small cell lung cancer, ovarian cancer, hepatocellular carcinoma, gliomas, renal cell cancer, bladder cancer, and CRC, as well as in some haematopoietic tumours such as B-cell lymphoma and erythroleukaemia [91-100]. *CD24* overexpression has also been linked with poor prognosis and reduced overall survival rates in multiple tumour types [97, 101, 102], and many researchers have addressed its role in inducing tumour cell proliferation, motility, and invasion [103-106]. It has been demonstrated that CD24 enhances breast cancer metastasis and rolls out of cancer cells into lung tissue by binding with P-selectin, an adhesion molecule expressed in endothelial cells and activated thrombocytes [107, 108]. Likewise, CD24 has been demonstrated to play a role in inducing cancer cell invasion based on its action in decreasing tissue factor pathway inhibitor-2 [109]. Other studies have revealed that silencing CD24 can inhibit cancer cell proliferation and invasion, inducing apoptosis and raising the sensitivity to chemotherapeutic agents in both breast and gastric cancers [110, 111]. Recent investigations have used CD24 as a marker of CSCs [112-114], yet as little is known about the precise mechanisms regulating CD24 function in CRC, further investigation is required to identify the functional activity of this molecule in context.

1.5.4 CD24 Proposed Signalling Mechanism

CD24 is localised on the cell surface and lacks a cytoplasmic domain through which to transmit intracellular signals. Any signalling process is thus likely to be activated directly on the cells where the gene is expressed or through direct physical interaction with cell surface receptors on adjacent cells (such as P-selectin, the L1 cell adhesion molecule (L1CAM), Siglec-G, TAG-1, or Contactin), mediated by the CD24 glycosylation pattern (Figure 1.10). However, *CD24* can initiate signalling by interacting with signalling proteins and other receptors such as Src-family protein tyrosine kinases, a potential binding pathway known for its role in transducing signals in cells [115]. Another signalling mechanism used by CD24 is its ability to change B cell receptor (BCR) location, moving through the membrane using lipid rafts to activate intracellular signalling. This association between CD24 and BCR may contribute to its activation of the binding of intracellular signalling proteins such as protein tyrosine kinase (PTK) and mitogen-activated protein kinase (MAPK) [116, 117]. Lipid rafts also act as platforms for signal transmission, and it is thought that CD24 performs a gatekeeping role within these lipid rafts by regulating their binding with integrins and other proteins [118]. CD24 has been shown to translocate CXCR4 and β1 integrins into lipid rafts and mediate cell adhesion and migration [103, 119]. It has also been suggested that CD24 triggers signalling through binding of lectin-like ligands to its projected carbohydrates; alternatively, CD24 may act independently by releasing secondary messengers derived from the CD24-GPI anchor membrane [78]. Although some of the

intracellular signalling pathways influenced by CD24 are well established in the literature, little is known about its signal-transducing capabilities overall, however.

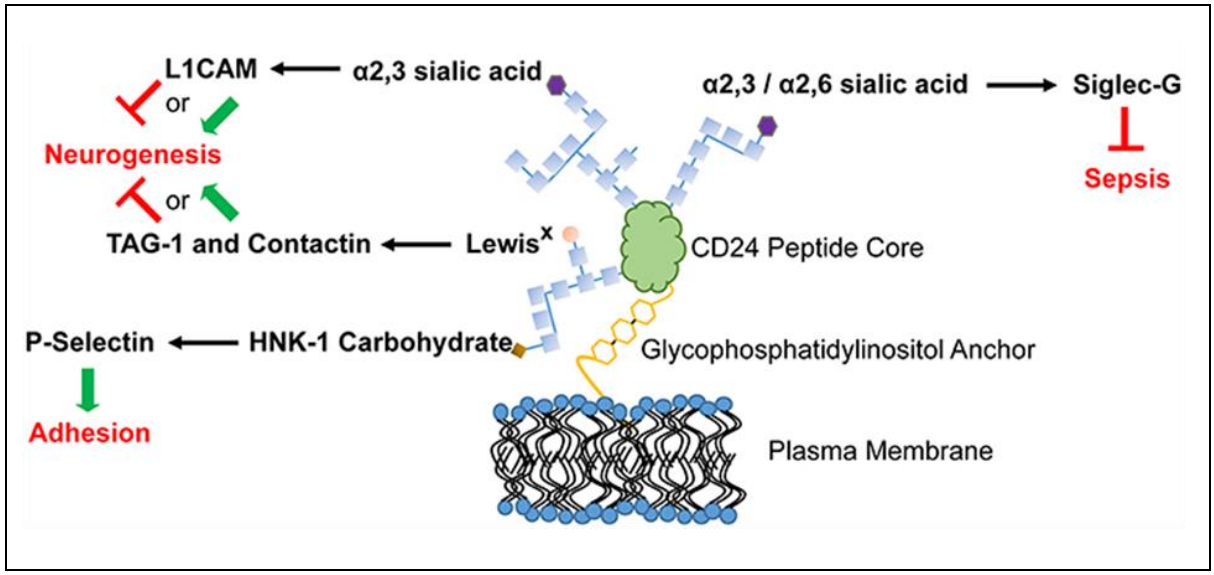


Figure 1.10 Schematic showing the possible associations of CD24 with partner receptors and ligands.

The binding of each specific CD24 glycosylation with specific ligands and the biological result of each binding is displayed. The blue squares indicate glycosylation, represented as a chain of carbohydrate monomers rather than a specific structure. The ligand interaction and the terminal carbohydrate moiety are also indicated [116].

1.5.5 CD24-Associated Signalling Molecules

CD24 has several potential binding molecules that have been significantly associated with controlling cell motility and enhancing stemness features [120]. Several downstream targets of this have been determined within the literature (Figure 1.11); however, for this project, the scope is constrained to the following downstream signalling pathways: Notch1 pathway, C terminal tensin like (Cten), Focal Adhesion Kinase (FAK), and Integrin-Linked Kinase (ILK).

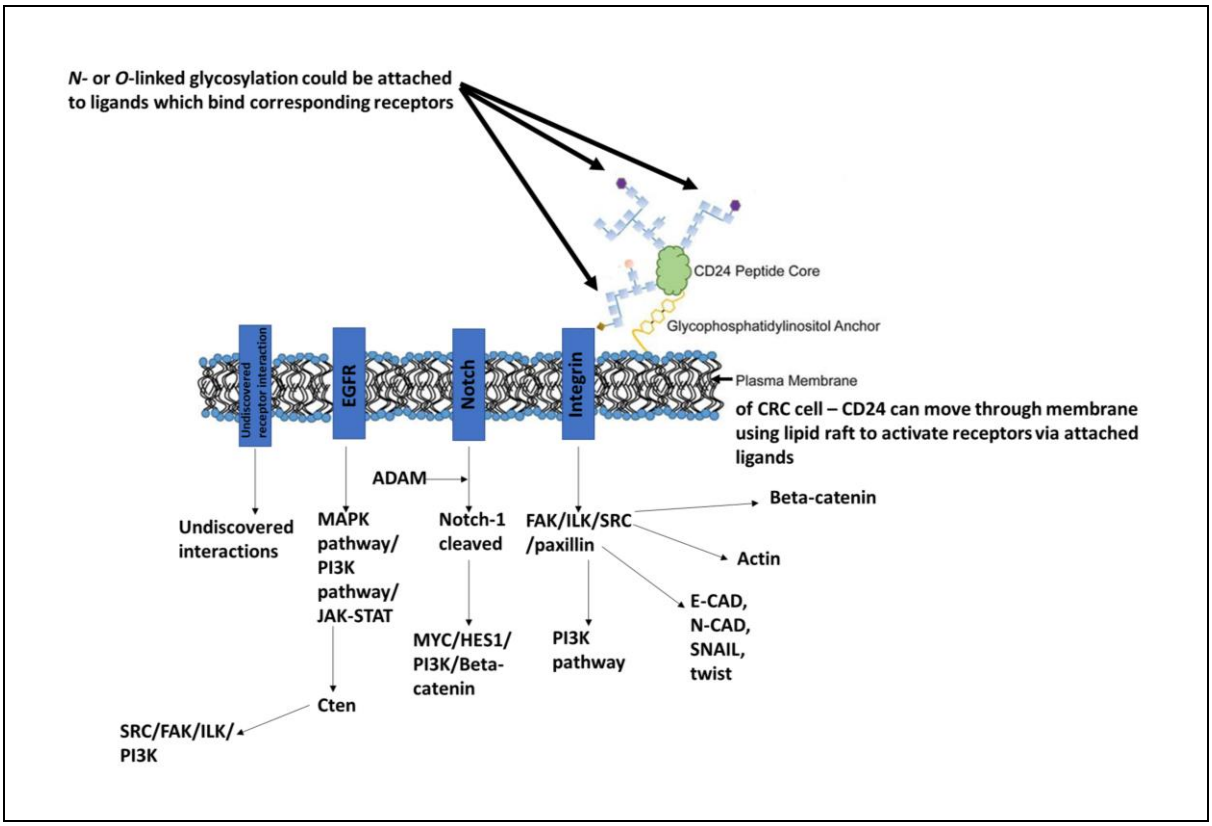


Figure 1.11 Network showing CD24 signalling pathways in CRC.

The signalling molecules and ligands that bind to CD24 and activates several targeted genes, leading to stimulation of cell migration, invasion and EMT. In addition, the importance of CD24 glycosylation in binding to ligands on adjacent cells are indicated. This network was created based on the finding from our group and others [116].

1.5.5.1 Notch-1

The notch pathway is a highly conserved pathway that was first discovered in 1917 in *Drosophila melanogaster*. The name of the Notch signalling pathway is derived from its receptors, with four of these being present in mammals, namely: Notch-1, Notch-2, Notch-3, and Notch-4. The notch pathway has multiple functions during embryogenesis as well as contributing to the haemostasis of organisms. Some of its functions include stem cell maintenance, cellular proliferation, differentiation, cell fate, and apoptosis [121].

The activation of Notch is triggered by ligands being present on the adjacent cell membrane; these can be categorised into two families, a jagged protein family, formed of JAG1 and JAG2, and a delta-like protein family that includes DLL1, DLL2, and DLL4 [122]. The Notch receptor itself is comprised of comprises three domains: the extracellular domain, a single transmembrane domain, and a notch intracellular domain (NICD). Upon binding the ligands of neighbouring cells to the Notch receptor, the receptor then undergoes two cleavage reactions mediated by ADAM-family metalloprotease and the γ-secretase complex. This cleavage process leads to the release of the Notch intercellular domain (NICD) into the cytosol, which then binds to a complex of proteins that include CBF1 (C protein factor 1) and Mastermind-like 1, which in turn binds to histone acetyltransferase P300. Eventually, the resulting complex of proteins translocates into the nucleus, where P300 acts as histone acetylase.

Accordingly, the whole complex can lead to activation of the transcription of Notch target genes such as *Myc*, *P21*, Cyclin D3, Slug, Nanog, and nuclear factor-kappa B (NF-κB) [122-124].

The upregulation of Activated Notch1 has been associated with cancer progression in multiple tumour types. For example, Notch1 has been found to induce CRC metastasis in models where *TP53* is mutated, and RAS/MAPK signalling is activated [125]. Similarly, Notch1 has been correlated with gastric cancer differentiation and found to play a role as an anti-cancer in gastric cancer cells [126, 127]. Some studies of breast cancer have linked CD24 and Notch1, based on silencing *CD24* resulting in lowered levels of Notch1 expression and the discovery that *CD24* stemness properties are mediated by downstream target Notch1 [128]. Among the previous researchers in our group, evidence that CD24 signals are passed through the Notch1 pathway, which stimulates the downstream target, Cten and several types of CRC cellular activities, has also been identified (unpublished data).

1.5.5.2 Cten

Cten or tensin 4 is a member of the tensin-like family proteins that consists of four homologous proteins, namely TNS1, TNS2, TNS3, and TNS4. Cten is generally localised in focal adhesion sites and shares a homology sequence with other tensin family members, which holds Src homology 2 (SH2) and phosphotyrosine-binding domains (PTB). However, Cten differs from other tensin family members in that it lacks an actin-binding domain

in its *N*-terminus site [129]. The SH2 and PTB domains thus play a significant role in binding the Cten to the cytoplasmic tails of β integrin and those proteins that possess phosphorylated tyrosine kinases, such as FAK and ILK [130]. The *Cten* gene maps to chromosomal region 17q21, with a total cDNA of 4,015 base pairs encoding 715 amino acid residues. It carries 12 exons, but only exon 4-11 shares the significant homology with other family members [131]. In normal tissue, Cten tends to be expressed in the prostate and placenta, where it has been found to serve as a tumour suppressor gene. In contrast, it acts as an oncogene in many solid tumours, including those found in CRC, breast, gastric, lung, and pancreatic cancers [129, 131].

The upregulation of Cten in CRC has been associated with increased cancer development. Albasri *et al.* found that the overexpression of Cten was linked to a greater than a 35-fold increase in five CRC cell lines out of 29 as tested by quantitative real-time (qRT)-PCR[132]. In the same study, Cten appeared to regulate cell migration and invasion by repressing the downstream target E-cadherin at the post-transcriptional level. While in a different study, Cten was shown to signals by means of ILK, in a manner that induced cell motility, with Cten overexpression increasing ILK levels and knockdown of Cten reducing the expression level of ILK, leading to cell motility suppression [130]. TGF-β was found to induce cell motility and stimulate EMT in CRC via Cten signalling [133]. The association of CD24 with Cten has also been investigated, and both molecules have been found to share similar stemness features such as induction of cell migration,

invasion, and adhesion; in some cases, they also act together with some focal adhesion molecules to modulate various cellular contexts [134, 135].

1.5.5.3 FAK

FAK is a non-receptor tyrosine kinase with 125 kDa molecular weight that is located at the focal adhesions. It thus plays an essential role in focal adhesion dynamics by mediating cell adhesion to the extracellular matrix via integrins, being activated through binding to multiple intercellular signalling pathways such as paxillin, vinculin, and phosphatidyl inositol-3 kinase (PI3K) [136]. FAK contributes to regulating many key cellular events, including cell proliferation, migration, adhesion and survival, and the overexpression of FAK has been associated with invasive and metastatic tumours [137]. The expression of FAK has also been correlated with stimulation of angiogenesis in breast cancer [138], while another study indicated that TGF-β induces EMT through downregulation of E-cadherin, which is mediated by FAK signalling in an Src dependant manner[139, 140].

Another study has suggested that CD24 accelerates FAK and paxillin phosphorylation and promotes integrin-dependent adhesion in breast cancer [103]. CD24 also relies on Src activity to mediate FAK and STAT3 dependent genes, which consequently may affect the control of cellular properties such as cell survival and proliferation that potentially contribute to tumour development [141]. The relationship between CD24, Cten, and phosphorylated FAK (p-FAK) has been explored by the previous researchers

in our lab, with results suggesting that CD24 knockdown results in abrogation of FAK activity in CRC [142, 143].

1.5.5.4 ILK

ILK is an intracellular protein that was discovered in 1996; it is connected directly to the cytoplasmic tails of integrin β1 and β3 subunits. ILK is a 59 kDa protein that maps to chromosome 11p15 and extensively expresses serine and threonine protein kinases at its focal adhesion [144]. With FAK, ILK plays an essential role in the transduction of multiple biochemical signals, beginning with cell-extracellular matrix interactions and moving on to the regulation of basic biological processes, such as cell cycle, apoptosis, proliferation, migration, invasion and angiogenesis [145, 146]. ILK consists of three structural domains: The *N*-terminal domain with four ankyrin-like repeats; the central pleckstrin homology (PH)-like domain; and the C-terminal protein kinase domain. The C-terminal domain of ILK is a catalytic domain that interacts with integrins, focal adhesion proteins such as paxillin and parvins, which in turn connect the integrins to the actin cytoskeleton and other intercellular signalling pathways [145-148].

The overexpression of ILK has been found to be correlated with tumorigenesis and progression. ILK plays a significant role in regulating EMT in melanoma cells, where silencing ILK leads to inhibition of N-cadherin expression and also inhibits nuclear translocation of β-catenin [149]. Similarly, inhibition of ILK in CRC cells reduces nuclear β-catenin expression and snail transcription as well as inducing E-cadherin expression[150].

Another study described ILK as playing a critical role in regulating cell proliferation and the growth of tumours based on ILK's upregulation of cyclin D1, Snail, and matrix metallopeptidase 9 (MMP-9) transcription [151]. Another study further indicated that ILK activation in tumour cells may induce secretion of VEGFA [152]. Previous researchers in our group have demonstrated the association of ILK with Cten and its role in promoting metastasis [130], while CD24 was found to signal through Cten-FAK/ILK to induce tumour features, such as invasion and migration, in CRC (unpublished data).

1.5.6 CD24 Ligands

1.5.6.1 P-selectin

Selectins are vascular cell-cell adhesion receptors that interact with sialylated carbohydrate determinants, such as sialyl Lewis A and X and mucin-like glycoproteins such as CD24[153]. Three types of selectin families have been identified: E-selectin, which is expressed on endothelial cells; L-selectin, which is expressed only on leukocytes; and P-selectin, which is expressed in thrombin-activated platelets and endothelial cells[65]. Selectins act as major mediators of white blood cells rolling on the surface of the endothelial tissue leading to activation of leukocytes integrins, which in turn facilitate firm adhesion to the cell surface of the endothelium and transmigration to the inflamed tissue [108, 154].

CD24 is a well-established ligand for P-selectin [82]. Physiologically, CD24 has been shown to mediate the adhesion of monocyte or neutrophil to the

activated platelets and endothelium-expressing P-selectin, and this binding could be inhibited by either CD24 or P-selectin antibodies. Interestingly, the B-lymphocyte is another cell that is express CD24 shows no adhesion to P-selectin, suggesting that this was probably due to the glycosylation patterns of CD24 having a crucial role in controlling CD24/P-selectin binding [97, 99] (Figure 1.12). The interaction between P-selectin and CD24 has also been shown to mediate the migration of tumour cells throughout the vasculature, promoting metastasis [108].

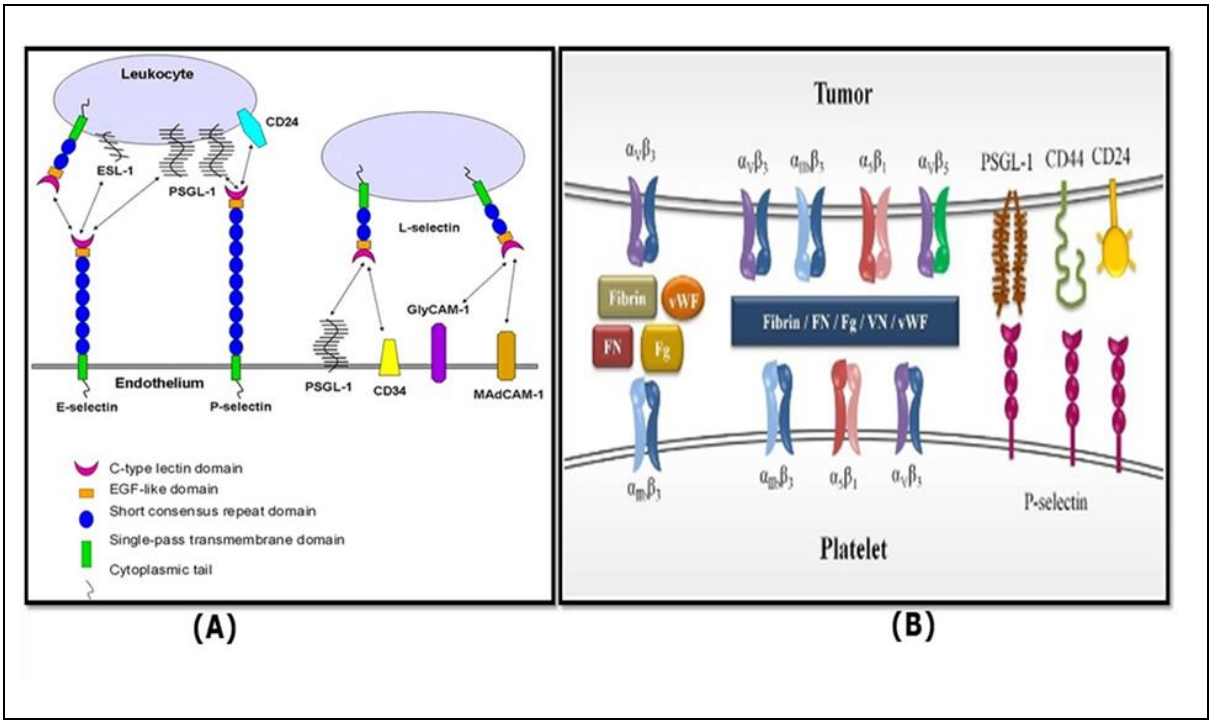


Figure 1.12 The interaction of P-selectin with its ligands on activated platelets and endothelium.

(A) P-selectin is expressed on activated vascular endothelium binding to PSGL-1 (P-selectin glycoprotein ligand) with high affinity. It also binds to CD24 [155]. (B) Interaction of platelet P-selectin with its selectin-ligands as expressed on tumour cells: PSGL-1, CD44, and CD24 [156].

1.5.6.2 Other Ligands

Multiple ligands have been associated with CD24, such as Sialic acid-binding Ig-like lectins (Siglecs), which are a group of immunoglobulin proteins expressed on numerous cell types in the innate and adaptive immune systems that aid in the discrimination between self and non-self, thus influencing host-pathogen interactions [157]. CD24 binds to the Siglec-10 expressed by tumour-associated macrophages, enhancing immune evasion (anti-phagocytosis) in many tumours [158].

Another ligand for CD24 is adhesion molecule L1, or LCAM-1, which is a member of the immunoglobulin superfamily. L1 is expressed in both neuron and lymphoid cells [159] as well as in many tumour cell types, including CRC, where it is associated with tumour progression and poor overall survival outcomes[160]. The cooperation of CD24 and L1 depends on the presence of α2,3-linked sialic acid, which promotes signal transduction and neurite outgrowth [161].

TAG-1 and Contactin are other identified ligands for CD24 that have been found to interact with the Lewis-x glycan present on the surface of CD24. Both molecules are required for CD24 to modulate neurite outgrowth of cerebellar and dorsal root ganglion (DRG) neurons [162].

1.5.7 Protein Glycosylation

During synthesis, many proteins undergo posttranslational modifications in their endoplasmic reticulum and Golgi apparatus, which affect their ultimate function. One example of such modification is glycosylation, which approximately half of the proteins expressed by cells undergo. Glycosylation is a posttranslational modification that involves an enzymatic glycosidic linkage reaction between the anomeric hydroxyl group of sugar and a protein [163]. During glycosylation, sugar groups are added covalently to amino acids, though only certain amino acids are suitable for this addition. The glycosylation family is thus categorised according to the nature of binding linking the amino acid to the sugar, creating five different groups. The most common glycosylation groups are *N*- linked glycosylation, *O*-linked glycosylation, and glypiation (GPI-anchor) [164, 165].

1.5.7.1 Common Types of Protein Glycosylation

1.5.7.1.1 *N-linked glycosylation*

N-Glycosylation of proteins is a posttranslational modification process that exists in all eukaryotic cells. It primarily takes place in the endoplasmic reticulum, continuing in the Golgi apparatus. This process uses the amino acid asparagine for carbohydrate attachment, where the asparagine must appear in sequences of tri-peptides known as sequons. The *N*-linked glycosylation target sequence is thus asparagine-(X)-serine/threonine, where X can be any amino acid with the exception of proline [166]. During normal growth and development, *N*-glycosylated residues play several

functional roles in protein folding, secretion, stabilisation, conformation, and trafficking to cellular and subcellular sites [167, 168]. In cancers, however, *N*-glycosylated proteins play a role in tumour growth and development based on their enhancement of the cancer cells' ability to evade immune detection and the promotion of uncontrolled proliferation, migration, cell-cell adhesion, and regulating glycoproteins binding to ligands [169-171]. However, many of these *N*-glycan features and their biological effects on various proteins, including CD24, remain under-investigated.

1.5.7.1.2 *O-linked glycosylation*

O-glycosylation is a process that occurs exclusively in the Golgi complex, where monosaccharides are bound to oxygen atoms present in the hydroxyl group of amino acids residues such as serine and threonine [163]. The standard form of *O*-linked glycosylation is β-*O*-*N*-acetylglucosamine (GlcNAc), which is referred to as mucin-type glycosylation and is usually found in extracellular and intracellular proteins in nuclear and cytoplasmic compartments [172, 173]. During normal growth and development, *O*-glycosylated residues generally play structural roles, though *O*-glycosylation in cell surface receptors plays a vital role in immunological processes such as inflammation response and ABO blood antigen formation [174]. In cancers, the mucin-type glycosylation seen in many glycoproteins is involved in tumour progression and metastasis [175, 176].

1.5.7.1.3 *Glypiation*

Glypiation is another common form of posttranslational modification, most frequently observed on the surface of the glycoproteins in eukaryotes and archaebacterium [177]. This process connects GPI via phosphoethanolamine to the target protein's C-terminal region during posttranslational modification. As with *N*-linked glycosylation, GPI synthesis occurs in the cytoplasmic leaflet of the endoplasmic reticulum and is eventually translocated to the lumen where protein ligation occurs [164].

1.5.7.2 *N*-glycans Association with Cancers

Several proteins with glycosylation moieties are present on the cell surfaces of cancer cells, though their expression is affected by several factors, including neoplastic and dysplastic changes. Their expression pattern is thus considered a useful indication of such changes. Different types of gastrointestinal malignancy are marked by overexpression of glycosylation-dependant proteins such as CEA, Ca19-9, MUC1, MUC5AC, and Ca125, for example, and these glycoproteins can thus be used to aid diagnosis (e.g., identifying Ca19-9 for pancreatic malignancy) and prognostic surveillance (e.g., identifying CEA for colorectal adenocarcinoma)[178-180].

Several previous studies have highlighted the role of *N*-glycosylation in promoting various cancer types. For example, two studies have indicated that most glycoproteins with increased *N*-glycosylation residues are associated with signalling pathways mediating pancreatic cancer progression, including TNF, TGF-β, and NF-kappa-B [181] as well as being

found in focal adhesion molecules and integrins [175]. Similarly, another study on pancreatic cancer showed that *N*-glycosylation inhibition reduces receptor tyrosine kinases, which in turn increases sensitivity to chemotherapeutic drugs [182].

In oral cancer, one study revealed that the disruption of *N*-glycosylation-related glycoproteins such as E-cadherin was involved in determining pathogenicity. In that study, the hypothesis was that impairing the regulatory mechanism of DPAGT1, an enzyme that regulates the *N*-glycosylation of E-cadherin and other cancer-associated proteins, affects both cell-cell interaction and cytoskeleton dynamics [167].

A recent study by Zhang *et al*. performed a point mutation in the three potential *N*-glycosylation sites of the epithelial cell adhesion molecule (EpCAM). These researchers found that the de-glycosylation of EpCAM caused an increase in apoptotic mechanisms and suppressed breast cancer cells' proliferative capacity, highlighting the significance of the *N*-glycosylation of EpCAM (referred to as an apoptotic regulator) as a targeted therapy for breast cancer [183]. The same group also stressed the importance of *N*-glycosylation of EpCAM in terms of regulating EMT in breast cancer [184].

Additional studies of *N*-glycome profiling of colorectal adenocarcinoma tissue and adjacent non-tumour colon tissue have found a protein *N*-glycosylation signature specific to CRC associated with a particular stage of tumour [185]. A similar study compared the *N*-glycomes in colorectal

adenomas and carcinoma cases and found differences in the glycosylation variants between adenomas and carcinomas and between carcinoma stages I, II, and III [186].

1.5.7.3 CD24 Glycosylation

CD24, as described above, is a triple-exon gene mapped to chromosome 6q21, which encodes a small, heavily-glycosylated protein with 80 amino acids [79, 80]. The mature form of CD24 has two potential *N*- and 16 *O*-glycosylation sites, which render it as a mucin-like protein. As multiple glycosylation residues decorate the CD24 protein structure, its molecular weight ranges from 30 to 70 kDa [97].

Few studies thus far have sought to investigate the glycosylation patterns in CD24. For example, *N*-glycosylation in mouse CD24 protein has been compared to human CD24, with a little similarity between the two proteins identified [187]. Another study exclusively analysed *N*-glycan using matrix-assisted laser desorption ionisation (MALDI) and electrospray ionisation ion trap (ESI) mass spectrometry, finding heterogeneous glycans that express different sugar epitopes, such as lewis^X, 3-linked sialic acid, or blood group H antigens, bisecting *N*-acetylglucosamine residues and *N*-acetyllactosamine, as well as high-mannose and hybrid type classes [188].

Further analysis performed by the same researchers on the *O*-glycosylation of murine CD24 found several significant epitopes, including 3-linked sialic acid, disialyl motifs, and Lewis X, sialyl-Lewis X, or HNK-1 units [189]. Some of these epitopes are associated with cellular biology processes, such

as cell-cell adhesion, binding, and migration: for instance, carbohydrate sialyl lewisX is necessary for CD24 to mediate the rolling of cancer cells on P-selectin [107], while the presence of α- 2,3- linked sialic acid residues on CD24 facilitates binding to L1, which in turn modulates neurite outgrowth [161].

Motari *et al*. studied the structure of carbohydrates bound to CD24-Fc proteins using matrix-assisted laser desorption/ionization-time-of-flight mass spectrometry (MALDI-TOF-MS). The study found that more than half of the oligosaccharides in CD24 glycans were Neu5Ac Galβ-1,3GalNAc, also referred to as sialyl-tumour antigens (sialyl-T). Accordingly, they suggested that CD24 could be the main carrier of sialyl-T in tumour cells, thus contributing to metastasis [190].

Collectively, these previous studies have highlighted the importance of the *N*-glycosylation presented in CD24 protein and thus raised the possibility that these *N*-sugars may act as mediators for CD24 activity in tumour cells.

1.5.8 CD24 as a therapeutic target for cancer

CD24 is overexpressed in about 90% of early-stage CRC and is known to have a role in tumour progression and metastasis in multiple tumours, as well as being a potential CSC marker; this could make it a potential therapeutic option for certain cancers [83]. Studies have already indicated that the use of CD24 monoclonal antibody to inhibit cancer growth and progression is feasible in many cancer types: for example, one study

showed that targeting CD24 with monoclonal SWA11 antibody (mAb) effectively inhibited tumour growth in xenograft tumours by changing the cytokines' milieu and increasing the accumulation of macrophages in tumour tissue [191].

SWA11 mAb was also found to inhibit multiple myeloma cell growth and prevent cancer development [192], and in terms of CRC, Shapira et al. developed a SWA11 mAb conjugated to pseudomonas exotoxin (PE-38) combined with a ZZ domain (Fc binding domain from Staphylococcal protein), and the resulting immuno-conjugated SWA11 antibody significantly reduced the growth of human CRC cell lines (HT29) in mice [193].

Another study showed that anti-CD24 mAb prevents tumour growth and reduces metastasis in human bladder carcinoma xenografts [194]; moreover, CD24-Fc binding to Siglec-10 on immune cells such as T-cells, B-cells, and phagocytic cells, can activate immunosuppression and prevent autoimmunity, while inhibition of the CD24-Siglec-10 binding in cancer cells by monoclonal antibodies can protect cancer cells from phagocytosis [83, 195].

1.6 Hypothesis and Aims

1.6.1 The role of *N*-glycosylation sites in CD24 in CRC progression

CD24 confers various features of stemness and enhances cell motility in CRC. It contains numerous *O*-glycosylation sites but contains just two *N*-glycosylation sites (N36, N52). As *N*-glycosylation is thought to be important in mediating glycoproteins' function, it is hypothesised that CD24 might depend on *N*-glycosylation for its activities. Based on this hypothesis, the following aims were developed:

1. To replace the target asparagine residue at N36 and N52 sites with glutamine residue using site-directed mutagenesis to create single mutant constructs of CD24 ($CD24^{N36Q}$ and $CD24^{N52Q}$).
2. To create a double mutant construct of CD24 at both sites ($CD24^{N[36,52]Q}$).
3. To study the impact of mutating *N*-glycosylation sites of CD24 on downstream molecule signalling.
4. To investigate the functional effect on cell proliferation, migration, and invasion using CD24 mutant constructs and compare them to wild-type CD24 and EVC.
5. To investigate the impact of $CD24^{WT}$ and CD24-mutant clones ($CD24^{N[36,52]Q}$) on regulating EMT in CRC.

1.6.2 The Role of CD24/P-selectin in CRC metastasis

CD24 acts as a ligand for P-selectin, an endothelial cell surface molecule, as well as regulating cancer cell metastasis [82]. However, the interaction of CD24 with P-selectin and their joint impact on CRC cell behaviour has not been specifically studied. It is hypothesised that CD24 mediates CRC cell adhesion to endothelial cells via its binding to P-selectin, which consequently promotes CRC metastasis. Therefore, the objectives of this section included:

1. Performing a dual approach of CD24 overexpression in HCT116 (negative CD24 cells) and knockdown in SW620 (endogenously expressing CD24) followed by stimulation with recombinant P-selectin to determine the effects of this stimulation.
2. Investigation of the impact of heterogenic interaction (CD24/P-selectin) on cell viability, cell motility, and downstream signalling molecules' activation, comparing these with those seen in non-stimulated cells and EVC.
3. Performing co-immunoprecipitation to study whether CD24 interacts with P-selectin.
4. Studying the impact of CD24/P-selectin binding on the regulation of CRC cells adhesion to endothelial cells using an adhesion assay.
5. Developing transwell co-culture models by culturing CRC cells on top of an endothelial cell monolayer to study the correlation of CD24 with

P-selectin in the promotion of CRC cell migration through the endothelium.

6. Determining whether the *N*-glycosylation of CD24 plays a role in P-selectin binding.

1.6.3 Investigation of the association of CD24 with CRC Angiogenesis

CD24 upregulates several signalling pathways that mediate cellular activities in CRC. The overall metastatic process requires the establishment of an appropriate local microenvironment, including sufficient vascular supply, to support tumour growth; published data thus suggest that ILK activation in tumour cells may induce VEGF-A secretion [196]. As CD24 and Cten have been shown to induce ILK expression [130], it is hypothesised that CD24 could regulate VEGF-A-mediated angiogenesis in CRC, depending on ILK. Thus, the specific aims of this section were:

1. To determine whether CD24 regulates VEGF-A expression in CRC cells.
2. To study the role of CD24 in inducing endothelial cell proliferation, migration and tube formation.
3. To perform an ELISA assay to measure the level of secreted VEGF-A in the supernatant retrieved from cells expressing CD24.
4. To apply co-transfection techniques to determine whether CD24 regulates VEGF-A through ILK.
5. To investigate the impact of CD24-mutant clones ($CD24^{N[36,52]Q}$) on VEGF-A expression and the cellular activities of endothelial cells.

Chapter 2: Material and Methods

2.1 Cell culture

2.1.1 Cell lines

Three colorectal cell lines, including HCT116, SW480 and SW620, were used for the experimental work of this study. These cells were purchased from the American Type Culture Collection (ATCC). The cell lines' identity was also confirmed by short tandem repeat (STR) genotyping using PCR-single locus technology (see Appendix II). The molecular characteristics for the above cell lines are briefly described in Table 2.1 and Table 2.2. Human umbilical vein endothelial cells (HUVECs) were purchased from Promocell® (Heidelberg, Germany). All cell lines were regularly undergoing monthly screening for mycoplasma infection.

Table 2.1 The properties of the cell lines used for the study

CRC cells					
Cell line	**Differentiation**	**Site**	**Morphology**	**Growth properties**	**Stage/Disease**
HCT116	Well	Colon	Epithelial	Adherent	Dukes' D, colorectal carcinoma
SW480	Moderate	Colon	Epithelial	Adherent	Dukes' B, colorectal adenocarcinoma
SW620	Moderate	Colon (Lymph node)	Epithelial	Adherent	Dukes' C, colorectal adenocarcinoma

Table 2.2 Mutation profiling for the significant oncogenes in the used cells

Cell line	KRAS	P53	BRAF	PI3K	CD24	Cten
HCT116	Mutant	Wild Type	Wild Type	Mutant	Negative	Negative
SW480	Mutant	Mutant	Wild Type	Wild Type	Negative	Negative
SW620	Mutant	Mutant	Wild Type	Wild Type	Positive	Positive

2.1.2 Cell maintenance

All the cells were grown in T75 (Corning) flask in Dulbecco's Modified Eagle's Medium (DMEM) (GIBCO®, Invitrogen, UK) with 10% Fetal Bovine Serum (FBS) (Invitrogen, UK), 1% L-glutamine (Invitrogen). After achieving 85-90% confluency, the medium was removed from the cells, and the cells were washed two times with Dulbecco's Phosphate Buffered Saline (DPBS, Sigma-Aldrich). The cells then were trypsinised by adding 3 ml of trypsin-EDTA (ThermoFisher Scientific) and incubated for 5 min at 37 °C, 5% CO2 atmosphere in a humidified incubator to detach the adherent cells from the surface of the culture flask. Following this, 7 ml of fresh DMEM-(10 % FBS) was added to the trypsinised cells to deactivate the trypsin. Afterwards, the cell suspension was centrifuged at 1500 rpm (300 xg) for 5 min, the supernatant was discarded, and the cell pellet was resuspended with 10ml of DMEM-(10% FBS). The suspended cells were then cultured into a new culture flask in a dilution of 1:10 of the cell suspension with a fresh DMEM-(10% FBS) and incubated at 37 °C, 5% CO2.

The HUVEC cell line was cultured as the above protocol with a difference that the cells were maintained in endothelial cell growth medium-2 (ECGM2) with supplements (Promocell®). The cell growth and morphology were observed daily under the microscope.

2.1.3 Freezing cells and Thawing

The cells freezing was performed by taking an early cell passage number. The cells were grown to 90% confluence, then harvested according to the abovementioned protocol. However, instead of resuspending the cell pellet with culture media, the pellet was resuspended with a freezing media containing a mixture of 90% FBS and 10% dimethyl sulfoxide (DMSO). After which, 1 ml of the cell suspension was transferred into a labelled Cryo-Vial tube and transferred to a freezing pot containing isopropanol to slowly freeze at a cooling rate of -1 per minute and stored overnight at –80 °C. For long-term storage, the cells were transferred to liquid nitrogen storage after 48 hr of freezing at -80 °C.

For cell thawing, the cell vial was taken out from the -80 °C freezer into a box containing dry ice, and the lid was loosened to prevent pressure increase as a vial warmed. In a quick process, the cells were defrosted by immersion in a 37 °C water bath. Afterwards, the cells were transferred to a sterile universal tube containing 9 ml fresh warmed culture media; then was centrifuged at 1500 rpm for 5 min. The cell pellet was then resuspended in 10 ml of a complete fresh medium, and the whole mixture was transferred to a new flask and left to grow overnight in 37 °C

incubators. After 24 hr, the media were replaced with a fresh complete medium and cells were allowed to grow until confluency.

2.1.4 Cell counting

As many experiments required optimising an approximate cell number, the live cell counting was performed using the automated cell counter (BIO-RAD TC20) and trypan blue (0.4% trypan blue in distilled H_2O). Briefly, 20 µl of the homogeneous cell suspension was mixed thoroughly with 20 µl of trypan blue in a dilution of 1:1. Then 10 µl of the mixture was loaded into each well of the dual-chamber counting slide (BIO-RAD TC20). Separately, both sides of the slide were counted by adjusting the observed peak to 6-20 µm. The number of live cells and the percentage of viable cells was noted, and the mean value for live cells on both sides was counted to calculate cell density per millilitre (ml).

2.2 Cloning

2.2.1 Bacterial transformation

Before commencing the experiment, the agar plate was prepared as follows; 1.5 g of Luria broth (LB) agar (Sigma) supplemented with ampicillin was added into 100 ml of sterilised water and then microwaved to dissolve the particles completely. Once the agar cooled down to 60 C°, 20 ml was poured into 10 cm Petri dishes (Costar, UK) and was left at room temperature for 10-15 min to solidify. According to the provided protocol, the heat shock method was used to transform plasmids into competent cells

(New England BioLabs). In short, 50 µl of the competent cells were placed into an Eppendorf tube and then were mixed with 5 µl of the plasmid (pcDNA3.1 Empty vector and pcDNA3.1-CD24). The whole mixture was incubated on ice for about 30 minutes, then was heat shocked for 30 seconds at 42 ^{0}C and cooled down on the ice for 5 min. Following this, the whole mixture of competent cells and plasmid was added to 950 µl of SOC outgrowth media (New England Bio Labs, UK) and incubated for 1 hr at 250 rpm rotator (SANYO Orbital incubator) at 37 °C. After incubation, 100 µl of the mixture was spread onto an agar plate and incubated at 37 ^{0}C for 16 hr. On the next day, one colony was picked up by using a 10 µl sterile tip and re-grown in 5ml of LB broth supplemented with five µg/ml of ampicillin and incubated overnight at 250 rpm rotator (SANYO Orbital incubator) at 37 °C. Next, the mixture was added to the autoclaved flask containing 100 ml of LB media and incubated overnight at 37 °C/250 rpm for additional growth. The plasmid was extracted using a mini-prep kit (Sigma) or maxi-prep (QIAGEN) kit.

2.2.2 Plasmid purification

The QIAGEN plasmid Maxi Kit (QIAGEN) was used to purify the high-copy plasmid DNA. The bacterial culture was briefly harvested at 6000 xg for 15 min at 4 $^{\circ}$C, and the supernatant was discarded. Following this, the pellet was resuspended with 10 ml of re-suspension/RNase A buffer (P1) and then lysed by adding 10 ml of the lysis buffer (P2) and inverted vigorously until the lysate becomes viscous and incubated for 5 min at room temperature.

After that, to neutralise the lysed cells, 4 ml of chilled neutralisation buffer (P3) and mixed thoroughly by vigorous inverting (six times) and incubated for 20 min on ice. After incubation, the mixture was centrifuged at 20,000*xg* for 30 min at 4 °C, and the supernatant (contained the plasmid) was collected. The QIAGEN-tip was equilibrated by adding 10 ml of equilibration buffer (QBT) and allowed to empty by gravity flow. Subsequently, the supernatant was added into the QIAGEN-tip and allowed to pass through the membrane by gravity flow. The QIAGEN-tip was washed (two times) with 10 ml washing buffer (QC) and then eluted with 15 ml of elution buffer (QF) into a new collection tube. Next, the eluted DNA was precipitated by adding 10.5 ml of room-temperature isopropanol and centrifuged at 15,000 *xg* for 30 min at 4 °C. After centrifugation, the supernatant was discarded, and the DNA pellet was washed with 5 ml ethanol and centrifuged for 10 min at 15,000 *xg*. Lastly, the supernatant was discarded, air-dried the pellet for ten minutes and resuspended with sterile H_2O.

2.2.3 DNA quantification

The DNA concentrations were measured using a NanoDrop™ 2000 UV spectrophotometer (Thermo Scientific). The absorbance ratio of 260/280 was used for evaluating DNA purity. A 260/280 ratio of 1.8–2 was considered as a good DNA quality. Elusion buffer (1 µl) was used to blank the NanoDrop, and the DNA samples (1 µl) were assessed at 260/280 ratio.

2.3 Transient transfection

2.3.1 Gene overexpression

According to the Lipofectamine®2000 (Invitrogen) instructions manual, the transfection protocol was as follows; 5×10^5 cells were seeded into 6-well plates containing 2 ml fresh growth media and incubated 24 hr. The medium was discarded, and the cells were serum-starved for 1 hr by adding 1.5 ml Opti-MEM® reduced-serum medium (Gibco, Life Technologies) per well before transfection. During incubation, the transfection mixture was prepared as follows: 8 µl/well of LipofectamineTM 2000 was added to 250 µl Opti-MEM® and incubated at room temperature for 5min. In a separate tube, 4 µg/well of $CD24^{WT}$, CD24-mutant plasmids or empty vector control were added to 250 µl Opti-MEM®, and the two tubes were then combined and incubated for 20 min at room temperature. The plasmid and Lipofectamine mixture was added to the well plates, incubated for 4-6 hr. After incubation, the transfection media was replaced with a 2 ml fresh growth medium and the cells were harvested 24-48 hr post-transfection for protein extraction and in vitro functional assays.

2.3.2 Gene knockdown

The SW620 cell line ($5x10^5$) was cultured 24 hr in a six-well plate, similar to the above protocol. Next, the medium was replaced with Opti-MEM® I reduced-serum medium (Gibco, Life Technologies) and incubated for one hour. During incubation, a mixture of Lipofectamine2000 (Thermo Fisher)

with silencer-select CD24 siRNA (Invitrogen) in a total volume of 2000 µl of Opti-MEM was added to each well and incubated for six hours. Likewise, the HUVEC cells were transfected with On-target plus P-selectin siRNA (DharmaconTM) mixed with the DharmaFECT-4 transfection reagent (DharmaconTM) in a total volume of 2000 µl of Opti-MEM. The medium was then replaced with a complete fresh medium (DMEM-10%FBS) for the SW620 cell line or ECGM-2 for the HUVEC cell line), and the cells were used for experimental work after 24 hr. Table 2.3 contains the target sequence for used siRNA.

2.3.3 Co-transfection

The Co-transfection technique was used to determine the putative signalling pathways of CD24. This experiment included establishing a system in which CD24 overexpression and ILK knockdown were performed simultaneously. The cells were transfected when they reached 50% confluency. For each co-transfection condition, 8µl of Lipofectamine™ 2000 was added to 250 µl of Opti-MEM® reduced-serum medium. CD24-expressing vector and ILK siRNA were diluted together at the optimal concentration in 250 µl of Opti-MEM. Afterwards, the plasmid/siRNA mixture was added to the diluted Lipofectamine and incubated for 20 min. After incubation, the total transfection mixture was added to the cells and incubated for 6 hr. Finally, the transfection reagents were replaced with 2 ml of the fresh growth medium, and the cells were used for protein and functional assays after 24 hr.

Table 2.3 siRNA sequences used in knockdown and co-transfection.

Gene	Target sequence
CD24 silencer-select siRNA (Ambion®)	UCAAGUAACUCCUCCCAGATT, UCUGGGAGGAGUUACUUGAAG
ILK silencer-select siRNA (Ambion®)	UUCUCCGUGUUGUCCAGCCACAGGC, GCCUGUGGCUGGACAACACGGGAGAA
Luciferase Universal non-targeting siRNA (ThermoFisher)	CAGUGUAGUAGUCGUUUC, GAAACGACUACUACACUG
ON-TARGET plus human SLEP SMART pool siRNA (Dhrmacon™)	GCUGAGAGGAGCCGAUAUA, GCUGAGGAACUGGGCUGAUA, GUAAAGCUGUGCAGUGUCA, CUAGAGGGCCAGUUACUUA
ON-TARGET plus Non-targeting Pool (Dhrmacon™)	UGGUUUACAUGUCGACUAA, UGGUUUACAUGUUGUGUGA, UGGUUUACAUGUUUUCUGA, UGGUUUACAUGUUUUCCUA

2.4 P-selectin stimulation

After transfection, the cells were starved by adding 1.5 ml of serum-free medium for three hours. Then 10 µg of recombinant human P-selectin/CD62P (R&D system a bio-techne brand) was mixed with 1 ml of complete culture medium, added to the cells and incubated for 60 min at 37 ºC in a 5% CO2 incubator to activate adhesion with CD24. Subsequently, protein extraction and functional assays were performed. The non-treated cells were served as a negative control.

2.5 Western blotting

2.5.1 Protein extraction

For protein extraction, the cells ($0.7\text{-}1.0x10^6$) were seeded in a six-well plate containing 2 ml of 10% DMEM. The following day, the media was discarded, and the cells were washed (two times) with 2 ml of PBS. The cells were then lysed by adding Pierce® radioimmunoprecipitation assay buffer (Thermo Fisher Scientific) mixed with protease and phosphatase inhibitor cocktail (100×, Thermo Fisher Scientific) in a dilution of 1:100 and then kept on ice for 15-20 min to avoid protein degradation. The lysates were scraped using a cell scraper, transferred to cold labelled Eppendorf tubes, and centrifuged at 16,000 *xg* for 30 min at 4 °C. The pellets were discarded, and the supernatant was moved to new Eppendorf tubes and kept at -20 °C for protein quantification.

2.5.2 Protein quantification

Bicinchoninic acid (BCA) assay was performed to measure the protein concentration by using Pierce™ bicinchoninic acid assay (BCA) kit (Thermo Scientific). Before commencing the experiment, BCA standards and working solutions were prepared according to the manufacturer instructions. The protein concentration standards were prepared by diluting the albumin standard into nine clean vials with different concentration ranges from 0-2000 µg/ml and the protein lysis buffer used as a diluent. The working solution was prepared by adding 50 volume of BSA solution A to 1 volume

of BSA solution B. Following that, 10 µl protein concentration standards were added in three replicates in the first three rows of 96-well microplate (Thermo-Scientific pierce TM), and the protein lysates were added into separate rows in the same plate and mixed with 200 µl of prepared working solution. The plate was mixed using the Multitskan Ex shaker from (Lab System), then covered with a foil and incubated at 37 ºC for 30 min. The absorbance of protein lysates was measured using the Multitskan-Ex at 550 nm wavelength. The unknown samples concentration was obtained by comparing their absorbance value to a standard curve using a simple formula.

2.5.3 SDS-polyacrylamide gel electrophoresis

NuPAGE™ 4-12% Bis-Tris Protein Gels, 1.0 mm, and 10-well were placed into Invitrogen electrophoresis gel tank followed by filling the inner chamber of the tank with NuPAGE™ Tris-Acetate SDS Running Buffer (Invitrogen), and then the rested to cover the gel. 50 µg of protein samples were added to the loading buffer (one-third volume of protein sample) containing 1x NuPAGE™ sample reducing agent (10x, Thermo Fisher Scientific). The samples were then placed on the heat block at 95 °C for minutes to denature the protein for an additional 5 min on ice and then centrifuged for a few seconds at 12000 RPM. Protein fractionation occurred by running samples on a NuPAGE 4-12% Bis-Tris gel (Invitrogen) at 150V for 90 min. The gel was then transferred to Polyvinylidene Difluoride (PVDF) membrane (Amersham, GE Healthcare Life Sciences) between two wet filter

papers in NuPAGE™ transfer buffer (Invitrogen) and placed in a semi-dry transfer on Bio-Rad Transblot turbo transfer system (Bio-Rad, Watford, UK) for 30 min at 25 V. After transfer, the membrane was stained with Ponceau red stain to confirm the successful transfer, followed by two washes with Tris-buffered saline, 0.1% Tween-20 (TBST) to remove the stain. The membrane was then blocked for 1 hr at room temperature with an appropriate blocking solution, either 5% skim milk (Sigma-Aldrich) or BSA (ThermoFisher Scientific) in TBST. The membrane was then incubated overnight at 4 °C with a relevant primary antibody diluted in the same used blocking buffer. The primary antibodies and diluents used in this study are detailed in Table 2.4.

The following day, the membrane was washed three times for 5 min with TBST solution and then incubated with appropriate HRP-conjugated secondary antibody for 1 hr at room temperature. After secondary antibody incubation, the membrane was rewashed with TBST, and the visualisation occurred using enhanced chemiluminescence (ECL) detection kit (Thermo Fisher Scientific) on the Odyssey Fc imaging system (LI-COR Bioscience, UK). Protein expression was digitally calculated using the Image Studio-Lite Version 5.2 software (LI-COR Biosciences Ltd. UK). Protein expression was normalised by calculation of the ratio between target proteins to the housekeeper α-tubulin.

Table 2.4 List of the antibodies used for Western blot.

Antibody	Provider	Source	Diluent	Ab_1 dilution	Ab_2 dilution
CD24 (SWA11)	Prof. Altevogt P (DKFZ, Heidelberg)	Mouse	5% Skimmed Milk+0.1% Tween TBS	1:1000	1:5000
Notch1	Abcam	Rabbit	5% BSA+0.1% Tween TBS	1:500	1:2000
Cten	Sigma	Mouse	5% Skimmed Milk+0.1% Tween TBS	1:1000	1:5000
FAK	Cell signalling	Rabbit	5% BSA+0.1% Tween PBS	1:1000	1:2000
ILK	Abcam	Rabbit	5% BSA+0.1% Tween TBS	1:1000	1:2000
E-cadherin	Cell signalling	Rabbit	5% BSA+0.1% Tween TBS	1:1000	1:5000
N-cadherin	Cell signalling	Rabbit	5% BSA+0.1% Tween TBS	1:1000	1:5000
Snail	Cell signalling	Rabbit	5% BSA+0.1% Tween TBS	1:000	1:5000

Vimentin	Cell signalling	Rabbit	5% BSA+0.1% Tween TBS	1:000	1:5000
P-selectin	Abcam	Rabbit	5% BSA+0.1% Tween TBS	1:1000	1:5000
PSGL-1	R&D	Mouse	5% Skimmed Milk+0.1% Tween TBS	1:1000	1:5000
VEGF	Santa Cruz	Mouse	5% Skimmed Milk+0.1% Tween TBS	1:1000	1:5000
Angiostatin	R&D system	Goat	5% Skimmed Milk+0.1% Tween TBS	1:1000	1:5000
Tubulin	Abcam	Mouse	5% Skimmed Milk+0.1% Tween TBS	1:000	1:5000

2.5.4 Western blot re-probing

RestoreTMPlus Western Blot Stripping Buffer (Thermo Scientific, Ref. 46430) was used to re-probe the membrane with an alternative antibody. The membrane was washed with 1xTBS and incubated with stripping buffer for 15 min at room temperature. The blot subsequently was washed two times with TBS and blocked for 30-60 min. Then the membrane was re-blotted with any antibody overnight and applying the same above protocol.

2.6 *N*-glycosylation digestion

Transfection of the modified construct of CD24, which was less glycosylated than the wild type CD24, resulted in variation in the molecular weight on western blot. Therefore, the glycosylation of CD24 was removed using an *N*-glycosylation digestion mix that contains a combination of α2-3, 6, 8 Neuraminidase and Peptide -*N*-Glycosidase F (PNGase F) (New England BioLabs, UK). According to the provided instructions, the reaction was prepared in a reaction volume of 20 µl as follows: 25 µg of the protein was added to 1 µl of glycoprotein denaturing buffer (10X) H_2O to make 10 µl reaction volume. Next, the protein was denatured by heating the reaction at 100 °C for 10 min, followed by ice-chilled and centrifugation for 10 seconds. After that, the total reaction volume was made to 20 µl by adding 2 µl GlycoBuffer (10X), 2 µl 10% NP-40 and 6 µl of water. Following this, 1 µl PNGase F and 1 µl α2-3,6,8,9 Neuraminidase (2 µl/1 µg) were mixed with the 20 µl-volume reactions and incubated at 37 °C overnight. After

incubation, the enzyme was deactivated by incubating the protein at 68 °C for 10 min. The mixture then was run on an SDS-PAGE gel.

2.7 Co-immunoprecipitation

This experiment was used to investigate protein-protein binding. First, the cells were lysed by Pierce IP lysis buffer (Thermo Fisher) mixed with 1x of PPI. The protein was then pre-cleared by incubating it with protein A agarose beads (Sigma-Aldrich) at 4 °C with gentle agitation for 30 min to clear out nonspecific binding. Next, the protein lysate was centrifuged at 13000 RPM for 5 min at 4 °C. The supernatant was collected for Co-IP, and the beads were maintained for later use. Finally, the CD24 antibody (1 µg) or P-selectin (4 µg) were added to the pre-cleared protein (300 µg) and incubated with a gentle rotating at 4 °C overnight.

Similarly, the pre-cleared protein (300 µg) was added to the pre-cleared beads without the antibody to serve as a negative control. The IP reaction was incubated with fresh beads for an additional twenty-four hours. The beads were then pelleted with centrifugation at 13,000 rpm for 4 min and washed (2x) with precooled phosphate buffer saline. Following that, 20 µl of the IP lysate was mixed with 4x NuPAGE™ LDS sample buffer (Thermo Fisher) and heated at 90 °C for 5 min followed by 5 min on ice and loaded onto NuPAGE Bis-Tris protein gels for western blot analysis. For each IP reaction, 50 µg of the protein was included as an input in the gel.

2.8 Real-time quantitative PCR (qPCR)

2.8.1 Primers

A former postdoc in our group designed all primers used for qPCR. Each primer sequence's specificity was checked against the Refseq mRNA database, self-complementarity, melting temperature (Tm), and exon junction using the Primer-BLAST tool available on the National Centre for biotechnology information. Below Table 2.5 includes all primers used for RT-qPCR.

Table 2.5 Primers used for RT-qPCR

Gene	Forward primer (5'->3')	Reverse primer (5'->3')
CD24 NM_013230.3	GCTCCTACCCACGCAGATTTA	TGGTGGTGGCATTAGTTGGA
Notch1 XM_034929540.1	AAGCTGCATCCAGAGGCAAAC	TGGCATACACACTCCGAGAACAC
Cten NM_032865.5	CCTTCGTGTGCCAGCATTCC	GCACCTCCCAGTTCTCTCTGTG
ILK XM_003819084.3	AAGGTGCTGAAGGTTCGAGA	ATACGGCATCCAGTGTGTGA
FAK L05186.1	TCCTAATGTTG ATGCCTGCC	CCTTGAAAAGGCTTCACACC
E-cadherin NM_004360.4	CGTCCTGGGCAGAGTGAAT	TTTGAATCGGGTGTCGAGGG

N-cadherin NM_001792.4	AGGCTTCTGGTGAAATCGCA	TGCAGTTGCTAAACTTCACATTG
Vimentin NM_003380.3	CGGGAGAAATTGCAGGAGGA	AAGGTCAAGACGTGCCAGAG
Snail 1 NM_005985.3	AATCCAGAGTTTACCTTCCAGCA	TCCCAGATGAGCATTGGCAG
VEGFA XM_008958739	GAGCAAGACAAGAAAATCCC	CCTCGGCTTGTCACATCTG
PBGD (Reference)	GGAGCCATGTCTGGTAACGG	CCACGCGAATCACTCTCATCT

2.8.2 RNA extraction

Total RNA was extracted using GenElute™ Total RNA Purification Kit (Sigma-Aldrich) according to the manufacturer's protocol. Briefly, the cell pellets were lysed using 200 µl of lysis buffer containing β-Mercaptoethanol (1%) and mix by vortexing for 15 sec to dissolve the pellets completely. Then 200 µl of ethanol (100%) was added to the lysate and mix by vortexing for 10 sec. The lysate with ethanol was transferred to the binding column assembled with a collection tube, centrifuged for 1 min at 13,000 *xg* and the flow-through discarded. The spin column was washed with 400 µl with wash-1 buffer and centrifuged at 13,000 *xg* for 30 sec, and the flow-through was discarded. A master mix of DNase I Digestion (10 µl) with DNase buffer (70 µl) was prepared in a total volume of 80 µl/column and mixed by gentle inversion. The DNase master mix (80 µl) was added to the

column and incubated for 15 min at room temperature. After incubation, the column was washed with 400 µl of wash-1 buffer and centrifuged for 30 sec at 13,000 *xg* and the flow-through discarded. Next, the column was transferred to a new collection tube and washed two times with 500 µl of wash-2 buffer (containing ethanol), the first wash was centrifuged for 30 sec at 13,000 *xg,* and the second wash was centrifuged for two min at 13,000 *xg*. Finally, the column was placed into a new collection tube, and the RNA was eluted by adding 50 µl of elution buffer to the column and centrifuged for 1 min at 13,000 *xg*. The RNA concentration was quantified using a NanoDrop system (ThermoFisher Scientific).

2.8.3 Complementary DNA (cDNA) synthesis

The cDNA was synthesised from RNA templates as follows: 15 µl reverse transcription master mix per reaction was prepared by adding 0.5 µg random hexamers (Thermo Fisher Scientific) to 1-2 µg RNA, and nuclease-free water, incubated for 5 min at 70 °C, then by 5 min at 4 °C. Followed by making 10 µl/ reaction of the bulk mixture containing: 5µl M-MLV-RT buffer (5X Promega), 1.25 µl dNTPs (10mM, Promega), 1µl M-MLV-RT enzyme (Promega), 25U RNase inhibitor (0.625 µl) (Promega), made up to 10 µl with distilled water. Finally, 10 µl of the bulk mixture was added to the 15 µl M-MLV template: hexamer mix to a total volume of 25 µl and incubated for 1 hr at 37 °C, then 10 min at 95 °C.

2.8.4 RT-qPCR reaction

RT-qPCR was performed to determine the mRNA levels of CD24, Cten and EMT biomarkers (Table S3) using GoTaq® qPCR Master Mix with SYBR green (Promega). The qPCR was performed in a total volume of 20 µl per-reaction containing: 10 ng of cDNA, 0.250 µM each of the forward and reverse primers, 10 µl of GoTaq® qPCR Master Mix and made up to 20 µl with nuclease-free water. The PCR was run on the following thermal cycles: X1 cycle hot-start activation for 2 min at 95 °C, X40 cycles (denaturation at 95°C for 15 sec, annealing at 60 °C for 60 sec, extension at 72 °C for 60 sec), X1 cycle melting curve stage (95 °C for 60 sec, 55 °C for 30 sec, 95 °C for 30 sec). Relative mRNA levels of target genes in experimental conditions were normalised to porphobilinogen deaminase (PBGD, housekeeping control) and the empty vector control using Livak's comparative threshold cycle (2-ΔΔCT) method [197].

2.9 Immunofluorescence

2.9.1 CD24 and PSGL-1 staining

Cells were seeded at a density of 20×10^3 cells/well in a TC 8-wells chamber slide (Corning) and incubated at 37 °C in 5% CO2 for 24 hr. The following day, the cells were washed twice by phosphate-buffered saline (PBS), fixed by incubation in a 1:1 dilution of methanol and acetone precooled at -20°C for 20 min. Then rewashed twice with cold PBS and blocked for one hour with 1% BSA, 22.52 mg/ml glycine in PBS plus 0.1% tween 20. The cells

were stained with CD24 (SWA11) mouse anti-human antibody in a dilution of 1:100 or PSGL-1 anti-human in a dilution 1:200 (R&D system) and incubated overnight at 4°C. After incubation, they gently washed 3x/5 min with 0.1%Tween 20 in PBS (PBST) followed by adding secondary antibodies Alexa-Fluor 488 goat anti-mouse in a dilution of 1:100 (Invitrogen) and incubated for 60 min. Nuclei were stained by 15 min incubation with 4',6-diamidino-2-phenylindole (DAPI; Sigma-Aldrich) diluted 1:10000 of 1% BSA, followed by another 3x/5 min washes with PBST. The slides were mounted with Fluoroshield anti-fade mountant (Sigma Aldrich) and imaged using Leica DMI4000B microscope (20x objectives, confocal setup).

2.9.2 F-actin staining

Filamentous actin (F-Actin) was visualised by immunofluorescence. Cells were seeded at 2×10^4 cells/well in 8 well chamber slides (Corning) and incubated for 24 hr. They were fixed with a mixture of 4% paraformaldehyde and 5% sucrose for 10 min and permeabilised using 0.1% Triton X-100 in PBS (Sigma-Aldrich) for 5 min at room temperature. Cells were stained by incubating for 1 hr with Texas Red-X phalloidin (Thermo Fisher Scientific) in 100 µl of 3% bovine serum albumin (BSA, Fisher Scientific) diluted in PBS. The nuclei were stained by incubation with DAPI diluted 1:10,000 in 1% BSA for 15 min, and slides were mounted with Fluoroshield anti-fade mountant (Sigma-Aldrich). The slides were imaged using a confocal Leica DMI4000B microscope at x20 magnification.

2.10 Site-directed mutagenesis (SDM)

SDM was performed to mutate the potential two *N*-glycosylation sites (N36Q, N52) present in CD24 protein since these sites were thought to mediate CD24 activity in CRC. A flow chart below (Figure 2.1) briefly illustrates the steps of the SDM experiment.

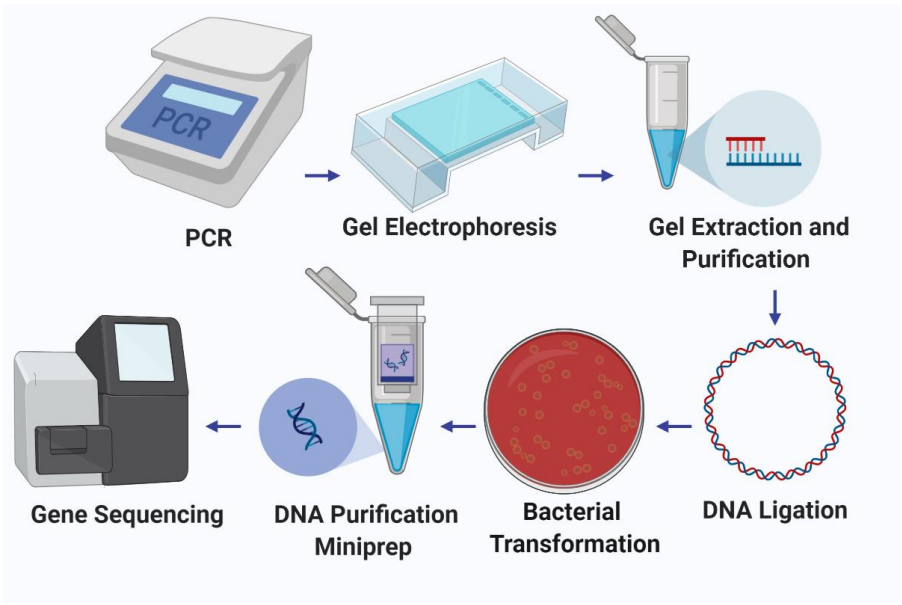


Figure 2.1 Flow diagram showing the process of the experimental plan for site-directed mutagenesis (SDM).

2.10.1 Primer designing

All primers for SDM were designed manually to match the following specification. Both forward and reverse primers were back-to-back to each other to avoid overlapping sequences and ensure they were amplified properly (Table 2.6). The mutation (AAC/AAT to CAA) was contained only

in the forward primers, and the mutant nucleotides were on the middle of the primer within 12-14 nucleotides on each side to anneal with the template strand. Also, the primers were checked for sequence homology to avoid dimerisation of the primers. To evaluate the gene specificity, the primers were subjected to the Blast tool available on the NCBI website.

Table 2.6 Site-directed mutagenesis Primers

SDM-Primers	Forward Phospho (5'->3')	Reverse Phospho (5'->3')
N36Q	GGAACTTCAAGTCAATCCTCCCAGAGT	AGTTGTTGTTTCACTGGAATAAATCTGCG
N52Q	CCAAATCCAACTCAAGCCACCACCAAG	GGCCAACCCAGAGTTGGAAGTACTC

2.10.2 Standard PCR

The Asparagine to Glutamine (N-Q) point mutation was performed using a Phusion SDM kit (Thermo Fisher Scientific, CAT# F541). In this assay, the mutation was introduced at each of the N-glycosylation sites (i.e. N36Q and N52Q) individually in a CD24 expression construct. Briefly, the PCR mix consisted of 10 µl Phusion HF buffer, 200 µM dNTPs, 0.5 µM each of forward and reverse primer (Table 6), 1 ng/µl template DNA, 0.02U/µl Phusion hot star II DNA polymerase (2U/µl), made up to 20 µl with nuclease-free water. Using the Primus 96 Thermal Cycler (MWG-Biotech Inc., Ebensburg, Germany), the cycling protocol was as follows: X1 initial denaturation cycle at 98 °C for 30-sec, X25 cycles of (denaturation at 98 °C for 10 sec,

annealing at 67-68 °C for 30 sec per primer, extension at 72 °C for 3 min), X1 final extension cycle at 72 °C for 10 min.

2.10.3 Agarose gel electrophoresis

One per cent of agarose gel was prepared by adding 0.5 g of agarose (Gibco-BRLife Technologies, USA) to 100 µl of 1X Tris-acetate EDTA (TAE) buffer (Bio-Rad). The mixture was heated in the microwave for 2-3 min until the agarose particles dissolve and cooled down to 50 °C. After that, five µl of GelRed® nucleic acid gel stain 10,000X (Biotium) was added to the mixture, poured into gel tray with a compatible comp, and allowed to sit at room temperature to solidify. The comp was removed, and the gel was transferred to the gel tank containing 1X TAE buffer. PCR products were tested on an agarose gel as the following: 4 µl of 6X DNA loading dye was added to 20µl of DNA and loaded into the gel. Then 1 KB of a ladder (Promega) was added to the first well, and the gel ran at 75 V for 1 hr. After running, the gel was placed in a Blue view transilluminator device to visualise the band, and the images were captured.

2.10.4 DNA purification from the agarose gel slice

The exact bands were excised from the agarose gel and placed into a clean Eppendorf tube. The excised bands' weight was then measured, and the DNA fragment was purified from the gel slice using GenEluteTM Gel extraction Kit (SIGMA-ALDRICH). Briefly, the three-gel volume of solubilisation solution was added to the gel slice and incubated at 55 °C for 10 min with a continuous vortexing every 2-3 min to dissolve the gel

completely. After that, the one-gel volume of isopropanol (100%) was added and mixed with the dissolved gel sample. The sample was loaded into a GenElute binding column with a volume of 700 µl and centrifuge for 1 min at 16,000 *xg*. The GenElute binding column was then washed by adding 700 µl of wash solution and centrifuge for one minute at 16,000 *xg*. The flow-through liquid was discarded, and the column was centrifuge without adding the wash solution to remove the excess of ethanol. The GenElute binding column was placed in a new collection tube. The DNA was eluted by adding 30 µl of preheated elution buffer at 65 °C to improve plasmid recovery and centrifuged for 1 min at 16,000 *xg*. Finally, the yielded DNA is ready for ligation.

2.10.5 Ligation and Bacterial transformation

The PCR products were circularized with T4 DNA ligase following the manufacturer's instructions (Thermo Fisher Scientific). 10-20 ng (made up to 5 µl) of DNA plasmid was added to 10 µl ligation reaction mixture (2.5 µl nuclease-free water, 2 µl rapid ligation buffer, and 0.5 µl T4 DNA ligase enzyme) and incubated at room temperature for 5 min. A ligation control mixture was prepared without T4 DNA ligase (Table 2.7). According to standard protocol, the ligated products were transformed into NEB 5α competent cells (New England BioLabs) using the above protocol.

Table 2.7 The component and concentration of the ligation reaction.

Reagent	Ten µl Ligation Reaction	Ten µl Ligation Control
Nuclease-free water	2.5 µl	3 µl
5X Rapid Ligation Buffer	2 µl	2 µl
Plasmid DNA	5 µl	5 µl
T4 ligase	0.5 µl	–

2.10.6 DNA purification (Miniprep)

Following the transformation, the GenElute™ HP Plasmid Mini-prep Kit (Sigma-Aldrich) was used to elute the plasmid. Briefly, according to manufacturer instructions, 3 ml of the bacterial culture was centrifuged at 13000 *xg* for 10 min, and the supernatant was discarded. This is followed by resuspending the pellet with 0.2 ml of re-suspension/RNase A solution, and then the resuspended cells were lysed by adding 0.2 ml of the lysis solution. After that, to neutralise the lysed cells, 0.35 ml of chilled neutralisation/binding solution and centrifuged at 13000 *xg* for 10 min. After placing the solution into a GenElute mini-prep binding column, 0.5 ml of column preparation solution was added and centrifuged for 1 min at 12,000 *xg*. Then the pre-cleared lysate was transferred to a binding column and centrifuged for 1 min at 12,000 *xg*. The flow-through was discarded, and the binding column was washed two times, first with 0.5 ml of optional wash solution followed by centrifugation for 1 min at 12,000 *xg* and discard

the eluate. The same procedure was applied for the second wash using the wash solution with ethanol and centrifuged again for 2 min without any additional wash solution to remove the excess of ethanol. After that, the binding column was transferred to a new collection tube, and the plasmid DNA was eluted by adding 0.1 ml of Elution solution.

2.10.7 Direct sequencing

Sanger sequencing was used to detect the presence of the targeted mutation and eliminated the presence of undesired mutations. Ten of the purified DNA plasmids from overnight bacterial culture were sent for Sanger DNA sequencing at a concentration of 100 ng/µl. T7 forward primers and BGH reverse primer present in our vector were used for sequencing in a concentration of 10 µg. The sequencing results were analysed using finch software and aligned via the BLAST2 alignment tool available on the National Centre for Biotechnology Information (NCBI) website to check the similarity between the nucleotide sequences.

2.11 In vitro functional studies

2.11.1 PrestoBlue cell viability assay

A cell viability assay was used to quantify cell numbers. Five thousand cells were seeded into each well of 96-well plates containing 100 µl growth medium and incubated 24 hr. The media was removed and washed twice with phosphate-buffered saline (PBS). The PrestoBlue® reagent (Invitrogen) was diluted in 10% FBS–DMEM (dilution of 1:10), and 100 µl

of the mixture was added to each well for 30 min. Fluorescence quantification of resazurin product (resorufin) was performed using the BMG FLUOstar OPTIMA plate reader (Ortenberg, Germany; FlexStation II, Molecular Devices, San Jose, CA, USA) at 544nm excitation and 612nm emission wavelength. Post-reading, the PrestoBlue® mixture was discarded, cells were washed once with medium and then replaced with fresh growth medium and incubated for a further 24 hr. Cell proliferation was evaluated at 0 hr, 24 hr, 48 hr, and 72 hr. Relative fluorescence unit (RFU) readings were normalised to the reading obtained at 0 hr and displayed relative to cell viability.

2.11.2 Transwell migration assay

Transwell inserts with 6.5 mm diameter and 8.0 µm pore size polycarbonate membrane, TC-treated, sterile (Costar, Corning) was used to measure the migration capability. The assay was performed in triplicate on at least two separate occasions. Firstly, 650 µl of fresh medium (containing 10% FBS) was added to the lower receiver wells as a chemoattractant. To the upper inserts, 1×10^5 cells were seeded in 100 µl DMEM (containing 0% FBS) and incubated at 37 °C in 5% CO2. After 24 hr of incubation, cell migration was assessed after 24 hr by incubating the inserts for 5 min in a new well-containing 650 µl trypsin-EDTA to detach the cells. Cells were then transferred to the original well and labelled with 3 µM calcein acetoxymethyl ester (Thermo Fisher Scientific) by incubation for 1 hr at 37 °C. Visualisation of the cell motility was performed using the Nikon Eclipse TiE

fluorescence microscope (fluorescein isothiocyanate filter, 488nm excitation). Four random microscopic fields per well were taken at ×10 magnification (see Appendix IV), and the cells were counted manually using ImageJ (National Institutes of Health, Bethesda, MD) and analysed by taking the average of the four fields per well.

2.11.3 Wound healing assay

Cell migration was also assessed using Culture-Insert 2-Well 24, ibiTreat (ibidi). Briefly, the inserts were placed in the centre of each well in 24-well plates. Following the manufacture's protocol, 1×10^6 cells were suspended in 1 ml DMEM (0% FBS), 70 µl/well was added to the insert and incubated for 24 hr. Following this, the inserts were removed, the cell layers were washed with PBS to remove non-adherent cells and covered by 1 ml fresh medium. Wound closure was visualised at 0 hr and 24 hr using a wide-field system Okolab microscope. Cell migration across the gap was measured by calculating the surface area of the wound using ImageJ. In this assay, 10 µg/ml mitomycin C (Sigma-Aldrich) was added to inhibit cell proliferation.

2.11.4 Matrigel invasion assay

The invasive capability of CRC cells was measured in the same way except that before seeding, the insert was prepared by coating in 300 µg/ml Matrigel (Matrigel® Matrix, Corning®). A day before commencing the experiment, the Matrigel was thawed overnight at 4 ºC. The Matrigel was prepared as follow: 300 µg/ml of Matrigel was diluted in 1000 µl of DMEM (containing 0% FBS) and added into the upper chamber to coat the filter

membrane of the Transwell and allowed to polymerise for 2 hr at 37 °C in 5% CO2. After incubation, the remaining liquid on the top layer of the formed Matrigel on the membrane was removed. The cells were then seeded, and the same protocol of transwell migration assay was used.

2.11.5 Adhesion assay

HUVECs ($5x10^3$/well) were cultured for 24-48 hr to confluence in a 96-well plate prior to initiating the assay. The HUVECs then was activated using either 20 ng/ml tumour necrosis factor-α (R&D System) for 4 hr or 1 U/ml of thrombin (Sigma-Aldrich) for 30 min, since the expression of P-selectin in endothelial cells appears at a lower level. CD24-expressing cells were serum-starved for 3 hr and then pre-labelled with calcein-AM. Next, the cancer cells were added directly to the formed monolayers of HUVECs and incubated at 37 °C in a CO2 incubator for 2-3 hr to adhere. After incubation, non-adherent cells were aspirated out, and the HUVECs were washed two times by PBS to remove the excess of medium and non-adherent cells (Figure 2.2). Then the RFU of the adherent cells were measured using FLUOstar OPTIMA Microplate Reader at (excitations 485nm/ emissions 520nm). In some experiments, P-selectin was knocked down in HUVECs using siRNA. The relative cell adhesion was determined by calculating the ratio of wash to non-washed cells for three repeated experiments.

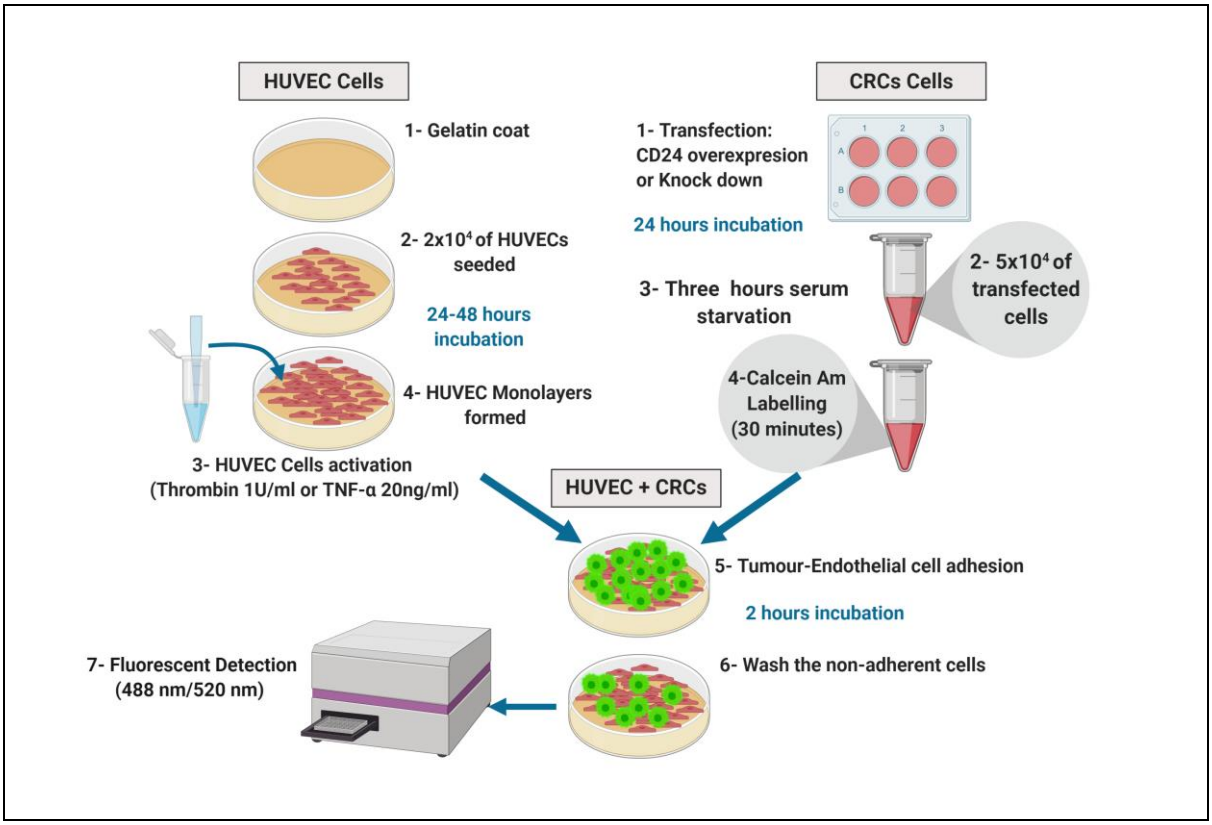


Figure 2.2 Illustration demonstrates the experimental steps of adhesion assay

2.11.6 Trans-endothelial migration assay

As with the adhesion assay, CRC cells were pre-labelled with calcein-AM before the experiment. Then the HUVECs were activated as the above assay. Using Transwells insert (6.5 mm diameter, 0.4 µm pore size), $1x10^5$ of HUVECs were seeded in the insert and incubated for 24-48 hr to form cells monolayer. Then $1x10^5$ of CD24-transfected cells were added on the top of the HUVECs monolayer in 100 µl of DMEM (0%FBS). The insert was afterwards transferred to the receiver well containing 650 µl of DMEM (10% FBS) as a chemoattractant. The plate was then incubated for an additional 24 hr at 37 °C. After incubation, the migrated cells were counted as the above Transwell migration assay.

2.12 Angiogenesis

2.12.1 Conditioned media preparation

The HCT116 and SW480 transfected with CD24 or EVC and SW620 with CD24 siRNA were chosen for conditioned medium preparation. A conditioned medium was briefly prepared by growing 2×10^6 cells to reach 70% confluency, and the medium was replaced with a serum-free DMEM medium. Conditioned medium was collected 24 hr after media change, and the media were filtered using a 0.2 µm filter (Sigma-Aldrich) and then stored at −20 °C for further experiments. After collecting the conditioned media, the attached cells were washed by cold PBS and lysed using RIPA buffer with protease phosphatase inhibitors. Then protein concentration was measured by BCA assay kit from Thermo Fisher Scientific and immunoblot with CD24 antibody.

2.12.2 Tube formation assay

Twenty-four hours before the experiment sat up, Matrigel® Matrix Basement Membrane (Corning) was placed on ice and thawed in the cold room (4 °C). 50 µl of 10 mg/ml Matrigel was added to a 96-well plate and incubated at 37 °C for 1 hr. After Matrigel polymerisation, 5 to $10x10^3$ in 96-well plate of HUVECs were cultured on the top of Matrigel and incubated with a conditioned medium for 12-16 hr at 37 °C. After incubation, the formed tube was quantified by counting the total tube's length from four fields per each replicate using ImageJ software.

For indirect co-culture tubule formation, Costar® Transwells, 0.4 µm pore size was used. First, HUVECs were cultured at a cell density of $5x10^4$ cells in the bottom coated well with 280 µl of Matrigel in a 24-well plate. After that, $1x10^4$ of either HCT116 overexpressed with CD24 or SW620 with silenced CD24 were added to the Transwells. Both cells were then incubated with 1:1 dilution of DMEM/ECGM-2 for 16 hr at 37 °C incubators. All images were taken at 10 X magnification, and the analysis was done by an angiogenesis analyser in ImageJ software. The experiments were performed using pre-chilled plates and tips to avoid Matrigel polymerisation. The total tube length was chosen to analyse the tube formation because other parameters, such as the number of nodes and the number of tubes, lead to false-positive results.

2.12.3 Enzyme-linked immunosorbent assay (ELISA)

The human VEGFA ELISA kit (R&D system) was used to detect the quantity of secreted VEGFA in CRCs transfected with CD24 according to the manufacturer's protocol. Before commencing the experiment, the supernatant was collected from CRC cells that were pre-transfected with CD24 or siRNA for CD24. Likewise, the ELISA buffers, biotin-conjugated, streptavidin-HRP, and VEGFA standards were prepared based on the manual's directions. The ELISA briefly was performed as follows: each well in the microwell strips was washed twice with 400 µl of wash buffer, and after the wash, the microwell strips was tapped on tissue paper to empty the wells. Then 100 µl of sample diluent was added in duplicate to all

standard wells. In the first well, 100 µl of the prepared standard (2000 pg/ml) was added to the diluent, mixed by pipetting and then 100 µl of the mixture transferred to the next well and the same procedure was done for the other wells respectively (Figure 2.3). Subsequently, 50 µl of sample diluent was added to the sample wells, followed by adding 50 µl of each sample in duplicate. The plate was covered with an adhesive film and incubated at room temperature for two hours in a microplate shaker. After incubation, the wells were emptied and washed four times, and then 100 µl of biotin-conjugated was added to all wells. Like the previous step, the plate was covered with an adhesive film and incubated for one hour at room temperature with shaking. Following incubation, the wells were washed four times, and 100 µl of streptavidin-HRP was added to each well, covered with a film and incubated for one hour at room temperature. After emptying and washing the wells, 100 µl of TMB substrate solution was added to all wells and incubated for 30 min at room temperature. Finally, the sample was incubated with 100 µl of stop solution for 20 min to inactivate the enzyme. The absorbance of both samples and standards were measured using Multitskan Ex from (Lab System) at 620nm. All assay stages were performed carefully to avoid intense exposure to light. The average absorbance values of each set of duplicate standards and samples were calculated and represented as means ±SD of two independent experiments.

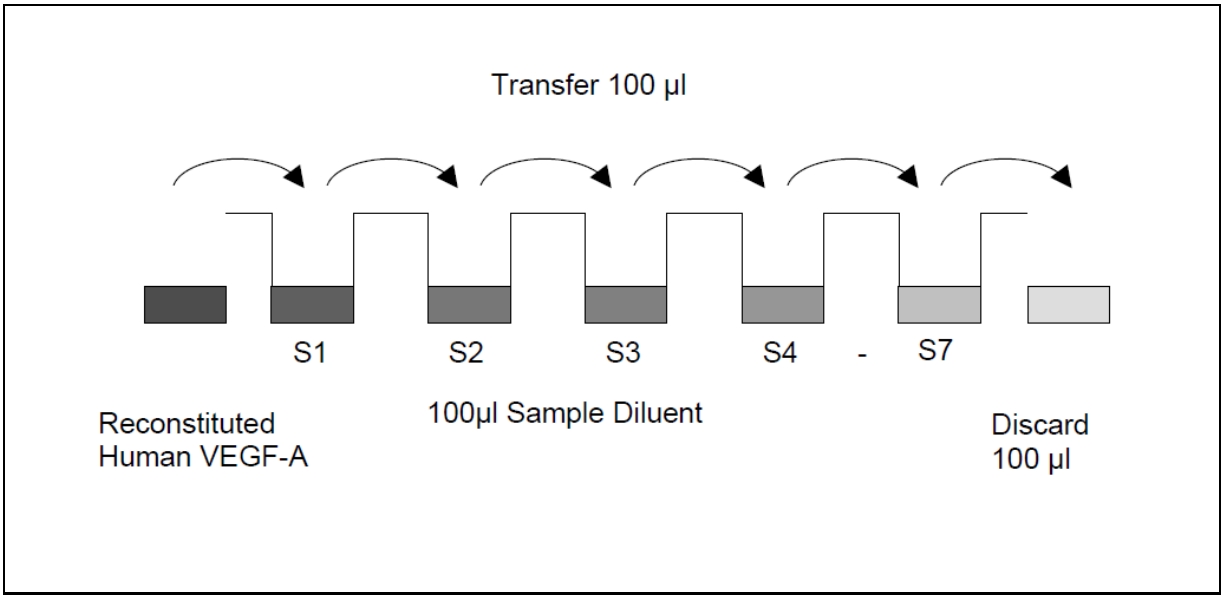


Figure 2.3 Representation of VEGF-A standard dilution ranging from 1000 to 15.6 pg/ml.

2.13 Flow cytometry

Transfection efficiency for cells overexpressed with $CD24^{WT}$ and mutant clones was determined using FACS analysis. Twenty-four hours post-transfection, the cells were detached using Trypsin-EDTA and resuspended in sterile-filtered PBA (Phosphate buffered saline +1% bovine serum albumin). The cell suspension was washed twice using PBA buffer by centrifugation for 5 min at 300 g. The cell was counted using an automated cell counter, and the volume of cells in PBA was adjusted at $2x10^6$/ml and pelleted by centrifugation at 300 *xg* for 5 min. Then the cell pellet was resuspended in 100 µl of PBA and incubated with CD24 (SWA11) antibody (1:100) for 60 min on ice. The antibody was washed twice by adding 1 ml of PBA and centrifuged for 5 min at 300 *xg*. The cell pellet resuspended in 100 µl of PBA and Alexa Fluor 488 goat anti-mouse conjugated secondary

antibody (Invitrogen) was added. The cells were incubated for 30 min on ice in the dark and then washed twice with PBA. The supernatant was removed, the pellet was vortexed and resuspended with 500 µl of 4% formaldehyde. The transfection efficiency was assessed by determining the ratio of cells overexpressing CD24 using a Beckman Coulter FC500 Flow Cytometer (Beckman Coulter) located in the Flow Cytometry Facility at Medical School, Queen Medical Centre. The data were analysed using Kaluza analysis 2.1 software (Beckman coulter Inc.), in which the cells were gated for identification of the CD24+ population using non-transfected cells as a control.

2.14 SWA11 antibody purification

Protein G sepharose column (Source Bioscience, ABE4749) was used to purify the SWA11 antibody from the supernatant (kindly gifted from Professor Altevogt Hans-Peter). Shortly, the SWA11 supernatant was diluted with 0.1 M sodium acetate pH 5.0. Then HiTrap Protein G sepharose column was equilibrated using 0.1 M sodium acetate pH 5.0. The mixture of supernatant and sodium acetate was applied to the column and allowed to pass. The flow-throw was applied repeatedly to the column several times. After that, the column was washed three times by 0.1 M sodium acetate pH 5.0. The bound antibody afterwards was eluted using 0.1 M glycine-HCL, pH 2.8. After elusion, the purified antibody concentration was quantified and ran in SDS-PAGE to check the IgG band using Coomassie Blue staining and Western blotting (see Appendix III).

2.15 Statistical analysis

Statistical analysis was performed using GraphPad Prism version 7.03 (La Jolla, CA) with the error bars representing the mean and standard deviation of mean (±SD) of at least two independent experiments. Before the statistical analysis, all data were examined for normality using the Shapiro-Wilk test.

To determine the normal distribution, the Student's T-test (non-parametric, two-tailed test) was applied for datasets that contain two groups (such as western blot).

For datasets that contain more than two groups, (such as cell proliferation, migration, invasion and cell adhesion), one-way and two-way analysis of variance (ANOVA) was applied with multiple comparisons by Tukey and Sidak tests, respectively. The difference with $P \leq 0.05$ was considered statistically significant.

Chapter 3: Investigation of the role of *N*-glycosylation sites on CD24 in CRC

3.1 Introduction

CD24 gene is located on chromosome 6q21, and it is a highly glycosylated, GPI protein [190]. Human mature CD24 comprises 31 amino acids, nearly half of which are serine and threonine residues, rendering it a mucin-like protein [78]. Analysis of the amino acid sequence shows that CD24 has 16 potential *O*-glycosylation sites and two potential *N*-glycosylation sites [190] (Figure 3.1). Because of the glycosylation, the CD24 protein molecular weight ranges from 30 kDa to 70 kDa [97, 187].

As mentioned in Chapter 1 (section 1.4.3), tumour metastasis follows distinct steps through EMT, a process in which epithelial cells undergo biological changes, including a loss in cell polarity, disruption of cell-cell adhesion and restructuring of the actin cytoskeleton. These changes contribute to the acquisition of invasive and migratory tendencies [198].

Interestingly, we have previously shown that CD24 induces cell invasion and migration in CRC, but it does not affect proliferation [120]. These changes are mediated through the CD24–Cten-ILK/FAK signalling pathways (unpublished data) and are accompanied by a 'cadherin switch', where epithelial cell expression of E-cadherin is reduced and N-cadherin expression, characteristic of mesenchymal cells, is increased [142].

Glycosylation is a post-translational modification involving the enzymatic glycosidic linkage reaction between the anomeric hydroxyl group of sugar and a protein [163]. As described in Chapter 1 (section 1.5.7.1.1), *N*-glycosylation is one of the common forms of protein glycosylation, primarily taking place in the endoplasmic reticulum and continuing in the Golgi apparatus. For *N*-glycosylation, carbohydrates are attached to an asparagine residue that appears in a specific sequon. Studies have shown that the target sequence for *N*-linked glycosylation is asparagine-(X)-serine/threonine, where X refers to any amino acid except for proline [168].

In normal growth and development, *O*-glycosylated residues have structural roles. In contrast, *N*-glycosylated residues have functional roles and have been shown to play a role in protein biology, including folding, secretion, stabilisation, conformation and trafficking to cellular and subcellular sites [164]. In cancer, several studies have indicated that *N*-glycosylated proteins play a role in tumour growth and development by enhancing the cancer cell's ability to evade immune detection, promoting uncontrolled proliferation, migration, and cell-cell adhesion [170, 173, 183].

The experimental work in this chapter is based on two observations. Firstly, *N*-glycosylation is thought to be important in mediating the function of many glycoproteins [167, 183, 184], including CD24. Secondly, *CD24* confers stemness features and enhances cell motility in CRC [120, 199]. Therefore, we hypothesised that CD24 might depend on *N*-glycosylation to

induce EMT and cell motility in CRC cells. To test this hypothesis, SDM was performed to mutate the two putative *N*-glycosylation sites in CD24 by substituting asparagine with glutamine. Mutant clones, including $CD24^{WT}$ and EVC, were overexpressed in two CD24 negative CRC cell lines: HCT116 and SW480 [200]. Following cell line transfection, functional studies on cell proliferation, migration and invasion *in vitro* and proteins and RNA analysis were performed.

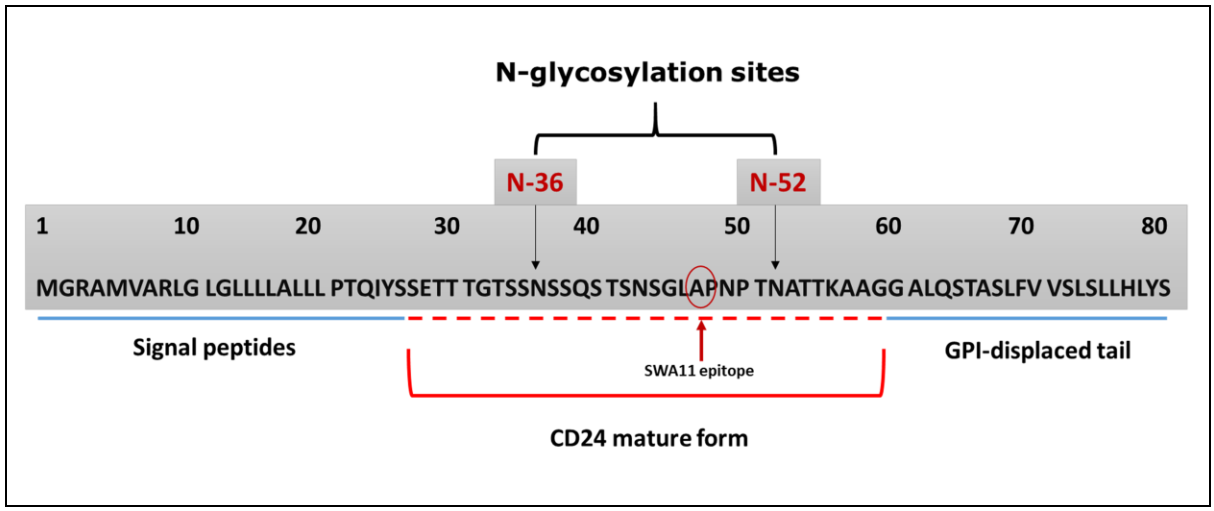


Figure 3.1 The sequence of CD24 glycosylation.

A simplified figure illustrates the sequence of the total CD24 protein (80 amino acids). The blue lines indicate signal peptide (1-26) and GPI-displaced tail (60-80). While the intermittent red lines indicate the mature form of CD24 (27-59) and within the mature peptide, the potential two glycosylation sites (N36 and N52) and the SWA11-Ab binding site are indicated by the arrows.

3.2 Results:

3.2.1 CD24^{WT} has no role in cell proliferation in CRC cells but induces cell motility

Our research group and others previously indicated that CD24 does not alter cell proliferation in CRC cells [120, 201]. To validate these findings, CD24 was ectopically overexpressed in HCT116 and SW480 cell lines (both express low levels of CD24 [200]) using a CD24-expressing vector. Likewise, CD24 was silenced in the SW620 cell line (highly expressed CD24) using small inhibitory RNA (siRNA). CD24 overexpression in HCT116 and SW480 and CD24 knockdown in SW60 were initially verified by Western blot, and both conditions affect the expression level of Cten, a downstream signalling molecule (Figure 3.2A and Figure 3.2B).

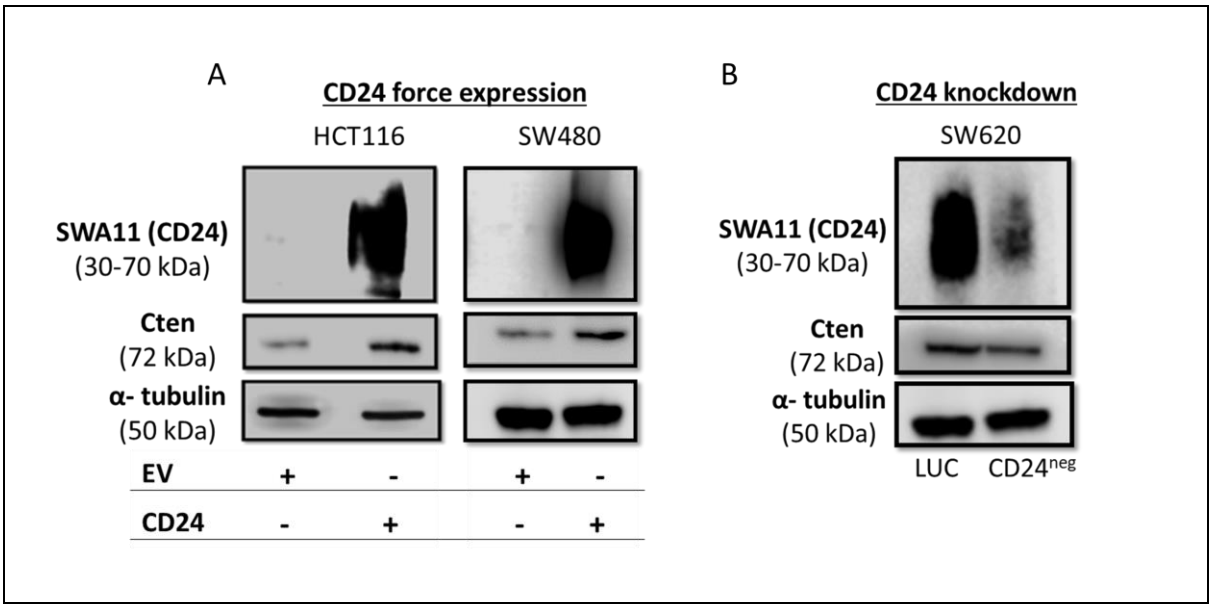


Figure 3.2 CD24 force expression and knockdown in CRC cells.

Western blot confirms a successful overexpression of CD24 in both HCT116 and SW480 cell lines compared to the empty vector control (EVC). It also showed an increase in the

level of Cten, a downstream signalling molecule (A). Similarly, Western blot showed that CD24 was successfully silenced in SW620 using siRNA compared to luciferase (LUC) siRNA control, but the level of Cten was reduced upon silencing of CD24 (B). Band intensities were analysed by image studio software. The western blot results shown are one representative experiment, repeated twice.

Cell proliferation was then assessed at 0 hr, 24 hr, 48 hr, and 72 hr by PrestoBlue proliferation assay (as described in Chapter 2, section 2.11.1). The data showed that the overexpression of CD24 in HCT116 and SW480 has no significant effect on cell proliferation when compared with the EVC (Figure 3.3A). Similar data were obtained in SW620, where silencing of CD24 did not change the cell proliferation compared to luciferase (LUC) siRNA control (Figure 3.3A).

Transwell migration and invasion assays (as described in Chapter 2, section 2.11.2) were used to determine CRC cells' ability to induce cell migration and invasion in the presence and absence of CD24. Compared to the EVC, CD24 overexpression in HCT116 and SW480 led to a significant increase in cell migration and invasion (Figure 3.3B). By contrast, silencing of CD24 in SW620 inhibited these activities compared to LUC (Figure 3.3C).

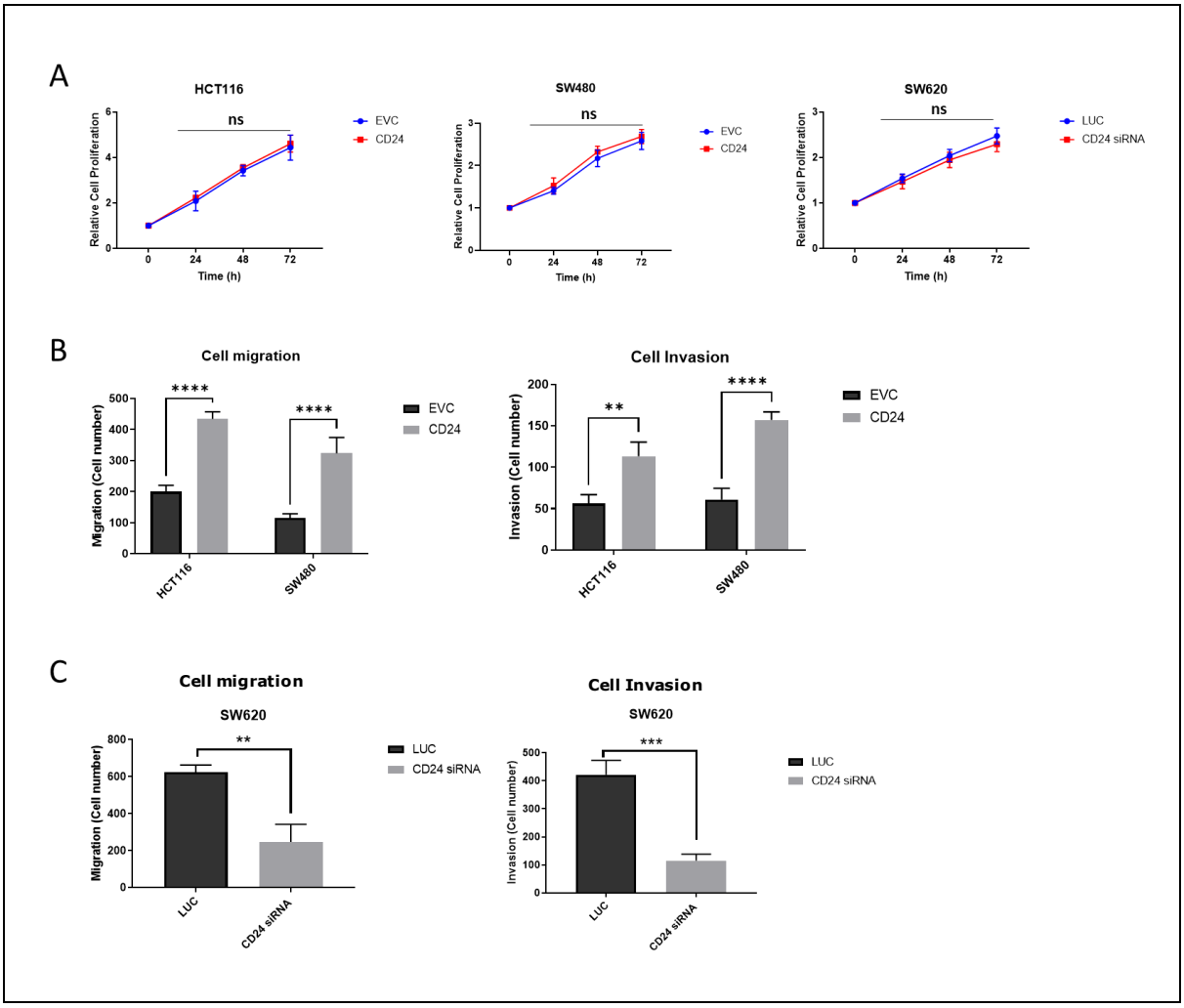


Figure 3.3 CD24 does not affect cell proliferation but induces migration and invasion in CRC cells.

PrestoBlue assay in both HCT116 and SW480 cells showed no significant difference between cells transfected with the CD24 expression vector and EVC. Likewise, SW620 transfected with CD24 siRNA or LUC did not affect cell proliferation (A), the graphs represent 6 replicates for each condition; collated results of two independent experiments shown. The relative cell proliferation displayed in cell proliferation graphs is based on the normalisation of relative fluorescence unit (RFU) readings to the reading obtained at 0 hr. Overexpression of CD24 resulted in a significant increase in cell migration and invasion of HCT116 and SW480 (B). However, silencing of CD24 in SW620 led to a reduction in the number of migratory and invasive cells (C). The statistical analysis were evaluated by GraphPad Prism by Two-way ANOVA with Tukey's multiple comparisons, $^{ns}P > 0.05$, **P <0.01, ***P <0.001, ****P <0.0001.

3.2.2 Mutating of functional sites of CD24 involved in CRC progression

3.2.2.1 Construction $CD24^{N36Q}$ and $CD24^{N52Q}$ plasmids

CD24 is *N*-glycosylated at N36 and N52 [190]. To create CD24 plasmids with a single mutation at either N36 or N52 sites, SDM has been performed as described in Chapter 2, section 2.10. Initially, two sets of back-to-back primers were designed to create $CD24^{N36Q}$ and $CD24^{N52Q}$. In this process, a codon for asparagine was replaced with a codon for glutamine (N-Q). Gradient PCR was performed to optimise the annealing temperature for both CD24 mutant construct primers. All tested annealing temperatures for $CD24^{N36Q}$ and $CD24^{N52Q}$ revealed discrete bands at 5747 kb (Figure 3.4A and Figure 3.4B). Thus, the annealing temperature of 68 °C was used for $CD24^{N36Q}$ and $CD24^{N52Q}$ amplification by PCR. As expected, gel electrophoresis displayed visible bands of the two mutant PCR products at the expected molecular weight (5747kb), and these bands were absent from the no-template controls (NTC) (Figure 3.4C). The amplified bands correspond to the mutant clones were extracted from the gel, ligated and transformed into NEF-5 competent cells (E-coli) as described in Chapter 2. The visible PCR product bands in the agarose gel along with the presence of colonies following bacterial transformation further validated a successful SDM. As clearly shown in Figure 3.4D, $CD24^{N36Q}$ and $CD24^{N52Q}$ plasmids were successfully ligated, as the colony-forming capacity was higher than that in NTC.

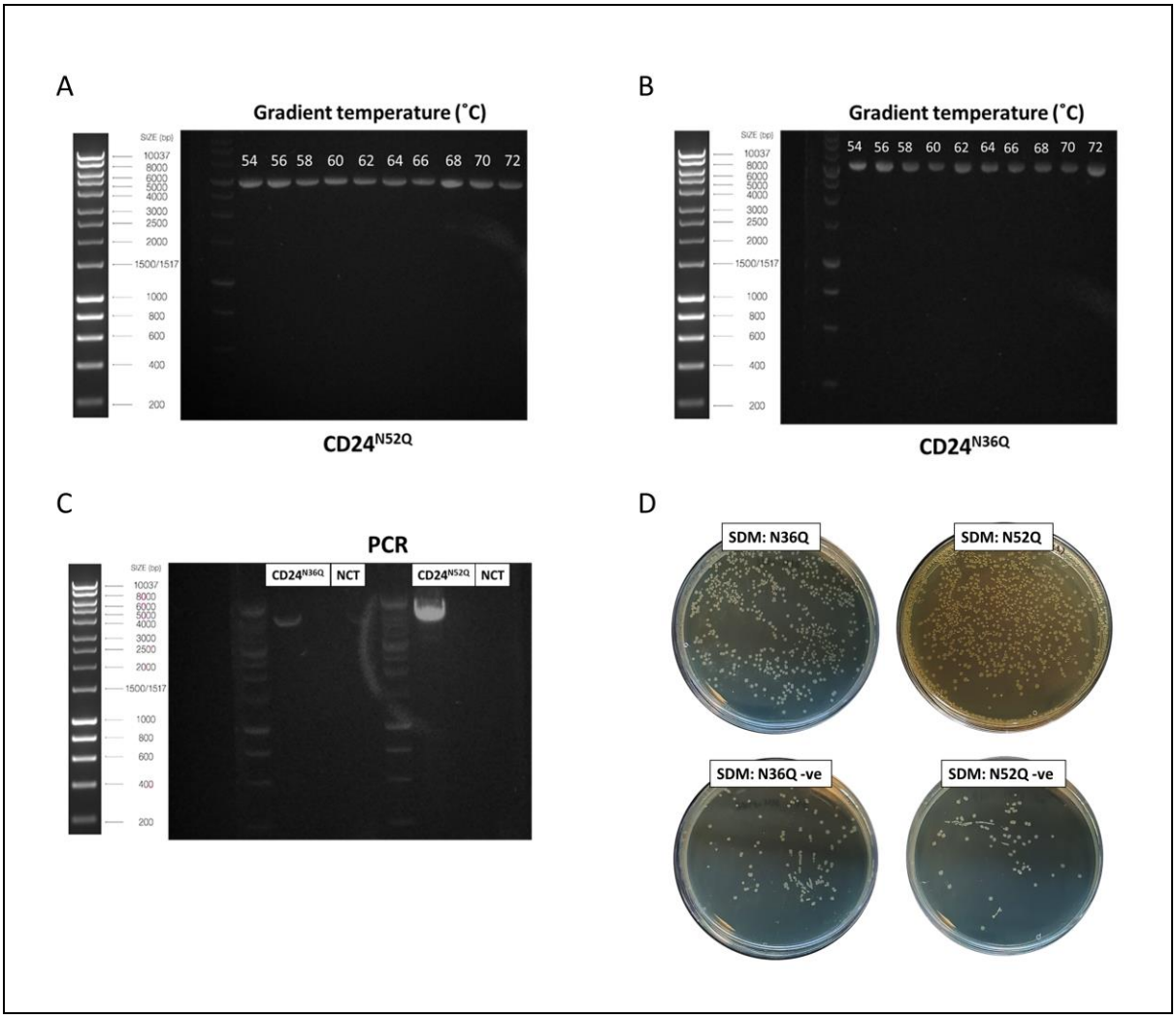


Figure 3.4 Construction of CD24 single mutant plasmids.

Site-directed mutagenesis was performed on two sets of back-to-back primers—a gradient PCR for optimising all designed primers' annealing temperatures (A and B). Gel electrophoresis of the $CD24^{N36Q}$ and $C24^{N52Q}$ products were amplified at 68°C and produced bright bands at the correct molecular size. No band was observed in the no-template control lane (NTC) (C). Bacterial transformation of the single mutant constructs showing a high colony number in mutant clones ($CD24^{N36Q}$, $CD24^{N52Q}$) compared to the negative control, confirming the successful ligation (D). The assay was performed in duplicate.

3.2.2.2 Validation of $CD24^{N36Q}$ and $CD24^{N52Q}$ mutation by direct sequencing

To confirm the presence of the required mutation and to eliminate the possibility of undesirable mutations, the plasmid DNA was sequenced using Sanger sequencing located at the sequencing facility, D-Floor, Queen's Medical Centre (QMC). First, ten colonies were selected, grown in LB media, and purified using a mini-prep technique as described in Chapter 2. All ten purified plasmids from the single mutant clones were sent for sequencing using universal primers, i.e., the T7 forward and BGH reverse primers present in our vector. The sequencing results were analysed using Finch software (Geospiza Inc., Seattle, WA), which confirmed the change of the asparagine codon (AAC/AAT) to the glutamine codon (CAA) in nine out of ten clones sent for sequencing (Figure 3.5A, B, and C). The sequencing results were also aligned via the BLAST2 alignment tool available on the National Center for Biotechnology Information (NCBI) website to check the similarity between the nucleotide sequences and confirm the full length of CD24 and mutant clones in the tested plasmids. The results showed that $CD24^{WT}$ plasmid identities were 100% similar to that of the CD24 reference gene (XM_024446293.1) in the NCBI GenBank (Figure 3.6A). However, the nucleotide sequences for $CD24^{N36Q}$ and $CD24^{N52Q}$ plasmids were 99% similar, and the change in AAC/AAT sequence to CAA was found (Figure 3.6B and Figure 3.6C), thereby confirming that the two mutant clones were successfully constructed.

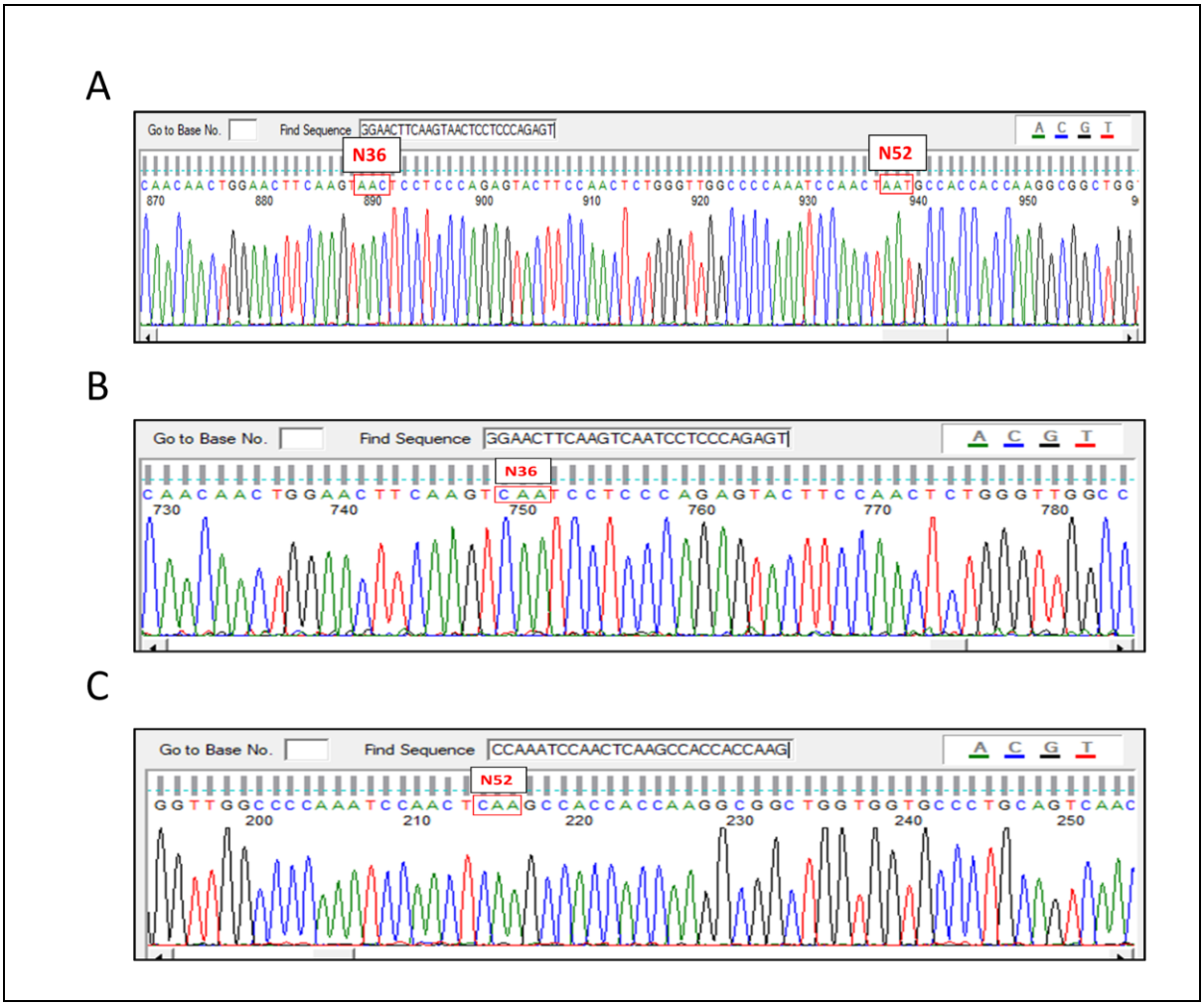
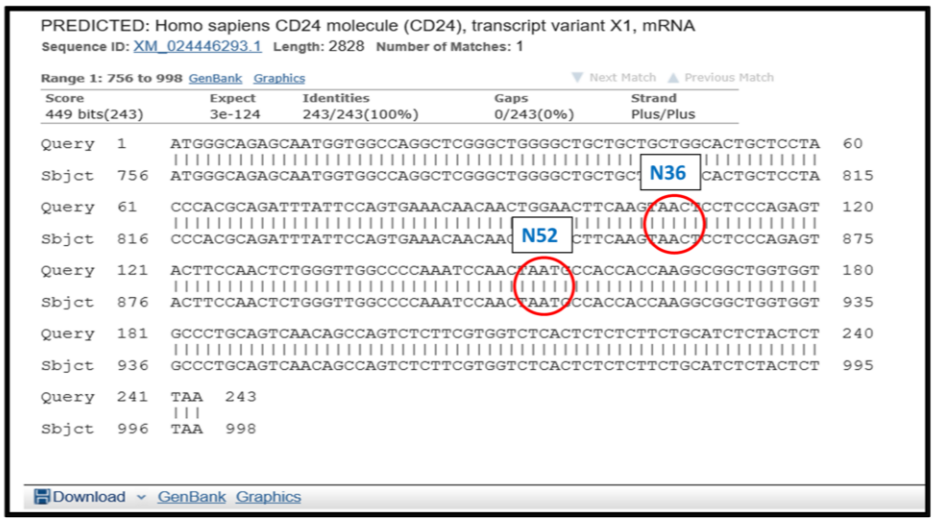


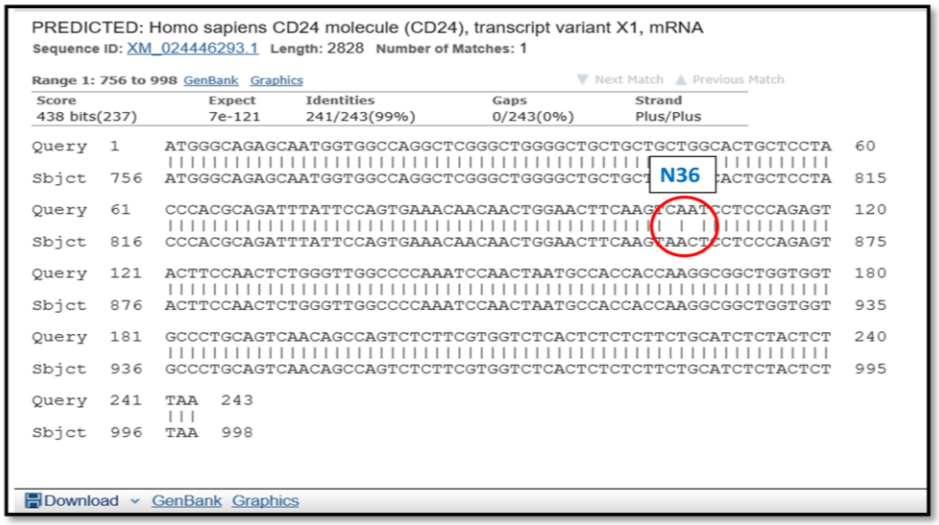
Figure 3.5 Gene sequencing analysis of CD24^{WT} and CD24^{N36Q} and CD24^{N52Q} using Finch software.

The sequence of CD24^{WT} indicated without any mutation at both N36 and N52 using the forward and complementary reverse primers (A). The sequencing data for N36 (B) and N52 (C) with introduced mutation. The sequences for CD24^{N36} and CD24^{N52} have been deposited on the GenBank database (accession MW694788 and MW694789) and will be released as soon as possible.

A


PREDICTED: Homo sapiens CD24 molecule (CD24), transcript variant X1, mRNA
Sequence ID: XM_024446293.1 Length: 2828 Number of Matches: 1
Range 1: 756 to 998 GenBank Graphics
Next Match Previous Match
Score 449 bits(243)
Expect 3e-124
Identities 243/243(100%)
Gaps 0/243(0%)
Strand Plus/Plus
Query 1 ATGGGCAGAGCAATGGTGGCCAGGCTCGGGCTGGGGCTGCTGCTGCTGGCACTGCTCCTA 60
Sbjct 756 ATGGGCAGAGCAATGGTGGCCAGGCTCGGGCTGGGGCTGCTGC CACTGCTCCTA 815
N36
Query 61 CCCACGCAGATTTATTCCAGTGAAACAACAACTGGAACTTCAAG CCTCCCAGAGT 120
Sbjct 816 CCCACGCAGATTTATTCCAGTGAAACAACAA CTTCAAG CCTCCCAGAGT 875
N52
Query 121 ACTTCCAACTCTGGGTTGGCCCCAAATCCAACTAATGCCACCACCAAGGCGGCTGGTGGT 180
Sbjct 876 ACTTCCAACTCTGGGTTGGCCCCAAATCCAACTAATGCCACCACCAAGGCGGCTGGTGGT 935
Query 181 GCCCTGCAGTCAACAGCCAGTCTCTTCGTGGTCTCACTCTCTCTTCTGCATCTCTACTCT 240
Sbjct 936 GCCCTGCAGTCAACAGCCAGTCTCTTCGTGGTCTCACTCTCTCTTCTGCATCTCTACTCT 995
Query 241 TAA 243
Sbjct 996 TAA 998
Download GenBank Graphics

B


PREDICTED: Homo sapiens CD24 molecule (CD24), transcript variant X1, mRNA
Sequence ID: XM_024446293.1 Length: 2828 Number of Matches: 1
Range 1: 756 to 998 GenBank Graphics
Next Match Previous Match
Score 438 bits(237)
Expect 7e-121
Identities 241/243(99%)
Gaps 0/243(0%)
Strand Plus/Plus
Query 1 ATGGGCAGAGCAATGGTGGCCAGGCTCGGGCTGGGGCTGCTGCTGCTGGCACTGCTCCTA 60
Sbjct 756 ATGGGCAGAGCAATGGTGGCCAGGCTCGGGCTGGGGCTGCTGC CACTGCTCCTA 815
N36
Query 61 CCCACGCAGATTTATTCCAGTGAAACAACAACTGGAACTTCAAG CCTCCCAGAGT 120
Sbjct 816 CCCACGCAGATTTATTCCAGTGAAACAACAACTGGAACTTCAAG CCTCCCAGAGT 875
Query 121 ACTTCCAACTCTGGGTTGGCCCCAAATCCAACTAATGCCACCACCAAGGCGGCTGGTGGT 180
Sbjct 876 ACTTCCAACTCTGGGTTGGCCCCAAATCCAACTAATGCCACCACCAAGGCGGCTGGTGGT 935
Query 181 GCCCTGCAGTCAACAGCCAGTCTCTTCGTGGTCTCACTCTCTCTTCTGCATCTCTACTCT 240
Sbjct 936 GCCCTGCAGTCAACAGCCAGTCTCTTCGTGGTCTCACTCTCTCTTCTGCATCTCTACTCT 995
Query 241 TAA 243
Sbjct 996 TAA 998
Download GenBank Graphics

C

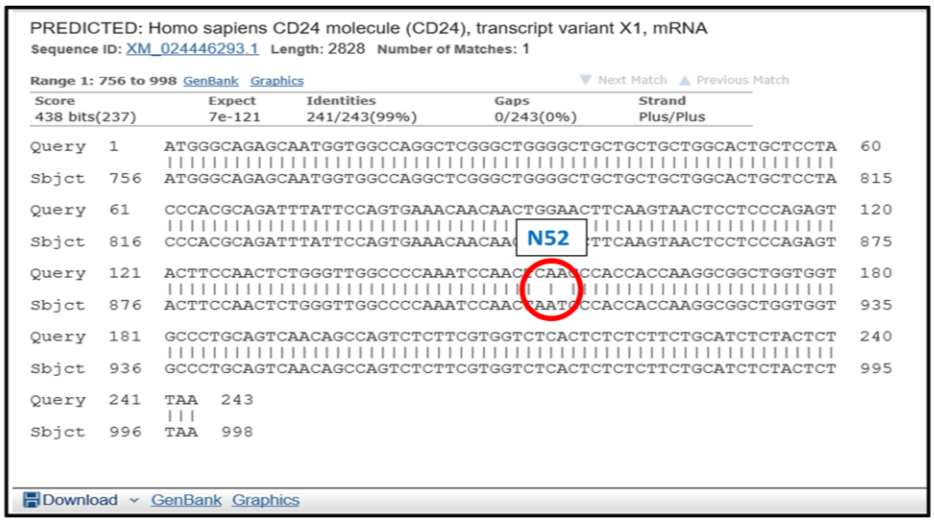

PREDICTED: Homo sapiens CD24 molecule (CD24), transcript variant X1, mRNA
Sequence ID: XM_024446293.1 Length: 2828 Number of Matches: 1
Range 1: 756 to 998 GenBank Graphics
Next Match Previous Match
Score 438 bits(237)
Expect 7e-121
Identities 241/243(99%)
Gaps 0/243(0%)
Strand Plus/Plus
Query 1 ATGGGCAGAGCAATGGTGGCCAGGCTCGGGCTGGGGCTGCTGCTGCTGGCACTGCTCCTA 60
Sbjct 756 ATGGGCAGAGCAATGGTGGCCAGGCTCGGGCTGGGGCTGCTGCTGCTGGCACTGCTCCTA 815
Query 61 CCCACGCAGATTTATTCCAGTGAAACAACAACTGGAACTTCAAGTAACTCCTCCCAGAGT 120
N52
Sbjct 816 CCCACGCAGATTTATTCCAGTGAAACAACAA TTCAAGTAACTCCTCCCAGAGT 875
Query 121 ACTTCCAACTCTGGGTTGGCCCCAAATCCAAC CCACCACCAAGGCGGCTGGTGGT 180
Sbjct 876 ACTTCCAACTCTGGGTTGGCCCCAAATCCAAC CCACCACCAAGGCGGCTGGTGGT 935
Query 181 GCCCTGCAGTCAACAGCCAGTCTCTTCGTGGTCTCACTCTCTCTTCTGCATCTCTACTCT 240
Sbjct 936 GCCCTGCAGTCAACAGCCAGTCTCTTCGTGGTCTCACTCTCTCTTCTGCATCTCTACTCT 995
Query 241 TAA 243
Sbjct 996 TAA 998
Download GenBank Graphics

Figure 3.6 Mutant constructs alignment using (BLAST2) tool.

BLAST2 tool of $CD24^{WT}$ plasmid showing 100% of nucleotide homology (A). The single-mutant clones showed the desired mutation at N36 (highlighted), i.e., AAC to CAA (B), and N52, i.e., AAT to CAA (C) with 99% homology in nucleotides sequence.

3.2.2.3 Construction of $CD24^{N[36,52]Q}$ plasmid

The abovementioned procedure used to create single mutant plasmids was also performed to produce a double mutant plasmid of CD24 at both N36 and N52 sites. In this process, the double mutation was produced either by using $CD24^{N36Q}$ plasmid with N52 primers or $CD24^{N52Q}$ plasmid with N36 primers. The gradient PCR was performed to optimise the annealing temperature for the designed primers, which showed a distinct band in agarose gel at all of the examined temperatures. Therefore, the annealing temperature of 68 °C was also chosen for PCR (Figure 3.7A). Both primers that contain the desired mutation in the presence of single mutant plasmids have been amplified. After running the PCR products in 1% agarose gel, a visible band of $CD24^{N[36,52]Q}$ mutant construct appeared at the expected molecular weight, 5747 kb, and there was no visible band in the NTC (Figure 3.7B).

$CD24^{N[36,52]Q}$ was ligated using a T4 ligase enzyme described above. In this step, no ligase enzyme was added for the control conditions. After ligation, the plasmids were transformed into competent cells (E. coli) on agar plates that contained a specific antibiotic. The transformation reaction shows a

higher number of growing colonies of CD24$^{N[36,\ 52]Q}$ than the number of colonies in the NTC (Figure 3.7C).

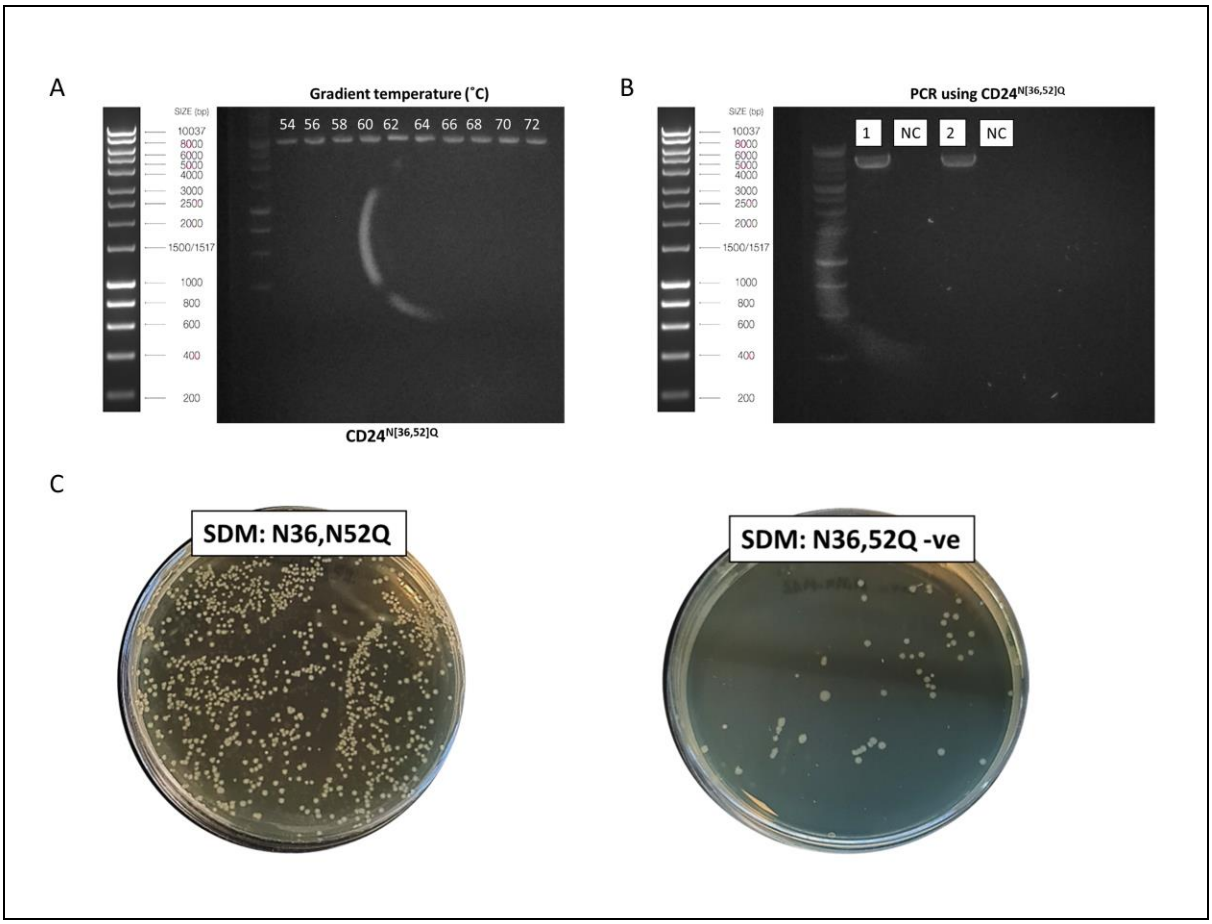


Figure 3.7 Construction of CD24 double mutant plasmids.

SDM was performed on either CD24^{N36Q} or C24^{N52Q} plasmid—a gradient PCR for optimising all designed primers' annealing temperature (A). Gel electrophoresis of the CD24$^{N[36,52]Q}$ product was amplified at 68 °C, and bright bands were produced at the correct molecular size and absence of a band in NCT (B). Bacterial transformation of the double mutant constructs showing high colony-forming in CD24$^{N[36,52]Q}$ plasmid compared to the negative control, confirming the successful ligation (C). The assay was performed in duplicate.

3.2.2.4 Validation of $CD24^{N[36,52]Q}$ mutation by direct sequencing

After the bacterial transformation, the growing bacteria were grown further by picking ten distinct pure colonies from ligated $CD24^{N[36,52]Q}$. Each colony was re-cultured separately in the LB broth medium with selective antibiotics for 16 hr. The multiplied plasmids in the LB broth were purified using the mini-prep technique. The ten purified $CD24^{N[36,52]Q}$ plasmids from overnight bacterial culture were sent for sequencing and analysed using Finch software. The sequencing results indicated the mutation at both N36 and N52 sites in ten clones out of ten sent for sequencing. Likewise, the alignment tool showed 98% similarity in the nucleotide sequence of $CD24^{N[36,52]Q}$ plasmid (Figure 3.8A, and Figure 3.8B); this verified the conversion of AAC/AAT sequence to CAA, confirming the successful construction of $CD24^{N[36,52]Q}$. The sequence for $CD24^{N[36,52]Q}$ has been deposited on the GenBank database (accession MW694790) and will be released as soon as possible.



Figure 3.8 Gene sequencing analysis of CD24$^{N[36,52]Q}$ using Finch software and alignment tool (BLAST2).

The sequence of CD24$^{N[36,52]Q}$ showed the desired mutation at both N36 and N52 (A). The BLAST2 tool indicates the change from AAC to CAA in the N36 site and the change of the AAT sequence to CAA in the N52 site with 98% homology in nucleotides sequence (B).

3.2.3 Mutant constructs show overexpression of CD24

The successful creation of the $CD24^{N36Q}$, $CD24^{N52Q}$, and $CD24^{N[36,52]Q}$ expression constructs was confirmed by direct sequencing (Figure 3.5 and Figure 3.7). The mutant expression constructs, alongside expression constructs for $CD24^{WT}$ and EVC, were transfected into HCT116 and SW480 cells. Western blotting also confirmed that mutant protein from all the constructs was successfully expressed in both cell lines (Figure 3.9A and Figure 3.9B).

It is well known that heavily glycosylated proteins, such as CD24, produce smeared bands on Western blotting, and the appearance may be influenced by both the pattern and amount of glycosylation. Since we altered putative *N*-glycosylation sites, a change in the banding pattern would be expected in the mutant protein if they were true glycosylation sites. However, assessment of expression levels and protein size is not reliable in Western blots of glycosylated proteins. To ensure that the banding alterations were not due to changes in expression of the core protein caused by an unidentified mutation in the plasmid, the lysates were digested using an *N*-glycosylation digestion mix (Neuraminidase and PNGase F enzymes) to remove sugar residues prior to Western blotting. A single 10kDa band was observed in all conditions, and similar levels of both mutant and wild-type proteins were shown to be expressed (Figure 3.9C and Figure 3.9D). This confirmed that any changes seen were due to changes in glycosylation rather than changes in protein expression.

Evaluation of the banding pattern shows that, compared to the wild-type protein, the protein expressed by both $CD24^{N36Q}$ and $CD24^{N52Q}$ ran more quickly and was less smeared in the western blot. Thus, in both cases, the protein appeared to be less glycosylated, and in both cases, the mutated protein had a similar pattern suggesting that the level of glycosylation was similar at each of these sites. Consistent with this, the protein expression by the construct $CD24^{N[36,52]Q}$ ran more quickly than that expressed by either of the single mutant constructs. The double mutant protein still had some smearing and did not run as quickly as the protein following neuraminidase digestion. This suggests that there is residual acetylation in the double mutant protein and, since the *N*-glycosylation sites have been removed, this must represent *O*-glycosylation. The appearances suggest that the majority of glycosylation in CD24 is at the *N*-glycosylation sites.

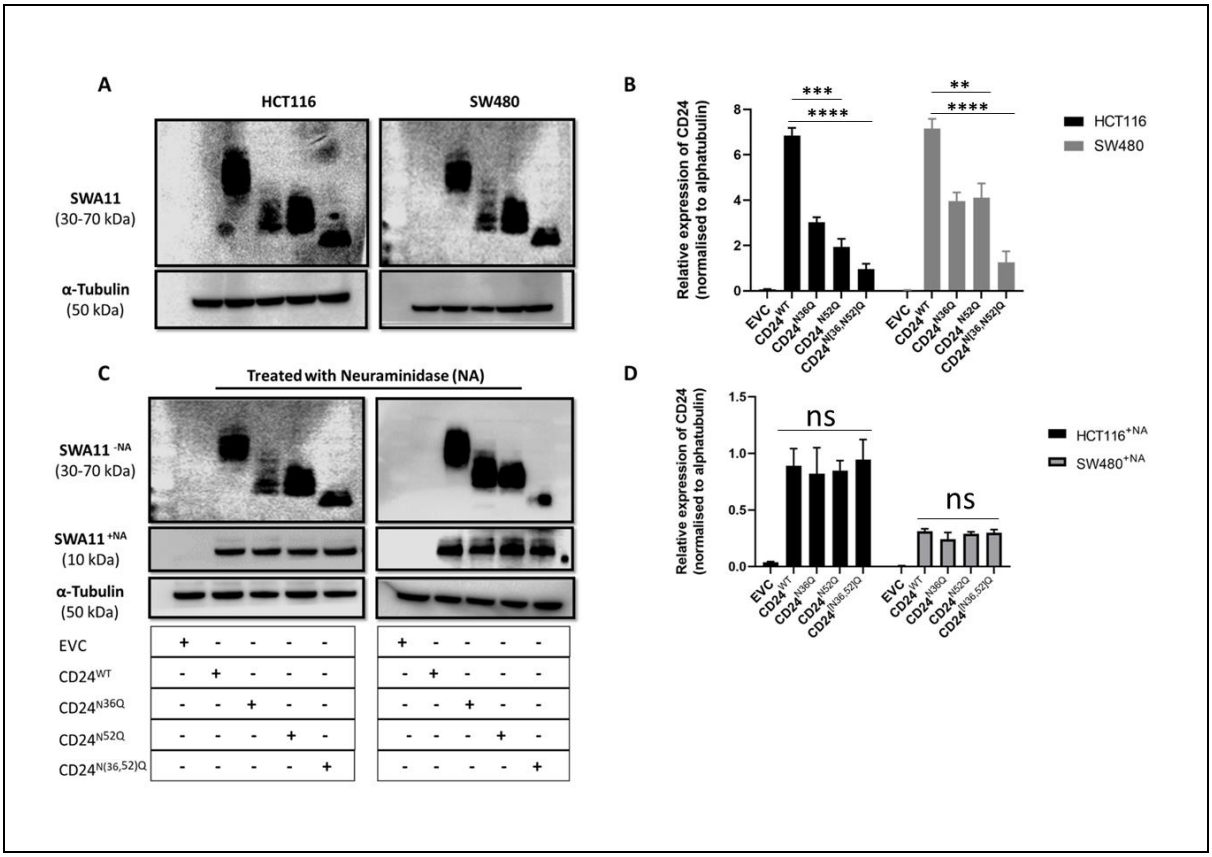


Figure 3.9 The expression level of CD24 shows variable glycosylation in the mutant constructs.

All mutant constructs were successfully overexpressed in both HCT116 and SW480 with band variation compared to $CD24^{WT}$ in Western blot (A). Densitometry and quantification of Western blot normalised to alpha-tubulin (B). After neuraminidase digestion, the relative protein expression of CD24 in HCT116 and SW480 cells expressing $CD24^{WT}$ and CD24 mutant constructs showed similar bands at approximately 10kDa (C). The bar graph (D) represents the quantitative densitometry analysis of Western blot for CD24 protein normalised to alpha-tubulin. The results shown are one representative experiment with three biological replicates. The band intensities were analysed by image studio software and compared using GraphPad Prism with Student's t-test (two-tailed, unequal variance), **P <0.01, ***P <0.001, ****P <0.0001. Abbreviation: -NA, with Neuraminidase; +NA, without Neuraminidase.

3.2.4 Transfection efficiency of CD24 and CD24 mutant constructs in CRC cells

Transient transfection was to be performed in HCT116 and SW480 using CD24-expressing vector or CD24 mutant clones. After transfection, the cells would be used for various experiments to study the effect of introducing these plasmids on cell activities. It was, therefore, necessary to confirm that transfection efficiency is relatively similar for all constructs and had not been altered by site-directed mutagenesis. Flow cytometry was used to calculate the percentage of CRC cells expressing CD24 following transfection. In this assay, the transfected cells were stained with a CD24 antibody (described in Chapter 2, section 2.13) and quantified by Beckman Coulter FC500. Data analysis, using Kaluza software, showed that in both HCT116 and SW480 cell lines, the transfection efficiency for $CD24^{WT}$ and all mutant constructs, including $CD24^{N36Q}$, $CD24^{N52Q}$, and $CD24^{N[36,52]Q}$, had the same efficiency of approximately 50% to 70% compared to the untransfected cells (Figure 3.10A and Figure 3.10B).

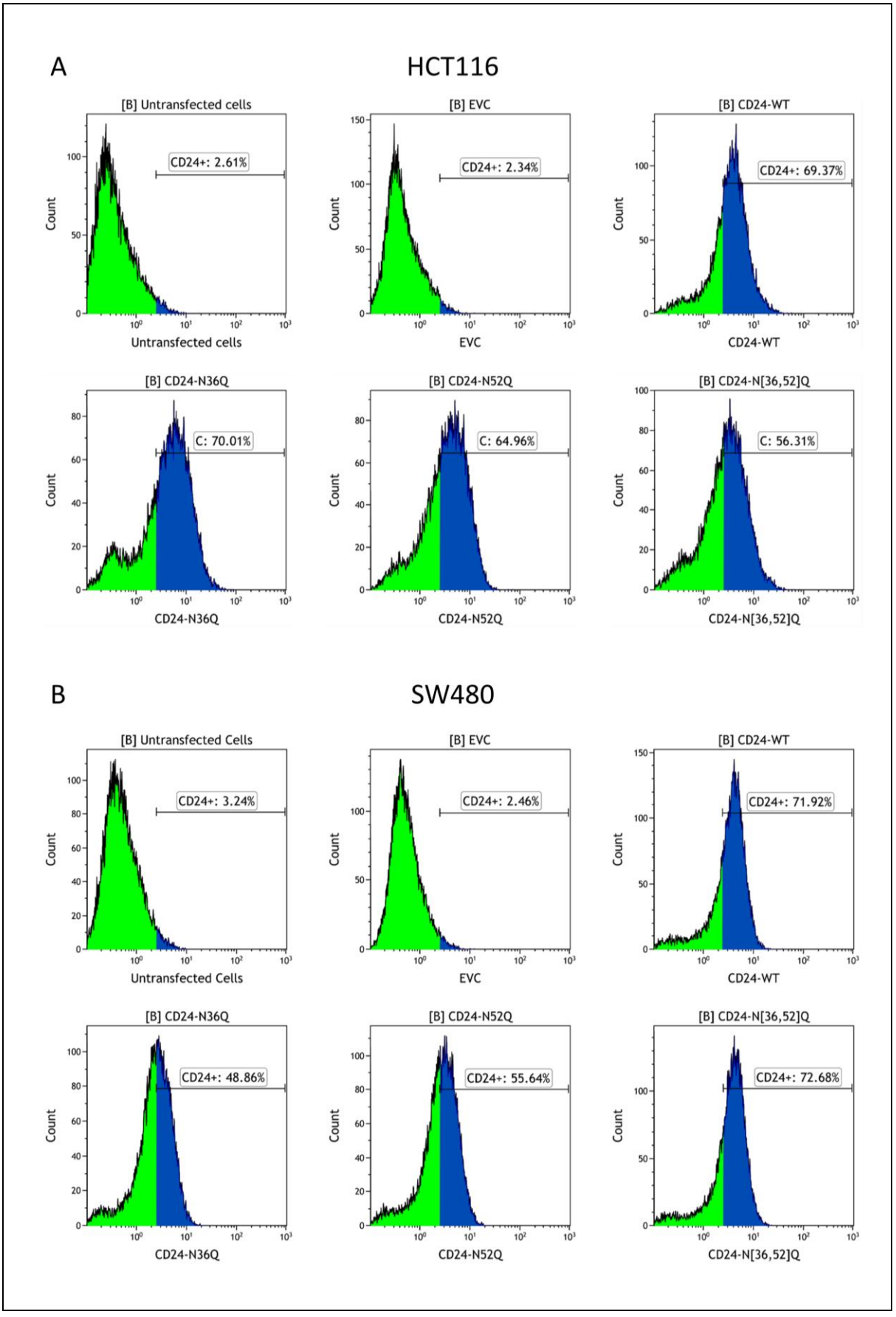

A
HCT116
[B] Untransfected cells
CD24+: 2.61%
Count
Untransfected cells
[B] EVC
CD24+: 2.34%
Count
EVC
[B] CD24-WT
CD24+: 69.37%
Count
CD24-WT
[B] CD24-N36Q
C: 70.01%
Count
CD24-N36Q
[B] CD24-N52Q
C: 64.96%
Count
CD24-N52Q
[B] CD24-N[36,52]Q
C: 56.31%
Count
CD24-N[36,52]Q
B
SW480
[B] Untransfected Cells
CD24+: 3.24%
Count
Untransfected Cells
[B] EVC
CD24+: 2.46%
Count
EVC
[B] CD24-WT
CD24+: 71.92%
Count
CD24-WT
[B] CD24-N36Q
CD24+: 48.86%
Count
CD24-N36Q
[B] CD24-N52Q
CD24+: 55.64%
Count
CD24-N52Q
[B] CD24-N[36,52]Q
CD24+: 72.68%
Count
CD24-N[36,52]Q

Figure 3.10 Evaluation of transfection efficiency of $CD24^{WT}$ and CD24 mutant constructs by flow cytometry.

HCT116 and SW480 were analysed 24h post-transfection with $CD24^{WT}$ and CD24-mutant constructs. The percentage of CD24 positive cells was indicated for each condition in both HCT116 (A) and SW480 (B). The untransfected cells and the cells expressing EVC served as controls. The shift to the right indicates the CD24+ cell population.

3.2.5 Loss of CD24 *N*-glycosylation sites results in increased cell proliferation

Our previous studies on the effect of CD24 on cell proliferation have shown that CD24 played no role in cell proliferation [202]. In order to investigate whether the N-glycosylation sites of CD24 play a role in regulating cell proliferation, a PrestoBlue cell proliferation assay was used to determine proliferation at four consecutive time points (Figure 3.11A and Figure 3.11B). As expected, there was no difference in cell numbers between cells transfected with $CD24^{WT}$ and cells transfected with EVC (i.e., $CD24^{WT}$ vs. EVC) in either HCT116 or SW480. Unexpectedly, transfection with the single-site mutant constructs $CD24^{N36Q}$ and $CD24^{N52Q}$ (i.e., $CD24^{N36Q}$ *vs*. $CD24^{WT}$ and $CD24^{N52Q}$ *vs*. $CD24^{WT}$) resulted in a significant increase in cell numbers from 24 hours onwards in both cell lines ($P < 0.0493$ at 24h and $P < 0.001$ at the other time points). The size of the effect was similar in each mutation, and no statistical difference was observed for $CD24^{N36Q}$ *vs.* $CD24^{N52Q}$. When the cells were transfected with the double mutant construct, the cell number was significantly greater than that seen in single mutant transfections, i.e., $CD24^{N[36,52]Q}$ *vs*. $CD24^{N36Q}$ and $CD24^{N[36,52]Q}$ *vs*.

$CD24^{N52Q}$ (P <0.0001 at each time point). The observations were similar in both cell lines, and the greatest effect was seen in the comparison of the double mutant with wild type, i.e., $CD24^{N[36,52]Q}$ *vs*. $CD24^{WT}$, P < 0.0001 at each time point for both HCT116 and SW480.

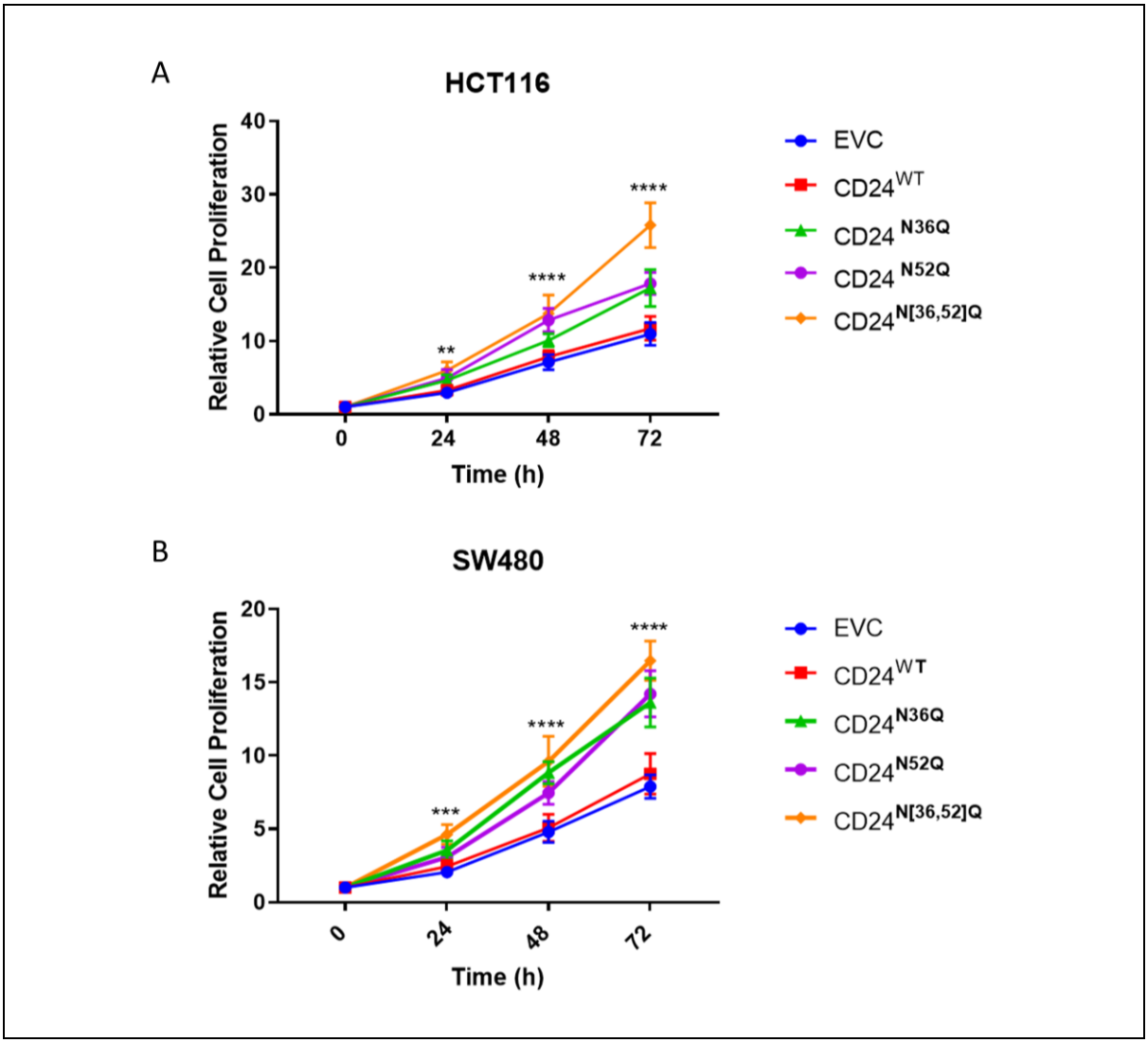


Figure 3.11 Mutations in the *N*-glycosylation sites of CD24 influence cell proliferation.

Relative cell proliferation values of HCT116 (A) and SW480 (B) cell lines expressing CD24 and CD24 mutant constructs. A significant increase in cell viability for all mutant constructs compared to the EVC and $CD24^{WT}$ at 24hrs (***P ≤ 0.001), 48hrs and 72hrs (****P ≤ 0.0001, respectively). The graphs represent 6 replicates for each condition; collated results of two independent experiments shown. Relative cell proliferation shows the relative fluorescence unit (RFU) readings that normalised to the reading obtained at 0hr. Results are representative of three biological replicates, and error bars indicate the SD. The multiple comparison was performed using two-way ANOVA test with Tukey's test (**P <0.01, ***P <0.001, ****P <0.0001).

3.2.6 Loss of CD24 *N*-glycosylation sites results in loss of motility induction

We have previously shown that CD24 can induce cell motility. Examinations into the potential role of *N*-glycosylation in cell migration were performed by comparative transwell migration assays and wound-healing assays using cells transfected with mutant constructs and $CD24^{WT}$. As expected, and in concordance with our previous data, $CD24^{WT}$ *vs*. EVC demonstrated a marked increase in transwell cell migration in HCT116 and SW480 (P <0.0001 for each) (Figure 3.12A). Transfection of the single mutant plasmids ($CD24^{N36Q}$ *vs*. EVC and $CD24^{N52Q}$ *vs*. EVC) showed increased cell migration, but this was significantly less than that induced by $CD24^{WT}$ ($CD24^{N36Q}$ *vs*. $CD24^{WT}$ and $CD24^{N52Q}$ *vs*. $CD24^{WT}$, P= 0.0018 for HCT116, P= 0.0045 for SW480). Transfection with the double mutant $CD24^{N[36,52]Q}$ caused a further reduction in cell transwell migration compared to $CD24^{WT}$ ($CD24^{N[36,52]Q}$ *vs*. $CD24^{WT}$, P <0.0001 in both HCT116 and SW480) (Figure 3.12A). The double mutant retained some ability to induce motility compared to the EVC in HCT116 ($CD24^{N[36,52]Q}$ *vs*. EVC, P <0.0114), but this ability appeared to be lost in SW480 (Figure 11A; $CD24^{N[36,52]Q}$ *vs*. EVC, P= not significant (NS).

Cell motility was also tested using a wound-healing assay, in which the residual wound size was measured over 24 hours (as described in Chapter 2). The data in Figure 3.12C and Figure 3.12D replicated those seen in the transwell migration assay in as much as the residual wound was significantly smaller in size in $CD24^{WT}$ vs EVC in both cell lines (HCT116 P

<0.0001, SW480 P <0.0001). The residual wound size was significantly smaller in $CD24^{N36Q}$ vs. EVC (HCT116 P > 0.0046, SW480 P <0.0072) and $CD24^{N52Q}$ vs. EVC (HCT116 P <0.0002, SW480 P<0.0045), but the residual wound was significantly smaller in $CD24^{WT}$ vs. $CD24^{N36Q}$ (HCT116 P <0.0242, SW480 P <0.0181 and $CD24^{WT}$ vs $CD24^{N52Q}$ (HCT116 P <0.0087, SW480 P <0.0367). Consistent with the transwell migration data, the difference in residual wound size was even more marked for $CD24^{N[36,52]Q}$ *vs.* $CD24^{WT}$ (P <0.0001 for HCT116 and SW480, respectively) and wound healing was almost the same in $CD24^{N[36,52]Q}$ *vs*. EVC for both HCT116 and SW480.

Our previous data showed that CD24 could also induce cell invasion through Matrigel (unpublished for cell invasion). Comparative transwell invasion assays performed examinations into the potential role of *N*-glycosylation in cell invasion. In concordance with our previous data, $CD24^{WT}$ vs EVC demonstrated a marked increase in cell invasion in HCT116 and SW480 (P <0.0001 for each) (Figure 3.12B). As with the migration assays, single mutant plasmids showed increased cell invasion than with EVC ($CD24^{N36Q}$ *vs*. EVC and $CD24^{N52Q}$ vs EVC) in both cell lines but were less significant than $CD24^{WT}$ (P =0.0012). Double mutants $CD24^{N[36,52]Q}$ caused further reduction and near-total abrogation in invasion ($CD24^{N[36,52]Q}$ vs $CD24^{WT}$, P <0.0001) in both HCT116 and SW480 (Figure 3.12B). No significant difference was observed in $CD24^{N[36,52]Q}$ *vs*. EVC for both cell lines.

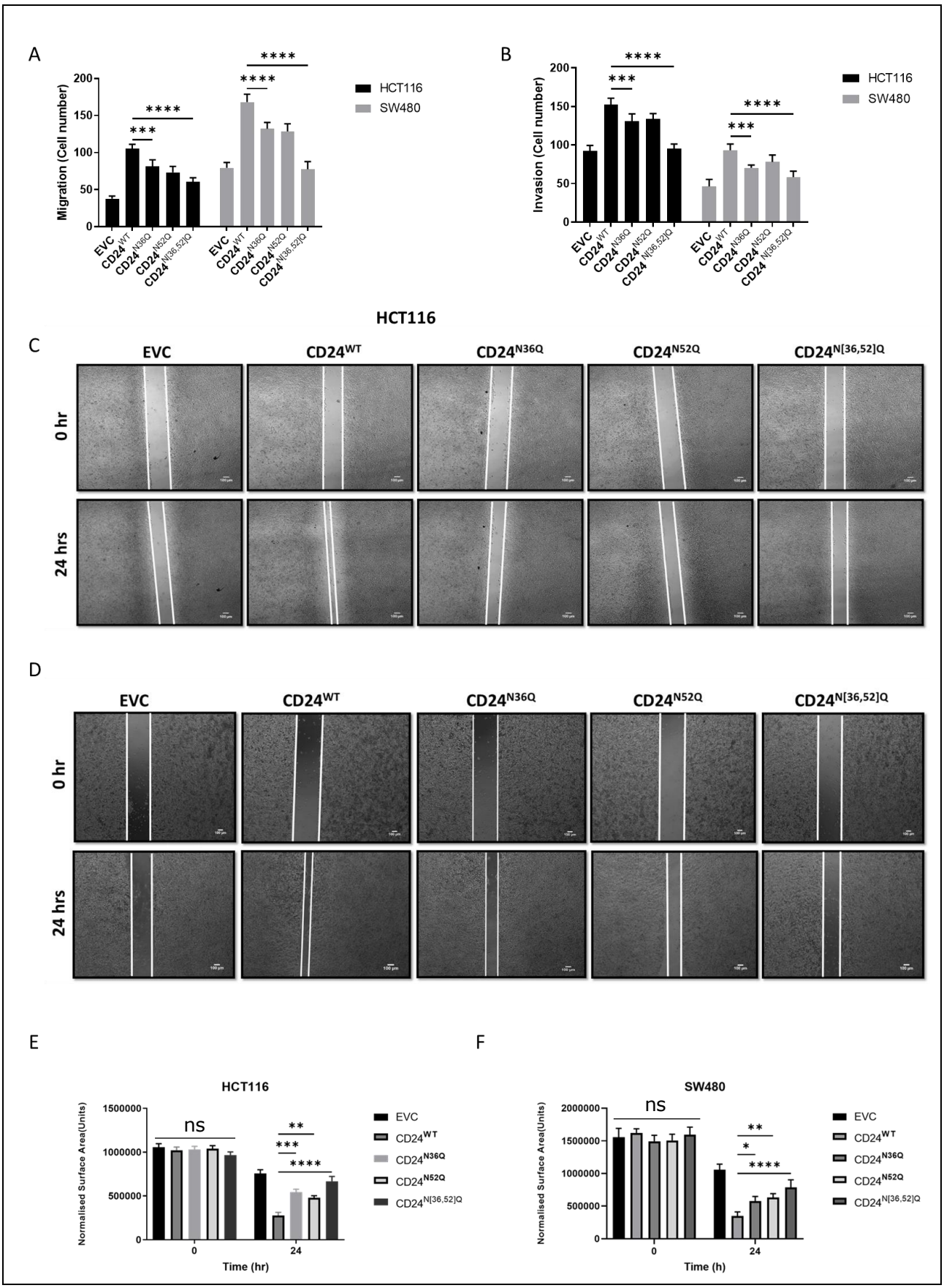

A
Migration (Cell number)
HCT116
SW480
EVC
CD24WT
CD24N36Q
CD24N52Q
CD24N[36,52]Q
B
Invasion (Cell number)
HCT116
C
D
0 hr
24 hrs
E
HCT116
Normalised Surface Area(Units)
Time (hr)
ns
F
SW480
Time (h)

Figure 3.12 *N*-glycosylation mutation causes inhibition in CD24-induced cell invasion and migration.

Transwell migration assay (A) and Transwell invasion assay (B) of HCT116 and SW460 cells transfected with $CD24^{N36Q}$ and $CD24^{N52Q}$ show a partial reduction in migration and invasion compared to the control CD24, whilst $CD24^{N[36,52]Q}$ cells show significant depletion in both assays. Results are representative of three independents experiments. Wound-healing assay of HCT116 cells (C) and SW480 (D) showed that overexpression of $CD24^{WT}$ results in a reduction of the wound gap compared to EVC. The migration ability was inhibited when both CD24 *N*-glycosylation sites are mutated. The lower panel graphs represent the normalized wound gap area of HCT116 (E) and SW480 (F). The graphs and wound healing assay's results shown in the figure are one representative experiment out of three experimental replicates. The results were evaluated by GraphPad Prism by two-way ANOVA with Tukey's multiple comparisons, ($^{ns}P>0.05$, *P< 0.05, **P <0.01, ***P <0.001, ****P <0.0001).

3.2.7 Loss of CD24 *N*-glycosylation sites result in loss of activation of downstream targets and reduction in EMT

We have shown previously in our lab that CD24 promotes EMT [60]. To investigate the potential role of N-glycosylation on EMT, HCT116 and SW480 were transfected with $CD24^{WT}$ and $CD24^{N[36,52]Q}$, and the expression of EMT-related markers (E-cadherin, N-cadherin, Snail, and Vimentin) was measured using Western blot and qPCR. The results showed that, compared to EVC, overexpression of $CD24^{WT}$ reduces the expression of E-cadherin and increases the expression of N-cadherin in both HCT116 and SW480 (Figure 3.13B and Figure 3.13C). This phenomenon is described in the literature as the 'cadherin switch' and is associated with EMT [203]. In the same context, the effect of overexpression of the single mutant constructs

(CD24^{N36Q} and CD24^{N52Q}) on the expression level of EMT markers was similar to that observed in CD24^{WT} (Figure 3.13A).

Conversely, transfection with CD24$^{N[36,52]Q}$ showed a complete failure to induce the cadherin switch in SW480 and a markedly diminished effect in HCT116. Complementing the cadherin switch, Snail and Vimentin levels were increased in HCT116 and SW480 by forced expression of CD24^{WT}. However, the level of these markers was lower in the forced expression of CD24$^{N[36,52]Q}$ *vs*. CD24^{WT}.

Our unpublished data suggest that CD24 may alter the levels of the target molecules at both the transcriptional and post-transcriptional levels. The mRNA levels of these targets were, therefore, evaluated by quantitative PCR. In both cell lines, the mRNA levels of N-cadherin, Snail and Vimentin were increased by transfection with either CD24^{WT} or CD24$^{N[36,52]Q}$. There was, however, no difference in levels of mRNA expression seen between the two constructs. Similarly, no difference was seen in the levels of E-cadherin mRNA following transfection of these constructs but, in SW480, the levels of E-cadherin mRNA were higher than that in HCT116 (Figure 3.13D).

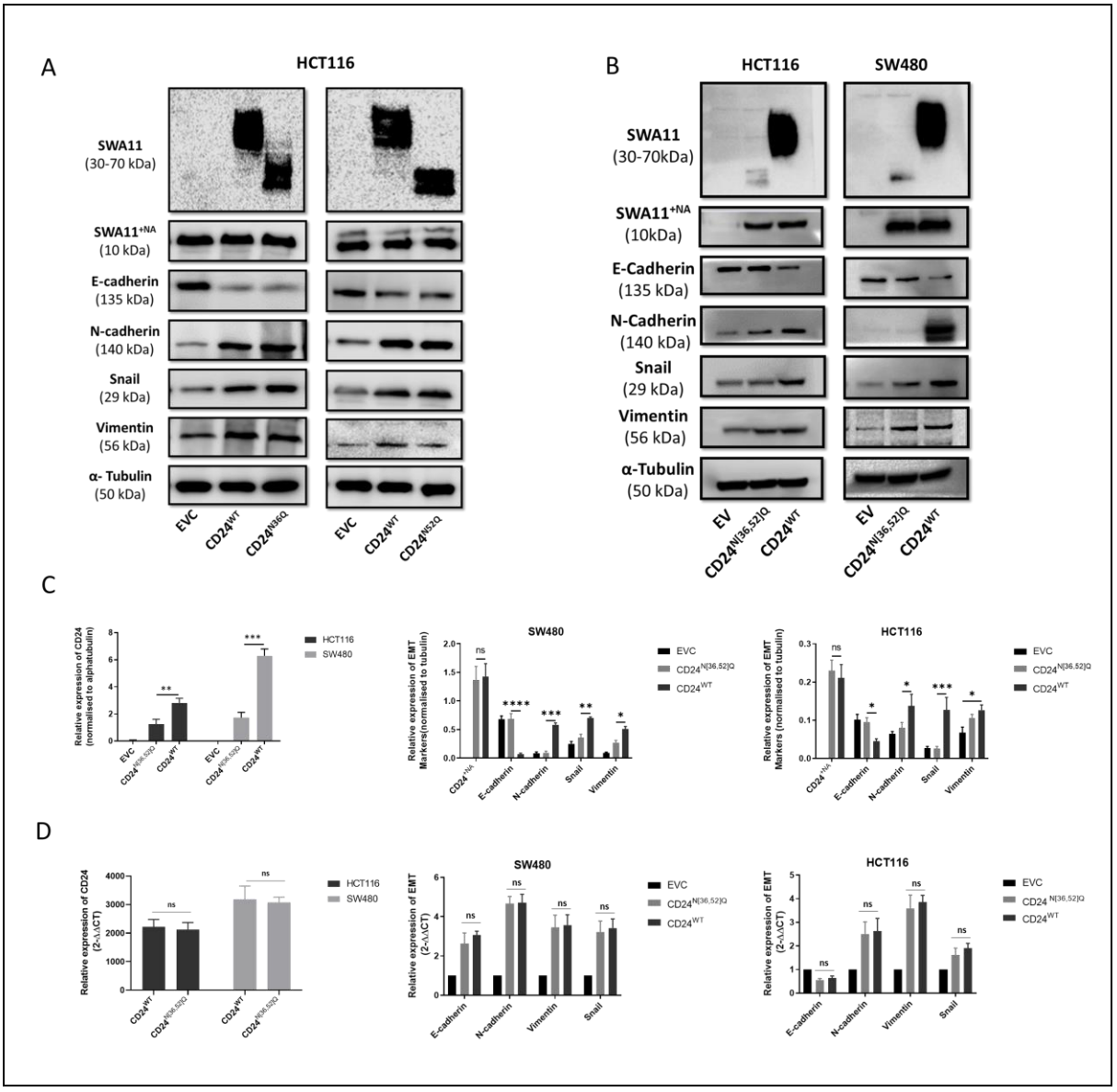
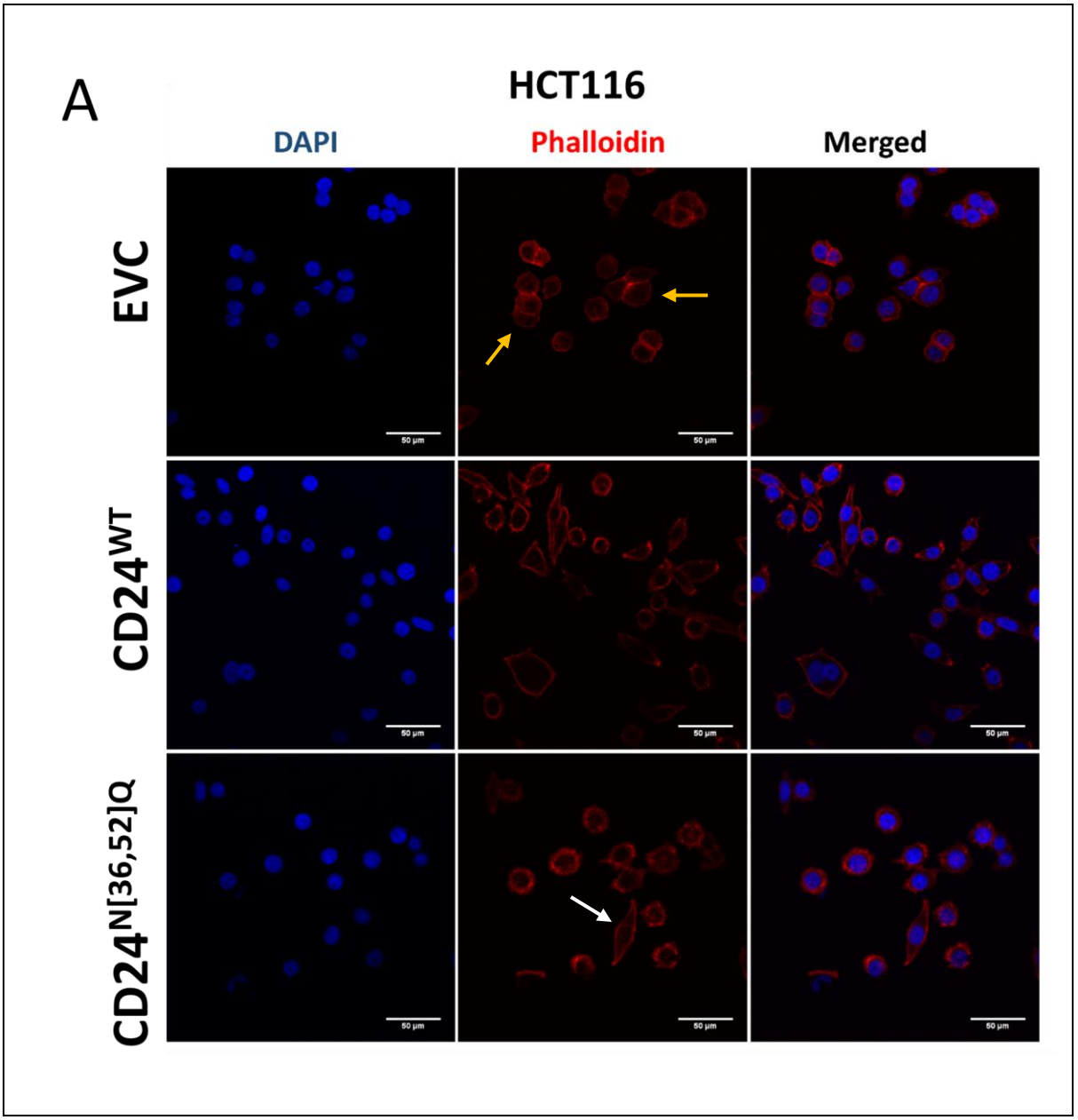


Figure 3.13 CD24 *N*-glycosylation inhibit the EMT mechanism in CRC cells.

Expression of CD24 along with EMT-related biomarkers (E-cadherin, N-cadherin, Snail, and Vimentin) were determined by Western blot post-transfection HCT116 and SW480 cells with EVC, $CD24^{WT}$, $CD24^{N36Q}$, $CD24^{N52Q}$ and $CD24^{N[36,52]Q}$ (A and B). The quantitative densitometry analysis of Western blot for CD24 and EMT proteins normalised to alpha-tubulin (C). RT-qPCR analysis of CD24 and EMT biomarkers in $CD24^{N[36,52]Q}$ showed no change in the mRNA levels than cells expressing $CD24^{WT}$ (D). The western blot and graphs shown are one representative experiment out of three experimental replicates. The band intensities were analysed by image studio software and the multiple comparisons by Student's T-test (two-tailed) compare the data between $CD24^{WT}$ and $CD24^{N[36,52]Q}$; a

significant difference in Western blot observed but not seen in qPCR. $^{ns}P > 0.05$, * $P < 0.05$, ** $P < 0.01$, *** $P < 0.001$.

EMT is a morphological change whereby tumour cells lose epithelial properties to gain a mesenchymal appearance. In order to investigate EMT further, phalloidin staining for F-actin was performed. In comparison to cells transfected with EVC, cells transfected with $CD24^{WT}$ acquired spindle-like features, and phalloidin staining showed actin polymerization and the formation of actin filaments in the cytoplasm. In contrast, cells overexpressing $CD24^{N[36,52]Q}$ maintained a rounded appearance, with only a few cells acquiring an elongated shape. However, the staining with phalloidin was similar in $CD24^{N[36,52]Q}$ *vs.* $CD24^{WT}$ suggesting that, despite the loss of the *N*-glycosylation sites, CD24 was still able to induce actin polymerisation (Figure 3.14A and Figure 3.14B).


A
HCT116
DAPI
Phalloidin
Merged
EVC
CD24WT
CD24N[36,52]Q
50 µm

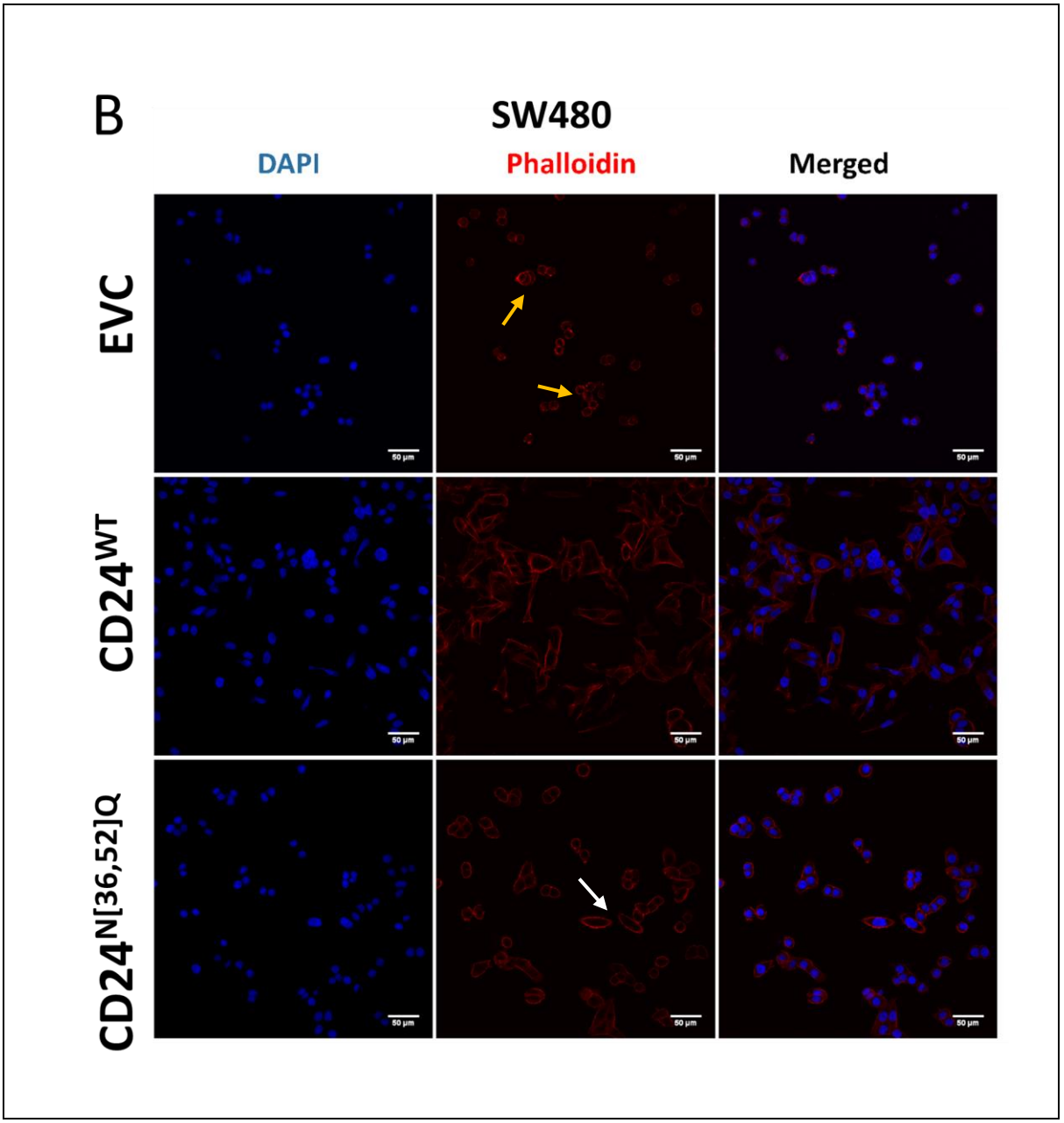


Figure 3.14 Loss of *N*-glycosylation inhibits CD24-mediated EMT phenotype alteration.

Confocal images of F-actin cytoskeleton staining at ×20 magnification for HCT116 (A) and Sw480 (B) shows that CD24-overexpressing ($CD24^{WT}$) cells acquired spindle-like structures, whilst cells overexpressing EVC displayed a rounded cell morphology and were present in cell clusters indicated by yellow arrows. In contrast, cells transfected with mutant CD24 ($CD24^{N[36,52]Q}$) maintained a rounded appearance with only a few cells retaining an elongated shape indicated by white arrows. The experiment was performed in triplicate. Scale bar 50µm.

3.3 Discussion

CD24 is a putative oncogene expressed in various cancer types, including CRC, where its overexpression is defined as a key early event in the development of CRC [202]. Glycosylation, in many proteins, plays a significant role in normal biological processes and cancer development, including tumour cell proliferation, invasion, angiogenesis and metastasis [203]. Changes in specific *N*-linked glycoproteins are associated with the development of many diseases, and thus, it is crucial to study *N*-linked glycoproteins to facilitate understanding of disease and help develop effective treatments [204, 205].

The structure of CD24 shows two putative *N*-glycosylation sites located around codon 36 and codon 52 [206]. In this study, we investigated the role of these sites in mediating the known functions of CD24, such as cell motility and EMT. Firstly, we proved that these sites were bona-fide *N*-glycosylation sites. At both sites, we substituted the asparagine with the glutamine (Figures 6 and 8), thereby removing the *N*-glycosylation target motif. This substitution would not affect the other *O*-glycosylation sites and would not create any new *O*-glycosylation sites as glutamine cannot bind to *O*-glycans [207]. Two constructs were created in which each *N*-glycosylation site was individually removed ($CD24^{N36Q}$ and $CD24^{N52Q}$), and a third construct was created in which both sites were removed ($CD24^{N[36,52]Q}$). Western blotting confirmed that each of the mutant constructs was expressing the protein although the banding patterns were

different from the protein expressed by $CD24^{WT}$. Plasmid transfection efficiency and expression of core protein were similar between the different constructs leading us to conclude that the variability in the Western blot banding patterns was due to variation in glycosylation. The wild-type protein showed the classical smeared band. Protein from each of the single-mutation constructs ($CD24^{N36Q}$ and $CD24^{N52Q}$) showed less smearing and quicker running speed than the wild-type protein; these features are consistent with reduced glycosylation. The single-mutation proteins bands were very similar, suggesting they had similar levels of glycosylation. Protein from the double mutant construct ($CD24^{N[36,52]Q}$) contains only *O*-glycosylation sites, and the smearing of the bands suggested that there was glycosylation. However, even though there are 16 putative *O*-glycosylation sites, the banding pattern suggests that the overwhelming majority of glycosylation of CD24 lies at the *N*-glycosylation sites. Our observations are the first description of this pattern of glycosylation in CRC.

Having shown that the putative *N*-glycosylation were indeed true glycosylation sites, we next investigated whether *N*-glycosylation was relevant to the known cellular function of CD24, e.g. regulation of EMT, cell migration, and cell invasion in CRC cells, as these are crucial steps for tumour metastasis [208]. All assays (transwell migration and wound healing for cell migration and transwell migration through Matrigel for invasion, immunofluorescence with phalloidin staining for EMT) showed similar results, i.e., the activity of the single mutants was significantly less that of the $CD24^{WT}$, thereby suggesting each of the sites contributed to

these functions. Furthermore, the effect seemed to be additive, as the activity of the double mutant ($CD24^{N[36,52]Q}$) was significantly less than the effect of a single mutation (leading to the near-total abrogation of the ability to CD24 to induce some of these processes) when both *N*-glycosylation sites were mutated. To our knowledge, this is the first report of the functional importance of *N*-glycosylation in CD24. Our data were complemented by Western blots showing that loss of *N*-glycosylation sites resulted in the failure of the cadherin switch and a reduced level of induction of the motility-related biomarkers Snail and Vimentin. The mRNA's evaluation showed similar levels of induction of gene transcription of *N*-cadherin, Snail, and Vimentin by both the wild-type CD24 and double mutant $CD24^{N[36,52]Q}$. This would suggest that the changes observed in protein expression were mostly due to post-transcriptional modifications.

Our results are comparable to other studies that identify the potential role of *N*-glycosylation in inducing migratory and invasion capabilities of tumour cells [107, 194, 209]. The exact mechanism through which the *N*-glycosylation sites induce these changes are uncertain, but we would conjecture that the glycosylated asparagine residues at codons 36 and 52 are able to form complexes with and activate target cell surface molecules. The additive effects could be explained by each glycosylated residue contributing a certain amount to the total avidity for the target molecules. Since both transcriptional and post-transcriptional effects are seen, it is likely that several different pathways are activated. This would fit with the multiple binding partners described for CD24 [142].

EMT is associated with the acquisition of cell motility [210]. We, and others previously, have demonstrated CD24 involvement in EMT of CRC cells [142, 211]. Immunofluorescence studies, in line with the cell motility studies, showed that cells transfected with $CD24^{WT}$ acquired a spindle-shaped mesenchymal phenotype (compared to cells transfected with EVC), and this was accompanied by actin polymerization. In cells transfected with the double mutant, $CD24^{N[36,52]Q}$, the cells retained a rounded epithelioid phenotype similar to that seen in cells transfected with EVC. The only inconsistency in our data is that cells transfected with $CD24^{N[36,52]Q}$ also showed actin polymerization at a level similar to that seen with $CD24^{WT}$. Thus, it is apparent that CD24 can induce actin polymerization and be mediated by mechanisms independent of *N*-glycosylation. It is uncertain what these mechanisms are, whether they are related to the residual low-level *O*-glycosylation and how they are coordinated with the *N*-glycosylation-dependent mechanisms of motility induction.

Previously, we have shown that CD24 has no influence on proliferation in CRC cell lines [120]. Therefore, it was surprising to observe that mutation of either of the *N*-glycosylation sites resulted in increased proliferation in both HCT116 and SW480 cells. As with the studies for motility, the size of the effect was similar for each mutation but, when combined together in the construct $CD24^{N[36,52]Q}$, the effects appeared to be additive. There is obviously a gain-of-function acquired through the removal of the *N*-glycosylation sites, which suggests that some signalling pathways are activated that are not activated by $CD24^{WT}$. We would conjecture that loss

of *N*-glycosylation may allow the CD24 to activate and form complexes with cell surface molecules (such as growth factor receptors) from which it would ordinarily be shielded by the sugar residues around codon 36 and 52. If it is a true biological phenomenon, it may be related to the role of CD24 as an inducer of stemness [212, 213]. Stem cells often have proliferative quiescence, and CD24 may induce this through *N*-glycosylation. Alternatively, it could be an artefact of our experimental system. Either way, our data warrant further investigation to identify the targets leading to this observed stimulation of proliferation.

To summarise, we have confirmed, in two different CRC cell lines, that the putative *N*-glycosylation sites of CD24 around codon 36 and codon 52 are true targets for glycosylation. For the first time, these sites have been shown to be functionally active mediators of CD24-induced EMT and cell motility (both cell migration and cell invasion) in CRC. The function of the *N*-glycosylation sites is mediated through both transcriptional and post-transcriptional mechanisms, although actin polymerisation may be mediated through *N*-glycosylation-independent pathways of CD24. Unexpectedly, the *N*-glycosylation sites may also play a role in cell proliferation. These results suggest that CD24 *N*-glycosylation may play a role in progression and metastasis in CRC. Further studies are necessary to elucidate the mechanisms of CD24 activity in CRC and explore whether it could be a target for therapy.

3.4 Summary of findings

- $CD24^{WT}$ played no role in CRC cells proliferation in CD24 expressing cells or in CD24-silenced cells.
- CD24 overexpression in CRC cells induces cell migration and invasion, whereas reducing the level of CD24 by siRNA decreased the migration and invasion capability.
- Single and double CD24 mutant constructs were created to understand the biological effect of *N*-glycosylation on the activities of CD24 in CRC cells.
- The mutant constructs were confirmed by direct sequencing and Western blot.
- Surprisingly, loss of *N*-glycosylation of CD24 increased CRC cell proliferation.
- The role of CD24 in the induction of cell motility was inhibited following transfection with a double-mutant clone, while single mutant clones showed an increase in these activities but were less significant than wild-type CD24.
- The ability of CD24 to regulate EMT and cadherin switch in CRC cells is dependent on *N*-glycosylation.

Chapter 4: Investigation of the role of CD24/P-selectin binding in CRC metastasis

4.1 Introduction

Tumour metastasis is the most common cause of cancer death, accounting for about 90% of all cancer mortality [214]. As described in Chapter 1, section 1.4.3, multiple molecular and cellular processes are required to occur in specific sequential steps in order for metastasis to occur [215]. Two important steps are the invasion of tumour cells into blood vessels and then the extravasation of tumour cells when they reach the secondary site [216]. The necessary intravasation and extravasation steps are mediated by the interaction between adhesion receptors, such as selectins, on endothelial cells and their cognate ligands on the surface of cancer cells [217].

Selectins are vascular cell-cell adhesion receptors that interact with sialylated carbohydrate determinants, such as sialyl Lewis A and X, and with mucin-like glycoproteins, such as CD24 [153, 218].

P-selectin (CD62) is the largest receptor within the selectin family. It is a calcium-dependent receptor and contains nine short consensus repeat (SCR) domains [219]. When stimulated with pro-inflammatory factors such as thrombin, P-selectin translocates rapidly from intracellular storage sites (the Weibel-Palade bodies) to the surface of the endothelial cells [220]. It plays a crucial role in promoting the adhesion of leucocytes to endothelium and extravasation during inflammation. It may play a similar role in terms

of cancer metastasis [221], and P-selectin has been found to bind particularly vigorously to various CRC cells [222-224].

The best-characterised ligand for P-selectin is P-selectin glycoprotein ligand-1 (PSGL-1), a 120 kDa glycoprotein that binds to all selectin family members but which has a particularly high affinity for P-selectin [225]. PSGL-1 is strongly expressed in haematopoietic cells and plays a significant role in mediating immune cell differentiation and leukocyte rolling on the endothelium [226].

CD24 has been shown to bind to endothelial P-selectin; however, apart from one study in breast cancer, which showed binding to E-selectin [227], it does not bind to other selectin families [107]. Some studies have shown that the interaction of CD24 with P-selectin enhances breast cancer metastasis and the migration of cancer cells into lung tissue [107, 108]; another study has indicated that CD24/P-selectin binding facilitates ovarian cancer cell adhesion to mesothelial cells [228].

It was thus hypothesised that, in CRC, endothelial P-selectin-CD24 interaction may occur, and it could be an essential factor in promoting haematogenous metastasis. To test this hypothesis, CRC cells expressing CD24 were stimulated with a recombinant human P-selectin protein, and the effect of this stimulation on activating CD24's downstream molecules, cell proliferation, and motility was investigated. Following this test, co-culture models were created by culturing CRC cells on top of an endothelial cell monolayer in order to develop a better understanding of the mechanisms through which the P-selectin/CD24 complex triggers CRC cell

adhesion to the endothelium and to begin to understand the contribution of this binding process to CRC metastasis.

4.2 Results

4.2.1 Stimulation of CD24 positive cell line (SW620) with recombinant P-selectin

As previously noted, PSGL-1 and CD24 have been identified as common P-selectin ligands in cancer cells [82, 229]. Consequently, the expression levels of PSGL-1 and CD24 were initially investigated using Western blot and immunofluorescence in three different CRC cell lines (HCT116, SW480 and SW620). The results showed that, as expected, CD24 was only expressed in the SW620 cell lines, while PSGL-1 was not expressed in any of the cells (Figure 4.1A and Figure 4.1B).

Recombinant human P-selectin (R-SELP) protein was added to the CRC cells expressing CD24 as a stimulant in order to determine whether such stimulation would activate CD24. SW620, the only cell line expressing a high level of CD24, was stimulated with two different concentrations (5 µg/ml and 10 µg/ml) of R-SELP protein. The cells were tested at different times after stimulation (30 min, 60 min, and 120 min) and blotted against the SWA11 (CD24) antibody. As Cten downstream signalling target of CD24 (unpublished data), it was also tested. The Western blot data showed that after one hour, there was an increase in the protein expressions of both CD24 and Cten, whereas no noticeable effect was observed in the control cells stimulated only with H_2O (Figure 4.2A and Figure 4.2B).

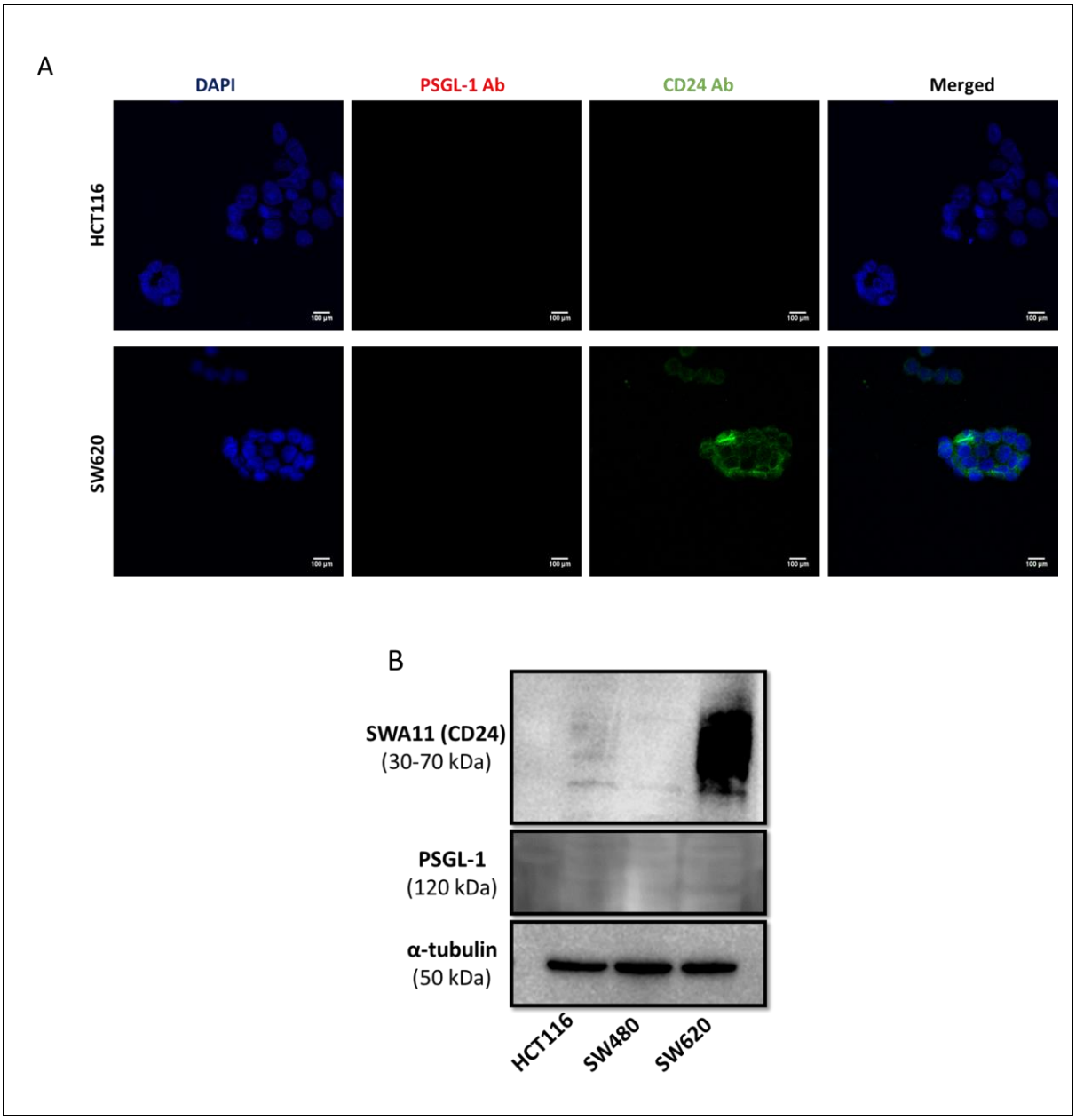


Figure 4.1 PSGL-1 does not express in CRC cells.

The expression level of CD24 and PSGL-1 in three different CRC cell lines using immunofluorescence staining (scale bar 100μm) and Western blot (A and B). CD24 was significantly expressed only in SW620 but not in other cell lines (HCT116 and SW480), while no expression of PSGL-1 was shown in any of the tested cell lines. The band intensities were analysed by image studio software and the results from one representative experiment. Abbreviation; PSGL-1: P-selectin glycoprotein ligand-1.

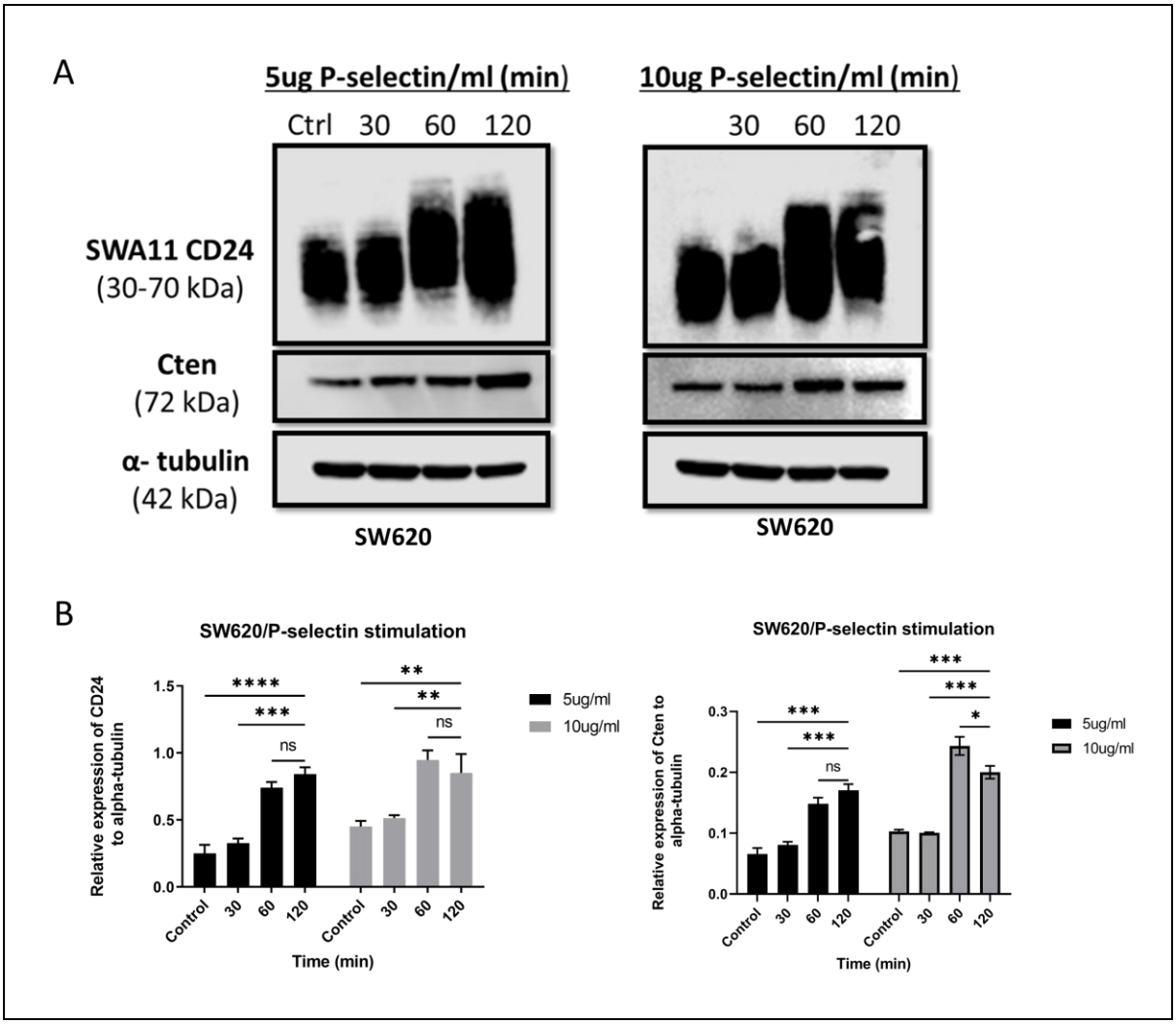


Figure 4.2 Stimulation of SW620 with P-selectin activates CD24 and its downstream target, Cten.

Western blot shows the expression of CD24 in only SW620 stimulated with different concentrations of recombinant P-selectin protein (5 ug/ml, left, and 10 ug/ml, right) at different time points and the expression level of CD24 and Cten as evaluated by Western blot (A), the western blot images shown are one representative experiment, repeated twice. Densitometry of the relative expression of CD24 and Cten normalised to alpha-tubulin (B). The band intensities were analysed by image studio software and compared using GraphPad Prism with Student's t-test (two-tailed, unequal variance), $^{ns}P>0.05$, * $P < 0.05$, ** $P <0.01$, *** $P < 0.001$.

4.2.2 P-selectin activates CD24 and its downstream signalling molecules

Stimulation of SW620 with soluble P-selectin caused an apparent increase in both CD24 and its downstream target Cten. It was necessary to determine whether this was mediated through CD24 or through another receptor. In order to do this, CD24 expression was modulated in CRC cell lines by stimulation with R-SELP.

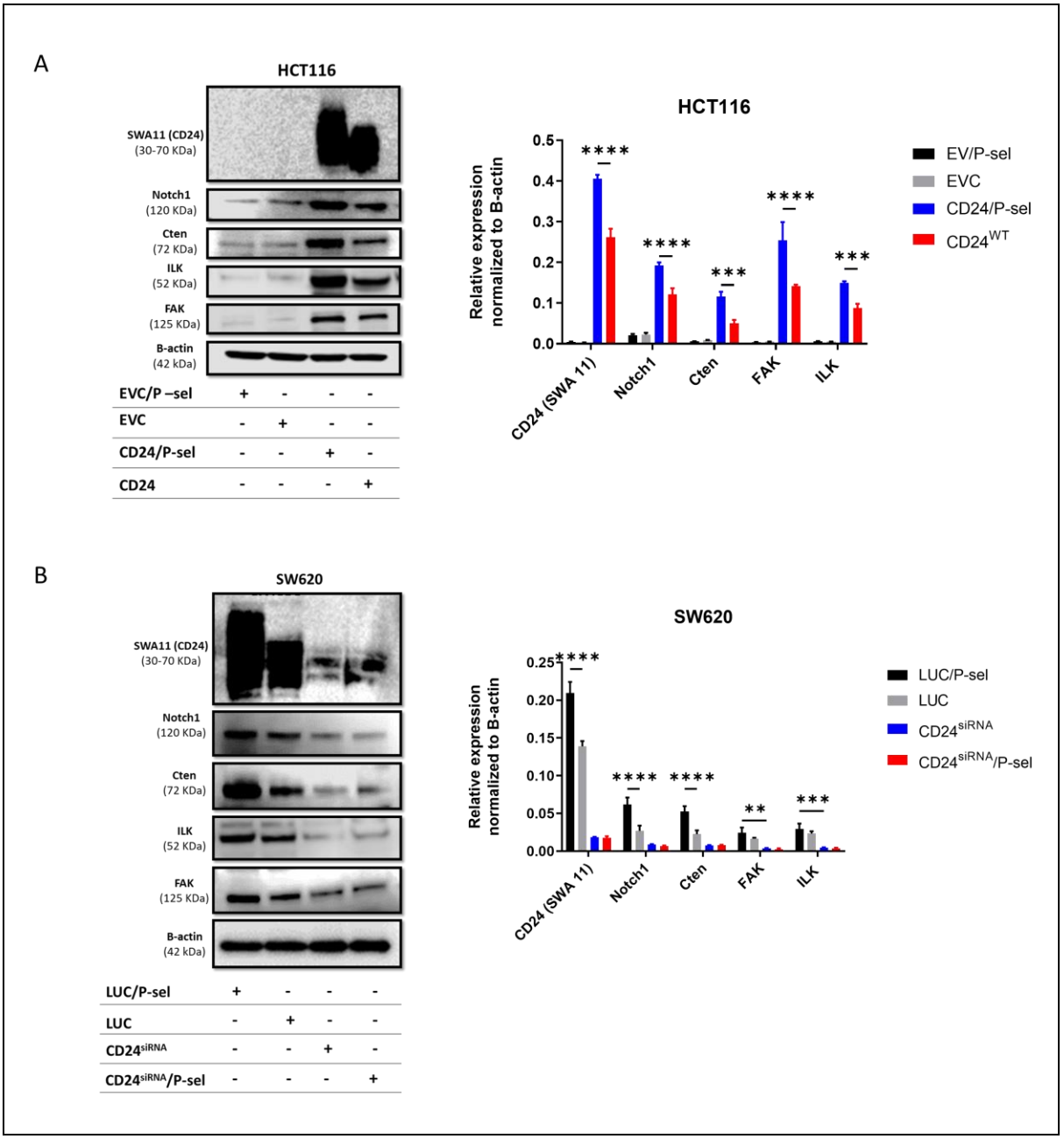
HCT116 and SW480 do not express CD24, and these were transfected with a CD24-expression vector. SW620 has high CD24 expression, and this was therefore transfected with anti-CD24 siRNA. Following transfection, the cells were stimulated with R-SELP protein for one hour, and the resulting protein lysates were collected and blotted with antibodies for CD24 and its downstream targets: Notch1, Cten, FAK, and ILK.

In HCT116, the control cells (i.e., those transfected with empty vector controls, $HCT116^{EVC}$, showed no difference in the expression of CD24 or its downstream targets when stimulated with R-SELP compared to stimulation with H_2O (or whatever we used). By contrast, in the cells transfected with the CD24 expression construct $HCT116^{CD24}$, there was an expression of CD24 and its downstream targets. However, when these cells were stimulation with R-SELP, the levels of CD24 seemed to be increased as well as the levels of the downstream targets (Figure 4.3A). The same results were seen in the SW480 cell line, similar to those for HCT116 (see Appendix VI).

SW620 normally expresses CD24, and in the control cells (i.e., those transfected with siRNA targeted to luciferase, $SW620^{Luc}$, there was an expression of CD24 and its downstream targets (as would be expected based on the data from the previous section). However, when these cells were stimulated with R-SELP, the levels of CD24 appeared to increase as well as the levels of the downstream targets. In the cells transfected with siRNA targeted to CD24 ($SW620^{CD24Neg}$), there was a loss of expression of CD24, and, in the absence of CD24, the expression of CD24 targets was not altered following stimulation with R-SELP (Figure 4.3B).

The results, taken together, show a significant increase in the expression of CD24 protein and its downstream-signalling molecules after R-SELP stimulation, but only in the presence of CD24 protein. This suggests that P-selectin binding with CD24 stabilise CD24 level and it activates the CD24 signalling pathways.

The regulatory effect of P-selectin on mRNA expression for CD24 and the CD24 signalling pathways in CRC cells was then investigated. The results show that there was a significant increase in the levels of CD24 and its downstream targets upon P-selectin stimulation compared to that seen under non-stimulated conditions (Figure 4.3C and Figure 4.3D).


A
HCT116
SWA11 (CD24)
(30-70 KDa)
Notch1
(120 KDa)
Cten
(72 KDa)
ILK
(52 KDa)
FAK
(125 KDa)
B-actin
(42 kDa)
EVC/P –sel + - - -
EVC - + - -
CD24/P-sel - - + -
CD24 - - - +
HCT116
Relative expression normalized to B-actin
0.6
0.4
0.3
0.2
0.1
0.0
****
****
***
****
***
CD24 (SWA 11)
Notch1
Cten
FAK
ILK
EV/P-sel
EVC
CD24/P-sel
CD24WT
B
SW620
SWA11 (CD24)
(30-70 KDa)
Notch1
(120 KDa)
Cten
(72 KDa)
ILK
(52 KDa)
FAK
(125 KDa)
B-actin
(42 kDa)
LUC/P-sel + - - -
LUC - + - -
CD24siRNA - - + -
CD24siRNA/P-sel - - - +
SW620
Relative expression normalized to B-actin
0.25
0.20
0.15
0.10
0.05
0.00
****
****
****
**
***
CD24 (SWA 11)
Notch1
Cten
FAK
ILK
LUC/P-sel
LUC
CD24siRNA
CD24siRNA/P-sel

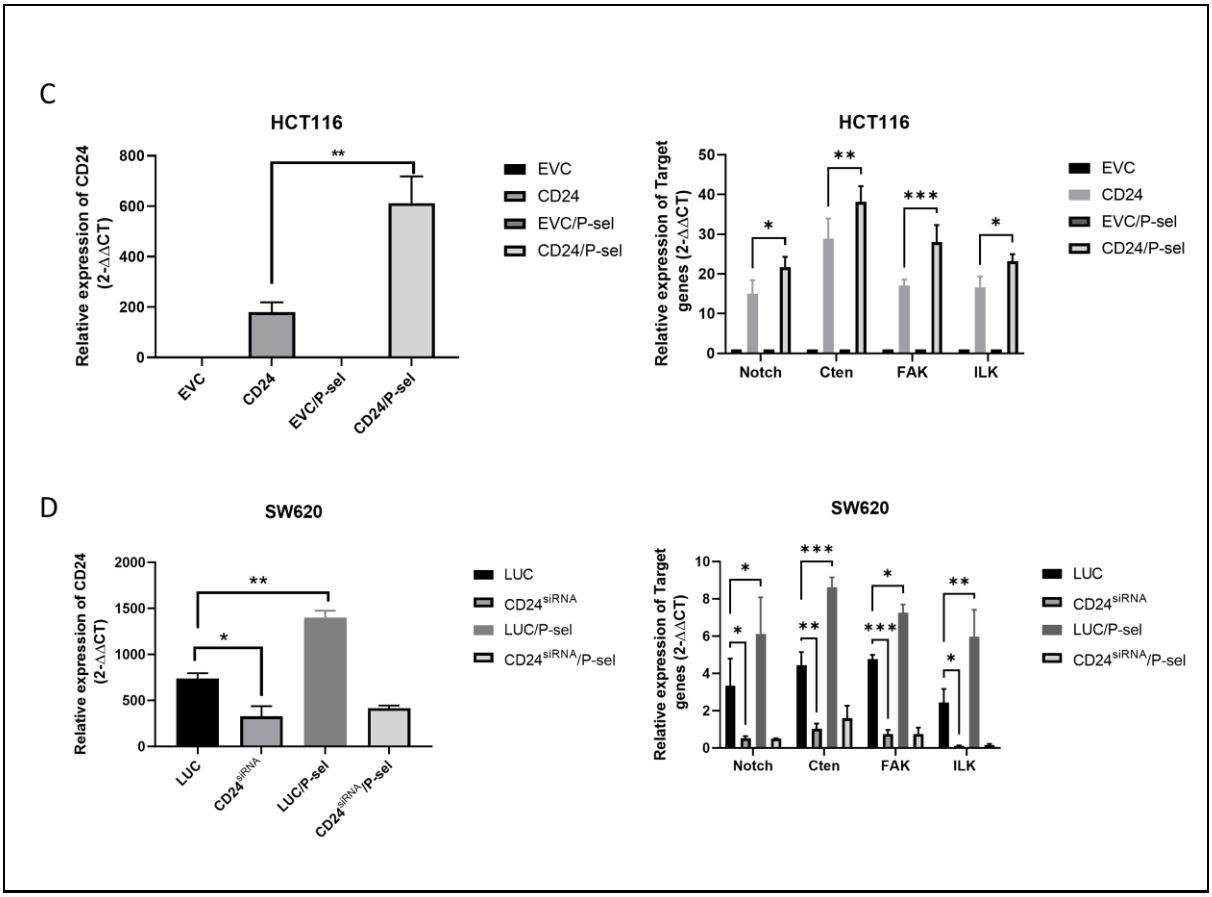


Figure 4.3 P-selectin/CD24 signalling pathways.

Western blot (left) and densitometry analysis (right) of the protein expression of CD24 and its downstream signalling pathways (Notch1, Cten, FAK, and ILK) after stimulation with P-selectin in HCT116 (A) and SW620 (B). The band intensities were analysed by image studio software and compared the stimulated and non-stimulated using GraphPad Prism with a student's T-test (two-tailed), ** P <0.01, *** P < 0.001, **** P < 0.0001. The effect of P-selectin on CD24 expression (left) and CD24 signalling pathways (right) at mRNA level in HCT116 (C) and SW620 (D). All values of PCR in graphs C and D were analysed by a One-Way ANOVA test with Sidak's multiple comparisons performed on GraphPad Prism, * P < 0.05, ** P <0.01, *** P < 0.001. The western blot and PCR results shown in the figure are one representative experiment with two biological replicates. Abbreviations: EVC: empty vector control; LUC: luciferase; P-sel: P-selectin.

4.2.3 CD24 binds to P-selectin

CD24 has been identified in several studies as a major ligand for P-selectin [82, 107], and our data suggest that the CD24-P-selectin interaction activates a signalling pathway. To further support this hypothesis, a protein binding assay was therefore performed using Co-IP to determine whether CD24 interacts with P-selectin in CRC cells. The HCT116 cell line was initially transfected with CD24, a process that was followed by a one-hour stimulation with R-SELP. The HCT116 cell overexpressing CD24 was then immunoprecipitated with a P-selectin antibody overnight before being immunoblotted using an anti-CD24 (SWA11) antibody. In the Western blot test, a clear smeared band corresponding to CD24 (30-70 kDa) was detected in the Co-IP product lane. There was no band seen in the control lane (beads alone), thus confirming that CD24 is pulled down by P-selectin and confirming that they do form a physical complex (Figure 4.4).

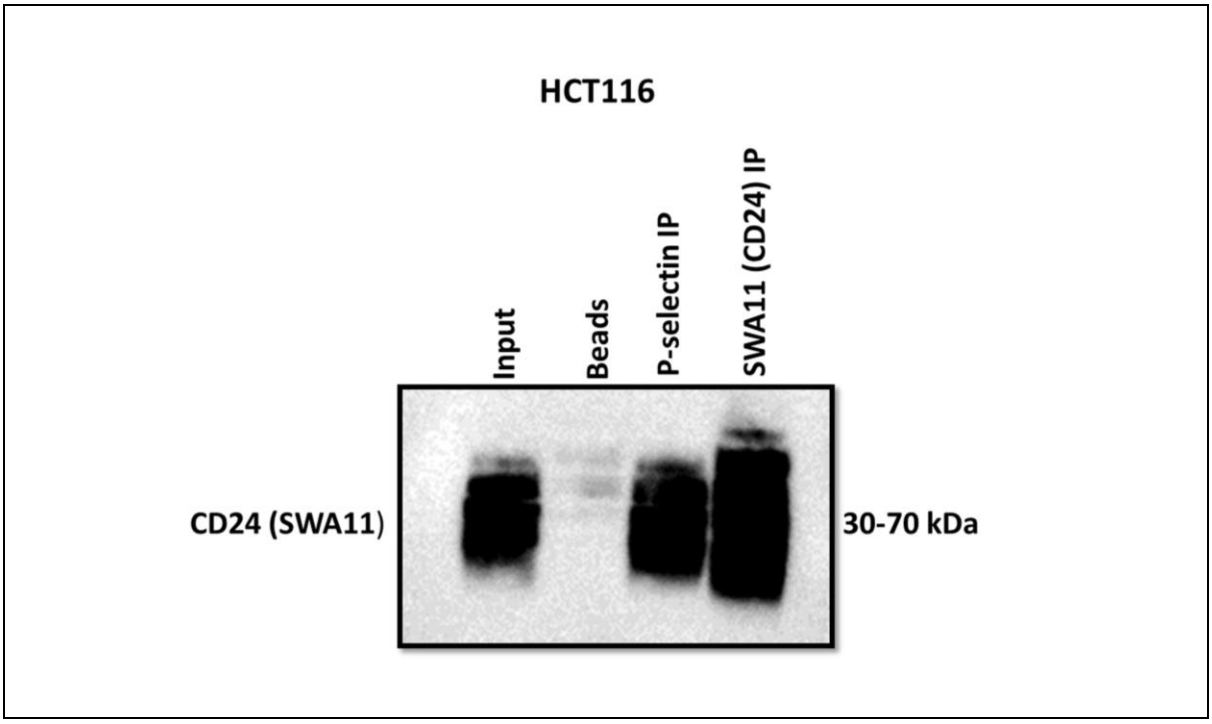


Figure 4.4 Interaction of P-selectin with CD24 as determined by Co-IP.

HCT116 was transfected with the CD24 expression vector and then stimulated with recombinant P-selectin. The cell lysate was immunoprecipitated using an anti-P-selectin antibody and blotted with an anti-SWA11 (CD24) antibody. The input was thus used as a positive control, while the beads served as a negative control, with the SWA11 (CD24) antibody used to determine the interaction of CD24 with P-selectin, as seen in the P-selectin IP lane. The results shown are one representative experiment, repeated twice.

4.2.4 P-selectin stimulation does not alter CRC cell proliferation, but it induces cell motility

After achieving confirmation that P-selectin interacts with CD24 to stimulate the expression of CD24 and its targets, we next sought to evaluate whether this resulted in any change in cellular function. The effect of P-selectin stimulation on cell proliferation was determined using a cell viability assay. No statistical difference was demonstrated in cell

proliferation between HCT116 transfected with CD24-expression vector and SW620 transfected with siRNA CD24 following P-selectin stimulation (Figure 4.5A and Figure 4.5B). These results are expected given that we have never shown an effect of CD24 on promoting cell proliferation. The data do, however, show that there is no effect of P-selectin stimulation on these cell lines through alternative cell surface molecules.

We have shown that CD24 can induce cell motility. Transwell chamber assays were used to examine whether the P-selectin interaction with CD24 could alter the capacity of CRC cells to migrate and invade the surrounding microenvironments. The data reflected the changes seen on Western blotting. After stimulation of $HCT116^{CD24}$ and $HCT116^{EVC}$ with R-SELP, a significant increase in the number of migrating and invading cells was observed in the $HCT116^{CD24}$ compared to that seen in the non-stimulated control cells, $P \leq 0.0001$. By contrast, no significant effect of stimulation with R-SELP was observed in the $HCT116^{EVC}$ (Figure 4.5C and Figure 4.5D). Similarly, in SW620, the cells transfected with the siRNA for luciferase ($SW620^{Luc}$) showed an increase in both cell migration and invasion following R-SELP stimulation, $P \leq 0.01$. However, P-selectin stimulation did not restore the migration and invasion capability in CD24-silenced cells ($SW620^{CD24Neg}$) (Figure 4.5E and Figure 4.5F). The data indicate that P-selectin stimulation can induce cell motility (both transwell migration and transwell invasion through Matrigel) and that this requires CD24.

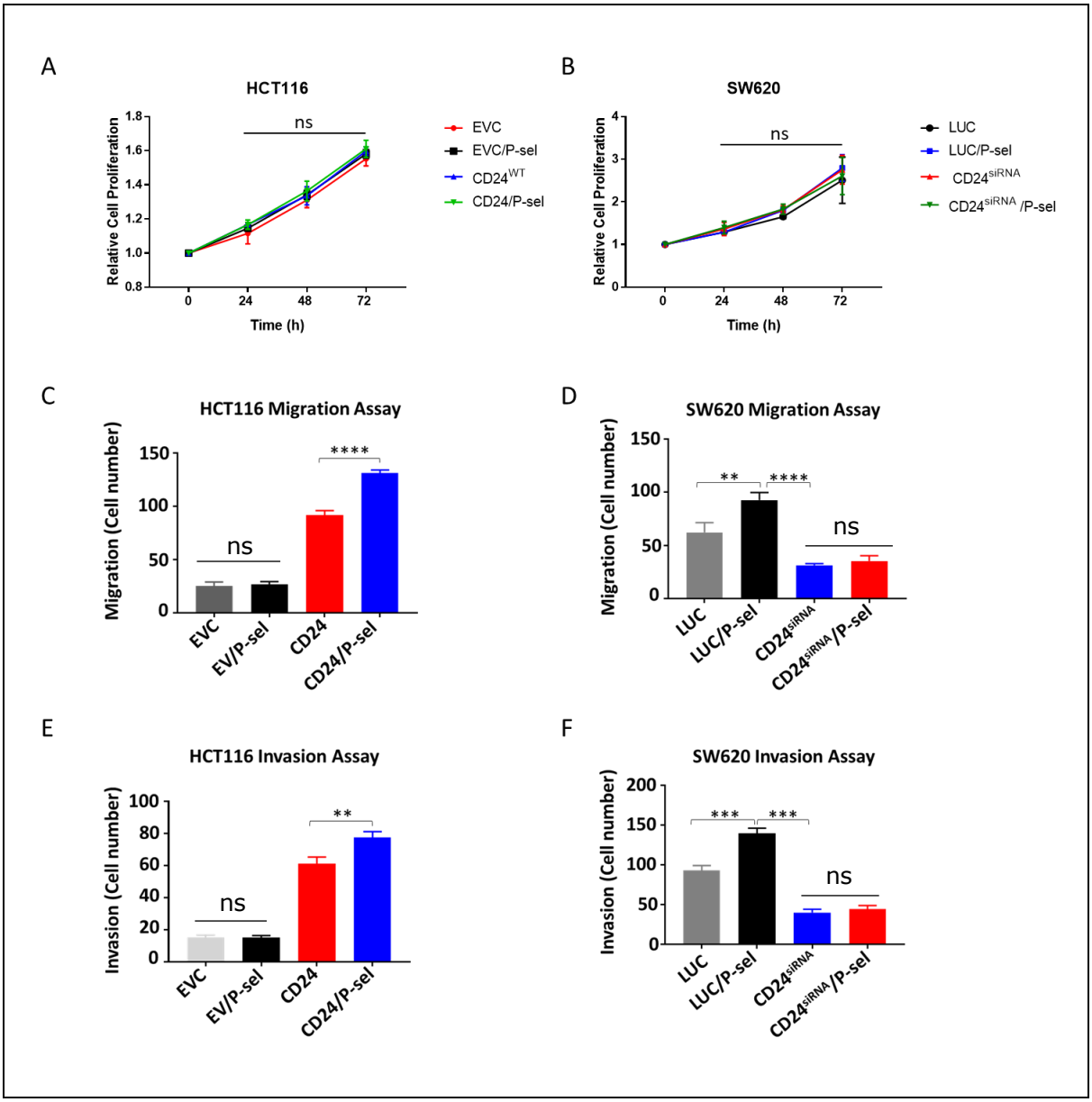


Figure 4.5 CD24/P-selectin binding did not alter cell proliferation, instead increasing cell motility.

A PrestoBlue assay showing cell proliferation unchanged in both HCT116 (A) and SW620 (B), with and without recombinant P-selectin. The transwell assay shows a significant increase in cell migration after stimulation with P-selectin ($HCT116^{CD24/P\text{-}selectin}$) compared to that seen in the non-stimulated cells ($HCT116^{CD24}$), which served as a control (C). Similarly, increased cell invasion is seen upon stimulation with P-selectin in HCT116 (D). A significant inhibition in cell migration (E) and invasion (F) was observed in CD24-silenced SW620 compared to that observed in the LUC control while stimulating SW620 cells with R-SELP after silencing CD24 with siRNA showed no effect on cell migration and invasion

abilities. The statistical analysis shows the mean ±SD of triplicates experiments based on two-way analysis of variance (ANOVA) with Tukey's multiple comparisons to analyse migration and invasion assays, $^{ns}P>0.05$, $^{**}P \leq 0.01$, $^{***}P \leq 0.001$, and $^{****}P \leq 0.0001$. The assay was performed in triplicate.

4.2.5 The CD24-P-selectin interaction regulates the adhesion of CRC cells to endothelial cells

Adhesion of tumour cells to endothelial cells is an essential step for tumour cell extravasation as part of the process of cancer metastasis [229]. Having shown that CD24 and P-selectin formed a physical complex, we hypothesised that this complex could regulate CRC cell adhesion to endothelial cells. To test this hypothesis, CD24 was overexpressed and silenced in HCT116 and SW620, respectively (as confirmed by Western blot, Figure 4.6A and Figure 4.6B). An adhesion assay was then carried out by co-culturing the CD24 transfected cells on top of pre-stimulated endothelial cells (HUVEC) with TNF-α for 4 hr (as described in Chapter 2, section 2.11.5). The presence of CD24 promoted adhesion in HCT116 as the number of adherent cells was significantly greater if CD24 was ectopically expressed ($HCT116^{CD24}$) when compared to those transfected with EVC ($HCT116^{EVC,}$ $P<0.001$) (Figure 4.6C). Conversely, CD24 knockdown resulted in a significant reduction in the adhesion of SW620 cells to HUVEC cells ($SW620^{CD24Neg}$ vs $SW620^{Luc}$, $P<0.01$ Figure 4.6D). These results suggest that CD24 plays an influential role in the adhesion of CRC cells to endothelial cells.

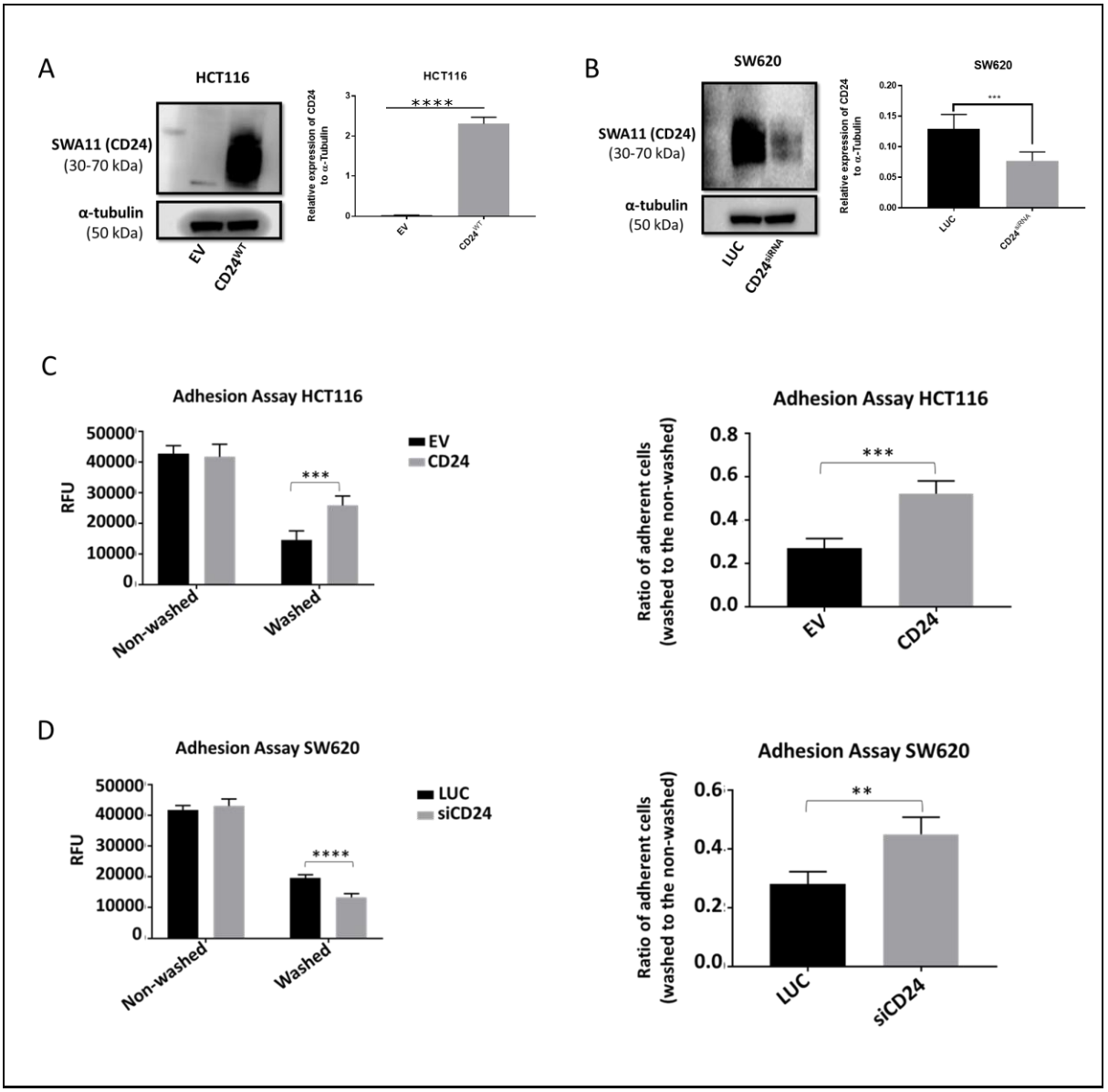


Figure 4.6 CD24 regulates the adhesion of CRC cells to endothelial cells.

Western blotting evaluation of CD24 protein expression following overexpression in HCT116 (A) and knockdown in SW620 (B). Densitometry analysis showing normalisation of the targeted protein to alpha-tubulin after evaluation with Student's T-test (two-tailed), **P <0.01, ****P <0.0001 (A and B, right). The western blot images shown are one representative experiment, repeated twice. The effect of CD24 on the adhesion of HCT116 (C) and SW620 (D) to the HUVEC. Cell adhesion statistical differences were determined by calculating the relative fluorescence unit (RFU) value ratio for washed cells to non-washed cells (C and D, right) and evaluated by GraphPad Prism by two-way ANOVA with Tukey's multiple comparisons, *P< 0.05, **P <0.01, ***P <0.001, ****P <0.0001. The

adhesion assay was performed in three replicates. Abbreviation: EVC: empty vector control; LUC: Luciferase control for siRNA.

Having shown that CD24 mediates adhesion to endothelial cells, we next sought to show that this was mediated through interaction with P-selectin rather than another endothelial receptor. Accordingly, adhesion assay was performed following modulation of P-selectin on HUVEC cells.

Before the assays were performed, HUVEC cells were stimulated either with TNF-α or thrombin to activate P-selectin expression. As shown by the Western blot results, both cytokines increase P-selectin levels compared to unstimulated cells (Figure 4.7A). In order to perform the experiments, Following HUVEC activation with TNF-α, P-selectin was down-regulated using siRNA targeted to P-selectin ($HUVEC^{PS\text{-}neg}$) whilst activated HUVEC cells transfected with siRNA for luciferase ($HUVEC^{Luc}$) were used as controls (Figure 4.7B).

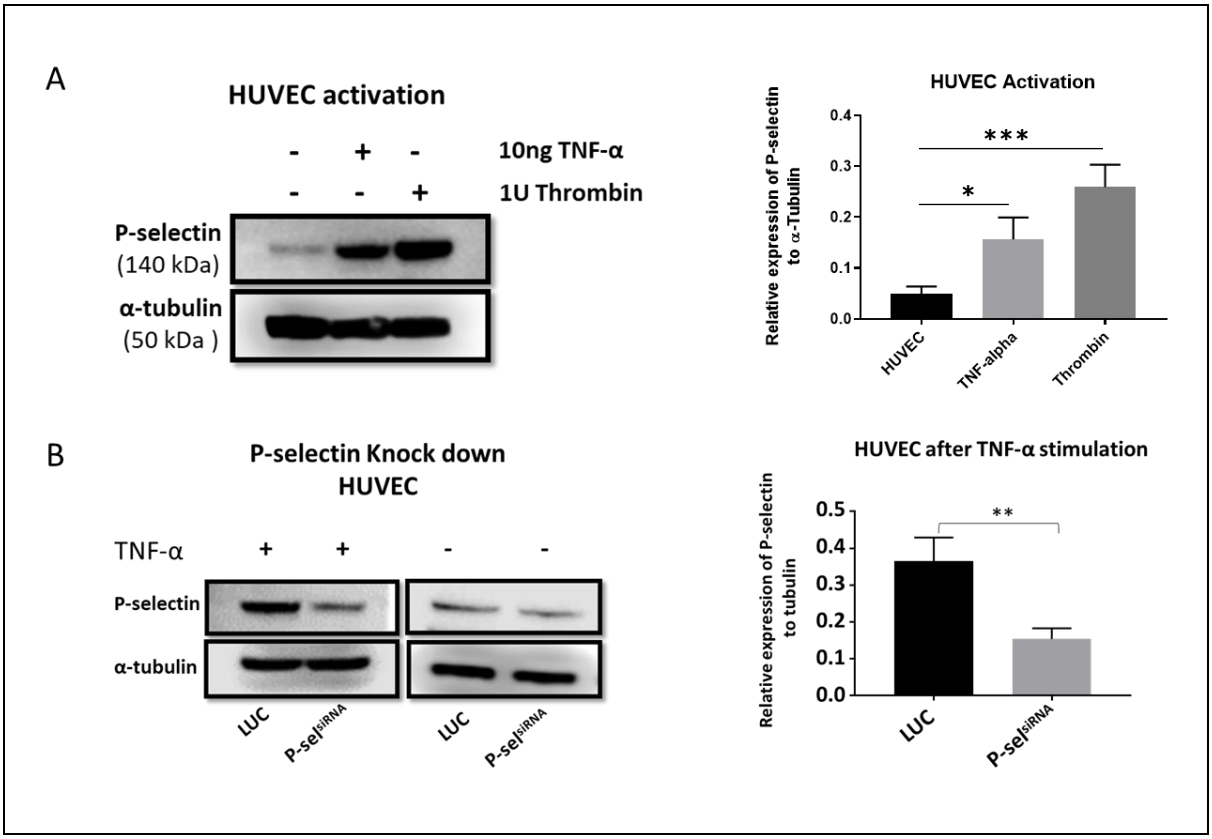


Figure 4.7 Western blot of CD24 in HCT116 and SW620, P-selectin in HUVEC.

Western blot results confirming the activation of P-selectin in HUVEC with 10ng/ml TNF-α and 1 Unit/ml thrombin (A). P-selectin knockdown using siRNA targeting P-selectin in HUVEC cell that stimulated with TNF-α (left-B) and non-stimulated cells (right-B). The band intensities were analysed by image studio software and compared using GraphPad Prism with Student's t-test (two-tailed, unequal variance), *P< 0.05, **P <0.01, ***P <0.001. The western blot images shown are one representative experiment, repeated twice

Adhesion assays were therefore performed on endothelial cells which had variable levels of P-selectin expression. The assays were also performed using HCT116 and SW620 cells in which, as with the earlier assay, the levels of CD24 expression were modulated (Figure 4.6A and Figure 4.6B).

The adhesion assays showed that the interaction between CD24 and P-selectin was necessary to promote adhesion between the CRC cells and the HUVECs. In HCT116, strong adhesion with HUVECs occurred only when both molecules were present in the co-culture (i.e., HCT116^{CD24}/ HUVEC ^{Luc}, P<0.0001). This was significantly reduced if CD24 was absent HCT116, but P-selectin was present in HUVECs (i.e., HCT116^{EVC}/ HUVEC^{Luc}) or CD24 was present on HCT116, but P-selectin was absent on HUVECs (HCT116^{CD24}/ HUVEC^{PSneg}). The absence of either one of the molecules resulted in a similar level of adhesion to that seen when both molecules were absent (i.e., HCT116^{EVC}/ HUVEC^{PSneg}) (Figure 4.8A). The data were identical in SW620; the presence of both molecules (SW620^{Luc}/ HUVEC^{Luc}, P<0.01) resulted in strong adhesion, which was abrogated when CD24 was lost in SW620 (SW620^{CD24neg}/ HUVEC^{Luc}) or P-selectin was lost in the HUVECs (SW620^{Luc}/ HUVEC^{PSneg}). The loss of either one of the molecules resulted in a similar level of adhesion to that seen when both were missing (SW620^{CD24neg}/ HUVEC^{PSneg}) (Figure 4.8B).

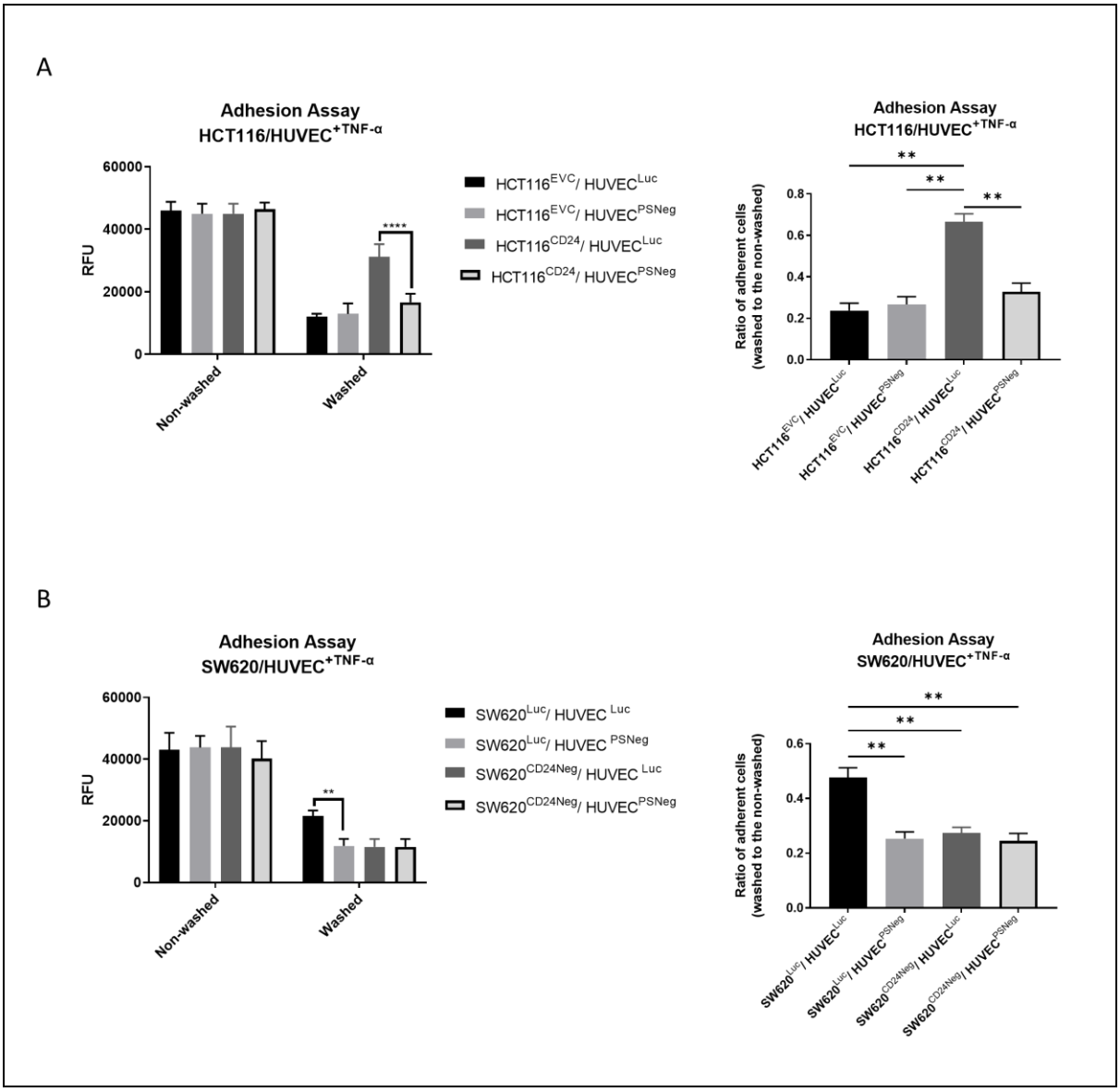


Figure 4.8 interaction of CD24/P-selectin regulates the adhesion of CRC cells to endothelial cells

Adhesion of HCT116^{CD24} was inhibited when co-culture with HUVEC^{PSneg} compared to HCT116^{CD24}/HUVEC^{LUC} (A). Similarly, inhibition of the adhesion of SW620^{LUC} to HUVEC^{PSneg} was observed when compared to SW620^{CD24neg}/ HUVEC^{PSneg} (B). This experiment was performed in three replicates. The statistical analysis were evaluated by GraphPad Prism by two-way ANOVA with Tukey's multiple comparisons, *P< 0.05, **P <0.01, ***P <0.001, ****P <0.0001. Abbreviation: EVC: empty vector control; LUC: Luciferase control for siRNA; PSNeg: P-selectin siRNA.

4.2.6 CD24-P-selectin interaction mediates trans-endothelial migration

Following adhesion to endothelium, the next step in the metastatic cascade is extravasation into the extravascular space in order to form a new colony. In a reversal of the process of vascular invasion, this would involve migration firstly across a barrier made of endothelial cells and then, for large blood vessels, migration through the muscular wall or, for capillaries, migration into the extracellular tissue of the metastatic site. Having shown that stimulation of CD24 by soluble recombinant P-selectin results in increased cell motility, we hypothesized that P-selectin expressed on endothelial cells could stimulate migration across the "endothelial barrier". We measured trans-endothelial migration using transwell co-culture assay. Firstly, HUVECs were layered onto the base of the insert. Once there was confluent, the epithelial cells were layered on top, and the migration of epithelial cells (labelled with calcein-AM) was measured. In order to test the importance of each of the molecules, the CD24 expression was modulated in the epithelial cells, and P-selectin expression was modulated in the endothelial cells (as described in the previous section).

Similar results were obtained from the trans-endothelial migration assay as were seen in the adhesion assay, where the interaction of CD24 and P-selectin in CRC cells promoted cell motility, but each molecule needed to be present for the effect to be seen. Thus, in HCT116, trans-endothelial migration occurred in the co-culture of $HCT116^{CD24}$/ $HUVEC^{Luc}$ (i.e., both molecules were present), but this was reduced if either CD24 or P-selectin

was absent (HCT116^{EVC}/ HUVEC^{Luc} and HCT116^{CD24}/ HUVEC^{Psneg}, P<0.0001). The experiments in SW620 also indicated that the presence of both molecules (SW620^{Luc}/ HUVEC^{Luc}) was necessary for trans-endothelial migration to occur but was lost when either one was lost (SW620^{CD24neg}/ HUVEC^{Luc} or SW620^{Luc}/ HUVEC^{Psneg}, P<0.0001). The loss of either one of the molecules resulted in a similar level of migration to that seen when both were missing (SW620^{CD24neg}/ HUVEC^{PSneg}) (Figure 4.9A and Figure 4.9B).

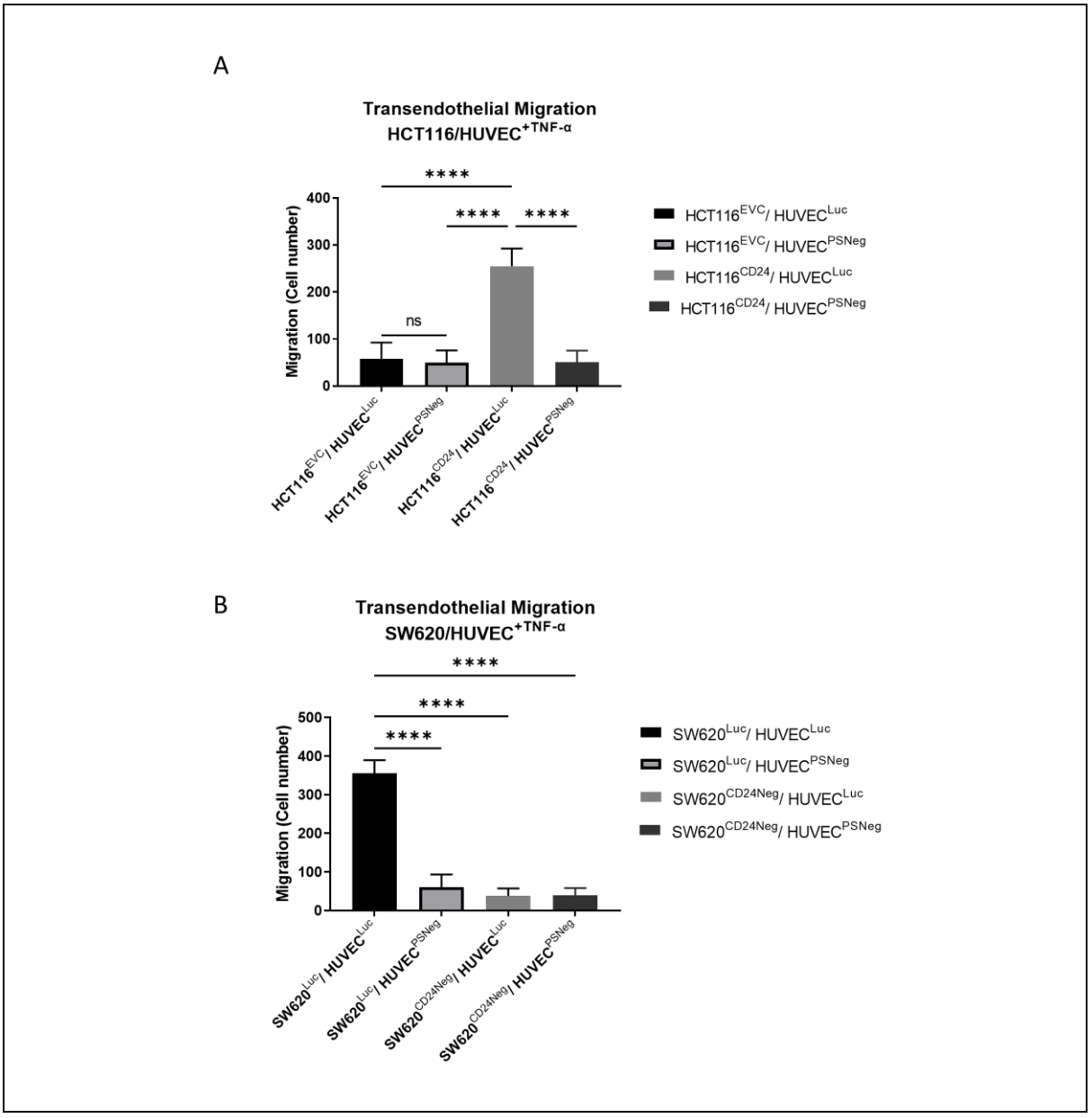


Figure 4.9 CD24/P-selectin interaction regulates trans-endothelial migration. Silencing CD24 and P-selectin individually or together in CRC cells and HUVECs, respectively, inhibited the migration of both HCT116 and SW620 through the endothelial monolayers (A and B). The graphs shown in the figure are one representative experiment out of three experimental replicates. The results were evaluated by GraphPad Prism by two-way ANOVA with Tukey's multiple comparisons $^{ns}P>0.05$, *P< 0.05, **P <0.01, ***P <0.001, ****P <0.0001). Abbreviation: EVC: empty vector control; LUC: Luciferase control for siRNA; PSNeg: P-selectin siRNA.

4.2.7 Loss of CD24 *N*-glycosylation disrupts CD24/P-selectin interaction and signalling pathway activation

In the previous chapter, loss of *N*-glycosylation of CD24 was shown to result in the inhibition of activities of CD24 in CRC cells. It was, therefore, of interest to see whether the CD24 *N*-glycosylation was relevant in the P-selectin/CD24 interaction. First, the physical interaction of CD24 with P-selectin was examined using Co-IP assay, as discussed above. The HCT116 cell was transfected with $CD24^{N[36,52]Q}$ and stimulated with R-SLEP protein. After this stimulation, the protein lysate was immunoprecipitated with an anti-P-selectin antibody and blotted with an anti-CD24 (SWA11) antibody. The resulting IP-products showed no physical interactions between $CD24^{N[36,52]Q}$ and P-selectin (Figure 4.10A); the reduction in band intensity in the input lane is instead most likely due to glycosylation modification, described in detail in Chapter 3. Overall, the Co-IP results indicate that N-glycosylation of CD24 is essential for P-selectin binding. Having shown that P-selectin stimulation led to the activation of CD24's downstream signalling molecules (Notch1, Cten, FAK, and ILK), more insights into P-selectin stimulation effects on CD24 signalling pathways were sought using HCT116 transfected with the CD24 double mutant construct ($CD24^{N[36,52]Q}$). The ensuring Western blot results were consistent with the previous data, with P-selectin stimulation leading to an increase in the expression level of CD24 downstream targets in cells expressing $CD24^{WT}$. By contrast, stimulation with P-selectin did not affect these molecules in cells transfected with $CD24^{N[36,52]Q}$ nor in EVC (Figure 4.10B, Figure 4.10C and Figure 4.10D).

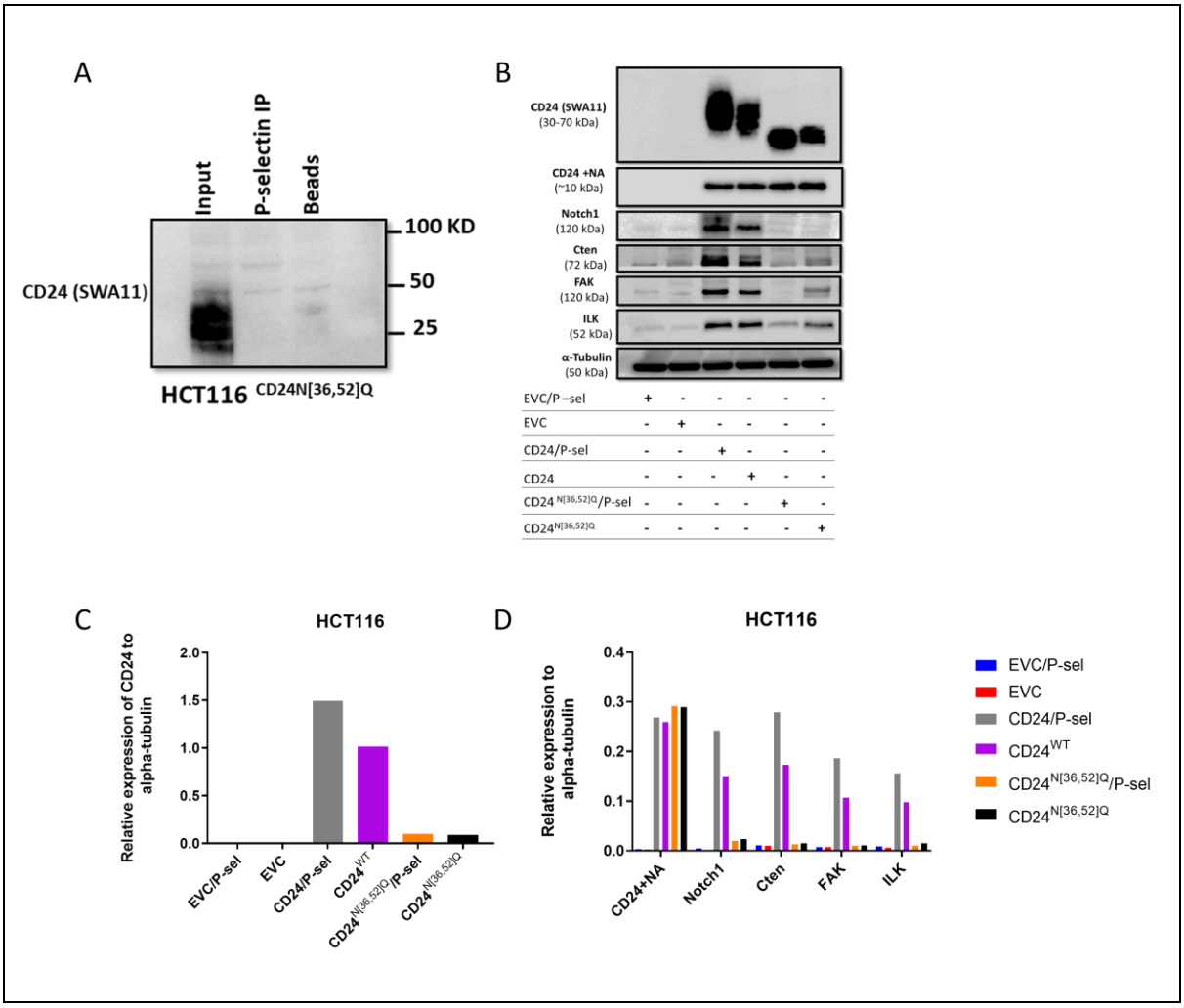


Figure 4.10 *N*-glycosylation mutation impairs CD24/P-selectin signalling in CRC.

CD24 did not bind to P-selectin when *N*-glycosylation sites were mutated (A). The co-IP results shown are one representative experiment out of two experimental replicates. P-selectin stimulation after overexpression of $CD24^{WT}$ and $CD24^{N[36,52]Q}$ in HCT116 led to an increase in the protein levels of CD24 downstream signalling pathways (Notch1, Cten, FAK, ILK). However, P-selectin did not affect these molecules' expression in HCT116 transfected with $CD24^{N[36,52]Q}$ (B). Protein densitometry of relative expression of CD24 and its downstream molecules after normalisation to alpha-tubulin (C, D). The band intensities were analysed by image studio software and the western blot experiment was performed once.

4.2.8 Loss of *N*-glycosylation in CD24 inhibits P-selectin-mediated cell adhesion and transendothelial migration.

Observations suggest that loss of *N*-glycosylation of CD24 leads to constraints on CD24-mediated CRC cell motility and disrupts the interactions with P-selectin. To investigate the effect of loss of CD24 N-glycosylation on CRC cell adhesion to HUVEC and transendothelial migration, HCT116 was transfected with $CD24^{N[36,52]Q}$ alongside activating the expression of P-selectin in HUVEC cells using TNF-α. Western blot testing then confirmed the $CD24^{N[36,52]Q}$ overexpression in HCT116 and P-selectin activation in HUVEC (Figure 4.11A and Figure 4.11B).

Following this confirmation, adhesion and transendothelial migration assays were performed. The adhesion assay data show that loss of CD24 *N*-glycosylation ($HCT116^{CD24N[36,52]Q}$) significantly decreased HCT116 adhesion to HUVEC cells when compared to $HCT116^{CD24}$, $P<0.001$ (Figure 4.12A and Figure 4.12B).

The importance of *N*-glycosylation of CD24 in facilitating the binding with P-selectin-mediated transendothelial migration was also investigated. The manipulated HCT116 cells with CD24 or $CD24^{N[36,52]Q}$ were co-culture with endothelial cells. The data showed that the loss of *N*-glycosylation in CD24 led to a decrease in the trans-endothelial migration of $HCT116^{N[36,52]Q}$ compared to $HCT116^{CD24}$, $P<0.001$ (Figure 4.12C). These results further confirm the potential role of *N*-glycosylation sites in CD24 in terms of modulating binding with P-selectin and the resulting cellular activities in CRC.

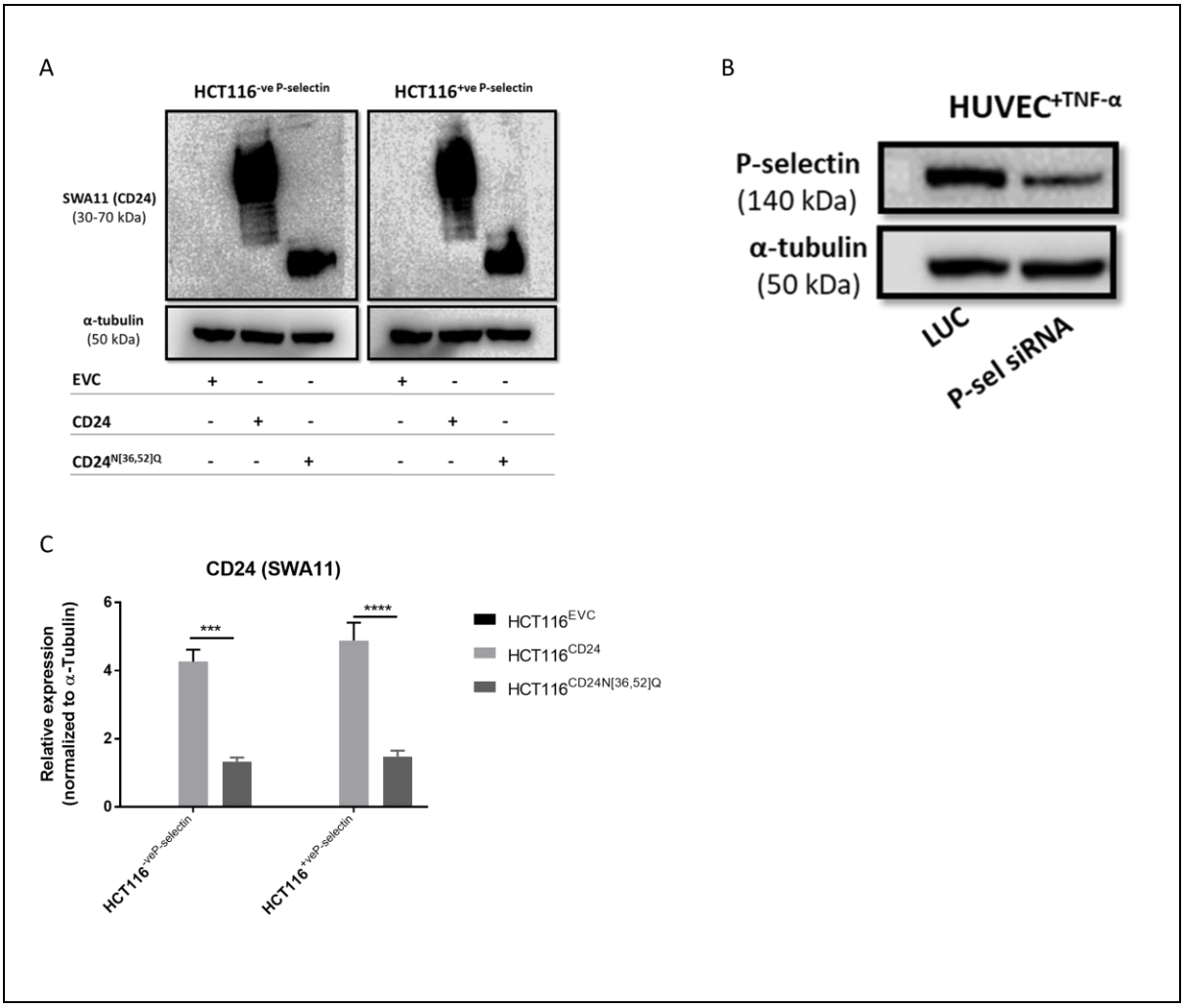


Figure 4.11 Western blot of CD24$^{N[36,52]Q}$ after stimulation with P-selectin and knockdown of P-selectin in HUVECs.

Confirmation of the overexpression of CD24^{WT} and double mutant construct (CD24$^{N[36,52]Q}$) in HCT116 stimulated with and without P-selectin (10 µg/ml) (A). Successful knockdown of P-selectin in HUVEC pre-stimulated with 1 Unit/ml thrombin (B). Densitometry analysis showing normalisation of the targeted protein to alpha-tubulin. The band intensities were analysed by image studio software and compared using GraphPad Prism with Student's t-test (two-tailed, unequal variance), ***P <0.001, ****P <0.0001. The western blot images shown are one representative experiment, repeated twice. Abbreviations: EVC: empty vector control; P-sel: P-selectin.

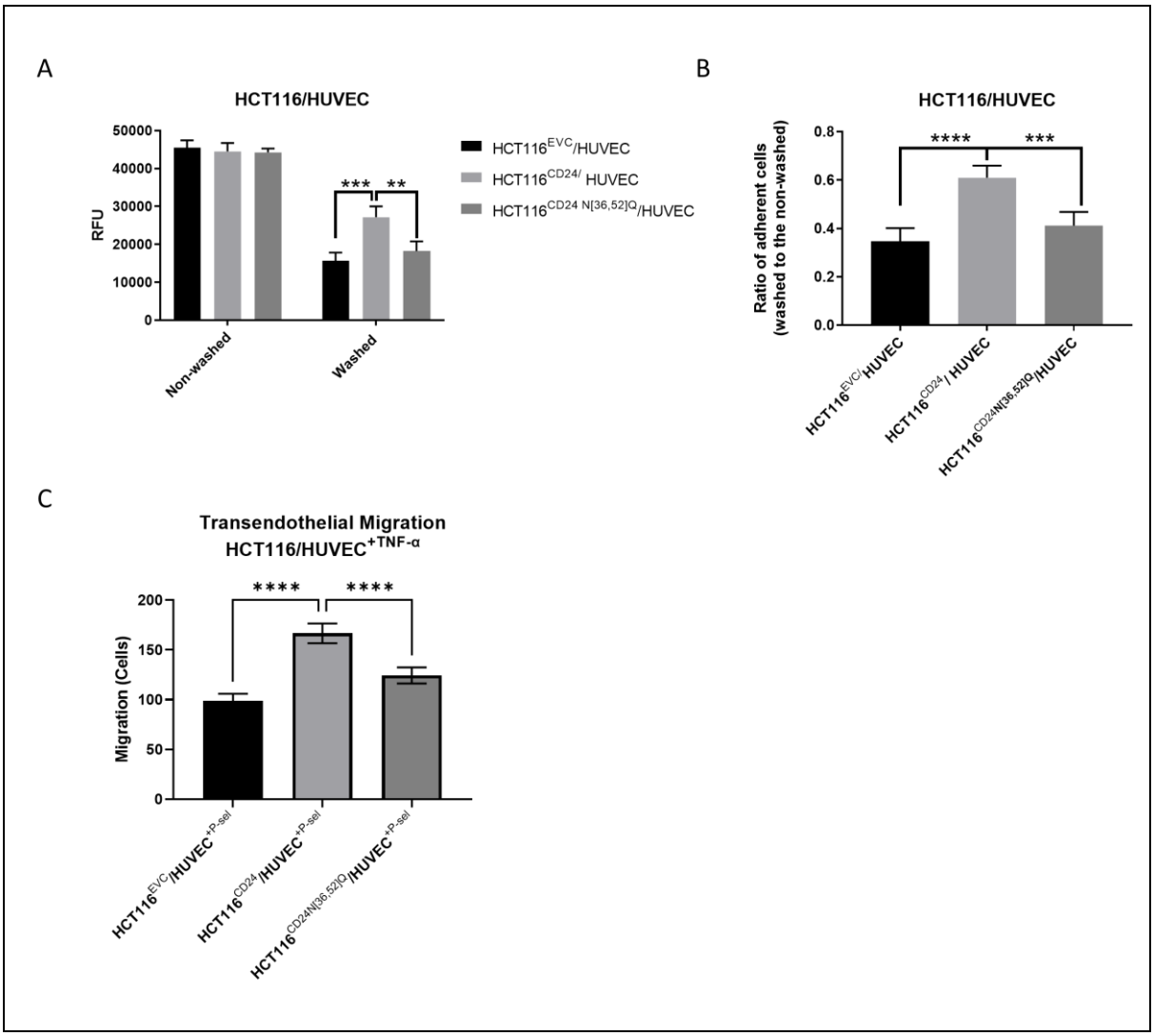


Figure 4.12 Loss of *N*-glycosylation in CD24 ($CD24^{N[36,52]Q}$) inhibits the HCT116 adhesion and transmigration through HUVEC cell monolayers.

Adhesion of HCT116 expressing $CD24^{N[36,52]Q}$ inhibited upon P-selectin silencing in HUVEC (A). Adhesion assay ratio of washed cells to the non-washed cells (B). Transendothelial migration assay after transfection of HCT116 with $CD24^{WT}$ and $CD24^{N[36,52]Q}$ and P-selectin knockdown in HUVECs (C). The error bar represents the SD means; the * indicate significant differences between means between three independent replicates. The results were evaluated by GraphPad Prism by two-way ANOVA with Tukey's multiple comparisons, *P< 0.05, **P <0.01, ***P <0.001, ****P <0.0001.

4.3 Discussion

The investigations discussed in this chapter were based on a study by Aigner et al., who first demonstrated the relationship between CD24 and P-selectin in human tumour cells. Their study indicated that CD24 could act as a ligand for P-selectin, and subsequent studies then suggested that this interaction might promote tumour metastasis [82, 230].

Based on such observations, this chapter aimed to explore the role of CD24's interactions with P-selectin and the impact of such interactions on the processes involved in cancer metastasis. The basic hypothesis was that CD24 mediates CRC cell adhesion to endothelial cells via its binding to P-selectin, consequently promoting CRC cell motility, leading to extravasation and metastasis. Several experiments *in vitro* examining this hypothesis were implemented using different cell lines and different methodologies (both via ectopic expression and gene knockdown).

Our data demonstrate that the protein expression of CD24 and its downstream target molecules (such as Cten) increased after stimulation with recombinant P-selectin. Using qPCR testing, we were able to show that P-selectin activates CD24 and its downstream targets at the mRNA level.

Furthermore, we were able to show that the CD24-P-selectin interaction is functionally relevant in promoting transendothelial migration. These observations were consistent with published data showing that P-selectin requires a receptor in tumour cells, such as CD24, to regulate metastatic processes [82].

Using Co-IP assays, we showed that CD24 physically formed a complex with P-selectin and that this binding promoted the adhesion of cancer cells to the endothelium.

Taken together, the data suggest that the CD24-P-selectin interaction can promote a number of the steps which are involved in the metastatic cascade. The interaction appears to be specific, and we were able to exclude PSGL-1 as a potential alternative; the possibility of other molecules interacting with P-selectin cannot be excluded.

The functional interaction between CD24 and P-selectin appears to require both proteins, and it increases levels of CD24 and its downstream targets. The altered expression suggests either increased transcription or stabilisation of the protein. There was an increase in CD24 mRNA, thus suggesting that there was transcriptional activation and a positive feedback loop. If that is the case, it begs the question of whether the effects seen on the other targets are due to direct activation of CD24 signalling pathways (in parallel to the pathway that activates CD24) or whether it is simply a phenomenon of increased expression of CD24 protein. The only way to resolve this would be to transfect CD24 which had been modified to have a cDNA sequence different from the endogenous wild-type sequence, and simultaneously knockdown the endogenous sequence. This would prevent a P-selectin induced expression of CD24 and, if the other targets were still up-regulated, it would show that P-selectin activated numerous downstream signalling pathways to induce targets of CD24

The impact of P-selectin/CD24 binding on cell viability was also investigated; stimulation with P-selectin did not affect cell viability either in HCT116 transfected with CD24 or in SW620 transfected with CD24 siRNA. These results agreed with those gathered by Ahmed *et al*., which suggested that CD24 does not play an influential role in cell proliferation [120]. This data supports the idea that the activity of CD24 in inducing cell motility is not dependent on cell proliferation and is actually a genuine induction of motility.

The findings in the previous chapter showed that *N*-glycosylation plays a vital role in CD24-mediated cell motility and EMT in CRC. Similarly, other studies have indicated that the glycosylation of cancer cell surface glycoproteins might mediate the binding to endothelial P-selectin [231-233]. In this chapter, therefore, the impact of CD24 *N*-glycosylation on binding to P-selectin was assessed. HCT116 was transfected with $CD24^{WT}$ and $CD24^{N[36,52]Q}$, followed by P-selectin stimulation. The resulting CD24/P-selectin interaction was examined by Co-IP. The data showed that the CD24/P-selectin interaction was disrupted by the loss of *N*-glycosylation in CD24. In addition, stimulation of the HCT116 expressing $CD24^{N[36,52]Q}$ with P-selectin did not change CD24's downstream signalling molecules' protein expression. These data suggested the possibility that CD24 requires *N*-glycosylation moieties to bind to P-selectin.

Given that the previous chapter showed that the majority of glycosylation in CD24 appears to be *N*-glycosylation, this is not altogether surprising. The loss of the *N*-glycosylation sites resulted in a failure of CD24 activity. This

re-iterates the importance of *N*-glycosylation to the function of CD24 and the importance of glycosylation to molecular function.

The noticeable limitations in this chapter are that the results were only obtained from *in vitro* models, which may not reflect what happens in patients at the molecular level. In addition, the Co-IP assay was restricted to using only HCT116 cells, as this cell line does not express CD24.

Overall, this chapter suggests that the CD24/P-selectin complex is crucial in terms of facilitating the interaction of CRC cells and endothelial cells. Therefore, it may act as a regulator of CRC cell adhesion to the endothelium and a facilitator of transendothelial migration, which in turn leads to metastasis formation. Moreover, this chapter's investigations highlighted the important role played by *N*-glycosylation of CD24 in developing this CD24/P-selectin complex, as the mutation of *N*-glycosylation was found to lead to the inhibition of both CRC cell adhesion to endothelial cells and migration through endothelial cell monolayers.

4.4 Summary of findings

- Stimulation with P-selectin activates both CD24 and CD24 signalling pathways at both protein and mRNA levels.
- Co-IP confirmed the interaction of CD24 with P-selectin.
- An increase in cell migration and cell invasion was observed upon stimulation with P-selectin.
- Both CD24-mediated cell adhesion to the endothelium and transendothelial migration are dependent on binding to P-selectin.
- Loss of CD24 *N*-glycosylation blocked the interaction with P-selectin.
- The decreased in the expression level of CD24's downstream signalling in the condition where CD24 *N*-glycosylation mutated failed to respond to P-selectin stimulation.
- Loss of CD24 *N*-glycosylation inhibits the ability of the CD24/P-selectin complex to induce adhesion and transendothelial migration.

Chapter 5: Investigating the association between CD24 and angiogenesis

5.1 Introduction

Angiogenesis is a hallmark of cancer and is considered a crucial factor in cancer growth [234]. Tumours cannot grow without nutritional replenishment, which is delivered through the vasculature. The growth of this vasculature is mediated by several growth factors. Tumours thus produce angiogenic factors that result in new blood vessels' growth, mainly via sprouting angiogenesis [235]. During this process, VEGF is a key stimulus for angiogenesis. This growth factor is found in nearly all solid tumours, and its receptors are exclusively expressed in the cells that line the blood vessels, i.e., the vascular endothelium [235].

Tumour cells induce endothelial activity through VEGF and VEGF receptors via aggregate cytokine activity [235]. This system can stimulate and sustain endothelial cells, assist in their migration and invasion of surrounding tissues, and induce cell proliferation. This system is also responsible for the typical vascular permeability of tumour vasculature. Tumour angiogenesis follows a distinct four-step process that begins with injury to the local tissue inducing hypoxia. The second step involves the activation of endothelial cells by angiogenic factors produced by the damaged cells and cells that have migrated into the damaged area (such as polymorphs and macrophages). During the third step, the endothelial

cells undergo proliferation and stabilisation, and the last step is the maturation of endothelial cells [235].

VEGF is a homodimeric glycoprotein that binds to heparin. It is a potent inducer of angiogenesis, and different variants are generated by alternative RNA splicing from a single gene. These variants include VEGF-A_{111}, VEGF-A_{121}, VEGF-A_{145}, VEGF-A_{165a}, VEGF-A_{189}, and VEGF-A_{206}. However, the dominant angiogenesis stimulator is $VEGF_{165a}$, which is characterised as a typical pro-angiogenic isoform [236, 237].

VEGF interacts with two receptors, VEGFR1 and VEGFR2, which are expressed by endothelial cells [236, 238]. These receptors consist of a transmembrane domain, ligand-binding domain, and tyrosine kinase active cytoplasmic domain such as Src kinase [238, 239]. VEGF is released by both normal tissue and tumour tissue and then diffuses into the surrounding areas. In addition, it increases vascular permeability, and it affects both vasodilation and vasoconstriction, which can promote angiogenesis [238].

VEGF is crucial in promoting *in utero* angiogenesis, and it is equally crucial in wound healing. It is a key mediator of tumour angiogenesis, and it is up-regulated by hypoxia and tumour glycoproteins [240]. Tumours activate an angiogenic switch, leading to increased VEGF production and resultant tumour vascularisation, which permits exponential growth. Tumour vasculature, however, is morphologically abnormal, lacks normal

organisation making it tortuous, irregularly shaped and usually haemorrhagic [235].

The association of CD24 with VEGF-mediated angiogenesis has been previously described. For example, a study by Wang *et al*. (2016) reported that CD24 could promote CRC angiogenesis [241]. This process is mediated by the interaction of CD24 with Hsp90, which increases STAT3 activity and thus regulates VEGF expression [241]. Another study showed that upregulation of CD24 has been associated with increased VEGF expression in breast cancer cells [242]. Salnikov *et al*. showed that targeting CD24 using a monoclonal antibody (SWA11) inhibited cancer cell proliferation and angiogenesis in both *in vitro* and *in vivo* models [191]. Another study also indicated that CD24 might have an inhibitory role in neovascularisation in stage II of retinopathy of prematurity (ROP) development [243].

Several studies have indicated that some genes expressed by cancer cells play a major role in attracting and activating endothelial cells. For instance, ILK, a target of CD24 signalling, has been shown to activate VEGF expression in tumour cells [244-247]. ILK signalling has been shown to work together with *VEGF* receptors in promoting morphological changes that are favourable for cell proliferation and their motility in endothelial cells themselves. Therefore, it appears that ILK has a fundamental function in promoting vascular angiogenesis [152, 196].

In this chapter, our hypothesis was built based on two facts. Firstly, we have shown that CD24 has several downstream targets, including ILK.

Second, the activation of ILK in tumour cells can induce the secretion of VEGF-A, leading to angiogenesis. Since CD24 mediates endothelial cell adhesion and transendothelial migration, we hypothesised that CD24 might also promote metastasis through the induction of ILK-mediated angiogenesis. This hypothesis was investigated initially by determining the regulation of VEGF and ILK by CD24. We then investigated the effect of the conditioned medium (CM) retrieved from CD24-expressing cells on endothelial cell proliferation, migration, and tube formation. Finally, we simultaneously overexpressed CD24 and knocked down ILK in HCT116 and SW480 cell lines in order to ascertain whether ILK was important in mediating CD24-induced VEGF-A expression.

5.2 Results

5.2.1 CD24 stimulates the expression of VEGF in CRC cells

We have previously shown that CD24 overexpression activates various signalling pathways in its role in inducing cell invasion and migration in CRC. To explore whether CD24 overexpression stimulates VEGF expression in CRC cells, we ectopically expressed CD24 in HCT116 cells ($HCT116^{CD24WT}$) and then determined the expression level of VEGF-A using Western blot and qPCR. In Western blot, forced expression of CD24 in the HCT116 resulted in a marked increase in ILK and VEGF-A protein expression compared to cells transfected with empty vector controls ($HCT116^{EVC}$). (Figure 5.1A and Figure 5.1D). To validate these findings, CD24 was ectopically expressed in another CD24 negative cell line ($SW480^{CD24WT}$) with different characteristics to HCT116. We also observed the upregulation of VEGF-A in $SW480^{CD24WT}$ when compared to $SW480^{EVC}$ control cells. (Figure 5.1B and Figure 5.1D). Next, we measured the expression level of the VEGF-A mRNA in both cell lines. Complementary to the Western blot results, the VEGF-A and ILK mRNA levels were increased in CD24-expressing cells compared to the EVC (Figure 5.1E).

We sought to further confirm our results by using an alternative method to modulate CD24 expression to ensure that the results were not an artefact of the technology. CD24 was silenced in SW620 (endogenously expressing a high level of CD24) using targeted siRNA ($SW620^{CD24neg}$). CD24 silencing led to a decrease in the level of VEGF-A protein when compared to control

cells transfected with siRNA targeted to luciferase ($SW620^{LUC}$). Similarly, the protein level of ILK (a downstream target of CD24) was decreased in $SW620^{CD24neg}$ *vs.* $SW620^{LUC}$ (Figure 5.1C and Figure 5.1D). Using qPCR testing, the mRNA expression of VEGFA and ILK was also evaluated. The mRNA level of both targets was significantly decreased in $SW620^{CD24neg}$ *vs.* $SW620^{LUC}$ (Figure 5.1F). Together the data from three different CRC cell lines indicate the up-regulation of VEGF-A by CD24.

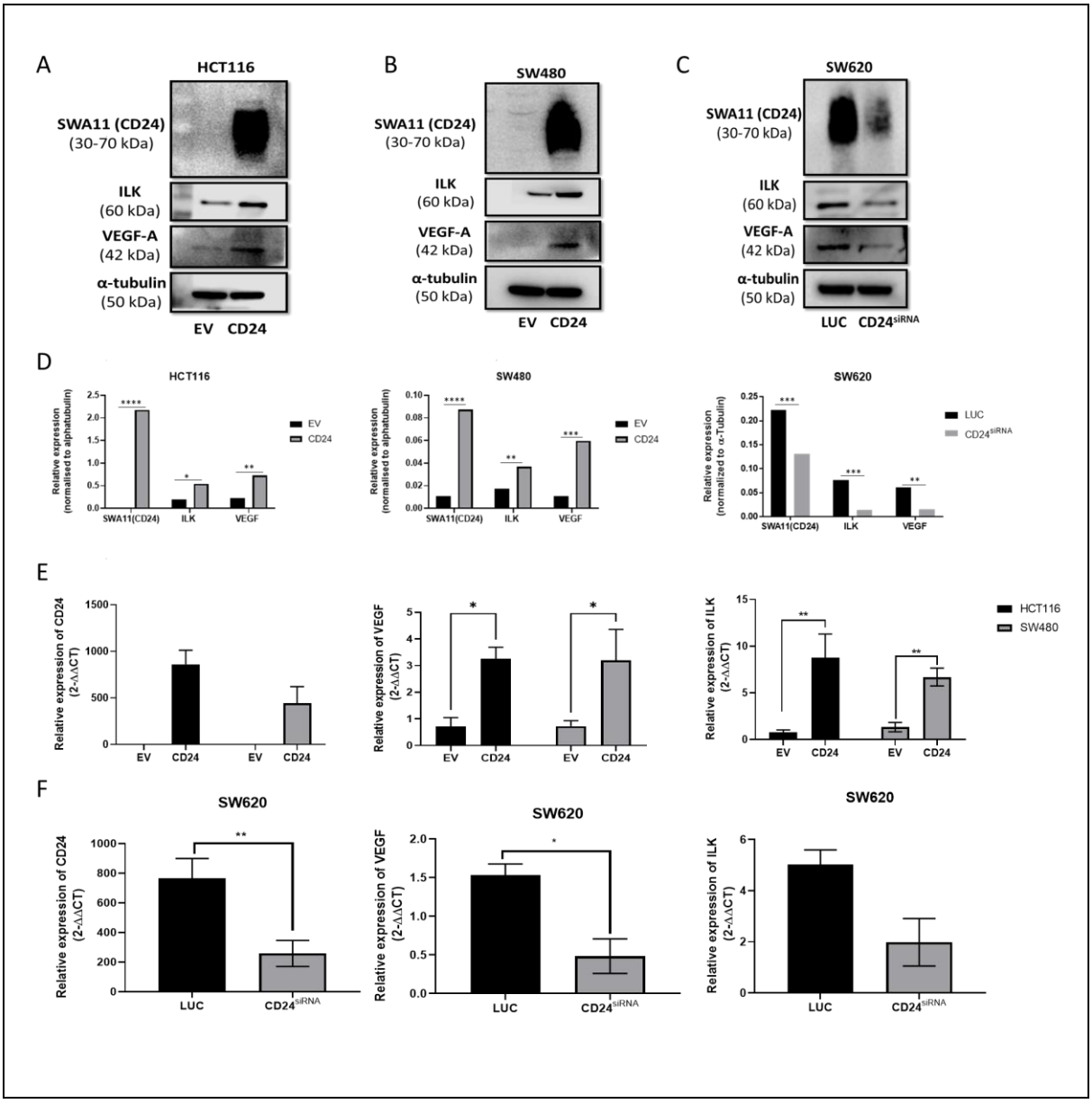


Figure 5.1 CD24 regulates VEGF-A expression in CRC cells.

Western blot analysis of ILK and VEGF-A in CD24 overexpressing cells, HCT116 (A), SW480 (B) and SW620 (C). Densitometry of relative expression of target proteins normalised to alpha-tubulin (D). The band intensities were analysed by image studio software and compared the stimulated and non-stimulated using GraphPad Prism with a student's T-test (two-tailed), *P < 0.05, **P < 0.01, ***P < 0.001, and ****P < 0.0001. RT-qPCR assessed the expression of CD24, ILK and VEGF-A in HCT116 and SW480 expressing CD24 (E). The mRNA expression level of CD24, ILK and VEGF-A in SW620 transfected with siRNA targeting CD24 and LUC control (F). All values of PCR in graphs C and D were analysed by

a One-Way ANOVA test with Sidak's multiple comparisons performed on GraphPad Prism, * P < 0.05, ** P <0.01, *** P < 0.001. The western blot and PCR results shown in the figure are one representative experiment with two biological replicates. Abbreviations: ILK: Integrin-linked Kinase; EVC: empty vector control; LUC: Luciferase.

5.2.2 CD24 enhances VEGF-A secretion to promote endothelial cell proliferation, migration, and vascular tube formation

Having shown that VEGF-A is a target of CD24 signalling, we sought to ascertain whether this induction resulted in the secretion of functionally active protein. Therefore, conditioned media (CM) was collected from CD24 expressing cells ($HCT116^{CD24WT}$ and $SW480^{CD24WT}$) as well as empty vector controls (as described in Chapter 2). The effect of the CM on proliferation, migration and tube formation on HUVEC was examined. For cell proliferation, the HUVEC cells were seeded at 5k cell density and culture for 24h. This was followed by incubation with the CM from CD24-expressing cells at different time points (0 hr,24 hr,48 hr and 72 hr) using PrestoBlue cell proliferation assay. For the cell migration, the assay was performed as follows: the endothelial cells were initially cultured on the upper Transwell chamber, and the CM-expressing CD24 was used as a chemoattractant on the receiver well and incubated for 24h. The Data from cell proliferation assay showed that the CM from CD24-expressing cells promoted HUVEC cell proliferation compared to cells expressing EVC or HUVEC cells stimulated with normal culture media alone (i.e., $HCT116^{CD24}$ *vs.* $HCT116^{EVC}$ or $HCT116^{CD24}$ *vs.* HUVEC, P<0.01 at 48 hr and P<0.001 at 72 hr) and ($SW480^{CD24}$ *vs.* $SW480^{EVC}$ or $SW480^{CD24}$ *vs*. HUVEC, P<0.05 at 48 hr and

P<0.01 at 72 hr) (Figure 5.2A and Figure 5.2C). Similarly, the migration of HUVEC cells increased when the CM retrieved from CD24 expressing cells used as a chemoattractant compared to cells expressing EVC and HUVEC alone (i.e., $HCT116^{CD24}$ *vs.* $HCT116^{EVC}$ or $HCT116^{CD24}$ *vs*. HUVEC, P<0.01) and ($SW480^{CD24}$ *vs.* $SW480^{EVC}$ or $SW480^{CD24}$ *vs.* HUVEC, P<0.01 and P<0.05, respectively) (Figure 5.2B and Figure 5.2D).

As with the previous section, we used an alternative method of modulation CD24 expression through silencing CD24 in SW620 using siRNA. CM was collected from $SW620^{CD24neg}$ and $SW620^{LUC}$ and used to stimulate HUVECs. The data show that both cell proliferation and cell migration of HUVEC were significantly reduced when the CM from $SW620^{CD24neg}$ was used compared to the CM from $SW620^{LUC}$ and HUVEC control cells (i.e., $SW620^{LUC}$ *vs.* $SW620^{CD24neg}$ or $SW620^{LUC}$ *vs.* HUVEC, P<0.05 and P<0.001, respectively) (Figure 5.2E and Figure 5.2F).

Having shown that CD24 induce HUVEC cell proliferation and migration, we next sought to investigate whether CD24 can promote the HUVEC cells ability to form tube-like structures. The tube forming assay was carried out by culturing the endothelial cells on top of the Matrigel layer, followed by overnight incubation using the CM from cells expressing CD24. The data showed that the CM from CD24 expressing cells efficiently enhanced HUVEC tube formation compared to that CM prepared from EVC expressing cells (i.e., $HCT116^{CD24WT}$ *vs.* $HCT116^{EVC}$ or $SW480^{CD24WT}$ *vs.* $SW480^{EVC}$, P<0.05) (Figure 5.3A and Figure 5.3B). However, the CM from $SW620^{CD24neg}$

stimulated significantly less endothelial tube formation compared to the CM from siRNA-LUC control (i.e., $SW620^{LUC}$ *vs.* $SW620^{CD24neg}$, $P<0.05$).

Since the above angiogenesis experiments were performed using the CM, the level of secreted VEGFA in the CM retrieved from the CD24-expressing cell was quantified using the ELISA test. The ELISA results showed that VEGF-A concentration was significantly higher in CM retrieved from CD24-overexpressing cells than EVC-overexpressing cells (i.e., $HCT116^{CD24}$ *vs.* $HCT116^{EVC}$ or $SW480^{CD24}$ *vs.* $SW480^{EVC}$, $P<0.01$) (Figure 5.3D). By contrast, the VEGF-A concentration significantly lowered in the CM collected from CD24 silenced SW620 compared to the LUC control (i.e., $SW620^{LUC}$ *vs.* $SW620^{CD24neg}$, $P<0.01$) (Figure 5.3D). Collectively, the results support the role of CD24 in promoting VEGF induced CRC angiogenesis.

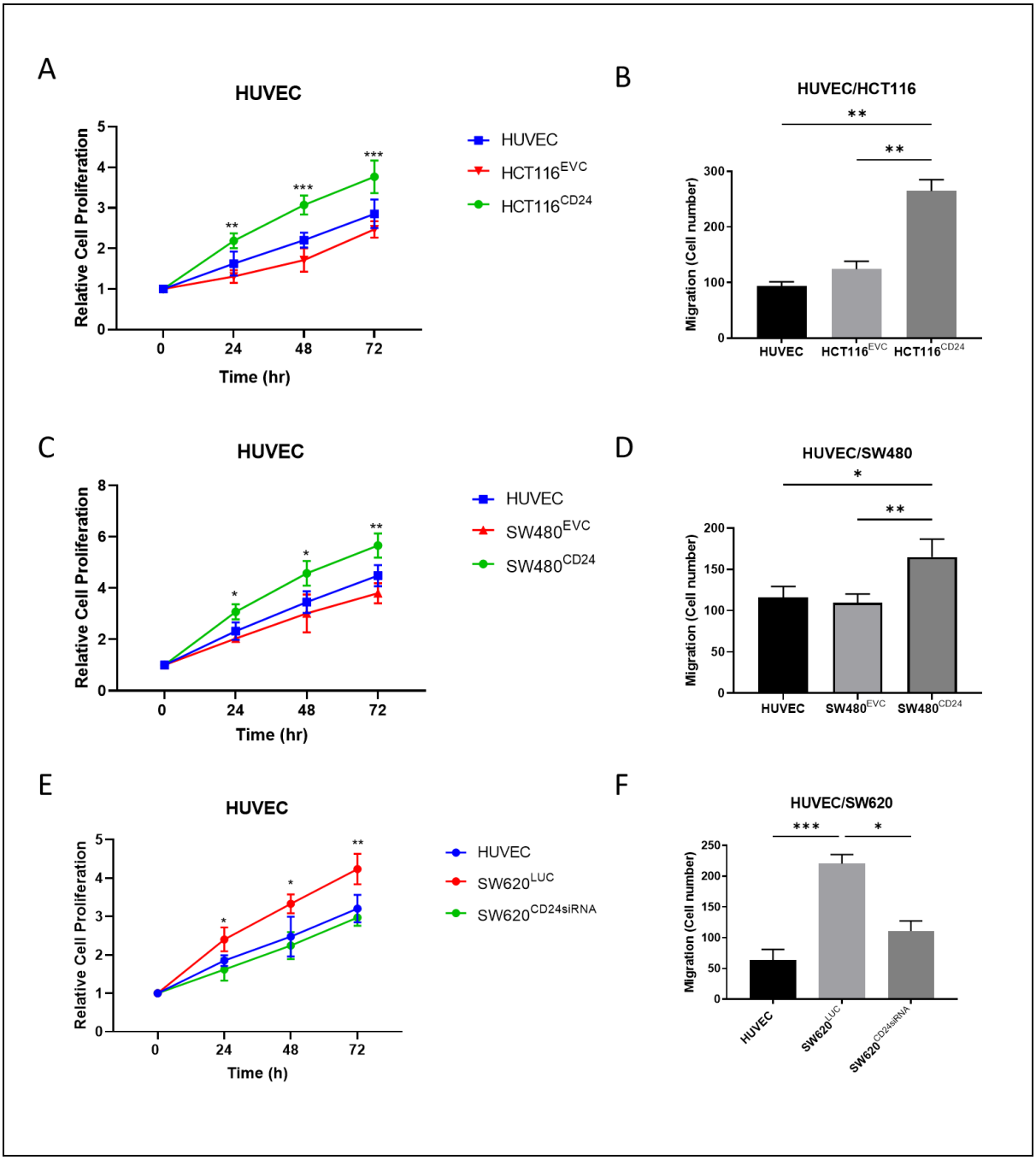
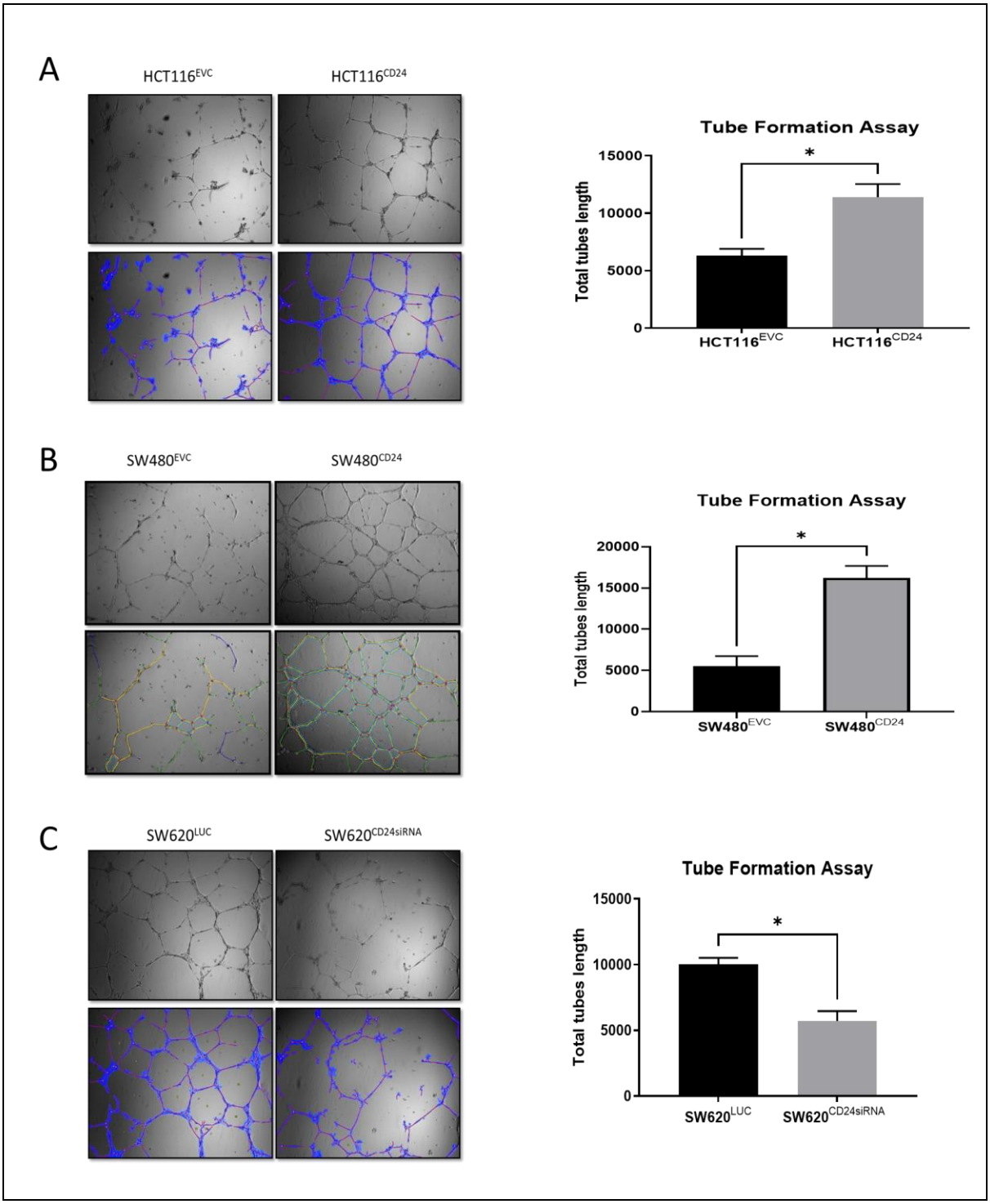


Figure 5.2 The effect of conditioned medium (CM) from CD24-expressing cells on HUVEC's cell proliferation and migration.

The increase in HUVECs' proliferation after using CM from CD24-expressing cells compared to HUVEC cell alone and EVC, HCT116 (A) and SW480 (C). Inhibition of HUVEC's proliferation by using CM from SW620^{CD24neg} (E). The graphs represent collated results from two independent experiments with 6 replicates for each condition. The relative cell proliferation displayed in cell proliferation graphs is based on the normalisation of relative fluorescence unit (RFU) readings to the reading obtained at 0 hr. Cell migration of HUVECs

was determined using transwell assay after plating the HUVECs with CM from HCT116 and SW480-expressing CD24 (B and D). The number of migrated HUVEC cells in transwell assay also decreased when incubated with CM from $SW620^{CD24neg}$ compared to $SW620^{LUC}$. The statistical analysis were evaluated by GraphPad Prism by two-way ANOVA with Tukey's multiple comparisons, $^{ns}P > 0.05$, $^{**}P < 0.01$, $^{***}P < 0.001$, $^{****}P < 0.0001$.



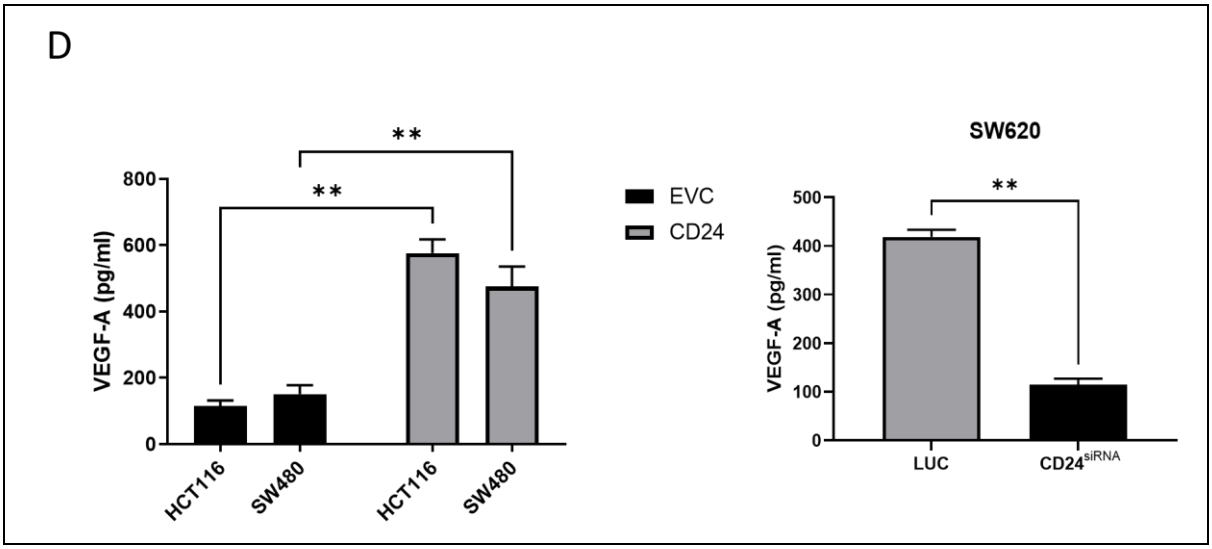


Figure 5.3 The effect of conditioned medium (CM) from CD24-expressing cells on angiogenesis.

The effect of HCT116 and SW480-expressing CD24 on HUVECs' tube formation (A and B). Scale bar 100μm. The CM from $SW620^{CD24neg}$ significantly reduced the tube formation ability of HUVECs (C). Analysis of total tube length by angiogenesis analyser in ImageJ software (A, B, and C right). Data for tube formation assay were compared using two-way ANOVA analysis; * $P < 0.05$ compared to control cells. ELISA test determined the VEGF-A concentration in the supernatant from the HCT116 and SW480-expressing CD24 and SW620 after transfecting with CD24 siRNA and LUC siRNA control (D), the statistical analysis was evaluated by GraphPad Prism by one-way ANOVA with Sidak's multiple comparisons, **P <0.01. The tube formation assay and ELISA results shown are one representative experiment with three biological replicates.

5.2.3 CD24 promoted VEGFA expression depending on ILK

ILK is an intracellular protein expressed by CRC cells and has been shown to regulate VEGF-A-mediated angiogenesis [152]. Since our data showed that CD24 positively regulates ILK and VEGF-A in CRC cells, we hypothesised that CD24 could promote the VEGF-A expression in CRC cells

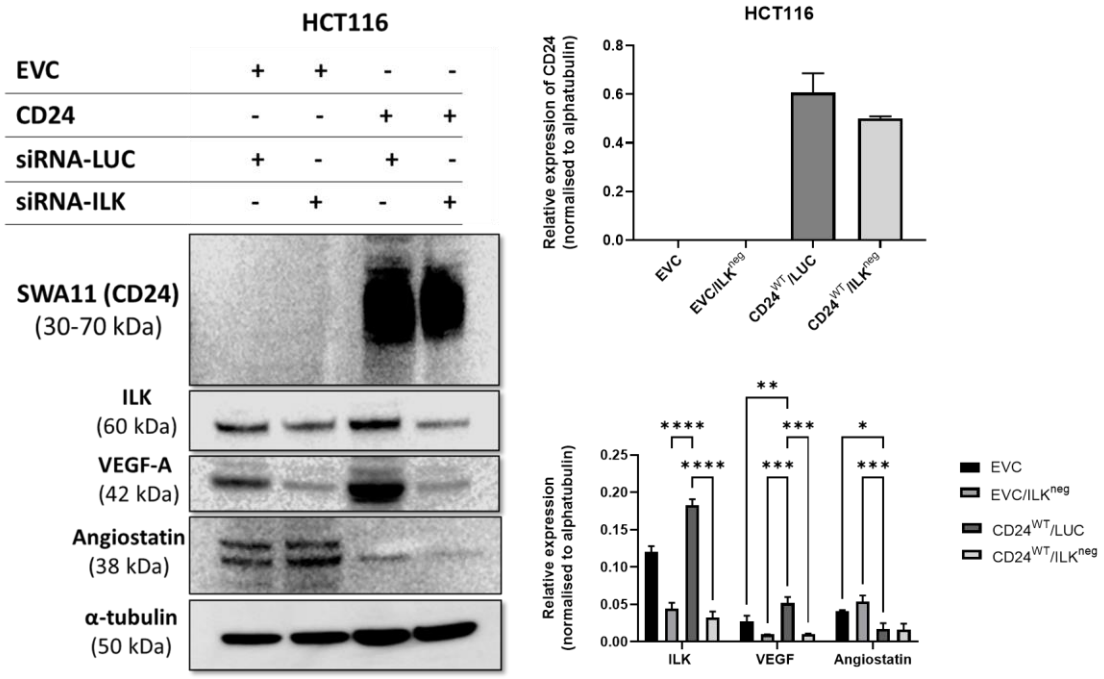
via ILK activation. To scrutinise this hypothesis, we performed a simultaneous co-transfection system in HCT116 and SW480 using a CD24-expression vector together with specific siRNA targeting ILK. A similar procedure was performed in SW620 (a cell line endogenously expressing CD24 and ILK) by silencing CD24 and ILK simultaneously using siRNA specifically targeting each molecule. The total protein lysates from the co-transfected cells underwent Western blotting to validate the transfection efficiency and evaluate the changes in ILK and VEGF-A proteins.

We found that the ectopic expression CD24 and simultaneous ILK silencing reduced VEGF-A protein level, i.e., ($HCT116^{CD24WT/ILKneg}$ *vs.* $HCT116^{CD24WT/LUC}$) and ($SW480^{CD24WT/ILKneg}$ *vs*. $SW480^{CD24WT/LUC}$) (Figure 5.4A and Figure 5.4B). Angiostatin is an angiogenic inhibitor of angiogenesis – performing the opposite role of VEGF-A – and has been reported to be produced by cancer cells. We, therefore, hypothesised that CD24, as well as activating VEGF-A, could inhibit the expression of angiostatin. As may have been predicted, ectopic expression of CD24 in both HCT116 and SW480 resulted in down-regulation of angiostatin, i.e., it was CD24-dependent. However, the expression of angiostatin was independent of ILK, i.e., the levels of angiostatin were the same in the condition of $HCT116^{CD24WT/LUC}$ *vs*. $HCT116^{CD24WT/ILKneg}$ and $HCT116^{EVC/ILKneg}$ *vs.* $HCT116^{EVC/LUC}$). The picture was the same for SW480, i.e., the levels of angiostatin were the same in the condition of $SW480^{CD24WT/LUC}$ *vs.* $SW480^{CD24WT/ILKneg}$ and $SW480^{EVC/ILKneg}$ *vs.* $SW480^{EVC/LUC}$) (Figure 5.4A and Figure 5.4B). Thus, the Western blot results confirm that CD24 induces

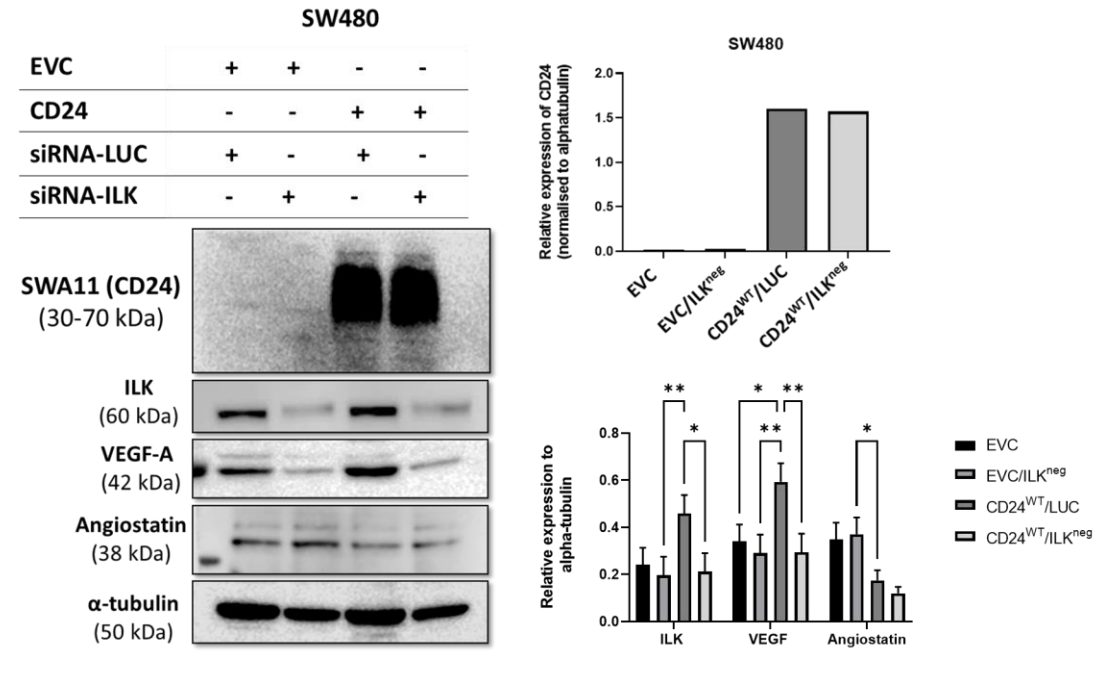
VEGF-A expression via ILK and inhibits the angiostatin expression in a mechanism independent of ILK.

The data were confirmed when CD24 and ILK were modulated in SW620 (which expresses endogenous CD24). Thus, when either CD24 or ILK was knocked down (i.e., $SW620^{CD24neg/LUC}$, $SW620^{ILKneg/LUC}$, $SW620^{CD24neg/ILKneg}$), there was a reduction of VEGF-A expression compared to the controls ($SW620^{LUC/LUC}$- these cells contained twice the amount of luciferase siRNA to ensure that siRNA concentration was not a confounder). This indicates that VEGF-A induction is dependent on a CD24-ILK signalling axis (Figure 5.4C). In contrast (in keeping with our earlier data), angiostatin expression was only up-regulated when CD24 was knocked down, i.e. $SW620^{CD24neg/LUC}$, $SW620^{CD24neg/ILKneg}$). Levels of angiostatin were not affected if endogenous CD24 was expressed and ILK was knocked down ($SW620^{ILKneg/LUC}$) or in the luciferase controls ($SW620^{LUC/LUC}$).

A


HCT116
EVC + + - -
CD24 - - + +
siRNA-LUC + - + -
siRNA-ILK - + - +
SWA11 (CD24)
(30-70 kDa)
ILK
(60 kDa)
VEGF-A
(42 kDa)
Angiostatin
(38 kDa)
α-tubulin
(50 kDa)
HCT116
Relative expression of CD24
(normalised to alphatubulin)
EVC
EVC/ILK^neg
CD24^WT/LUC
CD24^WT/ILK^neg
Relative expression
(normalised to alphatubulin)
ILK
VEGF
Angiostatin
EVC
EVC/ILK^neg
CD24^WT/LUC
CD24^WT/ILK^neg

B


SW480
EVC + + - -
CD24 - - + +
siRNA-LUC + - + -
siRNA-ILK - + - +
SWA11 (CD24)
(30-70 kDa)
ILK
(60 kDa)
VEGF-A
(42 kDa)
Angiostatin
(38 kDa)
α-tubulin
(50 kDa)
SW480
Relative expression of CD24
(normalised to alphatubulin)
EVC
EVC/ILK^neg
CD24^WT/LUC
CD24^WT/ILK^neg
Relative expression to
alpha-tubulin
ILK
VEGF
Angiostatin
EVC
EVC/ILK^neg
CD24^WT/LUC
CD24^WT/ILK^neg

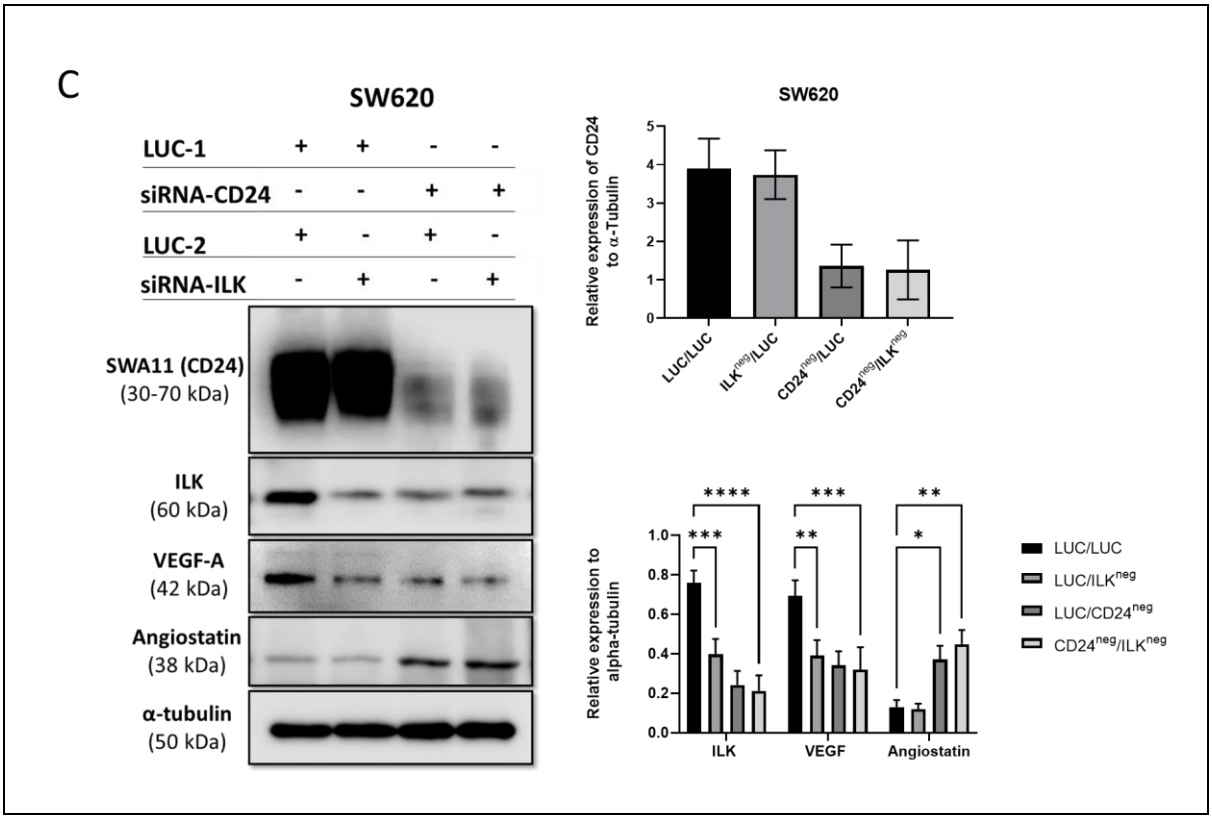


Figure 5.4 CD24 mediates VEGF-A expression via ILK in CRC cell lines.

Western blotting confirming the simultaneous delivery of CD24 plasmid and ILK siRNA in HCT116 (A) and SW480 (B), and the direct role of CD24/ILK signalling axis in regulating VEGF-A expression. However, Western blot showed that the regulation of angiostatin expression was autonomous of ILK. Validation of simultaneous knockdown of CD24 and ILK in the SW620 (C) cell line positively influenced the VEGF-A and angiostatin expression. The band intensities were analysed by image studio software and compared the transfected cells using GraphPad Prism with a student's T-test (two-tailed), *P < 0.05, **P < 0.01, ***P < 0.001, ****P < 0.0001). The western blot results shown are one representative experiment with two biological replicates. Abbreviations: EVC: empty vector control, LUC1: luciferase control for CD24-siRNA, LUC2: luciferase control for ILK-siRNA.

5.2.4 CD24 enhanced endothelial cells proliferation, migration and tube formation via ILK/VEGFA signalling axis

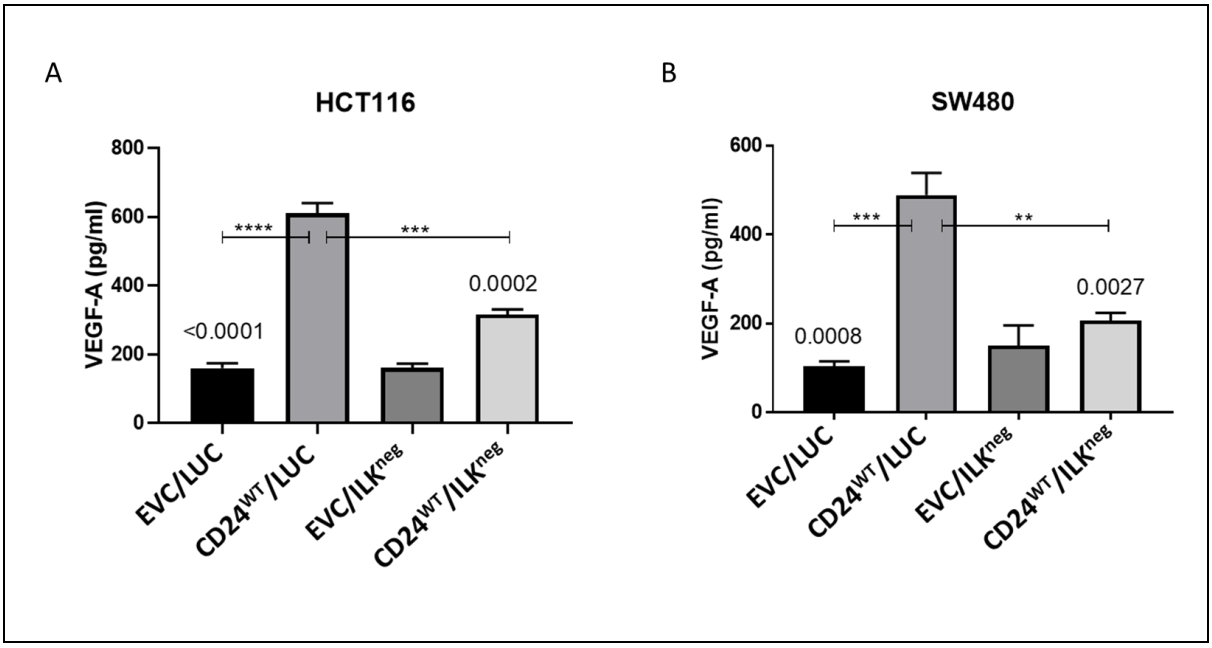
After confirming that ILK is necessary for CD24 to mediate VEGF-A expression, we sought to determine whether the ILK/VEGF-A signalling pathway is required for CD24 to enhance endothelial cell activities. In addition, by performing the functional assays, we would be able to see whether there were alternative non-ILK dependent pathways to activate VEGF-A.

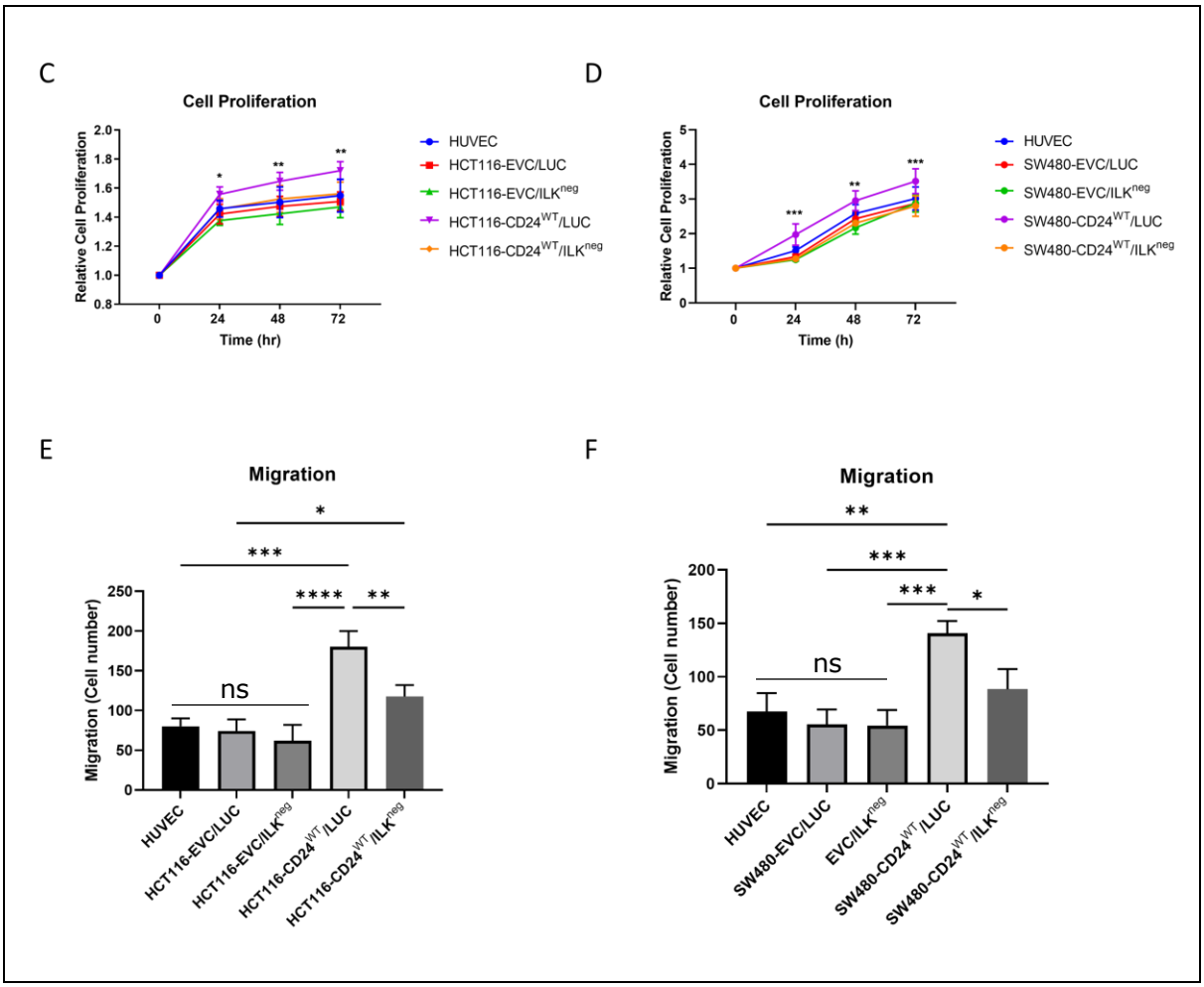
We used the same technique performed above by collecting the CM from transfected cells and testing the CM's effect on endothelial cell proliferation, migration, and tube formation. A quantitative ELISA test showed a decrease in the VEGF-A concentration in both HCT116 and SW480 following ILK silencing compared to the control conditions (i.e., $HCT116^{EVC/LUC}$ *vs.* $HCT116^{CD24WT/LUC}$ or $HCT116^{CD24WT/ILKneg}$ *vs.* $HCT116^{CD24WT/LUC}$, $P<0.0001$ and $P=0.0002$, respectively), and ($SW480^{EVC/LUC}$ *vs.* $SW480^{CD24WT/LUC}$ or $SW480^{CD24WT/ILKneg}$ *vs.* $SW480^{CD24WT/LUC}$, $P=0.0008$ and $P=0.0027$, respectively) (Figure 5.5A and Figure 5.5B).

For endothelial cell proliferation and migration assays, the CM retrieved from the conditions in which CD24 was overexpressed with simultaneous ILK silencing showed a significant reduction in cell proliferation and migration compared with the CM from control cells (i.e., $HCT116^{EVC/LUC}$ *vs.* $HCT116^{CD24WT/LUC}$, $HCT116^{CD24WT/ILKneg}$ *vs.* $HCT116^{CD24WT/LUC}$, or HUVEC *vs.* $HCT116^{CD24WT/LUC}$, $P<0.01$ and $P<0.05$), and ($SW480^{EVC/LUC}$ *vs.*

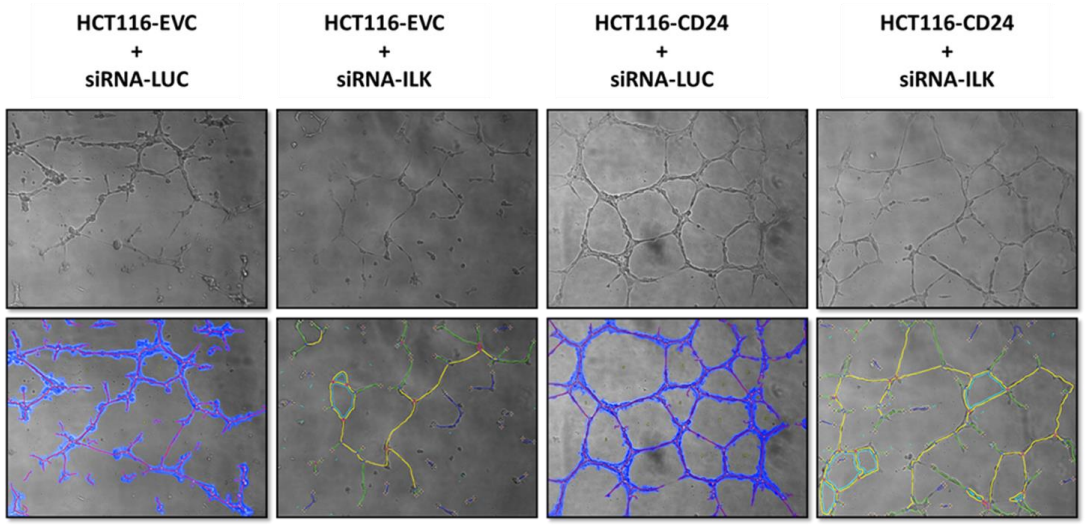
$SW480^{CD24WT/LUC}$, $SW480^{CD24WT/ILKneg}$ *vs.* $SW480^{CD24WT/LUC}$ or HUVEC *vs.* $SW480^{CD24WT/LUC}$, $P<0.01$ and $P<0.001$) (Figure 5.5C and Figure 5.5D, cell proliferation) and (Figure 5.5E and Figure 5.5F, cell migration). Thus, the data confirm the importance of ILK to CD24 for regulating these activities. The levels were not quite reduced to the levels of the controls suggesting that there may be non-ILK dependent pathways but, if they existed, they contributed less than the ILK-dependent pathways.

Tube formation was another assay used to demonstrate angiogenesis in vitro. The data showed that the HUVECs' tube formation ability was suppressed following incubation with CM from cells in which ILK was silenced compared with the control cells (i.e., $HCT116^{EVC/siRNA-LUC}$ vs. $HCT116^{CD24WT/LUC}$, $HCT116^{EVC/ILKneg}$ *vs.* $HCT116^{CD24WT/LUC}$, and $HCT116^{CD24WT/ILKneg}$ *vs.* $HCT116^{CD24WT/LUC}$, $P<0.01$ and $P<0.05$), or ($SW480^{EVC/LUC}$ *vs.* $SW480^{CD24WT/LUC}$, $SW480^{EVC/ILKneg}$ *vs.* $SW480^{CD24WT/LUC}$ and $SW480^{CD24WT/ILKneg}$ *vs.* $SW480^{CD24WT/LUC}$, $P<0.05$ and $P<0.01$) (Figure 5.5G and Figure 5.5H). The above results indicated that CD24-mediated tumour angiogenesis is mainly dependent on the ILK/VEGF-A signalling pathway.

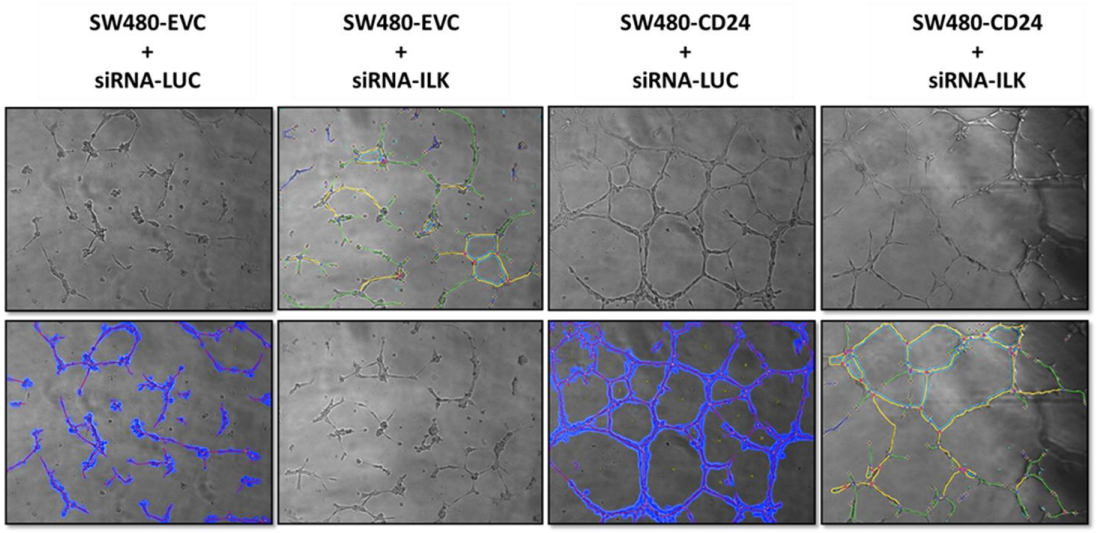

A
HCT116
VEGF-A (pg/ml)
800
600
400
200
0
****
***
<0.0001
0.0002
EVC/LUC
CD24WT/LUC
EVC/ILKneg
CD24WT/ILKneg
B
SW480
VEGF-A (pg/ml)
600
400
200
0
***
**
0.0008
0.0027
EVC/LUC
CD24WT/LUC
EVC/ILKneg
CD24WT/ILKneg


C
Cell Proliferation
Relative Cell Proliferation
2.0
1.8
1.6
1.4
1.2
1.0
0.8
0
24
48
72
Time (hr)
HUVEC
HCT116-EVC/LUC
HCT116-EVC/ILKneg
HCT116-CD24WT/LUC
HCT116-CD24WT/ILKneg
D
Cell Proliferation
Relative Cell Proliferation
5
4
3
2
1
0
0
24
48
72
Time (h)
HUVEC
SW480-EVC/LUC
SW480-EVC/ILKneg
SW480-CD24WT/LUC
SW480-CD24WT/ILKneg
E
Migration
Migration (Cell number)
250
200
150
100
50
0
*
***
****
**
ns
HUVEC
HCT116-EVC/LUC
HCT116-EVC/ILKneg
HCT116-CD24WT/LUC
HCT116-CD24WT/ILKneg
F
Migration
Migration (Cell number)
200
150
100
50
0
**
***
***
*
ns
HUVEC
SW480-EVC/LUC
EVC/ILKneg
SW480-CD24WT/LUC
SW480-CD24WT/ILKneg

G


HCT116-EVC + siRNA-LUC
HCT116-EVC + siRNA-ILK
HCT116-CD24 + siRNA-LUC
HCT116-CD24 + siRNA-ILK

H


SW480-EVC + siRNA-LUC
SW480-EVC + siRNA-ILK
SW480-CD24 + siRNA-LUC
SW480-CD24 + siRNA-ILK

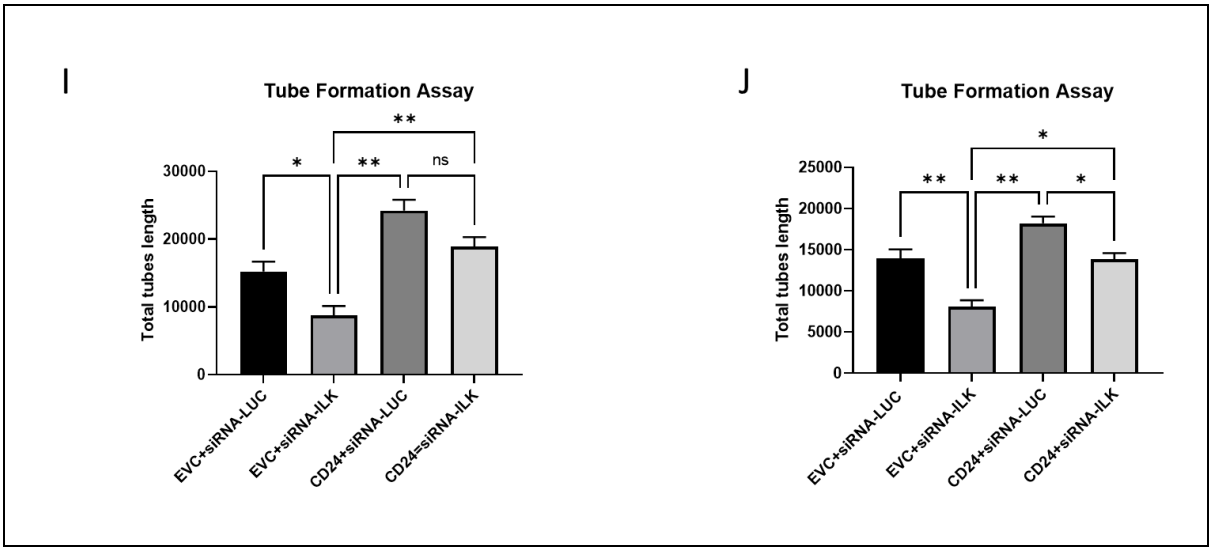


Figure 5.5 CD24 mediates angiogenesis via the VEGF-A/ILK signalling axis.

Quantitative ELISA test confirmed that the VEGF-A concentration decreased when ILK was knocked down in HCT116 (A) and SW480 (B). Conditioned medium (CM) from ILK siRNA cells decreased HUVECs' proliferation (C and D) and migration (E and F). The relative cell proliferation displayed in cell proliferation graphs is based on the normalisation of relative fluorescence unit (RFU) readings to the reading obtained at 0 hr. The graphs represent collated results from two independent experiments with 6 replicates for each condition. The HUVECs tube formation ability was inhibited after incubation with CM from cells transfected with ILK siRNA (G and H). ImageJ analysis of the total tube length using angiogenesis analyser (I and J). The statistical analysis were evaluated by GraphPad Prism by two-way ANOVA with Tukey's multiple comparisons, $^{ns}P > 0.05$, $^{**}P < 0.01$, $^{***}P < 0.001$, $^{****}P < 0.0001$. The results shown in the figure are one representative experiment with two biological replicates.

5.2.5 Loss of *N*-glycosylation of CD24 reduced the expression level of the ILK/VEGF signalling pathway

In the third chapter, *N*-glycosylation sites were shown to influence CD24 function in CRC cells and that an expression construct containing the mutation of both *N*-glycosylation sites ($CD24^{N[36,52]Q}$) expressed CD24 protein, which was functionally "inactivated". To confirm the role of *N*-glycosylation on the CD24-ILK induced VEGF-A protein expression, the HCT116 and SW480 cell lines were transfected with $CD24^{WT}$ and $CD24^{N[36,52]Q}$. Then the protein lysates were collected and underwent Western blotting. In line with our above findings, $CD24^{WT}$ overexpression in HCT116 and SW480 led to increased expression of ILK and VEGF-A proteins and decreased expression of angiostatin compared to EVC (Figure 5.6A and Figure 5.6B). In contrast, for both cell lines, the ectopic expression of $CD24^{N[36,52]Q}$ failed to induce either ILK, and VEGF-A expression whilst angiostatin expression remained at the same level as the empty vector controls (Figure 5.6A and Figure 5.6B).

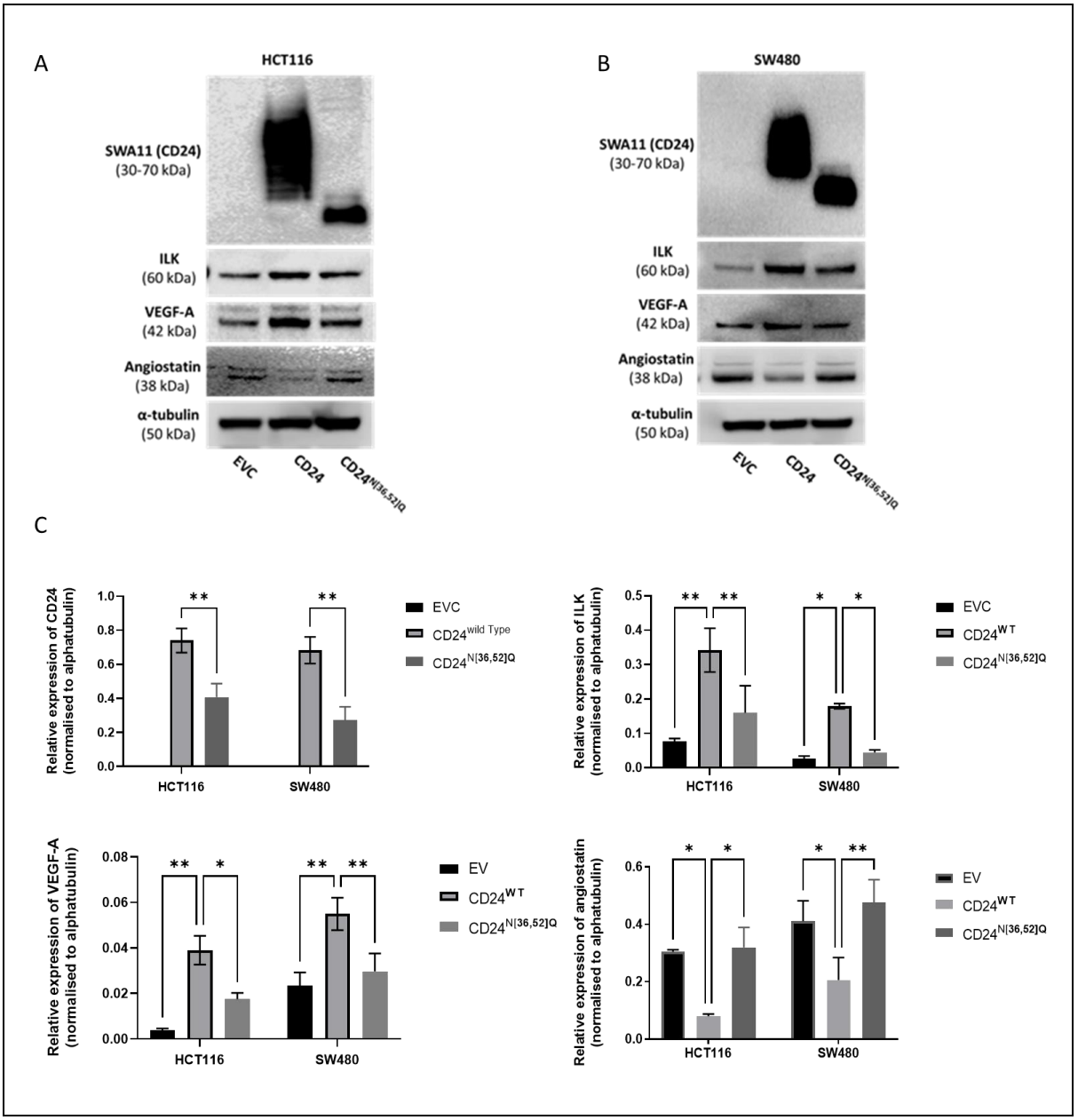


Figure 5.6 Loss of N-glycosylation disrupts ILK/VEGF-A signalling axis

Western blot analysis confirming the effect of loss of *N*-glycosylation on ILK/VEGF-A signalling axis and angiostatin in HCT116 (A) and SW480 (B). Densitometry of the targeted proteins after normalisation with alpha-tubulin (C). The band intensities were analysed by image studio software and compared the stimulated and non-stimulated using GraphPad Prism with a student's T-test (two-tailed), *P<0.05, **P<0.001. The western blot results shown are one representative experiment with two biological replicates.

5.2.6 Loss of *N*-glycosylation inhibits CD24-mediated endothelial cell proliferation, migration, and tubes formation

Western blotting revealed that loss of *N*-glycosylation in CD24 affects the expression of ILK/VEGF-A signalling. Here, we sought to investigate whether CM from cells transfected with CD24-mutant construct ($CD24^{N[36,52]Q}$) functionally affects HUVEC cell angiogenesis. First, the concentration of VEGF-A in CM was quantified by ELISA. Then proliferation, migration and endothelial tube formation assays were performed as previously described. ELISA results demonstrated that the CD24-mutant construct ($CD24^{N[36,52]Q}$) resulted in much lower levels of VEGF-A concentration in both HCT116 and SW480 (i.e., $HCT116^{CD24WT}$ *vs.* $HCT116^{CD24N[36,52]Q}$ or $SW480^{CD24WT}$ *vs.* $SW480^{CD24N[36,52]Q}$, P=0.0031 and P=0.0114, respectively (Figure 5.7A).

We next examined the proliferation and migration capability and tube formation potency of HUVECs using CM from $HCT116^{CD24N[36,52]Q}$ and $SW480^{CD24N[36,52]Q}$. As expected from the ELISA results, the proliferation and migration were inhibited when the HUVECs were incubated with the CM from cells expressing $CD24^{N[36,52]Q}$ compared to the cells expressing wild-type CD24 (Figure 5.7B, cell proliferation and Figure 5.7C, cell migration). Similarly, the tube forming ability of HUVECs was suppressed when incubated with CM from $CD24^{N[36,52]Q}$-overexpressing cells compared to that incubated with CM from cells expressing $CD24^{WT}$ (i.e., $HCT116^{CD24WT}$ *vs.* $HCT116^{CD24N[36,52]Q}$ or $SW480^{CD24WT}$ *vs.* $SW480^{CD24N[36,52]Q}$) (Figure 5.8A, Figure 5.8B and Figure 5.8C).

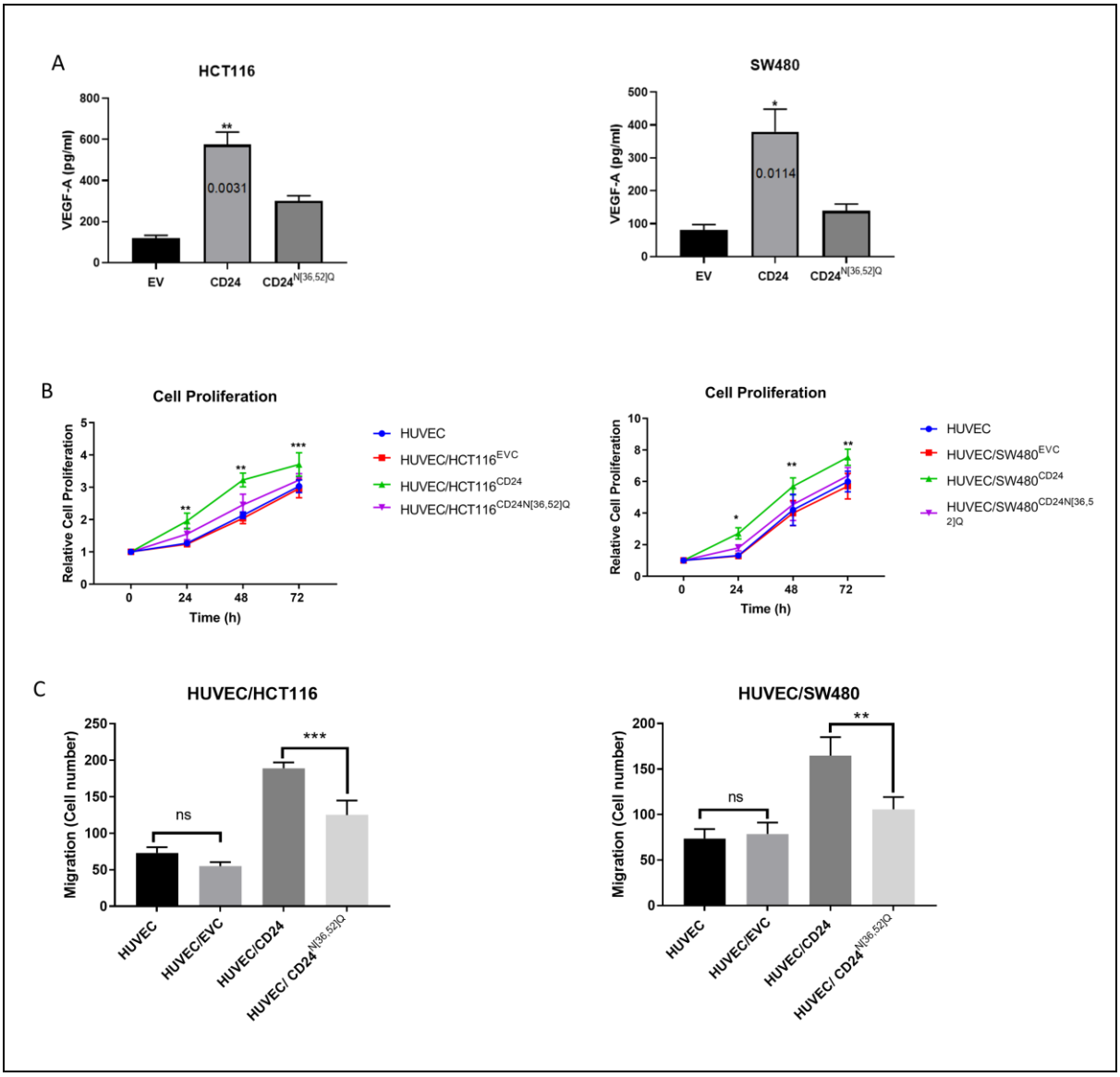
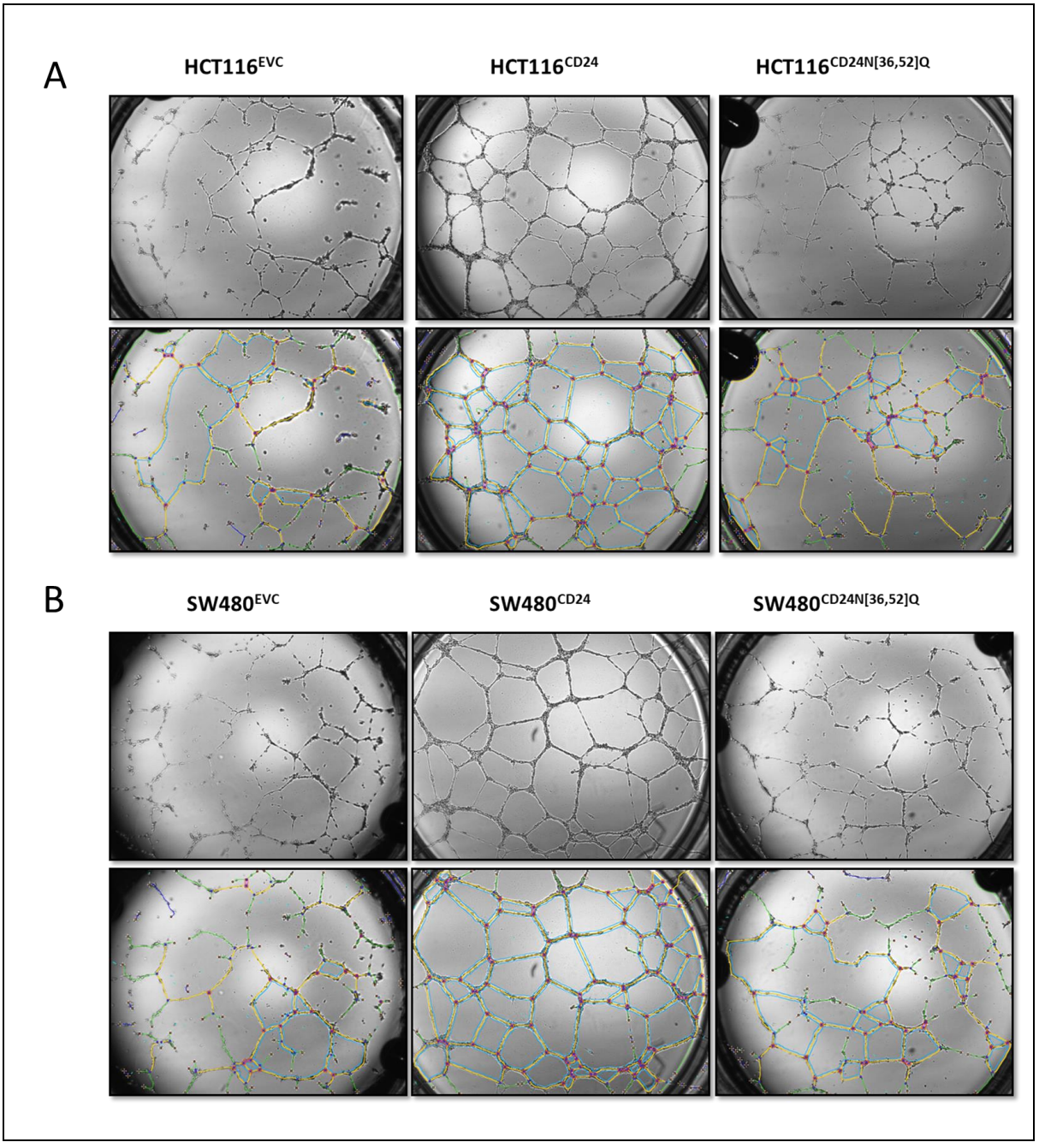


Figure 5.7 Loss of *N*-glycosylation in CD24 inhibits HUVEC cell proliferation and migration.

Quantitative ELISA test validating effect $CD24^{N[36,52]Q}$ on VEGF-A concentration in HCT116 (A-right) and SW480 (A-left). Conditioned medium (CM) from CD24-mutant clone ($CD24^{N[36,52]Q}$) decreased HUVECs' proliferation (B). The relative cell proliferation displayed in cell proliferation graphs is based on the normalisation of relative fluorescence unit (RFU) readings to the reading obtained at 0 hr. The graphs represent collated results from two independent experiments with 6 replicates for each condition. A reduction in the Transwell migration assay for HUVECs after incubating with CM from $CD24^{N[36,52]Q}$ (C). The statistical analysis were evaluated by GraphPad Prism by two-way ANOVA with Tukey's multiple

comparisons, ^{ns}P >0.05, **P <0.01, ***P <0.001, ****P <0.0001. The results shown in the figure are one representative experiment, repeated twice.



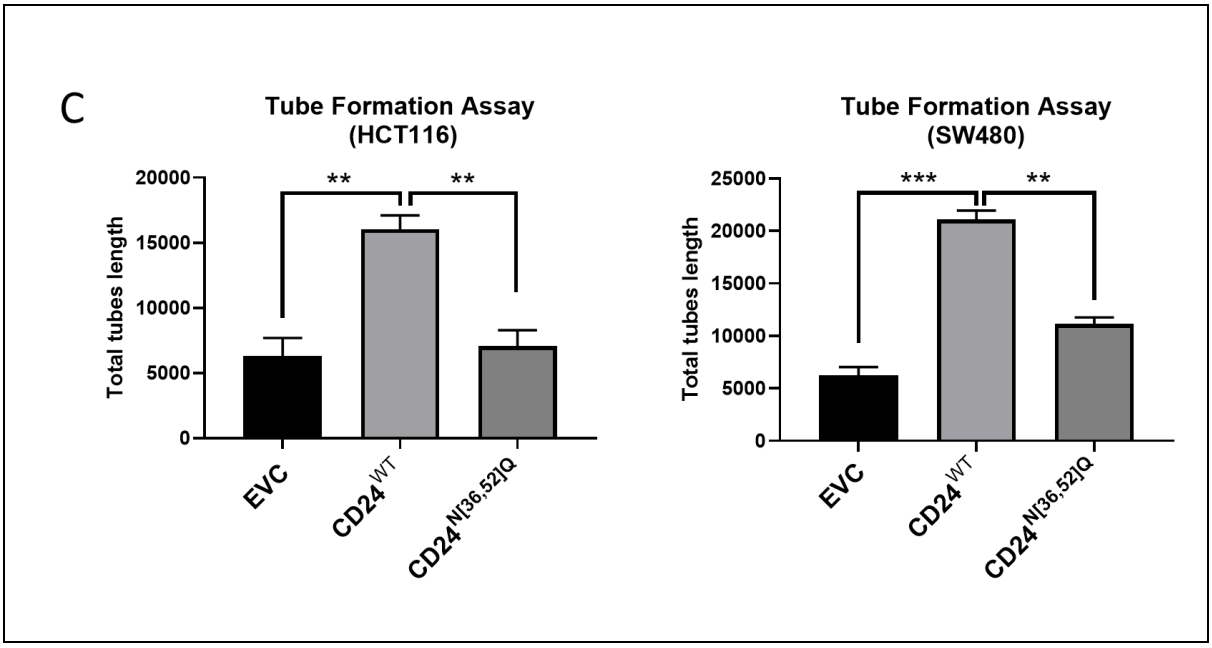


Figure 5.8 Loss of *N*-glycosylation in CD24 inhibits HUVEC tube formation.

The HUVECs' tube formation ability was inhibited after incubation with CM from HCT116 (A) and SW480 (B) that transfected with CD24-mutant construct ($CD24^{N[36,52]Q}$). Bar graph indicating the ImageJ analysis of the total tube length using angiogenesis analyser (C). The statistical analysis were evaluated by GraphPad Prism by two-way ANOVA with Tukey's multiple comparisons, $^{ns}P > 0.05$, $^{**}P < 0.01$, $^{***}P < 0.001$, $^{****}P < 0.0001$. The results shown in the figure are one representative experiment with two biological replicates.

5.3 Discussion

In our previous chapters, CD24 was demonstrated to regulate several cellular activities in CRC epithelial cells, including cell migration and invasion. Moreover, we found that CD24 binds to P-selectin expressed by endothelial cells and mediates adhesion to endothelial cells and transendothelial migration. These features are essential to the process of metastasis, and in this chapter, the aim was to investigate whether CD24 could contribute further to metastasis by promoting angiogenesis. Since angiogenesis is an essential process for the growth of the primary tumour, CD24 would also contribute to this [248, 249]. Angiogenesis is a complex process and is regulated by many growth factors and cytokines produced by tumour cells [250]. However, the principal growth factor promoting tumour angiogenesis is VEGF-A [251], which has been reported to be associated with vascularity and metastasis in human CRC [252].

This is the most comprehensive study of the role of CD24 in angiogenesis to date. We used three CRC cell lines (HCT116, SW480, SW620), and we used different methods to modulate CD24 levels – either an ectopic-expression vector in cell lines with low endogenous CD24 expression (HCT116 and SW480) or CD24-siRNA in a cell line with high endogenous CD24 expression (SW620). We found that the upregulation of VEGF-A in cells ectopically overexpressed with CD24 when compared to those overexpressed with empty vector control. In contrast, knockdown CD24 in SW20 resulted in a lower level of VEGF-A. These data were validated by

ELISA quantification of the secreted VEGF-A concentration in the supernatant retrieved from the transfected cells. The results showed that the altered expression of CD24 significantly affected the VEGF-A protein concentration in CRC cells. Taken together, CD24 appears to be essential for the regulation of VEGF-A expression in CRC cells. We believe that this is the first time the connection between CD24 and secreted VEGF-A has been observed.

To confirm that the CD24-driven VEGF-A was functionally active, we examined the effects on cell proliferation and migration of HUVECs. These are some of the key steps of angiogenesis [253], and we showed that the CM from CD24-expressing cells significantly enhanced proliferation and migration, while the CM from CD24-silenced cells failed to induce these activities. In addition, we explored the capillary like-tube formation capacity in HUVECs using *in vitro* tube formation assay, as it mimics *in vivo* angiogenesis and involves all of the angiogenesis steps [254]. We found that CD24 positively regulated tube formation in HUVECs.

Together, our results provide strong *in-vitro* evidence that CD24 could stimulate angiogenesis in CRC by regulating the VEGF-A expression. This would fit in with a role for CD24 in promoting metastasis through binding to the endothelium, stimulating extravasation and stimulating angiogenesis. Furthermore, the ability of CD24 to induce stemness would help the establishment of colonies. Metastasis also involves growth in a new environment, establishment of the appropriate cancer-stroma and evasion

of the local immune response. These studies would most probably require animal models to further investigate the role of CD24 in these processes.

Previous studies have indicated that ILK was found to mediate the expression of VEGF-A and angiogenesis [152, 196, 255]. This was the driver behind our initial studies since ILK is a downstream target for CD24 [199]. Therefore, we determined whether ILK is required for CD24 to regulate VEGF-A expression. Our results revealed that CD24 positively regulated ILK and VEGF-A expression and inhibited angiostatin expression (an endogenous angiogenesis inhibitor) [256]. However, totally unexpectedly, when we used siRNA targeting ILK in CD24 expressing cells, there was a failure to induce VEGF-A expression, whilst angiostatin expression remained unaltered. These results suggest that CD24 signals through ILK to promote VEGF-A expression in CRC cells and that it inhibits angiostatin expression but through a mechanism that is independent of ILK. Due to the time limitations at the current stage of research, we could not fully investigate which downstream CD24 signalling pathways are involved in regulating angiostatin in CRC. Future works are required to answer this question.

To demonstrate that the contribution of CD24 and ILK in the VEGF-A-mediated angiogenesis was functionally relevant, we collected the CM from our various experimental conditions and examined their effect on HUVECs' activities. Reflecting the Western blots, we found that the stimulatory effect of CD24 on HUVECs' proliferation, migration and tube formation were all

ILK dependent. The knockdown of ILK in the presence of CD24 did not completely abrogate the activities of CD24, raising the possibility of a minor alternative signalling pathway for CD24 mediated angiogenesis.

We have previously shown that loss of *N*-glycosylation sites in CD24 results in a marked reduction in the level of glycosylation (despite the presence of around 16 *O*-glycosylation sites) and an expression of a functionally inactivated CD24 molecule. Transfection of the functionally inactivated CD24 protein ($CD24^{N[36,52]Q}$) was equivalent to transfection with empty vector controls and resulted in failure to induce any of the features seen following transfection of the wild-type protein. Our data confirm the functional role of *N*-glycosylation of CD24 in CRC angiogenesis, which are compatible with studies that reported the contribution of *N*-linked glycosylation to tumour angiogenesis and metastasis [232, 257]. For example, Galectin-3, which is expressed in several tumours, including CRC, has been associated with angiogenesis induction by binding to glycoproteins on the surface of endothelial cells in an *N*-glycan-dependent manner [258, 259].

In conclusion, although the obtained results were from in vitro cellular experiments, this chapter provides strong data supporting the possible role of CD24 in inducing angiogenesis in CRC in an N-glycosylation and ILK dependent manner. The effects are mediated through induction and secretion of VEGF-A and inhibition of angiostatin. The latter is, however, mediated through an ILK-independent pathway which remains to be

elucidated. Thus, further investigations are necessary to reveal the role of CD24 in CRC angiogenesis, particularly which are the predominant splice variants and relevance *in vivo*.

5.4 Summary of findings

- Using three different CRC cell lines, CD24 was found to up-regulate VEGF-A expression and enhance angiogenesis.
- ILK was found to mediate the upregulation of VEGF-A via CD24 in CRC cells.
- Angiostatin, a potent angiogenesis inhibitor, is inhibited by CD24, and the mechanism was found to be independent of ILK.
- CD24 mediates HUVECs' proliferation, migration, and the ability to form tubes via upregulation of ILK and VEGF-A.
- Loss of *N*-glycosylation of CD24 resulted in failure to induce the VEGF-A expression and failure to inhibit angiostatin expression.
- Loss of *N*-glycosylation of CD24 resulted in failed angiogenesis in CRC by failure to induce HUVEC cell proliferation, migration, and tube formation.

Chapter 6: General Discussion

6.1 Introduction

CD24 is a triple-exon gene located at chromosome 6 on the long arm (q21). It encodes a small, heavily glycosylated protein (comprised of 80 amino acids) and is attached via GPI anchor to the cell surface membrane [79]. CD24 mature peptides consist of 16 *O*-glycosylation sites and two potential *N*-glycosylation sites, and, due to the variable glycosylation, its molecular weight ranges from 30 to 70 kDa [97, 187]. Although CD24 lacks a cytoplasmic domain to transmit signals, it localises to membrane lipid-rich microdomains known as lipid rafts. In these lipid rafts, CD24 serves as a mediator for the passage of many proteins into and out of the cell and regulates signal transduction [116].

CD24 expression was found to regulate many cellular functions in both healthy and cancerous tissues [83]. For example, its expression has been demonstrated in the normal murine colon and has been used to isolate $Lgr5^{+}$ putative colonic epithelial stem cells [90]. However, CD24 overexpression has been associated with induction of stemness and reduced overall survival in several tumour tissues, including CRC, which was used as a CSC marker [99, 211].

Although a growing body of studies has indicated some functional roles of CD24 in cancer development, our knowledge on the structural biology of CD24, its binding capacity with other cell surface molecules expressed by

the neighbouring cells, and its role in regulating cellular activities, particularly in CRC, remains incomplete.

The main purpose of this thesis is to understand the biological role and contribution of CD24 in CRC progression; thus, the aims were specifically based on the following theories:

I. *N*-glycosylation sites were thought to regulate the function of many glycoproteins; thus, the first aim was to investigate the role of *N*-glycosylation in CD24 in regulating its functional activities in CRC.

II. CD24 is a cell surface molecule that can interact with other cell surface molecules or can act as a receptor for other cell adhesion molecules expressed by endothelial cells such as P-selectin. This feature may allow CD24 to bind and mediate multiple signalling pathways and cellular activities, which are possibly relevant to metastasis. Therefore, the second aim of this research was to study the mechanism of CD24 binding to P-selectin and the effect of this binding on signalling pathways that enhance cell motility and CRC cell adhesion to endothelial cells.

III. The metastatic process requires the establishment of an appropriate local microenvironment, including a vascular supply, to support tumour growth. Published data suggest that activation of ILK in tumour cells may induce secretion of VEGF

and, since we have shown that CD24 can induce ILK, we hypothesise that this may be a component of the metastasis-promoting activity of the CD24 pathway. Based on these facts, the third aim of this thesis was to investigate the association between CD24 and VEGF-A and their joint role in regulating CRC angiogenesis and investigating whether ILK plays a role in this activity.

To verify the above aims, CD24 mutant constructs were generated, followed by manipulating the wild-type CD24 expression vector and the mutant constructs in two different CRC cell lines. Various *in vitro* cellular experiments and protein analyses were then conducted to study the CD24 function and to map the functional sites involved in regulating the signalling pathways and the interaction between CRC cells and endothelial cells.

This thesis provides many novel observations related to the CD24's function, i.e., signalling partners and ligands, which have made robust insights into future work on CD24 as a potent oncogene in CRC.

6.2 Key findings

6.2.1 Mapping of the functional sites in CD24 that contribute to CRC progression

6.2.1.1 Validation of CD24 expression and its impact role on the cellular contexts involving proliferation, invasion, and migration in CRC

Clinically, CD24 is overexpressed in CRC tissue [99, 260]. However, our preliminary investigations into CD24 expression *in vitro* showed that its expression level varied between different CRC cell lines, as it was highly expressed in SW620, a cell line harvested from lymph node metastases of CRC, and there was a lower expression in HCT116 and SW480, cell lines that were collected from primary poorly differentiated Dukes D and primary moderately differentiated Dukes B CRC, respectively. This may reflect the variability between cells at different cancer stages and could be attributed to significant molecular differences between the cell types, resulting in the differences in CD24 expression.

Subsequently, functional studies on CD24 were investigated *in vitro* for parameters related to CRC cell proliferation, invasion, and migration because all these features are important for determining the early metastatic phenotype. The data showed that when CD24 was transiently overexpressed in HCT116 and SW480, there was an increase in CRC cell invasion and migration. By contrast, CD24 knockdown by siRNA in SW620 reduced CRC cell motility (both invasion and migration). For cell proliferation, neither CD24 overexpression nor CD24 knockdown affected

CRC cell proliferation. These results are consistent with those of Ahmed *et al.*, who also revealed that CD24 could induce CRC cell motility but not cell proliferation [120].

6.2.1.2 *N*-glycosylation sites appear to be important for CD24 to induce its activities

CD24 is a heavily glycosylated protein, and its structure shows many *O*- and *N*-glycosylation sites, which renders it a mucin-like glycoprotein [206]. Protein glycosylation plays a significant role in normal biological processes and cancer development, including tumour cell proliferation, invasion, angiogenesis and metastasis [203].

Evidence exists that glycosylation is responsible for many functions mediated by CD24. For example, it has been shown that carbohydrate sialyl Lewis X is necessary for CD24 to mediate cancer cells' rolling on P-selectin [107, 228]. Likewise, the presence of α- 2,3- linked sialic acid residues on CD24 facilitates its binding to L1, which in turn modulates neurite outgrowth [161]. However, to our knowledge, the functional activity of *N*-glycosylation in CD24 in CRC has not been studied.

In Chapter 3, the direct sequencing and Western blot results confirmed the successful creation of CD24 mutant constructs, in which the target asparagine (located at codons 36 and 52) was replaced with glutamine. However, the banding patterns in the Western blot were markedly altered compared to those seen in $CD24^{WT}$. The explanation for the variability and non-parallel Western blotting bands for the mutant constructs was

intuitively that there was variation in glycosylation due to the loss of one or more of the *N*-glycosylation sites. However, it was also possible that the variation was an artefact of changes in transfection efficiency. When the glycosylation residues for all mutant constructs and $CD24^{WT}$ were digested by the neuraminidase and PNGase enzymes, all showed almost identical bands for all conditions thus confirming that the variation of the banding pattern was due to the variation of glycosylation in CD24, and the *N*-glycosylation sites had been successfully removed. It was interesting that mutation of either one of the *N*-glycosylation sites resulted in a marked reduction in the smearing pattern of the bands and when both were removed, there was a further reduction. The implication from this is that the majority of the glycosylation lies on the *N*-glycosylation sites, and, despite the presence of 16 putative *O*-glycosylation sites, this is relatively low. *O*-glycosylation is considered a feature of proteins having a major structural role whilst *N*-glycosylation sites appear to have functional roles. The data suggest the CD24 has mostly functional activity. Since it has no transmembrane domain, it must be causing alterations in other cell surface molecules in order to induce signalling. The interaction with these other molecules may be through the sugar residues at the *N*-glycosylation sites.

Our study attempted to identify the mechanisms by which CD24 may exert its functions. We have shown that CD24 motility-inducing activity in CRC cells is dependent on two closely positioned *N*-glycosylation sites; altering each site individually reduces CD24 activity but knocking them both out together results in near-complete loss of activity (i.e. a functionally

inactivated protein almost equivalent to EVC). An unexpected observation was that loss of these *N*-glycosylation sites paradoxically induces cell proliferation (in an additive fashion). Since the transfection of wild-type CD24 does not affect whatsoever cell proliferation in CRC, these results suggest that CD24 *N*-glycosylation may suppress regulatory systems of CD24-mediated proliferation. Therefore, mutations in the *N*-glycosylation sites may allow binding to other signalling molecules or ligands involved in cell division stimulation. However, it remains unclear whether the increase in cell proliferation was due to loss of a function associated with CD24 *N*-glycosylation sites, which inhibits proliferation or due to gain-of-function experimental artefact. These data require further investigations to define the exact role played by the *N*-glycosylation in regulating CRC cell proliferation.

6.2.1.3 CD24 involvement in induction of the EMT

Metastasis is prompted by EMT, which enhances cell migration and invasion [210]. The process of EMT is characterised by the induction of mesenchymal markers, N-cadherin and Vimentin, and a simultaneous decrease in the epithelial marker, E-cadherin. CD24 overexpression in CRC cells was associated with enhancement of EMT and cell motility [211]. Our observations reported in this thesis showed consistency with the above literature as cadherin switching (a surrogate marker of EMT) was identified in CD24-overexpressing cells, whilst other EMT drivers, such as Snail and Vimentin, were also seen to increase. In contrast, transfection of cells with

(CD24$^{N[36,52]Q}$) hindered induction of these features, which indicated that the ability of CD24 to induce EMT and regulate the downstream targets was dependent on its *N*-glycosylation sites.

In agreement with other studies regarding the potential role of *N*-glycosylation in many glycoproteins in regulating EMT-related phenotypic alteration [167, 184, 261], F-actin staining showed that the cells transfected with CD24^{WT} acquired a mesenchymal phenotype compared to control cells and was accompanied by actin polymerisation. Conversely, the cells retained a rounded epithelioid phenotype upon transfection with the double mutant construct and showed actin polymerisation similar to that seen in CD24^{WT}. Thus, the data suggest that CD24 can induce actin polymerisation, which is mediated by mechanisms independent of *N*-glycosylation. It is uncertain which mechanisms are involved in this process, how they are coordinated with the *N*-glycosylation-dependent mechanisms of motility induction and whether they are dependent on the *O*-glycosylation.

6.2.2 P-selectin activates CD24 in CRC

In this thesis, we showed the physical interaction between CD24 and P-selectin, that this interaction was *N*-glycosylation dependent and that it had a number of functional effects on the epithelial cells. A positive feedback loop of P-selectin/CD24 was observed, where P-selectin stimulation increased CD24 expression in CRCs but was not observed in the absence of CD24. We also demonstrated that P-selectin/CD24 interaction triggers

downstream signalling molecules associated with CRC migration and invasion, which were not observed in CD24-silenced cells. However, cell proliferation showed no effect from P-selectin stimulation. We showed that P-selectin formed a physical complex with CD24 and that this was responsible for promoting adhesion between the cells expressing CD24. The results indicated that the interaction between CRC cells and endothelial cells and metastasis regulation is dependent on P-selectin/CD24 binding. Nevertheless, the exact mechanism is not clearly understood.

CD24 is a cell surface and GPI-anchored protein, which could bind and regulate many signalling pathways as it clusters within lipid rafts [116]. In the literature, CD24 has been shown to serve as a ligand for P-selectin and facilitate cancer cell dissemination [82, 108, 230]. Many studies have also indicated the role of P-selectin in regulating different signalling pathways. For example, Reyes-Reyes *et al*. found that P-selectin plays a crucial role in regulating integrin-mediated adhesion in CRC cells [224]. Bauman *et al.* found that CD24 activates a3β1 and a4β1 integrins, which enhance the binding to other cell adhesion molecules, such as selectins, leading to induction of cell migration [103]. Kyung-min Lee *et al*. also indicated that a decrease in β1 integrin bound with CD24 led to decreased Src/FAK activity [105]. A similar study also showed that CD24 silencing resulted in significant abrogation of FAK-mediated cell motility in CRC [142].

Other studies showed that P-selectin could activate the phosphorylation of FAK and Src [262, 263]. Both ILK and FAK expression were found to be up-

regulated by Cten, which is another adhesion molecule that is known as a downstream target for CD24 [130]. Since both CD24 and P-selectin have shown a common role in activating the same signalling pathways, we, therefore, propose that CD24/P-selectin interaction activates signal transduction in CRC cells and a polymeric interaction between CD24/P-selectin/integrins may be involved.

Thus, it is possible that P-selectin binding to CD24 could initiate the signalling amplification by which this binding might activate the interaction with other cell surface molecules, such as integrins within the lipid rafts. Consequently, CD24 via these cell surface molecules can induce Cten activity, which in turn binds and activates other intracellular-bound kinase complexes, such as ILK, FAK and Src kinase, leading to the promotion of cell adhesion and motility (Figure 6.1).

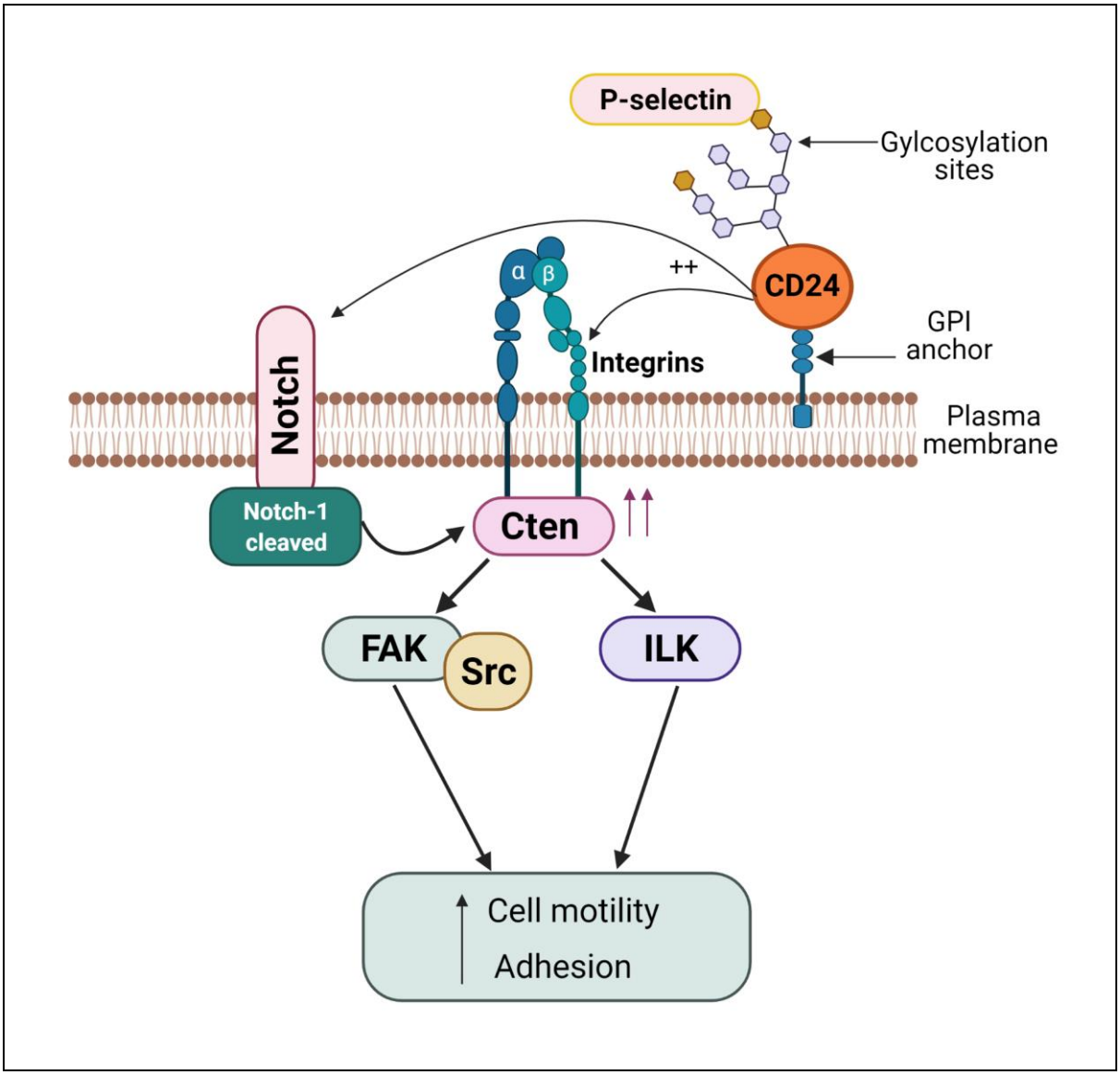


Figure 6.1 Summary diagram for CD24 signalling pathways following P-selectin stimulation in CRC cells.

The interaction of P-selectin with CD24 could initiate the signalling amplification by activating cell surface molecules, such as integrins and Notch1, within the lipid rafts. CD24, thus via Notch1 and integrins, augmented the activity of Cten, which in turn binds and activates ILK, FAK and Src kinase, leading to the induction of cell adhesion and motility. Abbreviations: GPI, Glycosylphosphatidylinositol; Cten, C-terminal tensin-like; ILK, Integrin-linked kinase; FAK, focal adhesion kinase.

6.2.3 The potential role of CD24 in the initiation of CRC angiogenesis

Angiogenesis is defined as the growth of new blood vessels from the pre-existing vessel network and is characterised as one of the primary steps required for tumour growth and metastasis [248, 264]. Tumour angiogenesis is mediated by several growth factors produced by cancer cells [264]. Among the many biomarkers of angiogenesis, VEGF-A plays a critical role in the migration of endothelial cells, invasion of surrounding tissues, differentiation and vascular permeability [235, 265]. VEGF is expressed in various human tumour cells and binds to many receptors found in vascular endothelial cells [252, 266]. Many signalling pathways have been indicated directly or indirectly in regulating VEGF-A expressions, such as CD24, ILK, STAT3, NF-κB, and AKT [152, 242, 267, 268]. In this study, we sought to investigate the contribution of CD24 to CRC angiogenesis as it has not been entirely elucidated.

We showed that CD24 is a positive regulator of VEGF-A expression. The experiments were performed in different CRC cell lines and using different methods of CD24 modulation to confirm that the data were not artefacts of methodology. The changes in the expression level of VEGF-A resulted in changes in secreted VEGF-A concentration in conditioned media, and this secreted protein was shown to be functionally active. It positively affected the endothelial cell proliferation and migration and tube formation capacity and provided strong evidence that CD24 regulates VEGF-A-mediated angiogenesis in CRC.

The exact mechanism for determining whether CD24 regulates VEGF-A directly or through another downstream target was not clear. This query guided us to study the CD24 signalling partners involved in VEGF-A regulation.

ILK was considered a good candidate as its expression has been associated with VEGF-A regulation, enhancing endothelial proliferation, migration and capillary formation [152, 196, 269]. Our research group has previously demonstrated that Cten signals through ILK and induce cell motility [130]. This thesis has shown that both Cten and ILK act as downstream signalling targets for CD24. Thus, we hypothesised that CD24 could signal through ILK and stimulate VEGF-A expression, leading to angiogenesis.

The data reported in Chapter 5: showed that if ILK was removed by knockdown, then the ability of CD24 to induce VEGF-A expression was abrogated. Similarly, CD24-mediated endothelial cell proliferation, migration, and tube formation were inhibited by ILK silencing. These data confirmed that CD24 signal through ILK to regulate VEGF-A and angiogenesis in CRC.

Given this potential role for CD24 in stimulating VEGF-A secretion, it was not surprising that we found that CD24 also down-regulated angiostatin expression, an angiogenesis inhibitory molecule. It was, however, surprising that the regulation of angiostatin seemed to be independent of ILK. This shows that there is more than one signalling pathway

downstream of CD24. Further examinations are necessary to determine the underlying mechanism behind the up-regulation of angiostatin.

Collectively, these outcomes indicate for the first time that CD24 can regulate angiogenesis via the ILK/VEGF-A signalling axis. Otherwise, CD24 regulates angiostatin independently of ILK, possibly via a unique mechanism. Hence, making CD24 is a potential therapeutic target against CRC.

6.3 Summary

This thesis describes a comprehensive analysis of the function and signalling partners of CD24 in different cellular models. The findings obtained from *in vitro* experiments confirmed that CD24 plays a crucial role in CRC development by enhancing cell motility. Moreover, a mutation of *N*-glycosylation sites in CD24 confirmed that these sites are important for CD24 function by regulating cell proliferation, migration, and invasion. The presence of these sites on CD24 was also shown to regulate downstream targets and EMT.

Our study also validated that CD24 interaction with P-selectin influences different signalling partners-mediated cell motility, adhesion to endothelial cells, and extravasation (transendothelial migration). Besides, the interaction of CD24 with P-selectin was dependent on *N*-glycosylation.

Finally, our investigation into the mechanism of CD24-driven angiogenesis was the first to identify that CD24 is a regulator of VEGF-A expression in CRC cells. Similarly, this thesis confirmed that the co-transfection technique was a valuable method for identifying the putative signalling pathway, such as ILK, which was found to be involved in CD24 up-regulation of VEGF-A. Nevertheless, these data require confirmation and further investigation to understand the CD24 function in regulating angiogenesis on a large scale.

6.4 Limitations

- This thesis generated very robust data, but all of these data were from *in vitro* experiments. Thus, the data require mechanistic evaluation highlighting how CD24 contributes to the tumour biology of CRC *in vivo*.
- Chapter 3 showed that CD24 loss of N-glycosylation induced CRC cell proliferation. However, only one technique was involved, and further studies are required.
- Another limitation of this study was that the interaction of CD24 with P-selectin was examined using a co-IP assay in only one cell line (HCT116).
- P-selectin expression in the HUVEC cell line was weak, which led us to stimulate the cells with thrombin or TNF-alpha before performing any experiment. However, the effect of the above cytokines on cell behaviour or the potential for stimulating other molecules has not been investigated.
- We showed that CD24 induce tube formation in HUVEC cells using *in vitro* tube formation assay. However, this assay was carried out within 24h, as the endothelial cells undergo apoptosis after 24h.
- In this thesis, we did not study the effect of the individual mutant clones of CD24 on binding to P-selectin or angiogenesis due to time restrictions.

6.5 Future directions

This thesis confirms the function of CD24 in regulating several cellular activities, including migration, invasion, and adhesion to endothelial cells. This work also shows that the functional activities of CD24 were dependent on its *N*-glycosylation patterns. However, the mechanism(s) by which the *N*-glycosylation of CD24 mediates these activities, particularly cell proliferation, are not fully understood. Therefore, the involvement of CD24 *N*-glycosylation in cell growth and proliferation regulation could be further investigated by establishing stable cell lines transfected with CD24-mutant constructs as the stable expression of the transfected plasmids last longer than those by transient transfection. The ability of the cell to divide and proliferate will then be determined by clonogenic survival assay or cell cycle analysis.

In another method, three-dimensional (3D) spheroid mono-culture models can be formed using the established stable cells, and then spheroid microarrays can be made, paraffin-embedded, sectioned and propped with Ki67 (cell proliferation marker).

Many pathways, such as EGFR/MAPK, PI3K and TGF-β, have been indicated to regulate cell proliferation and other biological processes in CRC [270]. Therefore, it would be interesting to study the association of CD24 with these pathways. This investigation will provide a broader understanding of how *N*-glycosylation mediates the function of CD24 and its interacting partners.

We have shown in this thesis that CD24 induce actin polymerization via F-actin staining. However, only the phalloidin immunofluorescence (F-actin staining) is not sufficient to conclude that $CD24^{WT}$ is able to induce actin polymerization because phalloidin only stains actin filaments and not the actin globular form, so it would be interesting to perform the quantification of G- and F- actin cellular fractions through Triton-X 100 fractionation.

We have demonstrated in Chapter 4 that CD24 binds to P-selectin, and this binding regulates cell motility and the interaction between CRC cells and endothelial cells. Thus, it is possible to investigate the connection of CD24 or any of its downstream signalling targets with other selectin families (such as E-selectin and L-selectin) and study their effect on CRC cell activities.

Another method to study the interaction of CD24 with selectins is through the use of 3D models, which can be performed by co-culturing the CRC cells expressing CD24 with endothelial cells or platelet cells. Then the cell-cell communication and ligands or downstream signalling target of CD24 should also be investigated. The co-culture techniques will validate our acquired data from a 2D culture and identify the putative ligands for CD24 on endothelial cells and their role in cancer development and metastasis.

As noted, angiogenesis is a prerequisite for cancer growth and metastasis [248]. VEGF and hypoxia are the main regulators of angiogenesis [251]. Hypoxia-inducible factor-1α (Hif-1α) is one of the genes activated upon hypoxia response and plays a role in inducing the transcription of many genes, including VEGF-A [271]. This study demonstrated that CD24

regulates the VEGF-A-mediated angiogenesis via ILK. However, the involvement of hypoxia in this process was not investigated. It will be interesting to examine whether CD24 or its downstream target (ILK) are up-regulated under hypoxic conditions and examine the correlation between CD24 and Hif-1α.

Moreover, VEGF-C and VEGF-D are other growth factors connected to lymphangiogenesis [272]. Thus, it is possible to study whether CD24 has a role in regulating these growth factors and lymphangiogenesis.

Another method to further investigate CD24 involvement in angiogenesis and lymphangiogenesis regulation is a co-culture system. Briefly, CRC cells can be stably transfected with the appropriate constructs for CD24 (either the wild-type CD24 or the mutant CD24) and co-cultured with HUVECs or human lymphatic endothelial cells (HLECs) in Matrigel as previously described [273]. After co-culture for one week, the cells can undergo routine histological processing (i.e., they will be formalin-fixed and paraffin-embedded), and sections can be stained for CD34 or CD31 (markers of endothelial cells) and Haematoxylin and Eosin (H&E). Angiogenesis can be quantified in terms of the number of CD34 or CD31 positive tubular structures. Also, co-culture experiments set up in parallel can undergo RNA and protein extraction and evaluate the expression of VEGF-A, VEGF-C, VEGF-D.

Finally, it might be very interesting to investigate the clinical relevance of CD24 in the clinical context; the expression of CD24 and CD31 can be

tested in primary CRC and hepatic metastatic tissues by immunohistochemistry and correlated with the clinicopathological parameters of CRC.

References

1. Marley, A.R. and H. Nan, *Epidemiology of colorectal cancer.* Int J Mol Epidemiol Genet, 2016. **7**(3): p. 105-114.
2. Favoriti, P., et al., *Worldwide burden of colorectal cancer: a review.* Updates in Surgery, 2016. **68**(1): p. 7-11.
3. Rawla, P., T. Sunkara, and A. Barsouk, *Epidemiology of colorectal cancer: incidence, mortality, survival, and risk factors.* Przeglad gastroenterologiczny, 2019. **14**(2): p. 89-103.
4. Uk, C.R. *Bowel cancer incidence statistics*. 2015 2015-05-15; Available from: https://www.cancerresearchuk.org/health-professional/cancer-statistics/statistics-by-cancer-type/bowel-cancer/incidence#heading-Zero.
5. Macrae, F.A., *Colorectal cancer: Epidemiology, risk factors, and protective factors.* Uptodate. com [Internet].[ažurirano 9. lipnja 2017, 2016.
6. Bishehsari, F., et al., *Epidemiological transition of colorectal cancer in developing countries: Environmental factors, molecular pathways, and opportunities for prevention.* World Journal of Gastroenterology : WJG, 2014. **20**(20): p. 6055-6072.
7. Durko, L. and E. Malecka-Panas, *Lifestyle Modifications and Colorectal Cancer.* Current Colorectal Cancer Reports, 2014. **10**(1): p. 45-54.
8. Brenner, H. and C. Chen, *The colorectal cancer epidemic: challenges and opportunities for primary, secondary and tertiary prevention*, in *Br J Cancer*. 2018. p. 785-92.
9. Smith, D., et al., *Symptomatic presentation of early colorectal cancer.* Annals of the Royal College of Surgeons of England, 2006. **88**(2): p. 185-190.
10. Swiderska, M., et al., *The diagnostics of colorectal cancer.* Contemporary oncology (Poznan, Poland), 2014. **18**(1): p. 1-6.
11. Kolligs, F.T., *Diagnostics and Epidemiology of Colorectal Cancer.* Visceral medicine, 2016. **32**(3): p. 158-164.
12. Kuipers, E.J., et al., *Colorectal cancer.* Nature reviews. Disease primers, 2015. **1**: p. 15065-15065.
13. Damin, D.C. and A.R. Lazzaron, *Evolving treatment strategies for colorectal cancer: a critical review of current therapeutic options.* World journal of gastroenterology, 2014. **20**(4): p. 877-887.
14. Armaghany, T., et al., *Genetic Alterations in Colorectal Cancer*, in *Gastrointest Cancer Res*. 2012. p. 19-27.
15. Fearon, E.R. and B. Vogelstein, *A genetic model for colorectal tumorigenesis.* Cell, 1990. **61**(5): p. 759-67.
16. Davies, R.J., R. Miller, and N. Coleman, *Colorectal cancer screening: prospects for molecular stool analysis.* Nature Reviews Cancer, 2005. **5**: p. 199.
17. Walther, A., et al., *Genetic prognostic and predictive markers in colorectal cancer.* Nat Rev Cancer, 2009. **9**(7): p. 489-99.
18. Nguyen, H.T. and H.Q. Duong, *The molecular characteristics of colorectal cancer: Implications for diagnosis and therapy (Review).* Oncol Lett, 2018. **16**(1): p. 9-18.
19. Okita, A., et al., *Consensus molecular subtypes classification of colorectal cancer as a predictive factor for chemotherapeutic efficacy against metastatic colorectal cancer.* Oncotarget, 2018. **9**(27): p. 18698-18711.
20. Tariq, K. and K. Ghias, *Colorectal cancer carcinogenesis: a review of mechanisms.* Cancer Biology & Medicine, 2016. **13**(1): p. 120-135.
21. Guinney, J., et al., *The consensus molecular subtypes of colorectal cancer.* Nature Medicine, 2015. **21**(11): p. 1350-1356.
22. Dunne, P.D., et al., *Challenging the Cancer Molecular Stratification Dogma: Intratumoral Heterogeneity Undermines Consensus Molecular Subtypes and*

Potential Diagnostic Value in Colorectal Cancer. Clin Cancer Res, 2016. **22**(16): p. 4095-104.
23. Worthley, D.L. and B.A. Leggett, *Colorectal Cancer: Molecular Features and Clinical Opportunities*, in *Clin Biochem Rev*. 2010. p. 31-8.
24. Lüchtenborg, M., et al., *APC mutations in sporadic colorectal carcinomas from The Netherlands Cohort Study.* Carcinogenesis, 2004. **25**(7): p. 1219-1226.
25. Kw, et al., *Activation of beta-catenin-Tcf Signaling in Colon Cancer by Mutations in Beta-Catenin or APC.* Science (New York, N.Y.), 1997. **275**(5307).
26. Sánchez-Tilló, E., et al., *β-catenin/TCF4 complex induces the epithelial-to-mesenchymal transition (EMT)-activator ZEB1 to regulate tumor invasiveness.* Proc Natl Acad Sci U S A, 2011. **108**(48): p. 19204-9.
27. Jl, et al., *Genetic Alterations During Colorectal-Tumor Development.* The New England journal of medicine, 1988. **319**(9).
28. G., L., et al., *Chromosome 18q Allelic Loss and Prognosis in Stage II and III Colon Cancer.* International journal of cancer, 1998. **79**(4).
29. Sr, et al., *Clinical and Pathological Associations With Allelic Loss in Colorectal Carcinoma [Corrected].* JAMA, 1989. **261**(21).
30. Colussi, D., et al., *Molecular Pathways Involved in Colorectal Cancer: Implications for Disease Behavior and Prevention.* International Journal of Molecular Sciences, 2013. **14**(8): p. 16365-16385.
31. Al-Sohaily, S., et al., *Molecular pathways in colorectal cancer.* J Gastroenterol Hepatol, 2012. **27**(9): p. 1423-31.
32. Pino, M.S. and D.C. Chung, *THE CHROMOSOMAL INSTABILITY PATHWAY IN COLON CANCER.* Gastroenterology, 2010. **138**(6): p. 2059-2072.
33. Y., B., et al., *HIF1A Overexpression Is Associated With Poor Prognosis in a Cohort of 731 Colorectal Cancers.* The American journal of pathology, 2010. **176**(5).
34. Sinicrope, F.A. and D.J. Sargent, *Molecular Pathways: Microsatellite Instability in Colorectal Cancer: Prognostic, Predictive, and Therapeutic Implications.* Clinical Cancer Research, 2012. **18**(6): p. 1506.
35. R., B.C. and Goel, *Microsatellite Instability in Colorectal Cancer.* Gastroenterology, 2010. **138**(6).
36. Nojadeh, J.N., S. Behrouz Sharif, and E. Sakhinia, *Microsatellite instability in colorectal cancer*, in *EXCLI J*. 2018. p. 159-68.
37. Zali, M.M.H., et al., *Four novel germline mutations in the MLH1 and PMS2 mismatch repair genes in patients with hereditary nonpolyposis colorectal cancer.* International Journal of Colorectal Disease, 2009. **24**(8): p. 885-893.
38. Frankel, W.C. and L. Wendy, *A practical guide to biomarkers for the evaluation of colorectal cancer.* Modern Pathology, 2019. **32**(1): p. 1-15.
39. Jp and Issa, *CpG Island Methylator Phenotype in Cancer.* Nature reviews. Cancer, 2004. **4**(12).
40. Rhee, Y.Y., K.J. Kim, and G.H. Kang, *CpG Island Methylator Phenotype-High Colorectal Cancers and Their Prognostic Implications and Relationships with the Serrated Neoplasia Pathway*, in *Gut Liver*. 2017. p. 38-46.
41. Mojarad, E.N., et al., *The CpG island methylator phenotype (CIMP) in colorectal cancer*, in *Gastroenterol Hepatol Bed Bench*. 2013. p. 120-8.
42. Shen, L., et al., *Integrated genetic and epigenetic analysis identifies three different subclasses of colon cancer.* Proceedings of the National Academy of Sciences, 2007. **104**(47): p. 18654.
43. Ogino, S., et al., *CpG island methylator phenotype, microsatellite instability, BRAF mutation and clinical outcome in colon cancer.* Gut, 2009. **58**(1): p. 90-6.
44. Cs, et al., *Inflammatory Markers Are Associated With Risk of Colorectal Cancer and Chemopreventive Response to Anti-Inflammatory Drugs.* Gastroenterology, 2011. **140**(3).
45. Pachmayr, E., C. Treese, and U. Stein, *Underlying Mechanisms for Distant Metastasis – Molecular Biology*, in *Visc Med*. 2017. p. 11-20.
46. Guan, X., *Cancer metastases: challenges and opportunities.* Acta Pharm Sin B, 2015. **5**(5): p. 402-18.

47. Dillekås, H., M.S. Rogers, and O. Straume, *Are 90% of deaths from cancer caused by metastases?*, in *Cancer Med*. 2019. p. 5574-6.
48. Gomez-Cuadrado, L., et al., *Mouse models of metastasis: progress and prospects.* Dis Model Mech, 2017. **10**(9): p. 1061-1074.
49. Tauriello, D.V.F., et al., *Determinants of metastatic competency in colorectal cancer.* Molecular oncology, 2017. **11**(1): p. 97-119.
50. Brenner, H., M. Kloor, and C.P. Pox, *Colorectal cancer.* Lancet, 2014. **383**(9927): p. 1490-1502.
51. Riihimäki, M., et al., *Patterns of metastasis in colon and rectal cancer.* Scientific reports, 2016. **6**: p. 29765-29765.
52. Fabisiewicz, A. and E. Grzybowska, *CTC clusters in cancer progression and metastasis.* Med Oncol, 2016. **34**(1): p. 12.
53. Moure, A. and H. Gomez, *Phase-Field Modeling of Individual and Collective Cell Migration.* Archives of Computational Methods in Engineering, 2021. **28**(2): p. 311-344.
54. Friedl, P. and K. Wolf, *Tumour-cell invasion and migration: diversity and escape mechanisms.* Nature Reviews Cancer, 2003. **3**(5): p. 362-374.
55. Martin, T.A., Ye, Lin, Sanders, Andrew J., Lane, Jane and Jiang, Wen Guo *Cancer Invasion and Metastasis: Molecular and Cellular Perspective.* Landes Bioscience, 2000-2013.
56. van Zijl, F., G. Krupitza, and W. Mikulits, *Initial steps of metastasis: cell invasion and endothelial transmigration.* Mutat Res, 2011. **728**(1-2): p. 23-34.
57. J., M. and Wotton, *Transcriptional Control by the TGF-beta/Smad Signaling System.* The EMBO journal, 2000. **19**(8).
58. Yan, X., et al., *N-cadherin, a novel prognostic biomarker, drives malignant progression of colorectal cancer.* Mol Med Rep, 2015. **12**(2): p. 2999-3006.
59. Lazarova, D.L. and M. Bordonaro, *Vimentin, colon cancer progression and resistance to butyrate and other HDACis.* J Cell Mol Med, 2016. **20**(6): p. 989-93.
60. Vu, T. and P.K. Datta, *Regulation of EMT in Colorectal Cancer: A Culprit in Metastasis.* Cancers, 2017. **9**(12): p. 171.
61. Yun, J.A., et al., *Loss of E-Cadherin expression is associated with a poor prognosis in stage III colorectal cancer.* Oncology, 2014. **86**(5-6): p. 318-28.
62. Valastyan, S. and R.A. Weinberg, *Tumor metastasis: molecular insights and evolving paradigms.* Cell, 2011. **147**(2): p. 275-92.
63. Pretzsch, E., et al., *Mechanisms of Metastasis in Colorectal Cancer and Metastatic Organotropism: Hematogenous versus Peritoneal Spread.* Journal of Oncology, 2019. **2019**: p. 7407190.
64. Dong C, Z.N., Konstantopoulos K, *Biomechanics in Oncology | SpringerLink*, ed. N.Z.K.K. Cheng Dong. 2018: Name Springer, Cham.
65. Bevilacqua, M.P. and R.M. Nelson, *Selectins.* J Clin Invest, 1993. **91**(2): p. 379-87.
66. Massagué, J. and A.C. Obenauf, *Metastatic Colonization.* Nature, 2016. **529**(7586): p. 298-306.
67. Papaccio, F., et al., *Concise Review: Cancer Cells, Cancer Stem Cells, and Mesenchymal Stem Cells: Influence in Cancer Development*, in *Stem Cells Transl Med*. 2017. p. 2115-25.
68. C., P., et al., *Cancer Stem Cells: The Root of Tumor Recurrence and Metastases.* Seminars in cancer biology, 2017. **44**.
69. Steinbichler, T.B., et al., *Cancer stem cells and their unique role in metastatic spread.* Semin Cancer Biol, 2019. **60**: p. 148-156.
70. Mego, M., J. Reuben, and S.A. Mani, *Epithelial-Mesenchymal Transition (EMT) and Cancer Stem Cells (CSCs): The Traveling Metastasis*, in *Liquid Biopsies in Solid Tumors*, M. Cristofanilli, Editor. 2017, Springer International Publishing: Cham. p. 67-80.
71. Ricci-Vitiani, L., et al., *Colon cancer stem cells.* Journal of Molecular Medicine, 2009. **87**(11): p. 1097.

72. Salaria, S., et al., *Expression of CD24, a Stem Cell Marker, in Pancreatic and Small Intestinal Neuroendocrine Tumors.* Am J Clin Pathol, 2015. **144**(4): p. 642-8.
73. Zhou, Y., et al., *Cancer stem cells in progression of colorectal cancer*, in *Oncotarget*. 2018. p. 33403-15.
74. Zhou, Y., et al., *Cancer stem cells in progression of colorectal cancer.* Oncotarget, 2017. **9**(70): p. 33403-33415.
75. Springer, T., et al., *Monoclonal xenogeneic antibodies to murine cell surface antigens: identification of novel leukocyte differentiation antigens.* Eur J Immunol, 1978. **8**(8): p. 539-51.
76. Kay, R., F. Takei, and R.K. Humphries, *Expression cloning of a cDNA encoding M1/69-J11d heat-stable antigens.* J Immunol, 1990. **145**(6): p. 1952-9.
77. Wenger, R.H., et al., *The heat stable antigen (mouse CD24) gene is differentially regulated but has a housekeeping promoter.* Journal of Biological Chemistry, 1993. **268**(31): p. 23345-52.
78. Kay, R., P.M. Rosten, and R.K. Humphries, *CD24, a signal transducer modulating B cell activation responses, is a very short peptide with a glycosyl phosphatidylinositol membrane anchor.* J Immunol, 1991. **147**(4): p. 1412-6.
79. Hough, M.R., et al., *Mapping of CD24 and Homologous Sequences to Multiple Chromosomal Loci.* Genomics, 1994. **22**(1): p. 154-161.
80. Fang, X., et al., *CD24: from A to Z.* Cell Mol Immunol, 2010. **7**(2): p. 100-3.
81. Shulewitz, M., et al., *Repressor roles for TCF-4 and Sfrp1 in Wnt signaling in breast cancer.* Oncogene, 2006. **25**(31): p. 4361-4369.
82. Aigner, S., et al., *CD24, a mucin-type glycoprotein, is a ligand for P-selectin on human tumor cells.* Blood, 1997. **89**(9): p. 3385-95.
83. Altevogt, P., et al., *Novel insights into the function of CD24: A driving force in cancer.* International Journal of Cancer, 2021. **148**(3): p. 546-559.
84. Kinoshita, T., *Enzymatic mechanism of GPI anchor attachment clarified.* Cell cycle (Georgetown, Tex.), 2014. **13**(12): p. 1838-1839.
85. Tan, Y., et al., *CD24: from a Hematopoietic Differentiation Antigen to a Genetic Risk Factor for Multiple Autoimmune Diseases.* Clinical Reviews in Allergy & Immunology, 2016. **50**(1): p. 70-83.
86. Shakiba, N., et al., *CD24 tracks divergent pluripotent states in mouse and human cells.* Nature Communications, 2015. **6**: p. 7329.
87. *Heat-stable antigen is a costimulatory molecule for CD4 T cell growth.* The Journal of Experimental Medicine, 1992. **175**(2): p. 437-445.
88. Liu, Y. and P. Zheng, *CD24: a genetic checkpoint in T cell homeostasis and autoimmune diseases.* Trends Immunol, 2007. **28**(7): p. 315-20.
89. Gilliam, D.T., et al., *The CD24 surface antigen in neural development and disease.* Neurobiol Dis, 2017. **99**: p. 133-144.
90. King, J.B., et al., *CD24 can be used to isolate Lgr5+ putative colonic epithelial stem cells in mice.* American journal of physiology. Gastrointestinal and liver physiology, 2012. **303**(4): p. G443-G452.
91. Deng, J., et al., *CD24 expression as a marker for predicting clinical outcome in human gliomas.* J Biomed Biotechnol, 2012. **2012**: p. 517172.
92. Pass, M.K., et al., *The 5'-flanking region of human CD24 gene has cell-type-specific promoter activity in small-cell lung cancer.* Int J Cancer, 1998. **78**(4): p. 496-502.
93. Kristiansen, G., et al., *CD24 Is Expressed in Ovarian Cancer and Is a New Independent Prognostic Marker of Patient Survival.* The American Journal of Pathology, 2002. **161**(4): p. 1215-1221.
94. Jacob, J., et al., *Expression of CD24 in Adenocarcinomas of the Pancreas Correlates with Higher Tumor Grades.* Pancreatology, 2004. **4**(5): p. 454-460.
95. Huang, L.-R. and H.-C. Hsu, *Cloning and expression of CD24 gene in human hepatocellular carcinoma: a potential early tumor marker gene correlates with p53 mutation and tumor differentiation.* Cancer Research, 1995. **55**(20): p. 4717-4721.

96. Sano, A., et al., *CD24 expression is a novel prognostic factor in esophageal squamous cell carcinoma.* Annals of Surgical Oncology, 2009. **16**(2): p. 506-514.
97. Kristiansen, G., M. Sammar, and P. Altevogt, *Tumour Biological Aspects of CD24, A Mucin-Like Adhesion Molecule.* Journal of Molecular Histology, 2004. **35**(3): p. 255-262.
98. Zarn, J.A., et al., *Association of CD24 with the kinase c-fgr in a small cell lung cancer cell line and with the kinase lyn in an erythroleukemia cell line.* Biochem Biophys Res Commun, 1996. **225**(2): p. 384-91.
99. Weichert, W., et al., *Cytoplasmic CD24 expression in colorectal cancer independently correlates with shortened patient survival.* Clinical Cancer Research, 2005. **11**(18): p. 6574-6581.
100. Kristiansen, G., et al., *CD24 expression is a new prognostic marker in breast cancer.* Clin Cancer Res, 2003. **9**(13): p. 4906-13.
101. Yang, X.R., et al., *CD24 Is a Novel Predictor for Poor Prognosis of Hepatocellular Carcinoma after Surgery.* Clinical Cancer Research, 2009. **15**(17): p. 5518-5527.
102. Kitaura, Y., et al., *Transforming growth factor beta1 contributes to the invasiveness of pancreatic ductal adenocarcinoma cells through the regulation of CD24 expression.* Pancreas, 2011. **40**(7): p. 1034-42.
103. Baumann, P., et al., *CD24 interacts with and promotes the activity of c-src within lipid rafts in breast cancer cells, thereby increasing integrin-dependent adhesion.* Cell Mol Life Sci, 2012. **69**(3): p. 435-48.
104. Baumann, P., et al., *CD24 expression causes the acquisition of multiple cellular properties associated with tumor growth and metastasis.* Cancer Res, 2005. **65**(23): p. 10783-93.
105. Lee, K.M., et al., *CD24 regulates cell proliferation and transforming growth factor beta-induced epithelial to mesenchymal transition through modulation of integrin beta1 stability.* Cell Signal, 2012. **24**(11): p. 2132-42.
106. Mierke, C.T., N. Bretz, and P. Altevogt, *Contractile forces contribute to increased glycosylphosphatidylinositol-anchored receptor CD24-facilitated cancer cell invasion.* J Biol Chem, 2011. **286**(40): p. 34858-71.
107. Aigner, S., et al., *CD24 mediates rolling of breast carcinoma cells on P-selectin.* The FASEB Journal, 1998. **12**(12): p. 1241-1251.
108. Friederichs, J., et al., *The CD24/P-selectin binding pathway initiates lung arrest of human A125 adenocarcinoma cells.* Cancer Res, 2000. **60**(23): p. 6714-22.
109. Bretz, N., et al., *CD24 promotes tumor cell invasion by suppressing tissue factor pathway inhibitor-2 (TFPI-2) in a c-Src-dependent fashion.* Clin Exp Metastasis, 2012. **29**(1): p. 27-38.
110. Ma, Z.L., et al., *Knockdown of CD24 inhibits proliferation, invasion and sensitizes breast cancer MCF-7 cells to tamoxifen in vitro.* Eur Rev Med Pharmacol Sci, 2015. **19**(13): p. 2394-9.
111. Jiao, X.L., et al., *Downregulation of CD24 inhibits invasive growth, facilitates apoptosis and enhances chemosensitivity in gastric cancer AGS cells.* Eur Rev Med Pharmacol Sci, 2013. **17**(13): p. 1709-15.
112. Yang, C.-H., et al., *Identification of CD24 as a Cancer Stem Cell Marker in Human Nasopharyngeal Carcinoma.* PLoS ONE, 2014. **9**(6): p. e99412.
113. Woodward, W.A. and E.P. Sulman, *Cancer stem cells: markers or biomarkers?* Cancer Metastasis Rev, 2008. **27**(3): p. 459-70.
114. Fillmore, C. and C. Kuperwasser, *Human breast cancer stem cell markers CD44 and CD24: enriching for cells with functional properties in mice or in man?* Breast Cancer Res, 2007. **9**(3): p. 303.
115. Parsons, S.J.P. and J. Thomas, *Src family kinases, key regulators of signal transduction.* Oncogene, 2004. **23**(48): p. 7906-7909.
116. Ayre, D.C. and S.L. Christian, *CD24: A Rheostat That Modulates Cell Surface Receptor Signaling of Diverse Receptors.* Frontiers in Cell and Developmental Biology, 2016. **4**: p. 146.

117. Suzuki, T., et al., *CD24 induces apoptosis in human B cells via the glycolipid-enriched membrane domains/rafts-mediated signaling system.* J Immunol, 2001. **166**(9): p. 5567-77.
118. Runz, S., et al., *CD24 induces localization of beta1 integrin to lipid raft domains.* Biochem Biophys Res Commun, 2008. **365**(1): p. 35-41.
119. Schabath, H., et al., *CD24 affects CXCR4 function in pre-B lymphocytes and breast carcinoma cells.* J Cell Sci, 2006. **119**(Pt 2): p. 314-25.
120. Ahmed, M.A., et al., *CD24 is upregulated in inflammatory bowel disease and stimulates cell motility and colony formation.* Inflammatory bowel diseases, 2009. **16**(5): p. 795-803.
121. Lobry, C., P. Oh, and I. Aifantis, *Oncogenic and tumor suppressor functions of Notch in cancer: it's NOTCH what you think*, in *J Exp Med*. 2011. p. 1931-5.
122. *Recent insights into the role of Notch signaling in tumorigenesis | Blood | American Society of Hematology.* 2020.
123. X., Y., et al., *Notch Signaling: An Emerging Therapeutic Target for Cancer Treatment.* Cancer letters, 2015. **369**(1).
124. Zacharioudaki, E. and S.J. Bray, *Tools and methods for studying Notch signaling in Drosophila melanogaster*, in *Methods*. 2014. p. 173-82.
125. Hedley, A., et al., *Epithelial NOTCH Signaling Rewires the Tumor Microenvironment of Colorectal Cancer to Drive Poor-Prognosis Subtypes and Metastasis.* Cancer cell, 2019. **36**(3).
126. Hu, S., et al., *The function of Notch1 intracellular domain in the differentiation of gastric cancer.* Oncology Letters, 2020. **15**(5): p. 6171-6178.
127. Zhou, W., et al., *The AKT1/NF-kappaB/Notch1/PTEN axis has an important role in chemoresistance of gastric cancer cells*, in *Cell Death Dis*. 2013. p. e847-.
128. Lim, J., et al., *CD24 regulates stemness and the epithelial to mesenchymal transition through modulation of Notch1 mRNA stability by p38MAPK.* Arch Biochem Biophys, 2014. **558**: p. 120-6.
129. Sh and Lo, *C-terminal Tensin-Like (CTEN): A Promising Biomarker and Target for Cancer.* The international journal of biochemistry & cell biology, 2014. **51**.
130. Albasri, A., et al., *Cten signals through integrin-linked kinase (ILK) and may promote metastasis in colorectal cancer.* Oncogene, 2011. **30**(26): p. 2997-3002.
131. Tb, L.S. H., and Lo, *Cten, a COOH-terminal Tensin-Like Protein With Prostate Restricted Expression, Is Down-Regulated in Prostate Cancer.* Cancer research, 2002. **62**(15).
132. A., A., et al., *C-terminal Tensin-like (CTEN) Is an Oncogene Which Alters Cell Motility Possibly Through Repression of E-cadherin in Colorectal Cancer.* The Journal of pathology, 2009. **218**(1).
133. Ilyas, A.A., et al., *TGFβ1-induced cell motility is mediated through Cten in colorectal cancer.* 2018.
134. Jp, et al., *CD24 Interacts With and Promotes the Activity of C-Src Within Lipid Rafts in Breast Cancer Cells, Thereby Increasing Integrin-Dependent Adhesion.* Cellular and molecular life sciences : CMLS, 2012. **69**(3).
135. Thorpe, H., et al., *Multiple pathways regulate Cten in colorectal cancer without a Tensin switch*, in *Int J Exp Pathol*. 2015. p. 362-9.
136. Wang, D., et al., *Focal adhesion kinase and paxillin promote migration and adhesion to fibronectin by swine skeletal muscle satellite cells*, in *Oncotarget*. 2016. p. 30845-54.
137. Wg, et al., *Focal Adhesion Kinase as a Marker of Invasive Potential in Differentiated Human Thyroid Cancer.* Annals of surgical oncology, 1996. **3**(1).
138. D., H.Y. and Zhang, *[Focal Adhesion Kinase Expression and Angiogenesis in Breast Carcinoma].* Nan fang yi ke da xue xue bao = Journal of Southern Medical University, 2007. **27**(9).
139. Mc, A. E., and Frame, *Src and FAK Signalling Controls Adhesion Fate and the Epithelial-To-Mesenchymal Transition.* Current opinion in cell biology, 2005. **17**(5).

140. C., C., et al., *TGFbeta-induced EMT Requires Focal Adhesion Kinase (FAK) Signaling.* Experimental cell research, 2008. **314**(1).
141. Bretz, N.P., et al., *CD24 controls Src/STAT3 activity in human tumors.* Cellular and Molecular Life Sciences, 2012. **69**(22): p. 3863-3879.
142. Hasan Ahmed, M.A. and M. Ilyas, *CD24 expression is associated with epithelial mesenchymal transition (EMT) phenotype and alterations in actin cytoskeleton in colorectal cancer.* Pathology, 2014. **46**: p. S105.
143. A., A., et al., *Nuclear Expression of Phosphorylated Focal Adhesion Kinase Is Associated With Poor Prognosis in Human Colorectal Cancer.* Anticancer research, 2014. **34**(8).
144. S., P. and Dedhar, *The Role of Integrin-Linked Kinase (ILK) in Cancer Progression.* Cancer metastasis reviews, 2003. **22**(4).
145. C., M.P., A.B. Fielding, and Dedhar, *Integrin-linked Kinase--Essential Roles in Physiology and Cancer Biology.* Journal of cell science, 2008. **121**(Pt 19).
146. Zheng, C.C., et al., *Significance of integrin-linked kinase (ILK) in tumorigenesis and its potential implication as a biomarker and therapeutic target for human cancer.* Am J Cancer Res, 2019. **9**(1): p. 186-97.
147. Wu, C. and S. Dedhar, *Integrin-linked kinase (ILK) and its interactors: a new paradigm for the coupling of extracellular matrix to actin cytoskeleton and signaling complexes*, in *J Cell Biol*. 2001. p. 505-10.
148. E., H.G., et al., *Regulation of Cell Adhesion and Anchorage-Dependent Growth by a New Beta 1-integrin-linked Protein Kinase.* Nature, 1996. **379**(6560).
149. Overdevest, J.B., et al., *CD24 offers a therapeutic target for control of bladder cancer metastasis based on a requirement for lung colonization.* Cancer Res, 2011. **71**(11): p. 3802-11.
150. C., T., et al., *Inhibition of Integrin Linked Kinase (ILK) Suppresses beta-catenin-Lef/Tcf-dependent Transcription and Expression of the E-cadherin Repressor, Snail, in APC-/- Human Colon Carcinoma Cells.* Oncogene, 2001. **20**(1).
151. K., A., et al., *Integrin-linked Kinase Regulates Cell Proliferation and Tumour Growth in Murine Colitis-Associated Carcinogenesis.* Gut, 2008. **57**(7).
152. Tan, C., et al., *Regulation of tumor angiogenesis by integrin-linked kinase (ILK).* Cancer Cell, 2004. **5**(1): p. 79-90.
153. Varki, A., *Selectin ligands.* Proceedings of the National Academy of Sciences of the United States of America, 1994. **91**(16): p. 7390-7397.
154. Springer, T.A., *Traffic signals for lymphocyte recirculation and leukocyte emigration: The multistep paradigm.* Cell, 1994. **76**(2): p. 301-314.
155. St Hill, C.A., *Interactions between endothelial selectins and cancer cells regulate metastasis.* Front Biosci (Landmark Ed), 2011. **16**: p. 3233-51.
156. Amo, L., et al., *Involvement of Platelet–Tumor Cell Interaction in Immune Evasion. Potential Role of Podocalyxin-Like Protein 1.* Frontiers in Oncology, 2014. **4**(245).
157. Macauley, M.S., P.R. Crocker, and J.C. Paulson, *Siglec-mediated regulation of immune cell function in disease.* Nat Rev Immunol, 2014. **14**(10): p. 653-66.
158. Barkal, A.A., et al., *CD24 signalling through macrophage Siglec-10 is a new target for cancer immunotherapy.* Nature, 2019. **572**(7769): p. 392-6.
159. G., K., et al., *Evidence for Cis Interaction and Cooperative Signalling by the Heat-Stable Antigen Nectadrin (Murine CD24) and the Cell Adhesion Molecule L1 in Neurons.* The European journal of neuroscience, 1995. **7**(5).
160. Boo, Y.J., et al., *L1 expression as a marker for poor prognosis, tumor progression, and short survival in patients with colorectal cancer.* Ann Surg Oncol, 2007. **14**(5): p. 1703-11.
161. Kleene, R., et al., *The neural recognition molecule L1 is a sialic acid-binding lectin for CD24, which induces promotion and inhibition of neurite outgrowth.* J Biol Chem, 2001. **276**(24): p. 21656-63.
162. Lieberoth, A., et al., *Lewisx and α2,3-Sialyl Glycans and Their Receptors TAG-1, Contactin, and L1 Mediate CD24-Dependent Neurite Outgrowth*, in *J Neurosci*. 2009. p. 6677-90.

163. *Protein Glycosylation, an Overview*, in *eLS*.
164. Spiro, R.G., *Protein glycosylation: nature, distribution, enzymatic formation, and disease implications of glycopeptide bonds.* Glycobiology, 2002. **12**(4): p. 43R-56R.
165. Rudd, P.M. and R.A. Dwek, *Glycosylation: heterogeneity and the 3D structure of proteins.* Crit Rev Biochem Mol Biol, 1997. **32**(1): p. 1-100.
166. Rao, R.S.P. and W. Bernd, *Do N-glycoproteins have preference for specific sequons?* Bioinformation, 2010. **5**(5): p. 208-212.
167. Varelas, X., M.P. Bouchie, and M.A. Kukuruzinska, *Protein N-glycosylation in oral cancer: dysregulated cellular networks among DPAGT1, E-cadherin adhesion and canonical Wnt signaling.* Glycobiology, 2014. **24**(7): p. 579-591.
168. Aebi, M., *N-linked protein glycosylation in the ER.* Biochim Biophys Acta, 2013. **1833**(11): p. 2430-7.
169. Radcliffe, C.M., et al., *Identification of specific glycoforms of major histocompatibility complex class I heavy chains suggests that class I peptide loading is an adaptation of the quality control pathway involving calreticulin and ERp57.* J Biol Chem, 2002. **277**(48): p. 46415-23.
170. Sriram, V., et al., *Importance of N-linked glycosylation in the functional expression of murine CD1d1.* Immunology, 2008. **123**(2): p. 272-281.
171. Bergeron, J.J., et al., *The role of the lectin calnexin in conformation independent binding to N-linked glycoproteins and quality control.* Adv Exp Med Biol, 1998. **435**: p. 105-16.
172. Gw, C.F. I., and Hart, *O-Glycosylation of Nuclear and Cytosolic Proteins. Dynamic Interplay Between O-GlcNAc and O-phosphate.* The Journal of biological chemistry, 2000. **275**(38).
173. Reily, C., et al., *Glycosylation in health and disease.* Nature Reviews Nephrology, 2019. **15**(6): p. 346-366.
174. S., T. and Fukuda, *Roles of O-linked Oligosaccharides in Immune Responses.* BioEssays : news and reviews in molecular, cellular and developmental biology, 2001. **23**(1).
175. Peixoto, A., et al., *Protein Glycosylation and Tumor Microenvironment Alterations Driving Cancer Hallmarks.* Frontiers in Oncology, 2019. **9**(380).
176. Stowell, S.R., T. Ju, and R.D. Cummings, *Protein Glycosylation in Cancer.* Annu Rev Pathol, 2015. **10**: p. 473-510.
177. T., K., R. Nishizaki, and Ikezawa, *The Presence of GPI-linked Protein(s) in an Archaeobacterium, Sulfolobus Acidocaldarius, Closely Related to Eukaryotes.* Biochimica et biophysica acta, 1997. **1334**(1).
178. Kirwan, A., et al., *Glycosylation-Based Serum Biomarkers for Cancer Diagnostics and Prognostics.* BioMed research international, 2015. **2015**: p. 490531-490531.
179. Irimura, T., et al., *Diverse glycosylation of MUC1 and MUC2: potential significance in tumor immunity.* J Biochem, 1999. **126**(6): p. 975-85.
180. Brockhausen, I., J. Schutzbach, and W. Kuhns, *Glycoproteins and their relationship to human disease.* Acta Anat (Basel), 1998. **161**(1-4): p. 36-78.
181. Pan, S., et al., *Quantitative glycoproteomics analysis reveals changes in N-glycosylation level associated with pancreatic ductal adenocarcinoma.* Journal of proteome research, 2014. **13**(3): p. 1293-1306.
182. Contessa, J.N., et al., *Inhibition of N-Linked Glycosylation Disrupts Receptor Tyrosine Kinase Signaling in Tumor Cells.* Cancer Research, 2008. **68**(10): p. 3803-3809.
183. Zhang, D., et al., *The role of epithelial cell adhesion molecule N-glycosylation on apoptosis in breast cancer cells.* Tumour Biol, 2017. **39**(3): p. 1010428317695973.
184. Liu, X., et al., *Deglycosylation of epithelial cell adhesion molecule affects epithelial to mesenchymal transition in breast cancer cells.* Journal of Cellular Physiology, 2019. **234**(4): p. 4504-4514.

185. Sethi, M.K., et al., *In-depth N-glycome profiling of paired colorectal cancer and non-tumorigenic tissues reveals cancer-, stage- and EGFR-specific protein N-glycosylation.* Glycobiology, 2015. **25**(10): p. 1064-1078.
186. Kaprio, T., et al., *N-glycomic profiling as a tool to separate rectal adenomas from carcinomas.* Molecular & cellular proteomics : MCP, 2015. **14**(2): p. 277-288.
187. Ohl, C., et al., *N-glycosylation patterns of HSA/CD24 from different cell lines and brain homogenates: a comparison.* Biochimie, 2003. **85**(6): p. 565-73.
188. Bleckmann, C., et al., *Glycomic Analysis of N-Linked Carbohydrate Epitopes from CD24 of Mouse Brain.* Journal of Proteome Research, 2009. **8**(2): p. 567-582.
189. Bleckmann, C., et al., *O-glycosylation pattern of CD24 from mouse brain.* Biol Chem, 2009. **390**(7): p. 627-45.
190. Motari, E., et al., *Analysis of Recombinant CD24 Glycans by MALDI-TOF-MS Reveals Prevalence of Sialyl-T Antigen.* American journal of biomedical sciences, 2009. **1**(1): p. 1-11.
191. Salnikov, A.V., et al., *Antibody targeting of CD24 efficiently retards growth and influences cytokine milieu in experimental carcinomas.* Br J Cancer, 2013. **108**(7): p. 1449-59.
192. Gao, M., et al., *Identification and Characterization of Tumor-Initiating Cells in Multiple Myeloma.* J Natl Cancer Inst, 2020. **112**(5): p. 507-515.
193. Shapira, S., et al., *An immunoconjugate of anti-CD24 and Pseudomonas exotoxin selectively kills human colorectal tumors in mice.* Gastroenterology, 2011. **140**(3): p. 935-46.
194. Overdevest, J.B., et al., *CD24 Offers a Therapeutic Target for Control of Bladder Cancer Metastasis Based on a Requirement for Lung Colonization.* Cancer Research, 2011. **71**(11): p. 3802.
195. Barkal, A.A., et al., *CD24 signalling through macrophage Siglec-10 is a target for cancer immunotherapy.* Nature, 2019. **572**(7769): p. 392-396.
196. Basaki, Y., et al., *Inhibition of angiogenesis by inactivation of integrin-linked kinase in human vascular endothelial cells.* Cancer Research, 2004. **64**(7 Supplement): p. 17.
197. Livak, K.J. and T.D. Schmittgen, *Analysis of Relative Gene Expression Data Using Real-Time Quantitative PCR and the 2−ΔΔCT Method.* Methods, 2001. **25**(4): p. 402-408.
198. Pearson, G.W., *Control of Invasion by Epithelial-to-Mesenchymal Transition Programs during Metastasis.* J Clin Med, 2019. **8**(5).
199. OTIFI, H., *INVESTIGATING THE SIGNALLING AND FUNCTIONAL ACTIVITY OF CD24 IN CANCER*, in *Molecular Pathology*. 2017, University of Nottingham.
200. Schneider, M., et al., *Characterization of colon cancer cells: a functional approach characterizing CD133 as a potential stem cell marker.* BMC Cancer, 2012. **12**(1): p. 96.
201. Zhuo, J. and X. Wang, *Combination of targeting CD24 and inhibiting autophagy suppresses the proliferation and enhances the apoptosis of colorectal cancer cells.* Mol Med Rep, 2019. **20**(1): p. 539-548.
202. Sagiv, E., et al., *CD24 Is a New Oncogene, Early at the Multistep Process of Colorectal Cancer Carcinogenesis.* Gastroenterology, 2006. **131**(2): p. 630-639.
203. Barkeer, S., et al., *Glycosylation of Cancer Stem Cells: Function in Stemness, Tumorigenesis, and Metastasis.* Neoplasia, 2018. **20**(8): p. 813-825.
204. Drake, R.R., *Glycosylation and cancer: moving glycomics to the forefront.* Adv Cancer Res, 2015. **126**: p. 1-10.
205. Schwarz, F. and M. Aebi, *Mechanisms and principles of N-linked protein glycosylation.* Curr Opin Struct Biol, 2011. **21**(5): p. 576-82.
206. Rodrigues, J.G., et al., *Glycosylation in cancer: Selected roles in tumour progression, immune modulation and metastasis.* Cell Immunol, 2018. **333**: p. 46-57.
207. Bause, E. and G. Legler, *The role of the hydroxy amino acid in the triplet sequence Asn-Xaa-Thr(Ser) for the N-glycosylation step during glycoprotein biosynthesis.* Biochem J, 1981. **195**(3): p. 639-44.

208. van Zijl, F., G. Krupitza, and W. Mikulits, *Initial steps of metastasis: cell invasion and endothelial transmigration.* Mutation research, 2011. **728**(1-2): p. 23-34.
209. Li, L., et al., *CD24 isoform a promotes cell proliferation, migration and invasion and is downregulated by EGR1 in hepatocellular carcinoma.* OncoTargets and therapy, 2019. **12**: p. 1705-1716.
210. Mittal, V., *Epithelial Mesenchymal Transition in Tumor Metastasis.* Annu Rev Pathol, 2018. **13**: p. 395-412.
211. Okano, M., et al., *Human colorectal CD24+ cancer stem cells are susceptible to epithelial-mesenchymal transition.* Int J Oncol, 2014. **45**(2): p. 575-80.
212. Kim, S.-K., et al., *Sustainability of CD24 expression, cell proliferation and migration, cisplatin-resistance, and caspase-3 expression during mesenchymal-epithelial transition induced by the removal of TGF-β1 in A549 lung cancer cells.* Oncology letters, 2017. **14**(2): p. 2410-2416.
213. Ahmed, M.A., et al., *CD24 is upregulated in inflammatory bowel disease and stimulates cell motility and colony formation.* Inflamm Bowel Dis, 2010. **16**(5): p. 795-803.
214. Dillekås, H., M.S. Rogers, and O. Straume, *Are 90% of deaths from cancer caused by metastases?* Cancer medicine, 2019. **8**(12): p. 5574-5576.
215. Christofori, G., *New signals from the invasive front.* Nature, 2006. **441**(7092): p. 444-50.
216. Fares, J., et al., *Molecular principles of metastasis: a hallmark of cancer revisited.* Signal transduction and targeted therapy, 2020. **5**: p. 28-28.
217. Bendas, G. and L. Borsig, *Cancer Cell Adhesion and Metastasis: Selectins, Integrins, and the Inhibitory Potential of Heparins.* International Journal of Cell Biology, 2012. **2012**: p. 676731.
218. Kansas, G.S., *Selectins and their ligands: current concepts and controversies.* Blood, 1996. **88**(9): p. 3259-87.
219. VESTWEBER, D. and J.E. BLANKS, *Mechanisms That Regulate the Function of the Selectins and Their Ligands.* Physiological Reviews, 1999. **79**(1): p. 181-213.
220. Blann, A.D., S.K. Nadar, and G.Y.H. Lip, *The adhesion molecule P-selectin and cardiovascular disease.* European Heart Journal, 2003. **24**(24): p. 2166-2179.
221. Ley, K., *Functions of selectins.* Results Probl Cell Differ, 2001. **33**: p. 177-200.
222. Mannori, G., et al., *Differential colon cancer cell adhesion to E-, P-, and L-selectin: role of mucin-type glycoproteins.* Cancer Res, 1995. **55**(19): p. 4425-31.
223. Aruffo, A., et al., *Granule membrane protein 140 (GMP140) binds to carcinomas and carcinoma-derived cell lines.* Proceedings of the National Academy of Sciences of the United States of America, 1992. **89**(6): p. 2292-2296.
224. Reyes-Reyes, E.M., et al., *P-Selectin Activates Integrin-mediated Colon Carcinoma Cell Adhesion to Fibronectin.* Experimental cell research, 2006. **312**(20): p. 4056-4069.
225. Moore, K.L., *Structure and function of P-selectin glycoprotein ligand-1.* Leuk Lymphoma, 1998. **29**(1-2): p. 1-15.
226. Laszik, Z., et al., *P-selectin glycoprotein ligand-1 is broadly expressed in cells of myeloid, lymphoid, and dendritic lineage and in some nonhematopoietic cells.* Blood, 1996. **88**(8): p. 3010.
227. Myung, J.H., et al., *Direct measurements on CD24-mediated rolling of human breast cancer MCF-7 cells on E-selectin.* Anal Chem, 2011. **83**(3): p. 1078-83.
228. Carroll, M.J., et al., *Alternatively-Activated Macrophages Upregulate Mesothelial Expression of P-Selectin to Enhance Adhesion of Ovarian Cancer Cells.* Cancer Res, 2018. **78**(13): p. 3560-3573.
229. Chen, M. and J.-G. Geng, *P-selectin mediates adhesion of leukocytes, platelets, and cancer cells in inflammation, thrombosis, and cancer growth and metastasis.* Archivum Immunologiae et Therapiae Experimentalis, 2006. **54**(2): p. 75-84.
230. Aigner, S., et al., *Heat stable antigen (mouse CD24) supports myeloid cell binding to endothelial and platelet P-selectin.* Int Immunol, 1995. **7**(10): p. 1557-65.

231. Läubli, H. and L. Borsig, *Altered Cell Adhesion and Glycosylation Promote Cancer Immune Suppression and Metastasis.* Frontiers in Immunology, 2019. **10**(2120).
232. Chandler, K.B., C.E. Costello, and N. Rahimi, *Glycosylation in the Tumor Microenvironment: Implications for Tumor Angiogenesis and Metastasis.* Cells, 2019. **8**(6).
233. Scott, D.W. and R.P. Patel, *Endothelial heterogeneity and adhesion molecules N-glycosylation: Implications in leukocyte trafficking in inflammation.* Glycobiology, 2013. **23**(6): p. 622-633.
234. Bossi, P., et al., *Angiogenesis in Colorectal Tumors: Microvessel Quantitation in Adenomas and Carcinomas with Clinicopathological Correlations.* Cancer Research, 1995. **55**(21): p. 5049.
235. Frezzetti, D., et al., *VEGF as a potential target in lung cancer.* Expert Opin Ther Targets, 2017. **21**(10): p. 959-966.
236. Peach, C.J., et al., *Molecular Pharmacology of VEGF-A Isoforms: Binding and Signalling at VEGFR2*, in *Int J Mol Sci*. 2018.
237. Ye, X., et al., *Altered ratios of pro- and anti-angiogenic VEGF-A variants and pericyte expression of DLL4 disrupt vascular maturation in infantile haemangioma.* J Pathol, 2016. **239**(2): p. 139-51.
238. Claesson-Welsh, L. and M. Welsh, *VEGFA and tumour angiogenesis.* J Intern Med, 2012. **273**(2): p. 114-27.
239. Chou, M.T., J. Wang, and D.J. Fujita, *Src Kinase becomes preferentially associated with the VEGFR, KDR/Flk-1, following VEGF stimulation of vascular endothelial cells.* BMC Biochemistry, 2002. **3**(1): p. 32.
240. Shibuya, M., *Vascular Endothelial Growth Factor (VEGF) and Its Receptor (VEGFR) Signaling in Angiogenesis: A Crucial Target for Anti- and Pro-Angiogenic Therapies.* Genes Cancer, 2012. **2**(12): p. 1097-105.
241. Wang, X., et al., *CD24 promoted cancer cell angiogenesis via Hsp90-mediated STAT3/VEGF signaling pathway in colorectal cancer.* Oncotarget, 2016. **7**(34): p. 55663-55676.
242. Cao, X., et al., *Upregulation of VEGF-A and CD24 gene expression by the tGLI1 transcription factor contributes to the aggressive behavior of breast cancer cells.* Oncogene, 2012. **31**(1): p. 104-15.
243. Newman, H., et al., *Involvement of CD24 in angiogenesis in a mouse model of oxygen-induced retinopathy.* Curr Eye Res, 2012. **37**(6): p. 532-9.
244. Wang, W., et al., *Inhibition of high glucose-induced VEGF and ICAM-1 expression in human retinal pigment epithelium cells by targeting ILK with small interference RNA.* Molecular biology reports, 2012. **39**(1): p. 613-620.
245. Guo, L., et al., *Targeting of integrin-linked kinase with a small interfering RNA suppresses progression of experimental proliferative vitreoretinopathy.* Experimental eye research, 2008. **87**(6): p. 551-560.
246. Edwards, L.A., et al., *Suppression of VEGF secretion and changes in glioblastoma multiforme microenvironment by inhibition of integrin-linked kinase (ILK).* Mol Cancer Ther, 2008. **7**(1): p. 59-70.
247. Wani, A.A., et al., *Integrin-linked kinase regulates melanoma angiogenesis by activating NF-κB/interleukin-6 signaling pathway.* Oncogene, 2011. **30**(24): p. 2778-88.
248. Zetter, B.R., *Angiogenesis and Tumor Metastasis.* Annual Review of Medicine, 1998. **49**(1): p. 407-424.
249. Bielenberg, D.R. and B.R. Zetter, *The Contribution of Angiogenesis to the Process of Metastasis.* Cancer journal (Sudbury, Mass.), 2015. **21**(4): p. 267-273.
250. De Palma, M., D. Biziato, and T.V. Petrova, *Microenvironmental regulation of tumour angiogenesis.* Nat Rev Cancer, 2017. **17**(8): p. 457-474.
251. Carmeliet, P., *VEGF as a key mediator of angiogenesis in cancer.* Oncology, 2005. **69 Suppl 3**: p. 4-10.
252. Takahashi, Y., et al., *Expression of Vascular Endothelial Growth Factor and Its Receptor, KDR, Correlates with Vascularity, Metastasis, and Proliferation of Human Colon Cancer.* Cancer Research, 1995. **55**(18): p. 3964.

253. Hoeben, A., et al., *Vascular endothelial growth factor and angiogenesis.* Pharmacol Rev, 2004. **56**(4): p. 549-80.
254. Ahmed, Z. and R. Bicknell, *Angiogenic signalling pathways.* Methods Mol Biol, 2009. **467**: p. 3-24.
255. Wang, X., Z. Zhang, and C. Yao, *Targeting integrin-linked kinase increases apoptosis and decreases invasion of myeloma cell lines and inhibits IL-6 and VEGF secretion from BMSCs.* Med Oncol, 2011. **28**(4): p. 1596-600.
256. Oh, H.-H., et al., *Impact of KITENIN on tumor angiogenesis and lymphangiogenesis in colorectal cancer.* Oncol Rep, 2016. **35**(1): p. 253-260.
257. Cheng, W.K. and C.E. Oon, *How glycosylation aids tumor angiogenesis: An updated review.* Biomedicine & Pharmacotherapy, 2018. **103**: p. 1246-1252.
258. Nangia-Makker, P., et al., *Galectin-3 induces endothelial cell morphogenesis and angiogenesis.* The American journal of pathology, 2000. **156**(3): p. 899-909.
259. Markowska, A.I., K.C. Jefferies, and N. Panjwani, *Galectin-3 protein modulates cell surface expression and activation of vascular endothelial growth factor receptor 2 in human endothelial cells.* The Journal of biological chemistry, 2011. **286**(34): p. 29913-29921.
260. Sagiv, E., et al., *Targeting CD24 for treatment of colorectal and pancreatic cancer by monoclonal antibodies or small interfering RNA.* Cancer Res, 2008. **68**(8): p. 2803-12.
261. Xu, Q., et al., *Specific N-glycan alterations are coupled in EMT induced by different density cultivation of MCF 10A epithelial cells.* Glycoconj J, 2017. **34**(2): p. 219-227.
262. Azab, A.K., et al., *P-selectin glycoprotein ligand regulates the interaction of multiple myeloma cells with the bone marrow microenvironment.* Blood, 2012. **119**(6): p. 1468-1478.
263. Nolo, R., et al., *Targeting P-selectin blocks neuroblastoma growth.* Oncotarget, 2017. **8**(49): p. 86657-86670.
264. Mousa, L., M.E. Salem, and S. Mikhail, *Biomarkers of Angiogenesis in Colorectal Cancer.* Biomarkers in cancer, 2015. **7**(Suppl 1): p. 13-19.
265. Leung, D.W., et al., *Vascular endothelial growth factor is a secreted angiogenic mitogen.* Science, 1989. **246**(4935): p. 1306.
266. Ferrara, N., H.P. Gerber, and J. LeCouter, *The biology of VEGF and its receptors.* Nat Med, 2003. **9**(6): p. 669-76.
267. Wei, D., et al., *Stat3 activation regulates the expression of vascular endothelial growth factor and human pancreatic cancer angiogenesis and metastasis.* Oncogene, 2003. **22**(3): p. 319-29.
268. Zhu, C.C., et al., *CCR6 promotes tumor angiogenesis via the AKT/NF-κB/VEGF pathway in colorectal cancer.* Biochim Biophys Acta Mol Basis Dis, 2018. **1864**(2): p. 387-397.
269. Kaneko, Y., K. Kitazato, and Y. Basaki, *Integrin-linked kinase regulates vascular morphogenesis induced by vascular endothelial growth factor.* Journal of Cell Science, 2004. **117**(3): p. 407.
270. Koveitypour, Z., et al., *Signaling pathways involved in colorectal cancer progression.* Cell & Bioscience, 2019. **9**(1): p. 97.
271. Kaur, B., et al., *Hypoxia and the hypoxia-inducible-factor pathway in glioma growth and angiogenesis.* Neuro-oncology, 2005. **7**(2): p. 134-153.
272. Shibuya, M., *Vascular Endothelial Growth Factor (VEGF) and Its Receptor (VEGFR) Signaling in Angiogenesis: A Crucial Target for Anti- and Pro-Angiogenic Therapies.* Genes & cancer, 2011. **2**(12): p. 1097-1105.
273. Amin, E.M., et al., *WT1 mutants reveal SRPK1 to be a downstream angiogenesis target by altering VEGF splicing.* Cancer Cell, 2011. **20**(6): p. 768-80.

Appendices

Appendix I. Homo sapiens CD24 gene, Complete cDNA

>NM_001291737.1 Homo sapiens CD24 molecule (CD24), transcript variant 2, mRNA

AGTTTGCAGCGTCAGGCAGCGGGTCTGCGCCCAGCGAGCGGCTCCCCAGCTCCTGGGAAGATGCGGACCC
GGGACGCCCCCGTGAGCTCACTGCGCCTGGCTGACACGAGGCGCTCACAGAACAAAGCAAGGGCTTCGGG
GAGGGCGCGGCCGCGGGGCCGAGCGCGCAGATCGCTCCGGACCCGGACACCGCCTGCGAGGAGCGCCGAC
CAGCCGGGAAGGGTTCGCGCTAGGCGGCGCCCGGGTCCCGTCGGCCAGGGTCTCGCCGGCTCGCCGCGCT
CCCCACCTTGCCTGCGCCCGCCCGGAGCCAGCGGTTCTCCAAGCACCCAGCATCCTGCTAGACGCGCCGC
GCACCGACGGAGGGGACATGGGCAGAGCAATGGTGGCCAGGCTCGGGCTGGGGCTGCTGCTGCTGGCACT
GCTCCTACCCACGCAGATTTATTCCAGTGAAACAACAACTGGAACTTCAAGTAACTCCTCCCAGAGTACT
TCCAACTCTGGGTTGGCCCCAAATCCAACTAATGCCACCACCAAGGCGGCTGGTGGTGCCCTGCAGTCAA
CAGCCAGTCTCTTCGTGGTCTCACTCTCTCTTCTGCATCTCTACTCTTAAGAGACTCAGGCCAAGAAACG
TCTTCTAAATTTCCCCATCTTCTAAACCCAATCCAAATGGCGTCTGGAAGTCCAATGTGGCAAGGAAAAA
CAGGTCTTCATCGAATCTACTAATTCCACACCTTTTATTGACACAGAAAATGTTGAGAATCCCAAATTTG
ATTGATTTGAAGAACATGTGAGAGGTTTGACTAGATGATGGATGCCAATATTAAATCTGCTGGAGTTTCA
TGTACAAGATGAAGGAGAGGCAACATCCAAAATAGTTAAGACATGATTTCCTTGAATGTGGCTTGAGAAA
TATGGACACTTAATACTACCTTGAAAATAAGAATAGAAATAAAGGATGGGATTGTGGAATGGAGATTCAG
TTTTCATTTGGTTCATTAATTCTATAAGGCCATAAAACAGGTAATATAAAAAGCTTCCATGATTCTATTT
ATATGTACATGAGAAGGAACTTCCAGGTGTTACTGTAATTCCTCAACGTATTGTTTCGACAGCACTAATT
TAATGCCGATATACTCTAGATGAAGTTTTACATTGTTGAGCTATTGCTGTTCTCTTGGGAACTGAACTCA
CTTTCCTCCTGAGGCTTTGGATTTGACATTGCATTTGACCTTTTATGTAGTAATTGACATGTGCCAGGGC
AATGATGAATGAGAATCTACCCCCAGATCCAAGCATCCTGAGCAACTCTTGATTATCCATATTGAGTCAA
ATGGTAGGCATTTCCTATCACCTGTTTCCATTCAACAAGAGCACTACATTCATTTAGCTAAACGGATTCC
AAAGAGTAGAATTGCATTGACCACGACTAATTTCAAAATGCTTTTTATTATTATTATTTTTTAGACAGTC
TCACTTTGTCGCCCAGGCCGGAGTGCAGTGGTGCGATCTCAGATCAGTGTACCATTTGCCTCCCGGGCTC
AAGCGATTCTCCTGCCTCAGCCTCCCAAGTAGCTGGGATTACAGGCACCTGCCACCATGCCCGGCTAATT
TTTGTAATTTTAGTAGAGACAGGGTTTCACCATGTTGCCCAGGCTGGTTTCGAACTCCTGACCTCAGGTG
ATCCACCCGCCTCGGCCTCCCAAAGTGCTGGGATTACAGGCTTGAGCCCCCGCGCCCAGCCATCAAAATG
CTTTTTATTTCTGCATATGTTGAATACTTTTTACAATTTAAAAAAATGATCTGTTTTGAAGGCAAAATTG
CAAATCTTGAAATTAAGAAGGCAAAAATGTAAAGGAGTCAAAACTATAAATCAAGTATTTGGGAAGTGAA
GACTGGAAGCTAATTTGCATTAAATTCACAAACTTTTATACTCTTTCTGTATATACATTTTTTTCTTTA
AAAAACAACTATGGATCAGAATAGCCACATTTAGAACACTTTTTGTTATCAGTCAATATTTTTAGATAGT
TAGAACCTGGTCCTAAGCCTAAAAGTGGGCTTGATTCTGCAGTAAATCTTTTACAACTGCCTCGACACAC
ATAAACCTTTTTAAAAATAGACACTCCCCGAAGTCTTTTGTTCGCATGGTCACACACTGATGCTTAGATG
TTCCAGTAATCTAATATGGCCACAGTAGTCTTGATGACCAAAGTCCTTTTTTTCCATCTTTAGAAAACTA
CATGGGAACAAACAGATCGAACAGTTTTGAAGCTACTGTGTGTGTGAATGAACACTCTTGCTTTATTCCA
GAATGCTGTACATCTATTTTGGATTGTATATTGTGTTTGTGTATTTACGCTTTGATTCATAGTAACTTCT
TATGGAATTGATTTGCATTGAACACAAACTGTAAATAAAAAGAAATGGCTGAAAGAGCAA

Appendix II. Cell lines authentication certificate



School of Medicine
Division of Cancer and Stem Cell
Teresa Pereira Raposo
D Floor, West Block QMC
Nottingham, NG7 2UH
UK

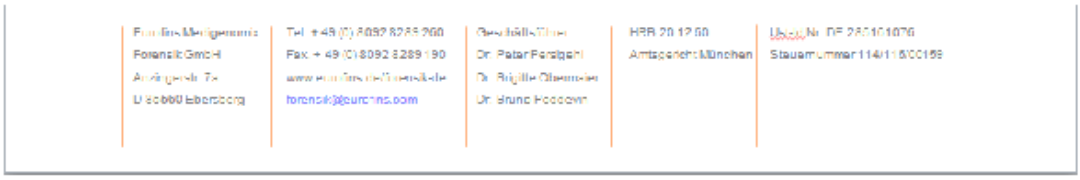
06.02.2017

Certificate

Order
By order of Teresa Pereira Raposo (School of Medicine) we were requested to perform a cell line authentication test. Following samples were examined:

Our sample number	Client sample name
CL170130_006	SW480
CL170130_007	DLD1
CL170130_008	SW620 (A)
CL170130_009	HCT116
CL170130_010	RKO
CL170130_011	SW620 (B)

Method:
Genetic characteristics were determined by PCR-single-locus-technology. 21 independent PCR-systems Amelogenin, D3S1358, D1S1656, D6S1043, D13S317, Penta E, D16S539, D18S51, D2S1338, CSF1PO, Penta D, TH01, vWA, D21S11, D7S820, D5S818, TPOX, D8S1179, D12S391, D19S433 and FGA were investigated (Promega, PowerPlex 21 PCR Kit).
In parallel, positive and negative controls were carried out yielding correct results.



Results:

DNA-System	DNA-criteria SW480 CL170130_006	DNA-criteria DLD1 CL170130_007	DNA-criteria SW620 (A) CL170130_008	DNA-criteria HCT116 CL170130_009	DNA-criteria RKO CL170130_010
AM	X, X	X, Y	X, X	X, X	X, X
D3S1358	15, 15	17, 17	16, 16	12, 16, 17, 18, 19	12, 16, 17, 18, 19
D1S1656	13, 14	17.3, 19.3	13, 14	12, 13, 14, 15	12, 13, 14, 16.3
D6S1043	11, 12	11, 13	11, 12	12, 13, 14	12, 13, 14.1, 20
D13S317	12, 12	8, 11	12, 12	10, 12, 13	8, 10, 11, 12
Penta E	10, 10	7, 14	10, 10	13, 14	10, 13, 14
D16S539	13, 13	12, 13	9, 13	11, 12, 13, 14	11, 12, 13
D18S51	13, 13	11, 17	13, 13	16, 17, 18	11, 12, 16, 17
D2S1338	17, 24	17, 25	17, 24	16, 16	16, 16
CSF1PO	13, 14	11, 12	13, 14	7, 10	7, 8, 10
Penta D	9, 15	9, 14	9, 15	9, 13	9, 10, 13
TH01	8, 8	7, 9.3	8, 8	8, 9	8, 9, 10
vWA	16, 16	18, 19	16, 16	17, 22, 23	17, 21, 22, 23
D21S11	30, 30.2	29, 32.2	30, 30.2	29, 30	29, 30
D7S820	8, 8	10, 12	8, 9	11, 12	11, 12
D5S818	13, 13	13, 13	13, 13	10, 11	10, 11
TPOX	11, 11	8, 11	11, 11	8, 8	8, 8
D8S1179	13, 13	15, 15	13, 13	12, 13, 14	9, 12, 13, 14
D12S391	17, 17	19, 22	17, 17	17, 18, 20, 21, 22	15, 17, 18, 20, 21, 22
D19S433	13, 13	14, 16	13, 13	12, 13	12, 13, 14, 18.2
FGA	24, 24	22, 22	24, 24	18, 19, 21, 22, 23	18, 19, 22, 23

DNA-System	DNA-criteria SW620 (B) CL170130_011
AM	X, X
D3S1358	16, 16
D1S1656	13, 14
D6S1043	11, 12
D13S317	12, 12
Penta E	10, 10
D16S539	9, 13
D18S51	13, 13
D2S1338	17, 24
CSF1PO	13, 14
Penta D	9, 15
TH01	8, 8
vWA	16, 16
D21S11	30, 30.2
D7S820	8, 9
D5S818	13, 13
TPOX	11, 11
D8S1179	13, 13
D12S391	17, 17
D19S433	13, 13
FGA	24, 24

Eurofins Medigenomix Forensik GmbH
Anzinger Str. 7a
D-85560 Ebersberg

Tel. +49 (0) 8092 8289 200
Fax. +49 (0) 8092 8289 190
www.eurofins-forensik.de
forensik@eurofins.com

Geschäftsführer
Dr. Peter Pongratz
Dr. Brigitte Obermeier
Dr. Bruno Hoogeveen

HRB 20 12 00
Amtsgericht München

Ust.-Id.-Nr. DE 240101876
Steuernummer 114/115/00159

Summary:
The following cell lines could be detected in the online database of the DSMZ (http://www.dsmz.de/de/service/services-human-and-animal-cell-lines/online-str-analysis.html):

Our sample number	Client sample name	DSMZ name
CL170130_006	SW480	SW-480
CL170130_007	DLD1	DLD-1
CL170130_008	SW620 (A)	SW620 [SW-620]
CL170130_009	HCT116	HCT-116
CL170130_010	RKO	RKO can be present in the mixture but the main component is HCT-116
CL170130_011	SW620 (B)	SW620 [SW-620]

Dr. Burkhard Rolf
Director Forensic Services

Dr. Michaela Bosch
Project Manager DNA-Forensics

Eurofins Medigenomix Forensik GmbH carries out all analyses with greatest care and on the basis of state of the art scientific knowledge. All results solely refer to the analysed samples. Our expert's reports must not be duplicated in extracts without consent of Eurofins Medigenomix Forensik GmbH.

Eurofins Medigenomix Forensik GmbH | Tel: +49 (0) 8092 8288 200 | Geschäftsführer: Dr. Peter Pongratz, Dr. Brigitte Obermeier, Dr. Bruno Hoogeveen | HRB 20 12 60 Amtsgericht München | Ust-Id-Nr. DE 281010876 Steuernummer 114/115/00159
Fax: +49 (0) 8092 8289 190 | www.eurofins-forensik.de | forensik@eurofins.com

Appendix III. SWA11 (CD24) antibody purification

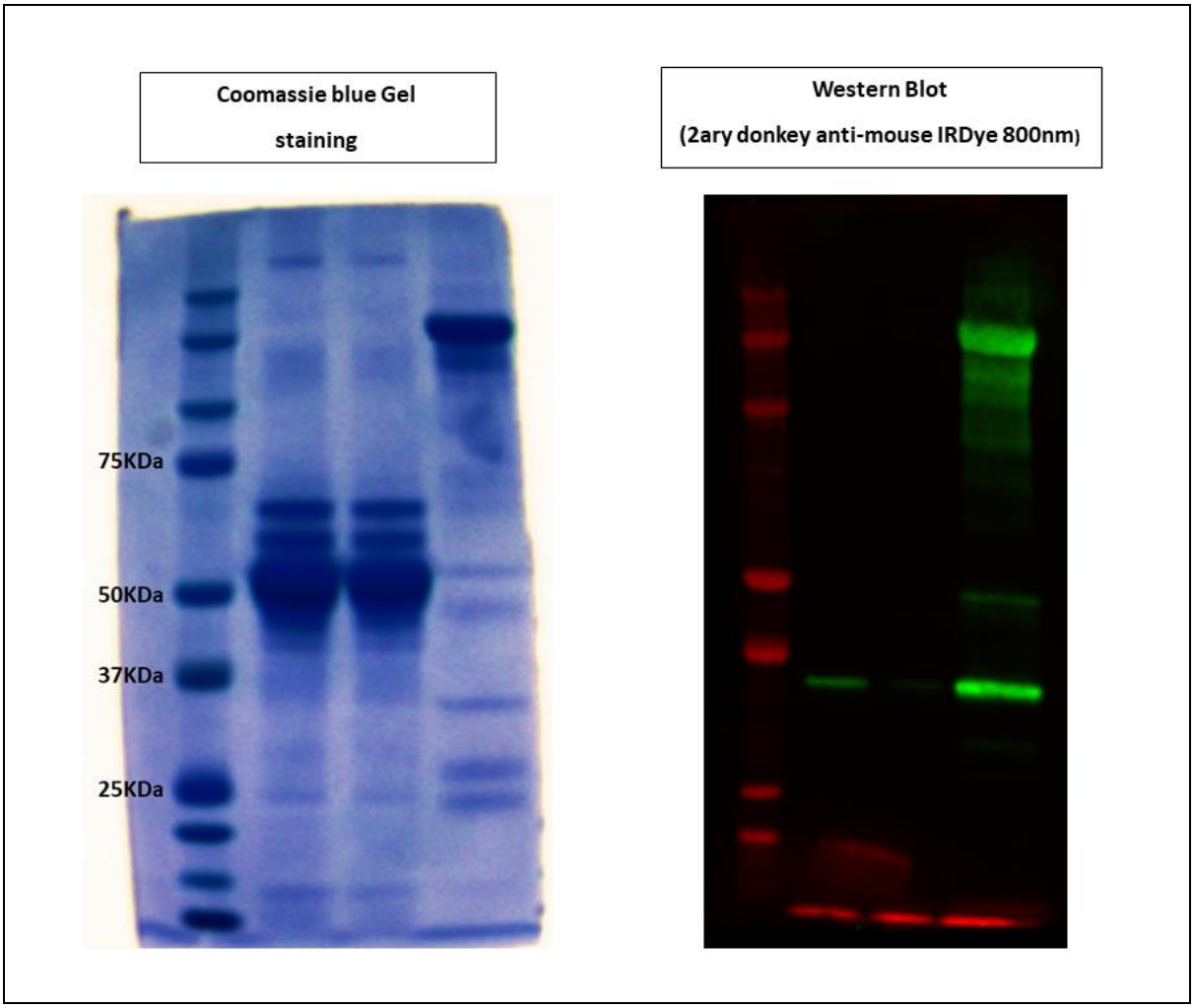


Figure S1 SWA11 (CD24) antibody purification IgG measurement.

Coomassie blue-stained gels and Western blotting using secondary donkey anti-mouse IRdye 800nm after SDS-PAGE of the purified antibodies.

Appendix IV. Transwell assays data analysis

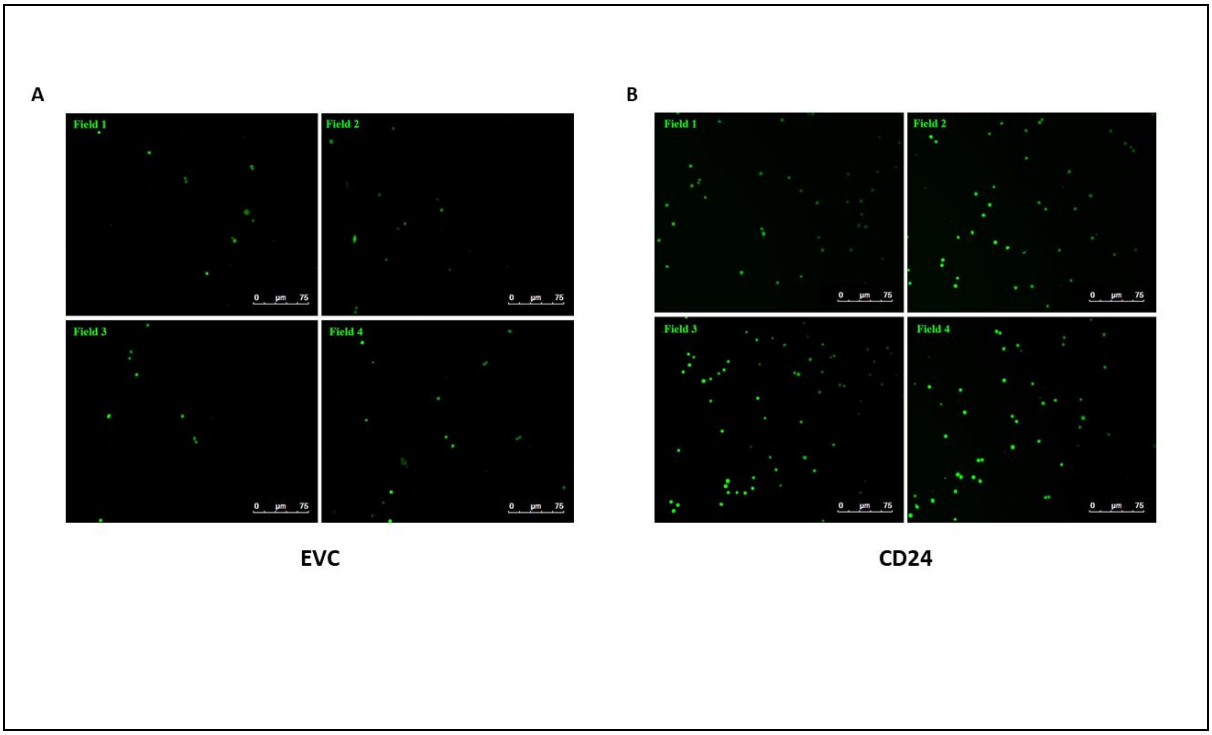


Figure S2 Representation of the transwell assay analysis of migrating and invasive cells.

Four random microscopic fields per well were taken at ×10 magnification, and the cells were counted manually using ImageJ (National Institutes of Health, Bethesda, MD) and analysed by taking the average of the four fields per well (A) empty vector control (EVC) and (B) CD24.

Appendix V. Stimulation of SW480-expressing CD24 with P-selectin

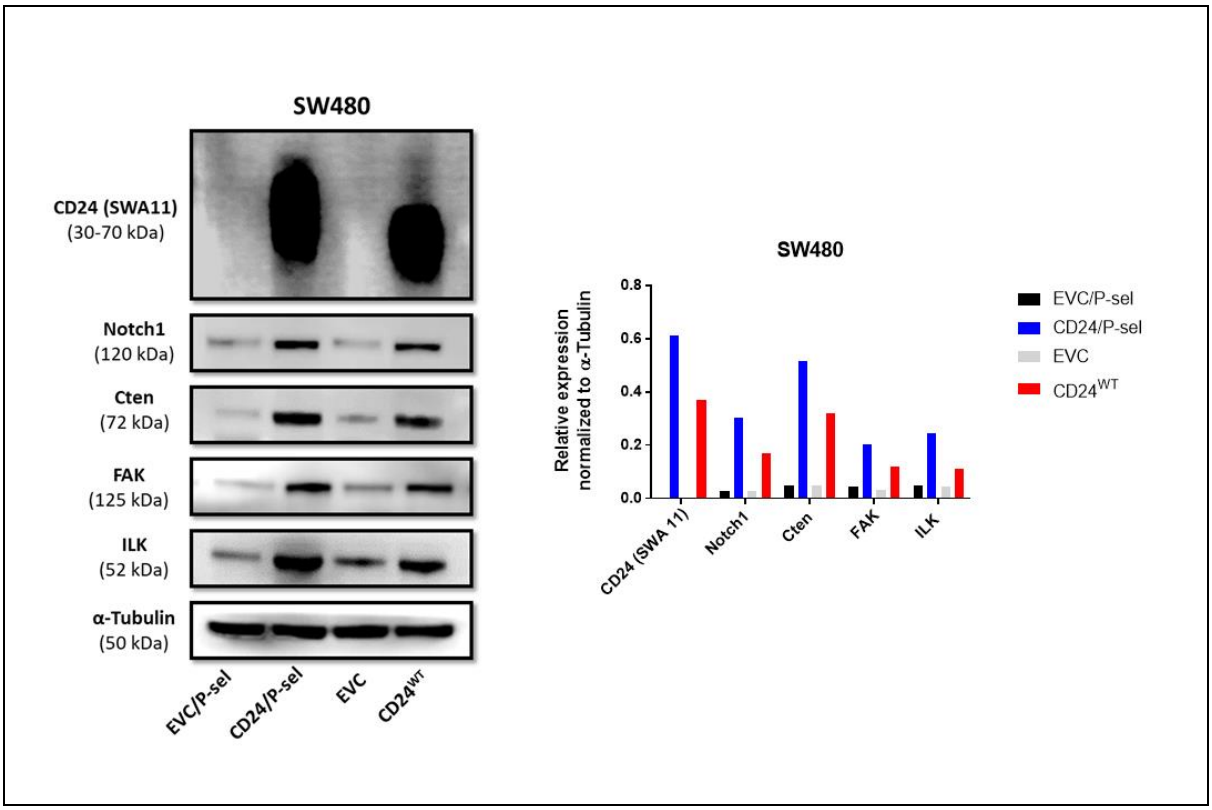


Figure S3 The effect of P-selectin stimulation on SW480 cell line.

Western blot analysis indicates the effect of stimulation with P-selectin on SW480-expressing CD24. As shown in the figure (left), the CD24 protein level and its end targets were increased compared to non-stimulated cells and EVC cells. Densitometry analysis of the relative expression of the target proteins normalised to alpha-tubulin.

Appendix VI. Optimisation of CD24 and ILK siRNA

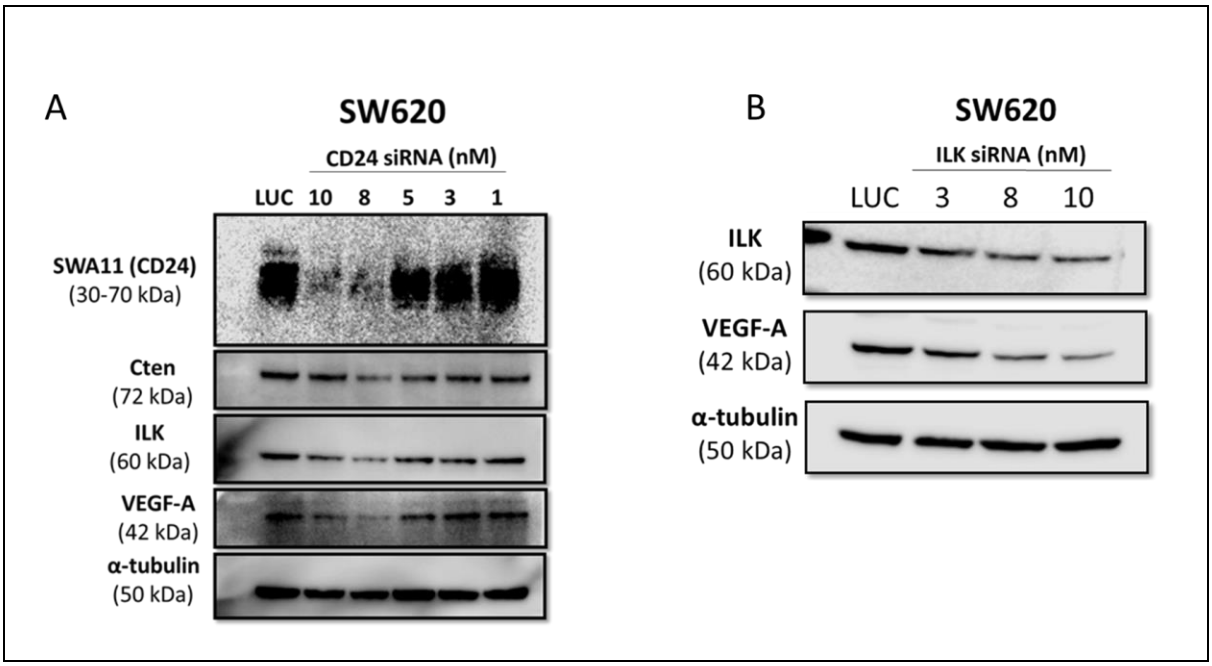


Figure S4 CD24 siRNA and ILK siRNA optimisation.

Western Blot confirmed CD24 silencing by siRNA in the SW620 cell line and showed the alteration of Cten, ILK, and VEGF-A proteins (A). In addition, ILK siRNA successfully led to ILK protein silencing compared to the luciferase control (LUC), and the optimum concentration of ILK siRNA was at 8 nM as indicated by western blotting. Similarly, the expression level of VEGF-A reduced in the ILK-silenced cells.